

GEOLOGY, PETROGRAPHY, AND GEOCHEMISTRY OF GRANITIC ROCKS FROM
THE COAST MOUNTAINS COMPLEX NEAR JUNEAU, SOUTHEASTERN ALASKA



OPEN-FILE REPORT 95-638

This report is preliminary and has not been edited or reviewed for conformity with U.S. Geological Survey editorial standards or with the North American Stratigraphic Code. Any use of trade, firm, or product names is for descriptive purposes only and does not imply endorsement by the U.S. Government.

About the cover: Juneau project field camp
on Hades Highway, Juneau Icefield. Michaels
Sword on the left, Devils Paw on the right,
elevation 8584 feet.
Photo by Art Ford, U.S. Geological Survey.

U. S. DEPARTMENT OF THE INTERIOR
U. S. GEOLOGICAL SURVEY

**GEOLOGY, PETROGRAPHY, AND GEOCHEMISTRY OF GRANITIC ROCKS
FROM THE COAST MOUNTAINS COMPLEX NEAR JUNEAU,
SOUTHEASTERN ALASKA**

By

James L. Drinkwater¹, David A. Brew¹, and Arthur B. Ford¹

Open-File Report 95-638

This report is preliminary and has not been reviewed for conformity with U.S. Geological Survey editorial standards or with the North American Stratigraphic Code. Any use of trade, firm, or product names is for descriptive purposes only and does not imply endorsement by the U.S. Government

¹Menlo Park, California 94025

CONTENTS

	Page
Abstract	1
Introduction	1
Previous Work	3
Methods and Procedures	5
Geologic Setting	6
General	6
Lithotectonic Terrane Reconstruction	7
Granitic Rocks of Transect	10
Geochronology	12
Admiralty-Revillagigedo Belt	12
Grand Island subbelt	12
Taku Harbor subbelt	15
Structure	17
Great Tonalite Sill Belt	18
Western subbelt	18
Structure	20
Coast Mountains Belt	20
Western subbelt	21
Eastern subbelt	24
Jointing	26
Miscellaneous plutons	27
Geochemistry	63
Admiralty-Revillagigedo Belt	64
Grand Island subbelt	64
Taku Harbor subbelt	65
Mainland Plutonic Belts	66
Great Tonalite Sill belt	66
Coast Mountains belt	67
Miscellaneous plutonic rocks	69
Summary of Chemical Features and Variations	70
Admiralty-Revillagigedo Belt	70
Mainland plutonic belts	70
Summary and Discussion	104
Petrogenetic Implications	105
Emplacement of the Mainland Batholith	109
Great tonalite sill belt	109
Coast Mountains belt	110
Resource Potential	112
References cited	113

LIST OF TABLES	<u>Page</u>
1. Major plutonic belts and subbelts.	28
2. Summary of isotopic ages	29
3. Radiometric age data: A) K-Ar analytical data; B) U-Pb analytical data.	30
4. Petrographic characteristics of plutons and plutonic units.	31
5. Modal analyses on samples from the Grand Island subbelt.	32
6. Modal analyses on samples from the Taku Harbor subbelt.	33
7. Modal analyses on samples from the Great tonalite sill belt.	34
8. Modal analyses from the southern unit of the western subbelt of the Turner Lake batholith .	35
9. Modal analyses from the central unit of the western subbelt of the Turner Lake batholith	36
10. Modal analyses from the northern unit of the western subbelt of the Turner Lake batholith	37
11. Modal analyses from the eastern subbelt of the Turner Lake batholith .	38
12. Modal analyses on samples from miscellaneous bodies.	39
13. Chemical characteristics of plutons and units across the Taku Inlet transect.	71
14. Chemical analyses of samples from the Grand Island subbelt (A and B).	72
15. Chemical analyses of samples from the Taku Harbor subbelt.	74
16. Chemical analyses of samples from the Great Tonalite Sill belt.	75
17. Chemical analyses for the southern unit of the western subbelt of the Turner Lake batholith .	76
18. Chemical analyses for the central unit of the western subbelt of the Turner Lake batholith .	77
19. Chemical analyses for the northern unit of the western subbelt of the Turner Lake batholith .	78
20. Chemical analyses for the eastern subbelt of the Turner Lake batholith .	79
21. Chemical analyses of samples from miscellaneous bodies.	80

List of Figures

	<u>Page</u>
1. Index map of southeastern Alaska showing location of study area and Coast Mountains complex.	2
2. Index map of the Taku Inlet transect area showing location of quadrangles and physical features along transect.	4
3. Lithotectonic terrane map of southeast Alaska	9
4. Generalized geologic map of study area.	11
5. Distribution of K-feldspar along transect	40
6. Magnetic susceptibility of plutonic subbelts from the Taku Inlet transect.	41
7. Generalized geologic maps of the Admiralty-Revillagigedo belt. A. Grand Island subbelt. B. Taku Harbor subbelt.	42
8. Modal compositions (K-f-qtz-plag plots) for rocks from the Admiralty-Revillagigedo belt (A, Grand Island subbelt; B, Taku Harbor subbelt).	44
9. Photographs of stain slabs of typical samples from; Admiralty-Revillagigedo belt: A, Grand Island subbelt; B, Taku Harbor subbelt.	45
10. Generalized geologic map of the Speel River pluton showing sample locations	46
11. Modal compositions (K-feld-qtz-plag) for rocks from the Great tonalite sill belt	47
12. Photographs of stain slabs of typical samples from Great tonalite sill belt.	48
13. Structural features of plutons from the Great tonalite sill belt.	49
14. Joint patterns in the Speel River pluton of the Great tonalite sill belt.	50
15. Generalized geologic maps of the western subbelt of the Turner Lake batholith. A. southern unit; B. central unit; C. northern unit.	51
16. Modal composition (K-feld-qtz-plag plots) for rocks from the Turner Lake batholith, western subbelt: A. southern unit; B. central unit; C. northern unit.	54
17. Photographs of stain slabs of typical samples from western subbelt of Turner Lake batholith: A. southern unit; B. central unit; C. northern unit.	55
18. Generalized geologic maps of the eastern subbelt of the Turner Lake batholith. A. Eastern unit; B. Stocks.	57
19. Modal composition (K-f-qtz-plag plots) - Turner Lake batholith, eastern subbelt: A. Eastern unit; B. Stocks.	59
20. Photographs of stain slabs of typical samples from eastern subbelt of Turner Lake batholith: A. Eastern unit; B. Wright Glacier stock	60
21. Modal compositions of Miscellaneous bodies of transect.	61
22. Synthesis of prominent joint sets for plutons from the Turner Lake batholith.(A-E).	62
23. SiO ₂ distribution in subbelts of transect.	81
24. A/CNK vs. SiO ₂ : A. Admiralty-Revillagigedo belt; B. Coast Plutonic belt	82
25. ALK* vs. SiO ₂ : A. Admiralty-Revillagigedo belt; B. Coast Plutonic belt	83
26. FeO*/Mg vs. SiO ₂ : A. Admiralty-Revillagigedo belt; B. Coast Plutonic belt	84
27. AFM diagram: A. Admiralty-Revillagigedo belt; B. Coast Plutonic belt	85

28. Ab-An-Or diagram: A. Admiralty-Revellagigedo belt; B. Coast Plutonic belt	86
29. K ₂ O-Na ₂ O-CaO diagram: A. Admiralty-Revellagigedo belt; B. Coast Plutonic belt	87
30. Trace element ranges for belts and subbelts of the Taku Inlet transect	88
31. Range charts of Rb, Sr, and SiO ₂ for plutons of transect (A, B, C).	89
32. Rb vs. Y+Nb tectonic affinity diagram: Taku Inlet transect.	90
33. Chemical characteristics of plutonic rocks from the Admiralty-Revellagigedo belt.	91
34. Harker diagrams: Rocks of the Admiralty-Revellagigedo belt.	92
35. REE plots: Grand Island and Taku Harbor subbelts.	93
36. Harker diagrams: Mainland plutonic belts	94
37. Binary diagram of Alk*/CaO versus SiO ₂ for subbelts of the Mainland batholith	95
38. Binary diagram of Fe*/Ti versus SiO ₂ for subbelts of the Mainland batholith.	96
39. Chemical characteristics of plutonic rocks from the mainland plutonic belts.	97
40. Harker diagrams: Great tonalite sill belt.	98
41. REE plots; Great tonalite sill belt.	99
42. Harker diagrams: Plutons of the Turner Lake batholith.	100
43. REE plots: Western subbelt of Turner Lake batholith.	101
44. REE plots: Eastern subbelt of Turner Lake batholith.	102
45. REE plots: Miscellaneous bodies of transect.	103
46. Summary diagram of plutonic subbelts and host terrane emplacement.	111

Geology, Petrography, and Geochemistry of Granitic Rocks from the Coast Mountains Complex near Juneau, Southeastern Alaska

BY James L. Drinkwater, David A. Brew, and Arthur B. Ford

Abstract

Granitic plutons of Late Cretaceous to middle Tertiary age comprise three major plutonic belts that occur in a large segment of the Coast Mountains Complex east of Juneau; they can be grouped, according to petrographic and chemical characteristics, into six northwest-trending subbelts. The Admiralty-Revillagigedo belt consist of two types of plutons; those of the Grand Island subbelt consist of magnetite-free, garnet- and epidote-bearing tonalites and quartz diorites, whereas the two plutons of the Taku Harbor subbelt are magnetite- and epidote-bearing, hornblende quartz monzodiorites. The two plutons of the Great tonalite sill belt are foliated, equigranular, magnetite-rich biotite-hornblende tonalites that differ from plutons from this belt to the northeast which are more acidic and felsic in composition. The Coast Mountains belt contains two major suites of plutons; the western subbelt consist of large plutonic units of predominantly massive, magnetite- and titanite-bearing biotite-hornblende granodiorite, whereas the eastern subbelt consist of undivided, massive, porphyritic, coarse-grained allanite-bearing hornblende-biotite granite and a stock of fine- to medium-grained seriate granite. Across the Coast Mountains Complex, the three major plutonic belts are distinguished by abrupt changes in age, structure, mineralogy, and composition, and the six subbelts are also distinguished by abrupt rather than gradual changes in chemical and modal composition, and magnetic susceptibilities.

Plutons of the Admiralty-Revillagigedo belt are characterized by high FeO^*/MgO ratios, high total alkalis and iron content, and high Sr abundances (700-1000 ppm). Rocks of the Great tonalite sill belt have restricted SiO_2 range (59-66 percent), high normative An content, and high ferromagnesian trace element (Sc, Cr, Co, and Zn) abundances, whereas rocks of the Coast Mountains belt are typically more acidic (64-74 percent SiO_2), less mafic, and contain higher abundances of K_2O , Rb, U, and Th. Granites of the eastern part of the Coast Mountains belt are further distinguished by low Sr (<400 ppm) and high Rb (>100 ppm) contents, pronounced negative Eu anomalies, and high Hf and Ta concentrations. The Wright Glacier stock is also characterized by very low Sr (<250 ppm) abundance and high Zr (280-380 ppm) and Y (30-50 ppm) concentrations.

The compositional differences between rocks of the various suites or subbelts reflect their differences in age and in the lithotectonic terranes and tectonic regimes into which they were emplaced. Plutons of the Admiralty-Revillagigedo belt represent an unrelated magmatic event from the plutonism of the mainland batholithic belts. Physical and chemical features support a common origin and magmatic evolution for most plutons of the Great tonalite sill and Coast Mountains belts, but some younger granites of the eastern part of the region may have been derived from a separate and unrelated magmatic event.

INTRODUCTION

Granitic plutons and batholiths of mostly Late Cretaceous to middle Tertiary age occupy a large part of the formally named Coast Mountains Complex (CMC of Brew and others, 1994) of southeastern Alaska (fig. 1). This segment of the North American cordillera, which extends the full length of the mainland Coast Mountains of southeastern Alaska and British Columbia, has previously been referred to as the Coast Range batholith (Buddington, 1927), Coast Mountains batholith (Gehrels and others, 1991), Coast Plutonic Complex (Douglas and others, 1970; Brew and Morrell, 1983), and Coast Mountains plutonic-metamorphic complex (Brew and Ford, 1984). These batholithic rocks represent post-accretionary magmatic activity (Brew, 1988)

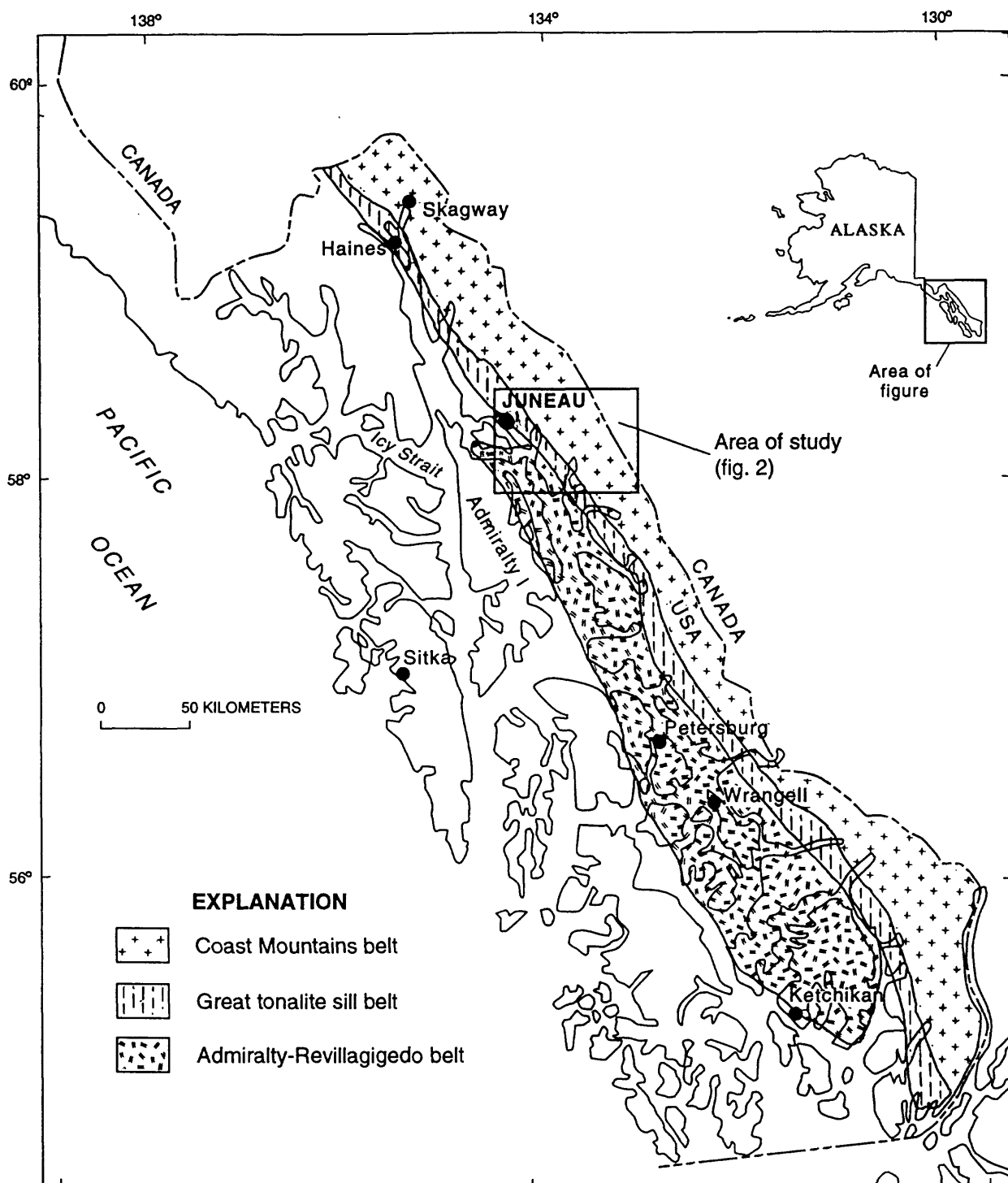


Figure 1. Index map of southeastern Alaska showing location of the Taku Inlet transect and major plutonic belts of the Coast Mountains complex.

Insular and Intermontane Superterrane (Wheeler and McFeely, 1991). Very little geologic and petrographic data are available on the granitic rocks of the northcentral part of the CMC in southeastern Alaska. The preliminary studies of Buddington (1927) and Buddington and Chapin (1929) focused primarily on the southern half of the batholith, and the two transect studies by Barker and Arth (1990) focused on the geochemistry, geochronology and isotope character of the batholithic rocks of the Skagway area in the northern part and Ketchikan area in the southern part of the CMC. We have investigated the geology, petrography, and chemistry of a segment of the CMC southeast of Juneau, termed the Taku Inlet transect (Drinkwater and others, 1991, 1994), which covers approximately 3500 sq kilometers of rugged mountainous and glaciated terrain between Taku Inlet and the Whiting River (Fig. 2).

The Taku Inlet transect area includes granitic rocks that belong to three major northwest-trending plutonic belts (Brew and Morrell, 1983). these belts are (fig. 1): (1) the Admiralty-Revillagigedo belt of Late Cretaceous plutons (Brew and Morrell, 1983); (2) the Great tonalite sill belt (Brew, 1988) of foliated tonalitic plutons of mostly Paleocene age; and (3) the Coast Mountains belt (Brew, 1988) of large, massive granodiorite and granite bodies of Eocene age. These plutons are believed to have been generated in response to the collision and accretion of the Alexander-Wrangellia terrane to the Stikine terrane in Late Cretaceous time (Crawford and others, 1987; Brew, 1988; Brew and others, 1991) and were emplaced along a complicated, linear, compressional structural zone that marks the boundary between these two major composite allochthonous terranes. These belts, in turn, can be subdivided into six subbelts on the basis of lithology, age, and magnetic susceptibility (Drinkwater and others, 1992) of the plutons and plutonic units.

This study delineates and describes the individual plutons and plutonic units that comprise the six subbelts of the CMC in the transect area. We also provide comprehensive chemical, geochronologic, and structural data for plutons that comprise the CMC in the Taku Inlet transect. The chemical characteristics of the three major plutonic belts within the transect was provided by Drinkwater and others (1994). This report provides additional modal and diagnostic chemical data that further supports the delineation and characterization of the subbelts and individual plutons and units. This information is instrumental in understanding the petrogenetic and emplacement history of this segment of the North American Cordillera and its implications to the complicated tectonic and terrane history of southeastern Alaska.

Previous Work

The Taku Inlet transect area lies within the region mapped in reconnaissance by Brew and Ford (1986) and partly in the area mapped and described by Brew and Grybeck (1984). Prior to this, geologic investigations were sparse and were centered at waterpower sites (Miller, 1962; Plafker, 1962). The transect area lies largely within four 1:63,360 quadrangles of the Taku River 1:250,000 scale quadrangle, and outer parts of the transect are within the Juneau 1:250,000 quadrangle. Peripheral parts of the transect area were included in the quadrangle mapping of Brew and Ford (1977) and Ford and Brew (1977), and in the reconnaissance mapping by Lathram and others (1965). More recently, Drinkwater and others (1992) used variations in magnetic susceptibility to delineate and characterize individual plutons and plutonic units within the transect, and Drinkwater and others (1989, 1990) provided preliminary petrographic and chemical descriptions of the Great tonalite sill rocks within the transect. Brew and others (1991) summarized the geophysical and geotectonic framework of a cross section of the northern (or Canadian) Cordillera that includes most of the Taku Inlet transect area. Studies on the metamorphic rocks

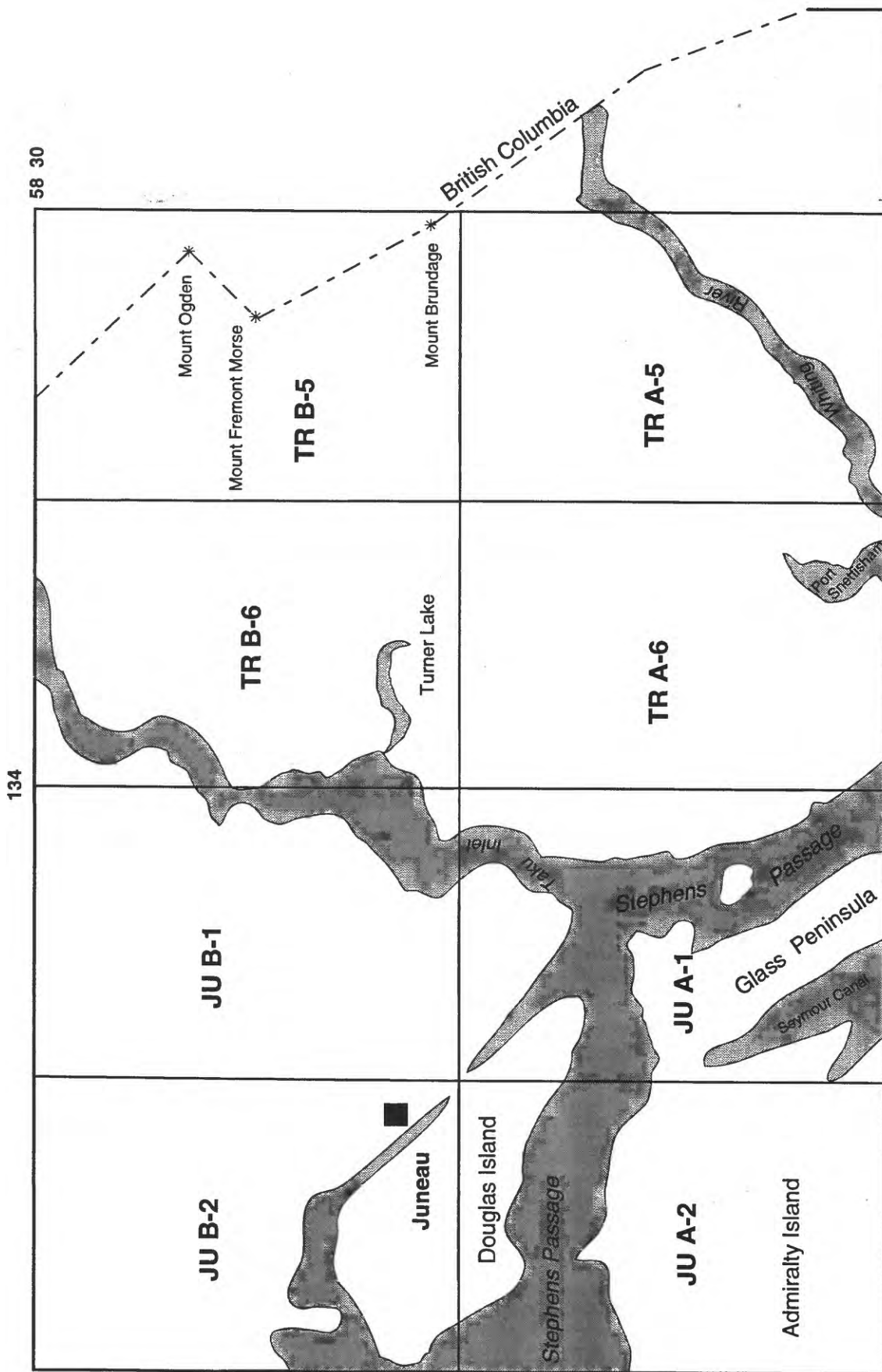


Figure 2. Index map of the Taku Inlet transect area showing location of Juneau (JU) and Taku River (TR) quadrangles. Area of study in this report lies between Taku Inlet and the Whiting River.

within the transect include those in the schist belt (west of the Great tonalite sill) by Himmelberg and others (1984a, b; 1986, 1991, 1995a, b) and Hooper and others (1990), and description of the migmatites by Karl and Brew (1983). Descriptions of mineral deposits and occurrences within the transect are found in Cobb, (1978); Kimball and others, (1984); and Wells and others, (1986).

Methods and Procedures

This report is based on information obtained or derived from field mapping in the Juneau region, and includes modal and chemical analyses, structural data, isotopic ages, and petrographic thin section analysis, as well as synthesis of previously published information. The rock classification used in this report is based on volume composition determined by modal analysis on stained rock slabs. Modal analysis (percent quartz, K-feldspar, plagioclase, and mafic minerals) were determined by counting a minimum of 1000 points per rock slab that were stained for K-feldspar and plagioclase by the method of Norman (1974). A grid of regularly-spaced points mounted on a glass plate was used, the spacing of the points were determined by the diameter of the larger rock grains. Biotite and hornblende were counted as total mafic minerals. The rock name of 235 samples was determined by plotting the modes (quartz, K-feldspar, and plagioclase recalculated to 100 percent) on the triangular classification (Q-A-P) diagram of Streckeisen (1976). Plutonic units or composite plutons were named by their average modal composition (Drinkwater and others, 1992).

Most major element oxides and minor element (Nb, Rb, Sr, Zr, Y, Ba, and Zn) abundances were measured by whole rock X-ray fluorescence (XRF) spectrometry at USGS laboratories in Denver, Colorado and Menlo Park, California. FeO was determined by wet chemical methods. The methods of analysis are summarized by Baedeker (1987). Pre-1980 samples were analyzed by rapid rock methods as described by Shapiro (1975), and the results are compatible with data from similar rocks analyzed by the more recent XRF methods. Rare-earth element abundances were determined prior to 1988 by inductively coupled plasma (ICP) atomic emission spectrometry, and after 1988 by instrumental neutron activation analysis (INAA). The analytical methods, techniques, and precision within the USGS laboratories are reviewed by Baedeker (1987). Additionally, the concentrations of selected trace elements (U, Th, Hf, Ta, Cs, Sc, Cr, and Co) were determined by INAA methods for 18 representative samples. The major element data were converted to normalized oxides and ratios, and CIPW norms and petrochemical indices by an upgraded version of the PETCAL 4 computer program (Bingler and others, 1976).

Isotopic ages have been obtained for many of the plutons or units by the K-Ar or U-Pb methods, but more isotopic dating is needed to establish the ages of all the plutons within the transect area. K-Ar ages were determined on either biotite or hornblende or both at laboratories in Menlo Park, California. Hornblende ages generally are more reliable indicators of the crystallization age of the rock than biotite, because the blocking temperature for hornblende is higher than that for biotite. Both mineral ages, however, may be younger than the age of crystallization because of reheating by younger intrusions or regional metamorphism. The U-Pb ages (zircon) presented here are from other published reports and from in-house analyses. The in-house ages are from single fraction analyses. The $^{206}\text{Pb}/^{238}\text{U}$ ages are used here but are in agreement with the $^{207}\text{Pb}/^{235}\text{U}$ ages within the limits of analytical error. Two $^{206}\text{Pb}/^{238}\text{U}$ vs. $^{207}\text{Pb}/^{235}\text{U}$ isochron intercept ages from Gehrels and others (1990) are also included here. The U-Pb zircon ages are generally better indicators of crystallization ages than K-Ar mineral ages because the closure temperature for U/Pb zircon is significantly higher than K/Ar in biotite or

hornblende; thus providing better retention of radiogenetic daughter elements in the U/Pb system. In some cases, ages from both methods may agree, but in other cases the K/Ar results may be reflecting the subsequent thermal history of the pluton rather than the crystallization age.

GEOLOGIC SETTING

The Taku Inlet transect segment (fig. 3) of the Coast Mountains Complex (Brew and others, 1994) includes representatives of many of the major plutonic belts (Brew and Morrell, 1983; Brew, 1988, 1994; Brew and others, 1992b; Drinkwater and others, 1994), metamorphic belts (Brew and others, 1992a) and at least two of the major structures (Brew and Ford, 1978; Ingram and Hutton, 1994) of southeastern Alaska. The proportion of gneisses and intrusive igneous rocks increases dramatically from west to east in the transect at the expense of schists and related rocks. As discussed below, the ages of the protoliths range from Late Proterozoic(?) to Cretaceous(?), and the ages of metamorphism and intrusion range from Late Cretaceous to middle Tertiary.

General

The following geologic sketch of the transect describes the major divisions from west to east. The western end of the transect consists of rocks of the western metamorphic belt of Brew and others (1989, 1992, 1994b); it consists mostly of pelitic schist, some metavolcanic rocks, and metacarbonate rocks that have been progressively metamorphosed from greenschist (pumpellyite-actinolite) facies on the west to amphibolite facies on the east (Brew and Grybeck, 1984; Stowell, 1989; Brew and others, 1992; Himmelberg and others, 1991, 1995). Within this belt are the 95-Ma plutons of the Admiralty-Revillagigedo belt (Brew and Morrell, 1983) that are discussed in detail in this report.

The Great tonalite sill (Brew and others, 1976; Brew and Ford, 1981, 1984a; Brew, 1988, 1994; Gehrels and others, 1991; Hutton and Ingram, 1992; Ingram and Hutton, 1994) marks the eastern limit of the western metamorphic belt and is the western part of the central metamorphic belt (Brew and Ford, 1984a). The Great tonalite sill is the name applied to a long and narrow composite set of sill-like plutons that extends from British Columbia on the south to Yukon Territory on the north. The individual plutons, some of which are described in detail later, range in age from about 55 to 70 Ma and generally consist of well foliated and locally lineated biotite-hornblende tonalite.

East of the Great tonalite sill are amphibolite-facies schists, gneisses, and migmatites (Karl and Brew, 1984) of the central metamorphic belt. Rock types include amphibolite-facies pelitic schist, semipelitic schist and gneiss, local quartz-rich schist, some large marble units, a variety of orthogneisses, and migmatites composed of original protolithic rocks together with neosomes related to all subsequent intrusive events. Their eastern limit is the western boundary of the central granitic belt. Mixed in with the schist and gneisses are scattered masses of metamorphosed ultramafic rocks (Grybeck and others, 1977) that now consist of serpentine, actinolite schist, and hornblende gabbro with locally preserved relicts of pyroxenite(?) and peridotite. These discontinuous bodies are the southern part of a belt of alpine(?) type ultramafic and associated gabbroic rocks that extends north almost to Skagway, Alaska (Brew and others, 1985; Brew and Ford, 1987; Himmelberg and others, 1985, 1986; G.R. Himmelberg, D.A. Brew, and A.B. Ford, unpublished data, 1991).

The Tertiary intrusions of the Coast Mountains belt are east of the Great tonalite sill. They are mostly massive sphene-hornblende-biotite granodiorite (Brew and Grybeck, 1984; Brew, 1988, 1994; Drinkwater and others, 1992, 1994).

The structure of the area is dominated by two major features, the steeply northeast-dipping Great tonalite sill shear zone and the near-vertical Coast Range megalineament. In addition to these two major features, the northeast-dipping metamorphic rock units record at least three earlier northeast-over southwest contractional and folding events that are closely associated with the metamorphism. The Great tonalite sill was intruded into an active northeast-over-southwest shear zone (Hutton and Ingram, 1992; Ingram and Hutton, 1994) in latest Cretaceous and Paleocene time (Brew, 1988, 1994; Gehrels and others, 1991). We currently interpret that shear zone to have been an original plate or terrane boundary, but its present expression and the actual location of the Great tonalite sill may be complicated by post-original-juxtaposition thin-skinned contractional faulting and subsequent break-throughs of those thrust sheets by the upward later continuations of the main deformation zone (D.A. Brew, unpub. data, 1992).

The Coast Range megalineament (Brew and Ford, 1978) is an enigmatic, poorly dated (but post-metamorphic) fault zone that is interpreted to reflect a fundamental contrast in the basement rocks on the opposite sides. That contrast is probably indirectly related to the Great tonalite sill shear zone close by and may be directly related to the differing proportion of underlying granitic rocks on the opposite sides of the zone.

Lithotectonic Terrane and Overlap Assemblage Reconstruction

In our lithotectonic terrane interpretation, the Taku Inlet transect includes, from west to east, parts of the: (1) Gravina overlap assemblage, which here consists of the Stephens Passage Group of Late Jurassic and Early Cretaceous age (Lathram and others, 1965); (2) the Behm Canal structural zone (Brew and Ford, 1993, 1994; Nokleberg and others, 1994); which here consists of structurally interleaved Stephens Passage Group and Wrangellia terrane of latest Paleozoic and Triassic age, and (3) Nisling terrane of inferred Late Proterozoic to Paleozoic age (Fig. 3). The Stikine terrane is exposed east of the Nisling.

The Gravina overlap assemblage (Brew and Karl, 1988; Cohen and Lundberg, 1993) consists mainly of flysch of the Seymour Canal formation together with intermediate to mafic volcanic breccias and flows of the Douglas Island Volcanics. Not far west of the Taku Inlet transect, along the eastern side of Admiralty Island, this unit unconformably overlies both Upper Triassic lithostratigraphic units.

In the Taku Inlet transect, Gravina overlap assemblage rocks are interpreted to occur both in healed-fault contact with the Behm Canal structural zone (see next paragraph) rocks and as units within that zone. Regionally, the contact of the Gravina overlap assemblage rocks with the Wrangellia terrane rocks is interpreted to be stratigraphic, with some post-metamorphic fault adjustments (Brew and Karl, 1988).

We are using the term "Behm Canal structural zone" (Brew and Ford, 1993, 1994; D.A. Brew, in W.J. Nokleberg and others, unpublished manuscript) in southeastern Alaska to denote the composite terrane consisting of large thrust slices composed of Gravina overlap assemblage and of Alexander, Wrangellia, Stikine, and Nisling terrane rocks, the Alava sequence of Rubin and Saleeby (1991), part of the Kah Shakes sequence and a early Paleozoic gneiss complex of Saleeby and Rubin (1990) and Rubin and Saleeby (1991). This terrane was considered as part of the Taku terrane of Berg and others (1978) and Monger and Berg (1987). The structural juxtaposition occurred in the Late Cretaceous, and the rocks were subsequently

metamorphosed (Late Cretaceous and early Tertiary) to greenschist- to amphibolite-facies mica schist, granitic orthogneiss, calc-silicate rocks, and minor marble and amphibolite. This metamorphism obscured most original fault features, generally leaving only contrasting lithologic sequences as field evidence of the juxtaposition. Brew and others (1991a, 1992a) used the abbreviation "YAWG" for this structural unit, an acronym formed from the first letters of Yukon prong, Alexander, Wrangellia, and Gravina, the original terrane rock-units juxtaposed in the structural zone.

We use the term "Nisling terrane" (from Wheeler and McFeely, 1991) here for the metamorphic rocks derived from Proterozoic and (or) lower Paleozoic depositional materials interpreted to have come from the western margin of ancestral North America. Nisling terrane rocks form the basement for most plutons of the Coast Mountains belt. The Nisling terrane has been correlated with the Yukon-Tanana terrane to the north (Mortenson and Jilson, 1985; Gehrels and others, 1990; Samson and others, 1991). Prior to the latest Cretaceous to middle Tertiary plutonism and metamorphism in the Coast Mountains, the terrane consisted of locally metamorphosed (in pre-Late Triassic time) quartz-rich and pelitic sedimentary rocks, carbonate rocks, ultramafic rocks, and intermediate- to mafic volcanic rocks that were sparsely intruded by middle Paleozoic granitoid rocks. Rocks in the terrane are now metamorphosed to amphibolite-facies mica schist, granitic orthogneiss, amphibolite, quartzite, marble, and calc-silicate rocks. In the field the Nisling terrane is recognized by the association of quartz-rich schist and gneiss, pelitic schist, and thick discontinuous marble units, with only rare amphibolite units. Where the quartz-rich units are missing, the association can well be confused with rocks of the Alexander terrane (Brew and Ford, 1984b) and isotopic methods may be required to differentiate the two terranes (Gehrels and others, 1990; Samson and others, 1991).

The contact of the Behm Canal structural zone rocks with Nisling terrane rocks is, as noted by Brew and others (1994a), one of the outstanding questions of Coast Mountains geology. In the Taku Inlet transect, we place the contact east of the locally fossiliferous metavolcanic rocks of the Wrangellia terrane and west of the schist and gneiss unit that we refer to as the Nisling terrane. The exact location is subject to discussion because Nisling terrane rocks are probably involved in the Behm Canal structural zone. The four diagnostic lithologic features used to define the Nisling; namely the thick discontinuous marble units, quartz-rich schists, meta-ultramafic rocks, and the orthogneisses first occur a few kilometers across strike from the fossiliferous Wrangellia terrane rocks. In the Taku Inlet transect itself, this places the contact somewhere within or at the contacts of the younger Speel River pluton, which is part of the Great tonalite sill. The isotopic evidence of Samson and others (1991), however, indicates that at least some of the lithic units immediately to the southwest of the Great tonalite sill belong with the Nisling terrane. Overall, the isotopic evidence of Samson and others (1991) indicates that the southwestern contact of the Nisling terrane in the Taku Inlet transect lies to the east of the Coast Range megalineament of Brew and Ford (1978).

As noted previously, the contact of Nisling terrane rocks with Stikine terrane rocks is believed to lie east of the study area, but it, too, is a subject of serious uncertainty in Coast Mountains geology (Brew and Ford, 1993, 1994; Brew and others, 1994a). A major structural break was mapped by Brew and Ford (1987), north of the transect area, as the Meade Glacier fault, which they extended south into the eastern part of the transect area. They initially interpreted this fault as a possible tectonic boundary between the Stikine terrane to the east and Alexander-Wrangellia terrane to the west, but it was later interpreted by Brew and others (1991) as a transtensional fault contact between upper and lower parts of the Stikine terrane.

Two other features in the Taku Inlet transect, the Sumdum fault and the Cape Fanshaw fault, have been proposed as major tectonic boundaries by Gehrels and

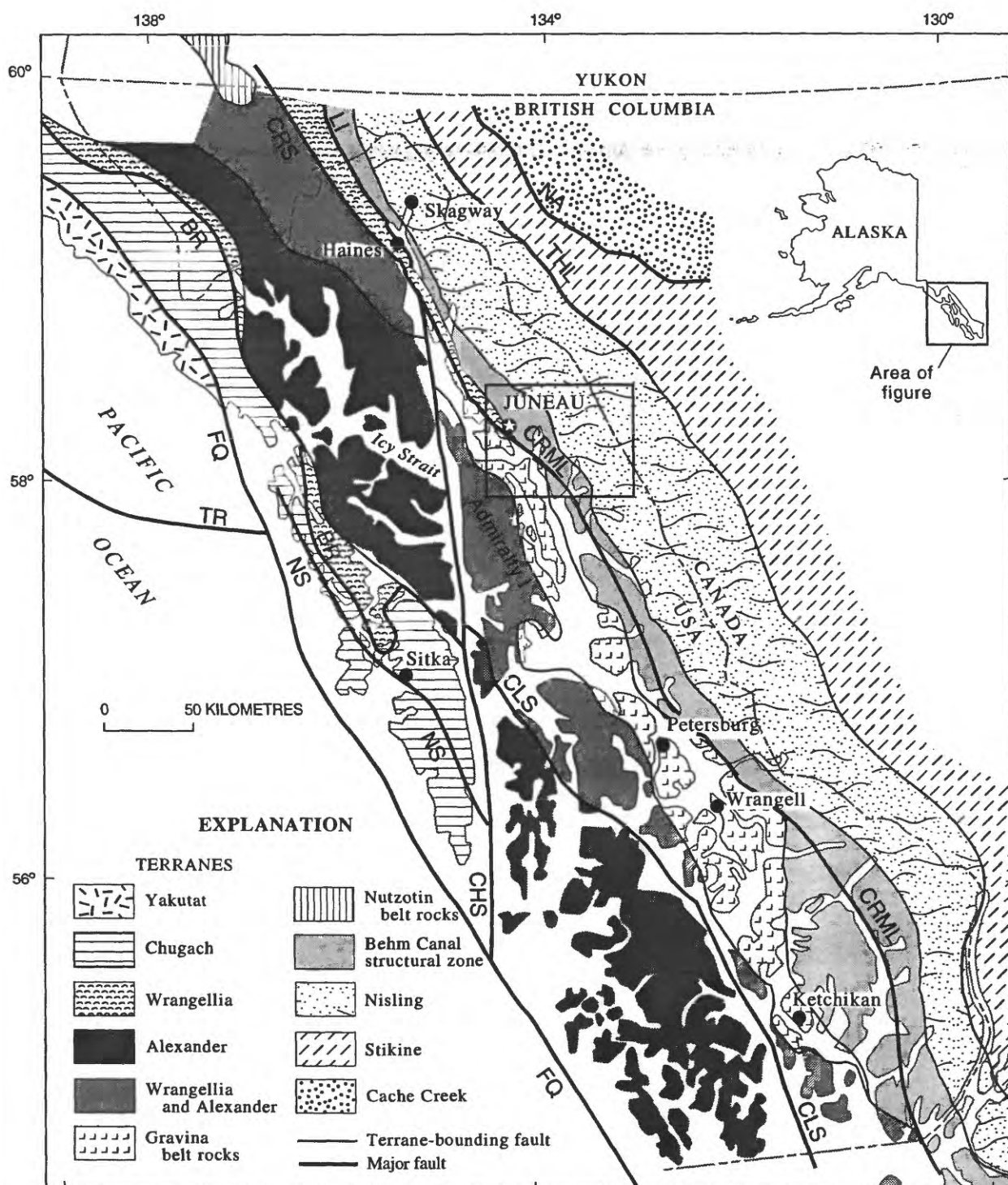


Figure 3. Lithotectonic terrane map of southeastern Alaska (modified from Brew and others, 1992) showing area covered by Taku Inlet transect (outlined). Faults: NA, Nahlin; CRML, Coast Range megalineament; FQ, Fairweather Queen Charlotte Islands; CHS, Chatham Strait; NS, Neva Strait; BR, Border Ranges; TR, Transition; CLS, Clarence Strait; CRS, Chililat River; THL, Tally Ho-Llewellyn.

others (1992) on the basis of their shoreline-only mapping and on their reinterpretation of Ford and Brew's (1973, 1977), Brew and Ford's (1977), and Brew and Grybeck's (1984) complete shoreline and high-country mapping. The Sumdum fault is postulated to be the contact between the Taku lithotectonic terrane of Berg and others (1978) on the west and the Yukon-Tanana terrane on the east. The Fanshaw fault is postulated to be the contact between Gravina overlap assemblage rocks (Berg and others, 1972) on the west and the the Taku terrane of Berg and others (1978) on the east. If these two major tectonic boundaries are present, they have been thoroughly obscured by post-juxtaposition metamorphism and intrusion, and we currently question their existence.

GRANITIC ROCKS OF TRANSECT

Granitic rocks of Cretaceous to early or middle Tertiary age in the CMC form plutons that range in size from small stocks to batholithic masses. They are largely tonalite and granodiorite calc-alkalic plutons but range in composition from quartz diorite to granite (Brew, 1988; Drinkwater and others, 1994). The CMC contains four major plutonic belts (Brew, 1992) that consist of NW-SE-trending array of plutons or granitic masses that are distinguish by age, size, structure, lithology, and chemistry (Brew, 1988; Brew and Morrell, 1983). Minor occurrences of older Mesozoic plutons (Brew, 1992, Gehrels and others, 1991) and Neogene alkalic granite stocks (Arth and others, 1988; Brew, 1992; Koch, 1993) also occur in parts of the CMC, but are absent or not identified in the Taku Inlet transect area. Three of the plutonic belts are represented in the Taku Inlet transect area (figs. 1, 4); they are the Admiralty-Revillagigedo, Great tonalite sill, and Coast Mountains belts. Plutons of the Great tonalite sill and Coast Mountains belts are spatially related (Brew and Ford, 1986) and close in age and petrologic affinity (Brew, 1988; Drinkwater and others, 1994). Plutons of the Admiralty-Revillagigedo belt were emplaced west of the megalineament and in different lithotectonic terranes. Because of their older age, distinctive mineralogy, and very low magnetic susceptibility, they are considered as a separate episode of plutonism unrelated to the emplacement of the mainland batholith (Great tonalite sill and Coast Mountains belts). A fourth belt, the 110 to 100-Ma Klukwan-Duke belt consists of Alaskan-type ultramafic bodies that are more prevalent in the southern part of the CMC. Small masses of more mafic-rich plutonic rocks occur throughout the Coast Mountains belt, and within the transect, only the larger ones are mapped (fig. 4). The age of these diorites and quartz diorites within the transect area has not been established but they may be age equivalent to the Early Cretaceous plutons dated by Arth and others (1988) in the Ketchikan area of the CMC. If so, they are interpreted as being older relict batholithic rocks that have been largely displaced by Eocene granitic batholithic rocks of the Coast Mountains belt.

The major plutonic belts of the transect area consist of subbelts (table. 1), which are characterized by plutons with distinctive lithology, magnetic susceptibility (Drinkwater and others, 1992), ages (Table 2), and by petrographic characteristics (table 4). The distribution of K-feldspar and mafic minerals is distinctive of each subbelt (fig. 5). The Admiralty-Revillagigedo belt is divided into two subbelts: the Grand Island subbelt consists of plutons of quartz diorite and tonalite that have very low magnetic susceptibility, and the Taku Harbor subbelt contains two plutons of quartz monzodiorite composition that have moderate magnetic susceptibility values (Drinkwater and others, 1992). The Great tonalite sill belt in the northern CMC is divided into two subbelts (Brew, 1988; Drinkwater and others, 1990, 1992): a western subbelt of relatively homogeneous, foliated tonalite and quartz diorite that gives very high magnetic susceptibility values, and an eastern subbelt of more felsic but heterogeneous rocks (Drinkwater and others, 1990) with

variable but generally high magnetic susceptibility. Only plutons of the western subbelt are represented along the transect. The southern extension of the Carlson Creek pluton penetrates the transect (fig. 4), but this pluton has been described in Drinkwater and others (1990) and will not be repeated here. The Coast Mountains belt within the transect area consist of the Turner Lake batholith. Although mapping has yet to determine the exact number of plutons in this part of the Coast Mountains belt, three large granodioritic units with moderately high magnetic susceptibility form the western subbelt, and undivided granite and granitic stocks with low magnetic susceptibilities form the eastern subbelt.

Geochronology

Most granitoids of the CMC were emplaced between Late Cretaceous and middle Eocene time. Plutons of the Admiralty-Revillagigedo belt have been dated from 101 Ma to 85 Ma, with an average age near 95 Ma (Brew and others, 1990). Within the Taku Inlet transect, they have been dated between 85 and 95 Ma (table 3). Plutons of the Great tonalite sill belt were emplaced from 70 to 55 Ma (Brew, 1988) but within the transect they are probably Paleocene in age (table 3). Just south of the Taku Inlet transect, in the Holkham Bay area, Wood and others (1991) reported a range of $^{40}\text{Ar}/^{39}\text{Ar}$ ages on biotite and hornblende of 63 to 53 Ma for rocks from the Great tonalite sill. The youngest group of plutons form the Turner Lake batholith of the Coast Mountains belt; they were emplaced from 54 to 49 Ma (K-Ar ages from Brew, 1988). Gehrels and others (1984) reported a U-Pb zircon age of 50 Ma for a granodiorite from the Turner Lake batholith near Taku Inlet. A small stock near Tease Lake, which has an intrusive contact with the tonalite sill, has yielded a K-Ar hornblende age of approximately 51 Ma (Table 4). Several granitic stocks near Wrights Glacier (Fig. 4) are suspected of being much younger than the rest of the Eocene plutons of the Turner Lake batholith, but they have not been dated.

Admiralty-Revillagigedo Belt

Late Cretaceous plutons of the Admiralty-Revillagigedo belt occur along the western margin of the CMC for approximately 400 miles from Juneau to Ketchikan. They form a discontinuous belt of isolated plutons, clusters of discrete plutons, and larger composite plutons, that are composed of foliated to gneissic, garnet- and epidote-bearing quartz diorite, tonalite, and granodiorite (Brew and Morrell, 1983; Burrell, 1984; Brew and others, 1992). Within the Taku Inlet transect area, these plutons occur as stocks and small dome-like intrusions that are clustered around Stephens Passage and the northeast tip of the Glass Peninsula (figs. 7A, 7B). These plutons are divided into two subbelts based on differences in lithology (fig 8A, 8B) and magnetic susceptibility (fig. 5.) (Drinkwater and others, 1992).

Grand Island Subbelt

The small stocks and dome-like intrusions that occur west of the Coast Range megalineament on Glass Peninsula and at Grand Island, Butler Peak and Irving Peak areas are part of the Grand Island subbelt (fig. 3). These plutons exhibit steeply-dipping foliations and contact-metamorphic aureoles, and are characterized by very low magnetic susceptibilities (Drinkwater and others, 1992). The plutons consist mostly of quartz diorite and tonalite (fig. 7) but range from diorite of the Irving Peak pluton to granodiorite of the Butler Peak pluton (fig. 8); modal analyses are given in table 5. The rocks show variable alteration and have deformational fabrics ranging from weakly to strongly foliated to locally gneissic; deformational flow banding and layering are more pronounced near margins. The presence of garnet and primary epidote in these rocks distinguish them from the rocks of the other belts, and a

characteristic feature of plutons of this subbelt is the presence of sulfides and ilmenite and absence of magnetite which gives these rocks a very low magnetic susceptibility signature (Drinkwater and others, 1992).

Glass Peninsula stocks: A group of tightly clustered, small oval-shaped, foliated intrusions, is found on the northeast tip of Glass Peninsula as steep, forest-covered mounds. Good exposures of these intrusions are limited and are found mostly at the highest peaks and along the shores of Stephens Passage and Doty Cove. A K-Ar hornblende age of 90.1 Ma was reported by Brew (unpublished data) for one of the stocks (table 3). The rocks, although being somewhat variable in texture and composition are mostly medium-grained, foliated, porphyritic to equigranular hornblende-biotite quartz diorite and tonalite (fig. 8 & 9). The intrusions contain mafic and hornfelsic inclusions, which are particularly common along the margins of the bodies, and are cut by 30-40 cm-thick felsic and aplite dikes (many of which are garnet and muscovite bearing). The stocks consist of plagioclase (50-80 percent), quartz (8-33 percent), hornblende and biotite (10-35 percent), and minor K-feldspar (0-9 percent).

The typical rock of the intrusions consists of phenocrystic to coarse-granular plagioclase, intergranular quartz, medium-grained and foliate hornblende and biotite, and interstitial to poikilitic K-feldspar. Mafic minerals are typically intergrown or clustered together. Garnet, titanite, epidote, apatite, ilmenite, and sulfides are common accessory minerals. Most rocks show some degree of mylonitic or cataclastic deformation, including recrystallized strained quartz aggregates; strained, bent, and abraded crystals (plagioclase and mafic minerals); fragmented grain margins, and overgrowths on plagioclase. Common secondary minerals include chlorite, sericite-muscovite, calcite, and granular opaque oxides. In some rocks, plagioclase is albitized.

Plagioclase is abundant and forms subhedral, stout tabular to subequant-shaped crystals. The plagioclase is nearly always altered to some degree by zonal and patchwork replacement by sericite, clinozoisite, and epidote. In some cases, sericite has recrystallized to coarser muscovite. Thin unaltered overgrowths of albitic plagioclase are common. Where relatively fresh, plagioclase exhibits multiple concentric zoning mostly of oscillatory-normal type. In most cases, deformation and alteration have obliterated twinning and much of the zoning in plagioclase.

Quartz and K-feldspar occur interstitially to plagioclase and mafic minerals. Quartz is common and forms anhedral, strained and recrystallized crystals and aggregates (mortar texture). Aggregates contain strained and unstrained subgrains with curved, jagged, and sutured boundaries. In more deformed rocks the quartz becomes stretched and develops polygonal boundaries. K-feldspar is uncommon and generally occurs in trace amounts as interstitial and poikilitic crystals; most show vague tartan twinning of microcline.

Hornblende and biotite are the major mafic minerals, although locally epidote occurs in significant amounts. Hornblende is generally more abundant than biotite, and both minerals are typically clustered in folia that define the conspicuous foliation in the rocks. Hornblende forms subhedral, tabular, pleochroic greenish-brown crystals that are fresh to partly altered to epidote, chlorite and opaque oxides; in some cases hornblende is replaced by light-green amphibole. Typically, the hornblende is twinned and may show broad concentric zoning. Biotite occurs as fine- to medium-grained, pleochroic brown to dark-brown or reddish-brown, ragged shards. It is fresh to partly altered to chlorite, titanite, and epidote: some biotite contains intergrowths of muscovite. Primary epidote is found as discrete subhedral crystals and as subhedral intergrowths with hornblende and biotite. It is typically zoned with cores of allanite, and exhibits euhedral boundaries to biotite and subhedral boundaries to hornblende.

Of the accessory minerals, titanite is the most common and widespread; it forms discrete, pleochroic gray-brown, euhedral crystals that typically exhibit diamond or spear-shaped and fish-tail twinned crystals. Garnet occurs as small subhedral crystals and clusters of crystals that are typically rounded and embayed; it is also found as euhedral inclusions in hornblende and biotite. Apatite is found as tiny euhedral inclusions in mafic minerals and as discrete crystals clustered with mafic minerals. Allanite is scarce and occurs as euhedral zoned cores in epidote. The nature of muscovite in these rocks is uncertain, its occurrence as intergrowths or bundles within biotite and as intersitial crystals indicate that it may be a late magmatic-hydrothermal mineral. Primary opaque minerals are scarce in these rocks, and where present they are either sulfides or ilmenite (which was identified by its elongated six-sided shapes). Sulfide minerals, although not common, are widespread; they were found in more than half of the sections we examined. They occur as granular interstitial crystals and aggregates that are typically associated with secondary iron oxides and hydroxides. Pyrite was identified in one sample by X-ray diffraction analysis.

Grand Island pluton: The pluton that forms Grand Island is a dome-like intrusion that exhibits steeply dipping concentric foliation. It consists of medium-grained, biotite-hornblende tonalite and quartz diorite. Most exposures are homogeneous, seriate to slightly porphyritic rocks, with a color index of 25 to 30. Mafic inclusions are common and are typically flattened, as well as stretched parallel with the foliation; locally they are sheared and flasered.

The rocks of the Grand Island pluton consist of coarse-grained to phenocrystic plagioclase, medium-grained tabular hornblende and foliate biotite, intergranular quartz, and minor interstitial K-feldspar. Plagioclase comprises 50 to 70 percent of the rocks and it forms subhedral blocky to tabular crystals and phenocrysts that are partly altered to fine-grained aggregates of sericite, clinozoisite, and prehnite. The plagioclase typically displays strong multiple concentric zoning, generally of oscillatory-normal type. Overgrowths and outer margins of plagioclase crystals are unaltered and generally reverse zoned. Quartz forms 11 to 23 percent of the rocks and occurs as intergranular strained crystals and polycrystalline aggregates. K-feldspar is rare (0 to 3 percent) and is found as interstitial crystals of microcline.

Mafic minerals (hornblende, biotite, and epidote) make up 15 to 38 percent of the rocks and define a folia of aligned tabular and lamellar crystals. Hornblende occurs as subhedral, twinned, pleochroic brown to greenish-brown crystals that are fresh to partly altered to granular epidote, opaques, and green amphibole. It typically contains inclusions of apatite and titanite. Biotite is pleochroic brown to reddish brown and forms platy or lamellar crystals which may be partly altered to chlorite, iron-oxides, and titanite. Primary epidote occurs as discrete subhedral crystals that enclose hornblende, it forms idiomorphic boundaries to biotite and symplectic boundaries to plagioclase and quartz.

The primary accessory minerals are titanite, apatite, and allanite; ilmenite and sulfides also occur but are much less common. Titanite forms euhedral twinned, arrow and diamond-shaped crystals that are typically clustered and aligned with mafic minerals. Apatite forms tiny euhedral inclusions in mafic minerals, and allanite occurs as subhedral cores in epidote and as inclusions in mafic minerals. Opaque minerals are scarce in these rocks, but where present they include primary ilmenite and sulfides, and as secondary magnetite or other iron oxides. Ilmenite was identified by its elongated, six-sided forms as inclusions in mafic minerals and plagioclase.

Irving Peak pluton: The Irving Peak pluton occurs east of Grand Island, and forms a poorly-exposed, forested mound along the ridge from Irving Peak to Taku

Mountain. The best exposures of this pluton are along the shore of Stephens Passage. It is a heterogeneous, foliated, altered dioritic body approximately 5 by 2 kilometers in size. The pluton contains mafic inclusions and xenoliths of finely banded country rock, and it is cut by mafic and trondhjemitic dikes on its western side and by granitic dikes in its southern part. The pluton is composed mostly of foliated, medium-grained, hypidiomorphic-granular, biotite-bearing hornblende diorite and quartz diorite that has a color index of 23 to 44.

The major constituents of the rocks are plagioclase (40 to 65 percent), quartz (1 to 15 percent), and hornblende and biotite (23 to 44 percent). The accessory minerals are titanite, apatite, ilmenite, and sulfides. Plagioclase is elongated to lens-shaped and is commonly highly altered to epidote or clinozoisite and sericite. Quartz forms interstitial strained crystals. Greenish-brown hornblende is typically rimmed by blue-green amphibole, and is partly altered to epidote and actinolite. Biotite is uncommon and is typically altered to chlorite (navy blue birefringence), and is often intergrown with hornblende. These rocks show strong deformational textures including strong undulatory extinction in quartz, bent and fractured crystals of plagioclase and hornblende, and stretched plagioclase.

Butler Peak pluton: A small oval-shaped stock of foliated granodiorite and leucotonalite forms Butler Peak along the eastern shore of Stephens Passage (fig. 4). Brew and others (1992) reported a U-Pb zircon age of 94 Ma for this pluton. It is partly surrounded by a narrow hornblende-hornfels aureole. The pluton is composed chiefly of foliated, medium-grained, hypido-granular garnet-bearing biotite granodiorite and leucotonalite which have a color index of 7 to 11. The rocks consist of plagioclase (45 to 69 percent), quartz (25 to 36 percent), K-feldspar (1 to 9 percent), and biotite (7 to 11 percent). The common accessory minerals are apatite, garnet, epidote, allanite, and ilmenite; titanite and sulfides were found in one sample. Plagioclase is commonly altered to muscovite and clinozoisite. Deformation and recrystallization have destroyed much of the twinning and zoning in plagioclase, although some oscillatory zoning remains. Quartz forms anhedral, strained, polycrystalline crystals or mosaics. Microcline occurs as intergranular or poikilitic crystals. Biotite is the chief mafic mineral, and it forms fine- to medium-grained shards that are fresh to partly altered to chlorite, muscovite, titanite and minor calcite. Primary epidote occurs as discrete, subhedral to euhedral, zoned crystals that form idiomorphic boundaries to biotite. Some epidote crystals contain cores of allanite. Garnet is found as euhedral inclusions and as discrete rounded and abraded crystals.

Taku Harbor Subbelt

Two oval-shaped stocks of Late Cretaceous age are located at Everett Peak and Arthur Peak along the eastern side of Stephens Passage in the southern part of the transect (figs. 4, 7B). These two plutons differ from plutons of the Grand Island subbelt by their high K-feldspar contents (table 6), absence of biotite, and presence of magnetite (Drinkwater and others, 1992). Both plutons exhibit strong planar fabric and moderately strong deformational textures indicative of mylonitic deformation. The Everett Peak pluton yielded a U-Pb zircon age of 86.7 Ma (Table 3).

Everett Peak pluton: The intrusion that encompasses the Everett, Webster, and Fillmore Peaks area (fig. 7B) consist of foliated, medium- to coarse-grained, porphyritic, epidote-bearing hornblende quartz monzodiorite. The pluton is approximately 5.5 by 5.7 km in size, has steeply-dipping concentric foliations and shows discordant intrusive contacts with the country rock. Although the pluton is compositionally homogeneous (table 6; fig. 8B), it varies texturally inward from a narrow plagioclase-porphyritic margin zone to a K-feldspar-porphyritic main phase

to a hornblende-porphyritic core zone. The mafic mineral abundance varies slightly, from less than 15 percent in the outer zone to greater than 20 percent in the central zone. Fine-grained streaky dioritic and granodioritic inclusions and schieren are common in the pluton and are aligned with the foliation. The pluton is cut by fine-grained felsic dikes.

The composition of the Everett Peak pluton is predominantly quartz monzodiorite (fig. 8B) with plagioclase (48 to 63 percent), K-feldspar (11 to 24 percent), quartz (7 to 20 percent) and hornblende plus epidote (15 to 22 percent) as the major constituents (table 6). Granodiorite, tonalite, and quartz diorite form minor lithic phases. The main phase of the pluton is distinguished by megacrysts of K-feldspar which are set in a hypidiomorphic-granular matrix of plagioclase, quartz, foliate tabular hornblende and epidote, and intergranular quartz and K-feldspar (fig. 9B). The core phase of the pluton consists of coarse-grained to phenocrystic, inclusion-rich, flow-aligned, tabular hornblende, fine to medium-grained plagioclase and quartz, and interstitial K-feldspar. Titanite, magnetite, apatite, zircon, and sulfides are the principal accessory minerals of both these major phases. Biotite is rare and is chiefly a secondary mineral after hornblende.

Plagioclase (An 33-36) forms subhedral, stout tabular to elongated crystals that show patchy and zonal alteration to sericite and clinozoisite, as well as patchy replacement by K-feldspar. It typically is well twinned and shows well-developed multiple zoning, which most commonly is oscillatory-normal type. Strained plagioclase crystals show patchy zoning and extinction.

K-feldspar is microcline and occurs as coarse-grained, anhedral, inclusion-rich crystals; blocky to stout tabular subhedral phenocrysts; and as intergranular crystals. The phenocrysts are inclusion-rich and microperthitic. K-feldspar is generally unaltered, but shows strained extinction. Tartan or cross-hatch twinning is well developed in granular and intergranular crystals.

Quartz forms intergranular, well-fractured, and strained crystals, and polycrystalline aggregates; less often, it forms stretched and strained granular crystals. It commonly shows trains of tiny inclusions.

The predominant mafic minerals are hornblende and epidote. Hornblende forms subhedral, elongated, tabular, brownish crystals that define the foliation of the rocks. It is typically twinned, pleochroic yellow brown to dark brown and greenish brown, and contains inclusions of titanite, magnetite, apatite, zircon, and biotite. Primary epidote occurs as discrete, subhedral, weakly pleochroic pale-green crystals that are commonly clustered or intergrown with hornblende. Biotite is rare and is found either as inclusions in hornblende or as secondary patches in hornblende.

Titanite is the most common accessory mineral and occurs in two primary phases. The most conspicuous phase is as discrete, medium-grained, euhedral, pleochroic gray-brown twinned crystals that typically exhibit fishtail or arrow-shaped forms. The other type of occurrence is as tiny, euhedral, equant, colorless to pale yellow-green crystals that occur as inclusions in plagioclase, K-feldspar, and hornblende.

Other commonly occurring accessory minerals include apatite, zircon, and opaque minerals. Apatite occurs as small (<0.5mm), discrete, euhedral crystals that commonly are clustered with mafic minerals, and as tiny euhedral inclusions in hornblende and plagioclase. Zircon is relatively scarce and occurs as tiny euhedral inclusions in hornblende and plagioclase. Primary opaque minerals are magnetite and sulfides. Magnetite forms subhedral equant-shaped inclusions, and sulfide granules typically form clots with magnetite.

Arthur Peak pluton: A small stock extends from Arthur Peak to the shores of Stephens Passage and Limestone Inlet. It is a foliated, medium-grained, leucocratic

(CI=5-17) body of altered and mylonitically deformed, porphyritic quartz monzodiorite; tonalite and quartz diorite form minor phases (fig. 8B). The oval-shaped intrusion is roughly 2.5 by 3.3 km in size, and has a discordant intrusive contact with the country rocks and a fine-grained aplitic border zone. The stock is cut by aplite dikes and contains fine-grained dioritic inclusions. Several outcrops show rusty staining and sulfide alteration. The rocks consist of megacrystic and phenocrystic K-feldspar in a foliated hypidomorphic granular mass of tabular plagioclase, hornblende, and epidote, and intergranular stretched quartz and K-feldspar.

The mineralogy and textures of the Arthur Peak pluton are similar to those of the Everett Peak pluton; plagioclase (50 to 64 percent), K-feldspar (2 to 24 percent), quartz (12 to 26 percent), and hornblende and epidote (5 to 17 percent) are the major constituents. Titanite, apatite, magnetite, and sulfides are the common accessory minerals, whereas zircon is rare. Plagioclase forms medium-to coarse-grained, subhedral, stout tabular crystals that show zonal alteration with cores of epidote-clinzoisite and margins and outer zones of sericite. Zoning and twinning have largely been obliterated in the plagioclase by alteration and mylonitic deformation. K-feldspar occurs as subhedral to euhedral, inclusion-rich phenocrysts and interstitial crystals of microcline. Hornblende forms subhedral, tabular, well-twinned crystals that are pleochroic in shades of brown and green. Granular aggregates of epidote are found in hornblende, but some well-formed subhedral epidote is also present. The accessory minerals apatite, titanite, magnetite, and zircon occur primarily as inclusions in hornblende, although titanite is also found as discrete euhedral crystals. Sulfides are scarce and are found with magnetite and hornblende.

Structure

The weak to strong foliation shown by the Grand Island group of plutons is defined by aligned tabular hornblende, plagioclase, epidote, and lamellar biotite. This foliation is steeply dipping (65-86 degrees) and parallels the contacts, and in three larger plutons it is concentric. Igneous textures are well preserved indicating that the foliation is primarily a result of magmatic flow. However, the foliation and degree of solid state deformation increases to the east and southeast towards Stephens Passage and Grand Island, whereas alteration appears to increase in the northern bodies where muscovite is more prevalent. The two smaller northern bodies show weaker foliation and more dominant igneous textures than the larger bodies to the southeast. This increase in deformational fabric towards the Coast Range megalineament suggest that the primary foliations in the plutons were affected and accentuated by a metamorphic-deformational episode during or just after emplacement.

The structural relations between the plutons and the enclosing country rocks indicate a record of several stages of deformation and metamorphism (Brew and others, 1989, 1990). The low-grade schist and phyllites of the Gravina overlap assemblage were deformed and metamorphosed prior to emplacement of the Grand Island group of plutons (Brew and others, 1990; Stowell and others, 1993), however, hornfel assemblages that rim the plutons indicate contact metamorphism from chlorite to kyanite plus staurolite facies (Stowell and others, 1993; Stowell and Menard, 1994). The hornfels aureoles and Gravina overlap assemblage were also overprinted by upper greenschist facies metamorphism that was associated with the emplacement of the Great tonalite sill (Brew and others, 1989, 1990; Stowell and others, 1993; Stowell and Menard, 1994) at about 70 to 60 Ma.

An oriented fabric is evident throughout all zones of the Everett Peak pluton. The foliation in the pluton is defined by aligned, thin to thick tabular hornblende and epidote, and less conspicuously by elongated plagioclase tablets. The more

deformed rocks have developed a nearly gneissic texture including bands of aligned K-feldspar phenocrysts. In map view, the foliation parallels the contact of the pluton and forms a concentric pattern of steep inward-dipping (60-90 percent) foliations. Prismatic hornblende forms a lineation that lies in the plane of foliation and plunges 60 to 80 degrees down dip. Locally (west side), the foliation conforms to the foliation of the adjacent country rock. Because igneous textures are still very evident and felsic dikes are undisturbed, the directional fabric which is largely discordant to the country rock fabric, is considered a primary magmatic feature related to late-synkinematic emplacement of the pluton. Mylonitic deformation may have continued briefly after crystallization.

Great Tonalite Sill Belt

Two segments of the Great tonalite sill belt, the Speel River pluton (Drinkwater and others, 1989) and Taku Inlet pluton (Drinkwater and others, 1990) occur within the transect area (fig. 4) and are described here (fig. 10). They are considered mostly Paleocene in age based on the K-Ar hornblende age of 60.5 Ma reported by Drinkwater and others (1992). Both plutons are part of the western subbelt of northwest-trending, steeply-dipping, thick, sheet-like foliated tonalitic intrusions (Ingram and Hutton, 1994). To the southeast, the Speel River-Fords Terror pluton is part of the Great tonalite sill (Brew and Grybeck, 1984) which was studied extensively in the Holkham Bay area by Hollister and others (1987) and Wood and others (1991). Brew and Grybeck (1984) reported a K-Ar minimum age of 66 Ma for the Speel River-Fords Terror pluton, and Stowell (1987) reported a $^{40}\text{Ar}/^{39}\text{Ar}$ hornblende age of 62 Ma for this pluton. The foliated granite, granodiorite, and leucotonalite of the Annex Lakes pluton (Drinkwater and others, 1990), which forms an eastern subbelt of the Great tonalite sill belt north of the transect, is briefly described in table 3 as a comparison to the western subbelt.

Western Subbelt

The Speel River and Taku Inlet plutons are tabular to thick sheet-like intrusions with concordant contacts; they dip steeply to the northeast. Both plutons are composed predominantly of tonalite (fig. 11), show a strong directional fabric (fig. 12), and exhibit very high magnetic susceptibilities (Drinkwater and others, 1992). The elongated Speel River pluton has a long axis that coincides with the trend of the regional foliation and the linear Great tonalite sill plutonic belt. A pervasive foliation, defined by northwest-striking aligned folia of tabular hornblende and lamellar biotite, is more intensely developed near the margins of the plutons and parallels the contact and regional foliation of country rocks (Drinkwater and others, 1989; Hutton and Ingram, 1992).

Speel River pluton: The Speel River pluton is a 6 to 8 kilometer-wide segment of the Great tonalite sill, that extends for 32 kilometers from just south of Taku Inlet to the Whiting River (fig. 4, 10). The pluton pinches out to the north, where the continuation of the Great tonalite sill is represented by the older Carlson Creek pluton (Drinkwater and others, 1990). To the south, the pluton appears to pinch out at the Whiting River but also shows a sharp contact with a granodiorite sill that separates the Speel River pluton from another segment of the Great tonalite sill belt. The nature of the contact zone and age progression of the three sills is unclear and has not been studied in detail, but it does indicate that contact zones between sills may be marked by thin granodiorite segregations or intrusions.

The Speel River pluton consists mostly of homogeneous, medium to coarse-grained, foliated biotite-hornblende tonalite (fig. 12A) with an average color index of 26, but varies locally from quartz diorite to granodiorite. Quartz diorite is more

common along the southwest margin, and leucocratic fine- to medium-grained granodiorite forms sill-like segregations or lenses in the pluton. The pluton is more deformed and gneissic in texture along the lower (southwest) margin (fig. 12b) than the rest of the body. Synplutonic mafic dikes are typically disrupted and deformed, but range from fairly coherent bodies in the central part of the pluton to separate inclusions in the marginal zones. Elongated mafic-rich inclusions and schlieren in the margin of the pluton are aligned parallel to intrusive contacts and regional foliation of the country rocks. Larger screens of country-rock schist and gneiss occur up to 800 meters in length and are elongated in the direction of the foliation and regional structure. Felsic dikes are typically undeformed and coherent, and range in composition from granite to quartz monzodiorite (Drinkwater and others, 1989); they generally trend along, or are parallel to, the northeast-trending cross joints.

Rocks of the Speel River pluton consist of subhedral plagioclase (50-63 percent), tabular hornblende and lamellar biotite (20-33 percent), anhedral granular and intergranular quartz (14-22 percent), and interstitial K-feldspar (0-3 percent). Titanite, apatite, and magnetite are the common-occurring accessory minerals; zircon is much rarer. Locally, particularly near the lower margin, biotite becomes more abundant than hornblende.

Plagioclase is of andesine composition (An₃₂₋₄₅) and forms subhedral, subequant to stout tabular crystals. It shows well-developed polysynthetic twinning and exhibits multiple concentric zoning of normal or oscillatory normal type. The plagioclase is generally fresh, but may show slight alteration to sericite and clinozoisite. It contains rare inclusions of apatite.

Quartz occurs as anhedral, subequant-shaped, strained crystals and as intergranular strained crystals and polycrystalline aggregates. In more deformed rocks, the quartz becomes more elongated or stretched.

K-feldspar is a minor constituent of most rocks and occurs as anhedral interstitial crystals of microperthitic orthoclase. Less frequently, it occurs as poikilitic masses which enclose hornblende, biotite, and plagioclase. It is generally strained.

Hornblende and biotite are the chief mafic minerals and are generally clustered in folia that define the conspicuous foliation of the rocks. Hornblende forms subhedral, pleochroic light-brown to brownish-green to green, tabular crystals. Crystals of hornblende are commonly twinned and are fresh to partly altered to epidote and opaque minerals. The hornblende contains inclusions of apatite, zircon, and magnetite. Pleochroic brown to reddish-brown biotite occurs as platy to lamellar crystals and aggregates. It is generally fresh but may show partial alteration to chlorite, titanite, and opaque minerals. Prehnite occasionally forms pods of sheaflike aggregates in biotite. Biotite typically contains inclusions of apatite and zircon.

The chief accessory minerals are magnetite, titanite, apatite, and zircon. Magnetite forms discrete euhedral to subhedral interstitial crystals and inclusions in mafic minerals. Titanite is locally common and occurs as euhedral flow-aligned crystals and as subhedral embayed and skeletal crystals. Apatite forms tiny euhedral inclusions and discrete subhedral crystals clustered with mafic minerals. Zircon is far less common than other accessory minerals, but is widespread in its occurrence as small euhedral inclusions in mafic minerals.

More-felsic rocks of the Speel River pluton consist of fine- to medium-grained, foliated hornblende-bearing biotite granodiorite. The rocks are strongly foliated to slightly banded with lamellar biotite forming streaky clusters and thin layers in the rocks. The rocks are also slightly porphyritic and alliotrimorphic granular in texture with plagioclase forming the coarser crystals. The common accessory minerals are allanite, magnetite, and apatite.

Taku Cabin Pluton: A small segment of the Great tonalite sill belt that is exposed north of the Speel River pluton along Taku Inlet has been described by Drinkwater and others (1990) as the Taku Cabin pluton (fig. 4). The pluton is very similar to the Speel River pluton in modal composition, petrographic characteristics, textures, and structure, but in contrast it contains a well-defined sill layer of allanite bearing hornblende-biotite granodiorite that has not been recognized in the larger Speel River pluton. This indicates that the Taku Cabin pluton is a composite pluton of at least three coalesced intrusive sheets. Modal analysis are given in table 7, and rock classification is depicted in figure 11. Rocks from the Taku Cabin pluton contain slightly more quartz and K-feldspar and less mafic minerals than rocks from the Speel River pluton.

Structure

The Speel River and Taku Cabin plutons exhibit a predominant northwest trending foliation that parallels the regional fabric and structure of the CMC. This foliation dips steeply (70-88 degrees) to the northeast (fig. 14) and is in accord with the regional foliation of the whole Great tonalite sill. Two sets of down dip lineations characterize these plutons (fig. 14). One set, that is defined by stretched inclusions and prismatic hornblende, has similar trend as the foliation and plunges steeply southeast. The other set of lineations is formed by prismatic hornblende and trends from north 20 to 30 degrees west and plunges 60-84 degrees north. The foliation is believed to have originated by both primary magmatic flow and solid-state deformation (Drinkwater and others, 1989) during synkinematic emplacement into an active contractional high-angle reverse shear zone (Hutton and Ingram, 1992; Ingram and Hutton, 1994).

Joint fractures are well developed in the Speel River and Taku Cabin plutons. Parallel and cross joints form the most predominant fractures (fig. 14), and they conform to the regional joint pattern (D.A. Brew, unpubl. data). Along the length of the Speel River pluton, the parallel joints trend from N 40 to 46 degrees W and dip approximately 71 degrees northeast (fig. 14). A complementary joint set dips from 24 to 50 degrees to the southwest. Cross joints are the most conspicuous fractures in the Speel River pluton and occur as a conjugate set; they are generally very uniform in orientation and spacing. On an average, the cross joints trend from N 50-52 degrees E and dip 80-81 degrees southeast (fig. 14) and the complementary set shows similar trend but dips 65 to 75 degrees northwest. Felsic dikes or segregations trend along or parallel to the cross joints. The trace of these joints in aerial view extends across the width of the pluton and crosses its contact into the country rock.

The emplacement of the Great tonalite sill is believed to involve multiple intrusions (Hutton and Ingram, 1992; Ingram and Hutton, 1994). The nearly 1000 meter-wide internal granodiorite sill in the southernmost part of the transect indicates the presence of separate intrusive bodies. The 150 to 300 meter-wide granodiorite sill layer in the Taku Cabin pluton indicates that this pluton was emplaced as three or more separate intrusive sheets. The presence of granodiorite segregations in the Speel River pluton may also be evidence for multiple sheets. This is in accord with the findings of Ingram and Hutton (1994) who determined that other plutons of this belt to the south and north of the transect consist of multiple inclined sheets, each separated by screens of metasedimentary rocks. The occurrence of screens of schist in the Speel River pluton indicates the presence of four to six separate intrusive sheets.

Coast Mountains Belt

The Turner Lake batholith is a large continuous mass of granitic rocks, east of the Great tonalite sill belt (fig. 4), that forms a segment of the Coast Mountains belt

along the transect. Mapping has yet to determine the exact number of plutons that occupy this part of the Coast Mountains belt, thus large masses are delineated as plutonic units or composite plutons. Rocks of the Turner Lake batholith range from granite to tonalite in composition and exhibit moderate to high magnetic susceptibility (Drinkwater and others, 1992). On the basis of lithology, the batholith can be divided into two subbelts; the western subbelt which consists of large massive plutons and composite plutons of predominantly granodiorite composition, and the eastern subbelt which consists of undivided massive granite and granitic stocks (Drinkwater and others, 1992).

Western Subbelt

Three large masses of granodiorite and two heterogeneous stocks comprise the western subbelt of the Turner Lake batholith (fig. 4, 15). These masses occupy the heart of the transect area and are mapped as plutonic units based on modal composition, textures, and magnetic susceptibility. These plutonic units are subequant to subrectangular in plan and show discordant to locally concordant intrusive contacts. They are well-jointed intrusions that are composed of largely homogeneous and massive textured rocks of granodioritic composition (fig. 16). Locally, near their margins, they exhibit a weak foliation and are texturally heterogeneous. Although no internal contacts have been found in these units, they are considered as composite plutons based on variations in lithology and textures across the bodies. Modal analyses are given in tables 8–10.

Southern unit: The southern part of the Turner Lake batholith (fig. 4) is a coherent homogeneous body (fig. 16A) that reaches 22.5 kilometers in length and varies between 5 and 13 kilometers in width (fig. 15A). The rocks are weakly foliated and finer grained near the margin of the body. Stretched inclusions and schlieren also define a weak foliation near the margins of this body. The body has mostly discordant intrusive contacts but locally shows concordant contacts with the country rock. No internal contacts have been found which indicates that the body may be a single intrusion. The unit is composed largely of homogeneous, massive, medium-to coarse-grained, biotite-hornblende granodiorite (fig. 17A) but varies from biotite-hornblende tonalite, near the margins, to biotite granodiorite which is common in the southern most part of the body. Leucocratic dikes are common and consist largely of fine-grained, garnet-bearing biotite aplite of granodiorite to granite composition (fig. 16A). Most dikes trend NE–SW and dip 65 to 90 degrees.

The most common rock phase is a hypidiomorphic equigranular sphene-bearing biotite-hornblende granodiorite, with a color index of 13 to 20. Locally the rocks are slightly porphyritic. The rocks consist of plagioclase (44–55 percent), quartz (21–31 percent), K-feldspar (4–12 percent), and mafic minerals (13–20 percent). Titanite is the most common accessory mineral; magnetite, apatite, and zircon are less common but widespread in their occurrence.

Plagioclase (An_{37–43}) forms subhedral, subequant-shaped, fresh to partly altered crystals that exhibit strong multiple zoning. The cores and interior parts of the plagioclase typically are replaced by sericite and clinozoisite. Zoning is most commonly of oscillatory normal type. Inclusions of apatite, magnetite, and hornblende, although uncommon, occur in the core and interior zones of plagioclase.

Felsic minerals make up 25 to 40 percent of the rocks (table 8). Quartz forms anhedral granular to intergranular strained crystals. K-feldspar occurs most often as intergranular and poikilitic crystals of orthoclase. K-feldspar oikocrysts enclose plagioclase, hornblende, biotite, and magnetite. Locally, K-feldspar forms medium-grained granular crystals.

The primary mafic minerals are hornblende and biotite. Hornblende forms stout tabular, pleochroic light-brown to brownish-green to green crystals and is fresh to partly altered to epidote, chlorite, and granular titanite. It is typically twinned, and contains inclusions of apatite, magnetite, biotite, and zircon. Biotite occurs as subhedral, pleochroic light- to dark-brown ragged columns, plates, and shards. It is orange-brown in some sections and may be partly altered to chlorite and granular titanite. Inclusions of apatite, magnetite, and zircon commonly occur in the biotite.

The common accessory minerals are magnetite, titanite, apatite, and zircon. Allanite occurs in the biotite granodiorite of the southern border zone. Magnetite forms small (<.5 mm) euhedral inclusions in mafic minerals, and subhedral interstitial crystals, and discrete crystals clustered with mafic minerals. Titanite is found as discrete euhedral, pleochroic gray-brown crystals. Apatite occurs as euhedral inclusions in mafic minerals and as subhedral intergranular crystals. Zircon is uncommon and forms euhedral inclusions in mafic minerals.

Central unit: A large subrectangular shaped igneous body occupies the middle part of the Turner Lake batholith; it is roughly 22–26 kilometers in long dimension and 13 kilometers in width (fig. 15B). The central unit of the Turner Lake batholith is largely a homogeneous, massive to weakly foliated, leucocratic body that is distinguished from other units of the Turner Lake batholith by its very high magnetic susceptibility (Drinkwater and others, 1992). The body has concordant to discordant intrusive contacts and the rocks become more heterogeneous or migmatitic near the margins. Slight changes in lithology and joint patterns suggest that the central unit is probably a composite pluton, although internal contacts have not been mapped.

The rocks range in composition from hornblende-biotite tonalite to hornblende-biotite granite, but the predominant rock type is a massive, medium- to coarse-grained, equigranular titanite-bearing biotite-hornblende granodiorite with a mafic index of 8–16 (fig. 16B, 17B). Slightly porphyritic rocks contain phenocrysts of plagioclase and coarse-grained quartz. Biotite and hornblende are about equal in abundance. Conspicuous large titanite crystals (up to 3 mm) are widespread throughout the central unit. Mafic inclusions are typically rounded and occur up to several meters in size. Aplite and pegmatite dikes and veins up to 10 cm wide are widespread but generally are uncommon.

The rocks of the central unit consist mainly of medium- to coarse-grained subhedral plagioclase (40–58 percent), anhedral quartz (23–35 percent), and euhedral to subhedral hornblende and biotite (8–16 percent), and interstitial to poikilitic K-feldspar (5–17 percent). Mafic minerals are generally coarse grained and typically intergrown or clustered. The commonly occurring accessory minerals are titanite, magnetite, apatite, and zircon. Clots of magnetite and apatite are common in the central unit, and some of these clots contain anhedral titanite and zircon crystals. Myrmekite commonly occurs between crystals of plagioclase and K-feldspar, but is not abundant.

Plagioclase occurs as subequant to stout tabular crystals of sodic andesine (An_{30–37}). The plagioclase is generally fresh but may show minor alteration to sericite and clinozoisite. It exhibits normal and oscillatory-normal zoning, sometimes with reversed-zoned overgrowths. Some crystals of plagioclase have anhedral or rounded inclusions (quartz, albite, and K-feldspar droplets) and mottled (recrystallized) interiors.

Quartz forms anhedral granular and intergranular strained crystals. It commonly shows strong undulatory extinction, deformational banding, and coarse subgrain development. It typically occurs in aggregates and occasionally forms subpoikilitic crystals that formed by margin recrystallization or overgrowths.

K-feldspar forms interstitial to coarse-grained poikilitic crystals of microperthitic orthoclase. It is typically strained, and oikocrysts engulf or partly engulf crystals of plagioclase, quartz, biotite, hornblende, and titanite.

The major mafic minerals are hornblende and biotite, although magnetite is also relatively abundant. Pleochroic light-brown to brownish-green to green hornblende forms euhedral to partly resorbed, twinned, and elongated prismatic to stout tabular crystals. It is generally fresh, but may be partly altered to titanite, magnetite, and epidote or light green amphibole. Hornblende hosts inclusions of apatite, zircon, and magnetite. Biotite occurs as subhedral to euhedral platy or columnar crystals and lamellar aggregates. It is pleochroic light brown to dark brown where fresh, but it is orange to reddish brown where oxidized. Biotite shows minor alteration to chlorite, titanite, and opaque oxides. Inclusions of apatite, magnetite, and zircon are common. Magnetite is relatively common and widespread in rocks of the central unit. It forms small euhedral to subhedral equant crystals as inclusions, interstitial fillings, and as aggregates clustered with other mafic minerals.

The common accessory minerals are titanite, apatite, and zircon. Allanite is rare and is found in rocks of more granitic composition. Titanite is the most commonly occurring and abundant accessory mineral of the central unit. It forms euhedral, pleochroic gray to brown, twinned crystals that occur as typical diamond- and wedge-shaped forms. The titanite is generally unaltered, and it contains inclusions of apatite and magnetite. Apatite occurs in three distinct forms; 1) as tiny euhedral inclusions, 2) as subhedral interstitial crystals, and 3) as discrete subhedral crystals clustered with mafic minerals. Zircon forms small euhedral and subhedral (rounded) inclusions in biotite, hornblende, and plagioclase, and less often it forms discrete interstitial crystals. Clots of magnetite, apatite, and zircon are found either with or near mafic minerals.

A heterogeneous, mafic-rich granitic phase occurs within the central unit; it trends north northeast and divides rocks of similar granodiorite compositions and textures to the east and west. The granitic phase or body contains coarse-grained to phenocrystic K-feldspar, allanite, and relict orthopyroxene that has rims of colorless, polysynthetic twinned cummingtonite. The nature of this porphyritic granitic phase is uncertain because no contacts have been found during mapping of the area. It may represent either a separate pluton or a wide, heterogeneous contact zone between plutons of similar composition.

Northern unit: The northern part of the Turner Lake batholith, within the transect, is a large irregular-shaped body (fig. 3) somewhat elongated for 16 kilometers in the northwest direction; it ranges up to 12 kilometers in width. It is largely a massive to weakly foliated, leucocratic, medium- to coarse-grained body that ranges in composition from granodiorite to granite (table 10; fig. 16C). Rocks become stronger foliated or heterogeneous textured near the margins of the body. Aplite dikes, up to one meter wide, are common. Inclusions are generally uncommon and consist of rounded and unoriented fine-grained mafic-rich quartz diorite; some are porphyritic. Several lithologic phases make up the northern unit. The most common rock is a homogeneous, massive, porphyritic to seriate, medium- to coarse-grained hornblende-biotite granodiorite (fig. 17C), that has a color index of 3-12. In porphyritic rocks, K-feldspar, plagioclase and less commonly, quartz form phenocryst. Most of the main phase rocks are K-feldspar porphyritic and allanite-bearing, but rocks of the southwest part of the northern unit are predominantly massive, seriate-textured, hornblende-bearing biotite-microcline granodiorite. Plagioclase-porphyritic rocks are more common in the northern part of the body. An oval-shaped core zone of massive, slightly porphyritic biotite granite outcrops just north of the headwaters of Davidson Creek. In general, rocks of this unit are

distinguished from other units of the western subbelt by their inequigranular textures, fine-grained mafic minerals, and the presence of coarse-granular to phenocrystic K-feldspar.

Rocks of the northern unit consist of variable amounts of plagioclase (38–50 percent), K-feldspar (12–25 percent), quartz (22–37 percent), and mafic minerals (3–12 percent), (table 10) and they are classified as granodiorite or granite (fig. 16C). Most rocks are composed of medium- to coarse-grained crystals and phenocrysts of plagioclase and K-feldspar, medium- to coarse-grained anhedral quartz, and fine- to medium-grained intergranular hornblende and biotite. Mafic minerals typically are clustered or intergrown in aggregates. The common accessory minerals are allanite, apatite, titanite, zircon, and magnetite. Sulfides occur locally, particularly in rocks of the north-central part of the body.

Plagioclase forms subhedral, subequant to stout tabular, strongly zoned crystals of calcic oligoclase and sodic andesine (An_{26–32}). It is generally fresh, but may show partial alteration to sericite and epidote minerals. Crystals of plagioclase commonly exhibit multiple normal or oscillatory-normal zoning, some crystals have albitic overgrowths, and some have mottled interiors with rounded inclusions of quartz and K-feldspar.

K-feldspar occurs as medium- to coarse-grained anhedral crystals and subhedral phenocrysts of microperthitic orthoclase, and also as interstitial crystals of microcline. The coarser grains and phenocrysts typically exhibit Carlsbad twinning. Microcline predominates in rocks of the southwest part of the body.

Quartz forms anhedral crystals with equant to subequant shapes. It also occurs as intergranular crystals, and locally, it forms subhedral phenocrysts. It is typically strained, fractured, and commonly exhibits recrystallization of its margins giving it a subpoikilitic appearance. Trains of tiny dark inclusions commonly occur in the quartz.

The primary mafic minerals are biotite and hornblende, which occur as subhedral intergranular crystals and crystal aggregates; locally, they are found as coarser-grained, discrete euhedral crystals. Biotite forms pleochroic light- to dark-brown, stout rectangular plates and columnar-shaped crystals, and oxidized reddish or orangish-brown hexagons. It is generally fresh, but some crystals show minor alteration to chlorite, granular titanite, and opaques. Hornblende forms stout prismatic to elongated crystals that are pleochroic light greenish brown to brownish green to green. It is fresh to partly altered to granular opaques, titanite, and epidote, and it is typically partly resorbed and corroded. Inclusions of apatite, zircon, and magnetite are common in both biotite and hornblende.

Of the commonly occurring accessory minerals, allanite is the most conspicuous in rocks of the northern unit because it is found as relatively large (up to 2 mm), euhedral dark-brown crystals. The stout prismatic crystals of allanite are pleochroic light brown to dark reddish brown, are typically twinned, and some contain thin rims of epidote. Apatite occurs as small (< .5 mm) euhedral inclusions, as discrete intergranular crystals (up to 1 mm), and clustered with mafic minerals. Titanite occurs primarily as anhedral to subhedral interstitial crystals and intergrowths with biotite and hornblende. Zircon forms small (< .3 mm) euhedral to subhedral inclusions in biotite and hornblende, and in overgrowths of plagioclase; less commonly, it is found as discrete crystals clustered with apatite and magnetite near mafic aggregates. Magnetite occurs as euhedral to subhedral equant inclusions and interstitial crystals.

Eastern Subbelt

Rocks of the eastern subbelt are divided into an eastern unit of undivided granite, and two granitic stocks (fig. 4). The main intrusive mass has been mapped (fig. 18A) as undivided massive, leucocratic, medium- to coarse-grained hornblende-

biotite granite. Exposures of fine- to medium-grained, biotite granite occur along the USA-British Columbia border and indicate that more than one pluton may form this granitic mass. The granite shows discordant to locally concordant intrusive contacts with the country rock, but its contact with the granodiorite units of the western subbelt is poorly defined because much of the contact zone is concealed under either river valleys or glaciers. The granite is cut by small aplite dikes and more rarely by mafic dikes. Dioritic inclusions occur up to 35 cm in size. Two, and possibly more, granitic stocks of presumed middle Tertiary age occur within the transect area. The two stocks near Wright Glacier (fig. 4) are of different composition and texture. The southern stock is ellipsoidal-shaped in plan, and has discordant intrusive contacts to the country rocks. The contact between the stock and the undivided granite of the eastern subbelt is concealed under glaciers, but the stock's finer-grain size and nonporphyritic texture contrast it with the much coarser-grained porphyritic granite of the eastern subbelt of the Turner Lake batholith. The northern body (Wrights River stock) is irregular shaped and more heterogenous in composition (fig. 16) and texture than the southern stock.

Undivided granite: The predominant rock type mapped as undivided granite (fig. 18A) is a homogeneous, massive, medium- to coarse-grained, porphyritic to seriate hornblende-biotite granite (fig. 19A) that has a color index of 4-13. Locally, the rocks vary in texture to allotrimorphic to slightly hypidiomorphic granular. The rocks consist primarily of coarse-grained and phenocrystic K-feldspar (22-38 percent), medium to coarse-grained plagioclase (26-37 percent) and quartz (26-34 percent), and intergranular biotite and hornblende (4-13 percent). Mafic minerals are fine-grained in most rocks, with biotite being more abundant than hornblende; in some rocks hornblende is absent. Mafic minerals are typically clustered around phenocrysts of K-feldspar. The rocks contain conspicuous brown allanite crystals and locally the rocks are titanite-bearing. The other common accessory minerals are apatite, magnetite, and zircon.

Plagioclase forms anhedral to subhedral zoned crystals of calcic oligoclase (An₂₆₋₂₉). The plagioclase is generally fresh or partly altered to sericite. It exhibits normal or oscillatory-normal-type zoning with albitic rims.

Felsic minerals make up as much as 70 percent of the rocks. K-feldspar occurs as subhedral to anhedral coarse-granular to phenocrystic crystals of perthitic orthoclase. It is typically inclusion-rich, and exhibits simple Carlsbad twinning. Quartz forms anhedral, fractured, subequant-shaped crystals.

Mafic minerals (biotite and hornblende) occur as fine-grained, intergranular crystals and aggregates, and in some rocks they are clustered in trains around K-feldspar phenocrysts. Biotite forms subhedral to anhedral, tabular to shard-like crystals that are pleochroic light to dark brown or reddish brown. It is generally fresh or partly altered to chlorite and granular titanite. Inclusions of zircon and apatite are common. Hornblende occurs as subhedral to anhedral crystals that are typically corroded; where fresh, it is pleochroic light brown to greenish brown to brownish green, but where altered it consist of pale green amphibole and or granular titanite and epidote. In some cases, it is replaced by colorless to pale cummingtonite. In some sections the cummingtonite appears to be a primary mineral. Relict orthopyroxene with rims of hornblende also occurs but is uncommon.

The accessory minerals allanite, apatite, zircon, and magnetite occur in most rocks of the eastern unit; titanite occurs locally. Allanite is the most conspicuous of the accessory minerals because it forms relatively large (> 1mm), euhedral, pleochroic light- to dark reddish-brown crystals. It is typically twinned; zoned crystals exhibit euhedral growth layers. Zircon forms euhedral to anhedral inclusions in biotite and plagioclase; it is commonly metamict in biotite. Apatite

occurs as numerous tiny (<0.1mm) euhedral inclusions in biotite, hornblende and plagioclase. Magnetite is relatively scarce and occurs as subequant-shaped crystals clustered with mafic minerals. Primary titanite is uncommon in these rocks and, where present, is found as anhedral to subhedral interstitial crystals or as intergrowths with mafic minerals, and thus it appears to be a late-magmatic mineral.

Middle Tertiary stocks: The rocks of the southern Wrights Glacier stock consist of homogeneous, massive, fine- to medium-grained, seriate to allotriomorphic granular hornblende-biotite granite (figs. 19B, 20B). The constituent minerals (table 11) are K-feldspar (24-33 percent), plagioclase (32-37 percent), quartz (27-35 percent), and biotite and hornblende (3-10 percent). The accessory minerals are allanite, apatite, zircon, and magnetite, of which allanite is the most conspicuous in hand specimen.

Plagioclase forms medium-grained, subhedral to anhedral, stout rectangular and lath-shaped crystals of oligoclase (An₂₄₋₂₇). It is generally fresh or partly altered to patches and mesh-like aggregates of sericite. Typical features include multiple normal or oscillatory normal zoning, and anhedral (melt) inclusions of K-feldspar and quartz which occur along cleavages.

Felsic minerals comprise as much 64 percent of the rocks. K-feldspar forms medium- to locally coarse-grained, subhedral, inclusion-rich crystals of microcline. It is generally strained, micropertitic, and exhibits faded tartan twinning of microcline. Quartz is found as anhedral granular and intergranular crystals; it is commonly strained and well-fractured.

Biotite and hornblende occur as fine-grained, anhedral to subhedral intergranular crystals. They are commonly clustered along the borders of K-feldspar and plagioclase. Biotite forms fresh to partly altered, pleochroic brown, ragged column- and shard-shaped crystals and reddish to orange brown hexagons. Alteration products include chlorite, titanite and opaque minerals. Inclusions of zircon, apatite, and magnetite are common. Hornblende is partly embayed and resorbed and pleochroic in shades of greenish brown and brownish green. It may show minor alteration to granular titanite and opaque minerals, and contains inclusions of apatite, magnetite, and biotite.

Of the accessory minerals, allanite is the most prevalent; it forms discrete, euhedral to subhedral, pleochroic brown to dark-reddish-brown crystals. It is typically clustered with other mafic minerals, and occasionally shows minor alteration to epidote. Apatite and zircon form tiny euhedral inclusions in mafic minerals. Magnetite occurs as subequant-shaped inclusions and as interstitial crystals.

The Wrights River stock is more varied in composition and texture than the more uniform Wrights Glacier stock. The stock ranges from granite to quartz diorite in lithology (fig. 24) and has an average modal composition of quartz monzodiorite. Texturally, it varies from seriate or slightly porphyritic to hypidiomorphic granular; the color index ranges from 14 to 36. Characteristic of these rocks is the presence of cumingtonite with cores of relict orthopyroxene.

Jointing

Mega-joints and lineaments in the Turner Lake batholith cross contacts and largely follow the regional joint pattern. The synthesis of primary-appearing prominent joint sets (fig. 22) in the three granodiorite units of the western subbelt shows a predominant pair of northeast-southwest trending and northwest-trending joint sets that conform to the regional joint pattern. In the southern and central units, the predominant northeast-southwest-trending conjugate set of cross joints dip steeply to the southeast (69-73 degrees) and northwest (75-76 degrees). In the northern unit, similar trending cross joints dip approximately 79 degrees southeast. The northwest-trending parallel joints conform to the regional fabric and structure,

and dip from 70 to 78 degrees to the northeast. Less prominent joints have more varied trends between the three units indicating that they may be local or primary joints.

In the eastern subbelt of the Turner Lake batholith, the prominent joint sets trend more north-south and east-west than the major joint traces in the western subbelt (fig. 22) indicating a possible change in the regional stress field during or prior to cooling of the granite. These joints cross contacts and conform to joint patterns in the adjacent country rock.

Miscellaneous Plutons

Three small intrusive bodies occur between the northern and southern units of the western subbelt (fig. 4). The nature and age of the two dioritic bodies is unclear; they may either be older relict plutons of Jurassic or Cretaceous age, or more mafic phases of the Turner Lake batholith. The nature and age of the granite body at the head of Turner Lake are also uncertain because its contacts have not been mapped or studied in detail. The outer parts of the granite are finer grained indicating a margin, and the body separates equigranular granodiorite of the central unit of the western subbelt from a large block of migmatitic gneiss.

The granite body consists largely of massive, medium- to coarse-grained, porphyritic to seriate hornblende-biotite granite (fig. 24). Plagioclase comprises 36 to 43 percent of the rocks (table 12) as subhedral, stout tabular or blocky crystals of calcic oligoclase (An₂₇₋₃₂). It typically exhibits oscillatory or irregular multiple zoning with clear overgrowths of albitic plagioclase, and it hosts inclusions of apatite, hornblende, and magnetite. K-feldspar makes up 23-31 percent of the rocks and occurs as medium- to coarse-grained, subhedral, inclusion-rich crystals and phenocrysts, and as intergranular or poikilitic crystals. It is typically twinned, strained, and microperthitic. Quartz varies in abundance from 23 to 31 percent and forms medium- to coarse-grained, anhedral, strained, and well-fractured crystals. Biotite and hornblende comprise less than 10 percent of the rocks, and they occur as fine- to medium-grained, intergranular crystals. Biotite is more common than hornblende and forms pleochroic light- to dark-brown or reddish-brown, columnar- and platy-shaped crystals. It is fresh to partly altered to chlorite and granular titanite and opaque minerals. Hornblende occurs as subhedral, partly resorbed, greenish crystals that, in some rocks, are intergrown with pale-green to colorless cummingtonite.

The easternmost dioritic body is largely concealed beneath a glacier, but exposures of it are found along the southeast and northwest edge of the glacier. Visible contacts between it and the central unit of the western subbelt are not well-exposed, but a gradational contact was observed at one locality in the southeast part. Outcrops are cut by felsic dikes and show zones of iron-staining. The body consists mostly of weakly foliated, medium-grained hornblende-biotite quartz diorite with a color index of 20-30, and biotite-hornblende diorite with a color index of 40-50. Most rocks contain parallel-aligned, subhedral tabular plagioclase which forms an igneous foliation not apparent in hand sample. Most of the rocks show intergranular or poikilophitic textures in which interstitial or poikilitic crystals of biotite, hornblende, and minor quartz and K-feldspar fill the interstices between plagioclase crystals. Magnetite is relatively common and forms small, discrete, euhedral, equant-shaped crystals and interstitial subhedral crystals. Titanite, apatite, and zircon are other commonly occurring accessory minerals in these rocks.

The body of quartz diorite, north of Turner Lake, forms a large, steep hillside at the head of Davidson Creek. The body is largely a foliated, heterogeneous, medium-grained mass of quartz diorite. Internal foliations trend northeast, but the contacts of this body are either concealed or unaccessable. Outcrops are cut by 2- to 50-centimeter thick, fine-grained, leucocratic dikes, and by pegmatitic dikes. The rocks,

Table 1. Major plutonic belts and subbelts of the Coast Mountains complex within the Taku Inlet transect, southeastern Alaska

Belt	Subbelt	Plutons	Main rock types	Age
Admiralty- Revillagigedo belt	Grand Island subbelt ----	Glass Peninsula stocks; Grand Island pluton; Irving Peak pluton; Butler Peak pluton	Quartz diorite; Tonalite; Diorite; Granodiorite	Late Cretaceous
	Taku Harbor subbelt ----	Everett Peak and Arthur Peak plutons	Quartz monzodiorite	Late Cretaceous
Great tonalite sill belt	Western subbelt -----	Speel River pluton and Taku Cabin pluton; Carlson Creek pluton	Tonalite, quartz diorite; Tonalite, granodiorite; Quartz diorite, tonalite	Early Tertiary Late Cretaceous
	Eastern subbelt -----	Annex Lakes pluton	Granodiorite, granite, and leucotonalite	Early Tertiary
Coast Mountains (Turner Lake batholith) belt	Western subbelt -----	Northern, central, and southern units; Tease Lake stocks	Granodiorite, and granite; Quartz monzodiorite	Tertiary (Eocene)
	Eastern subbelt -----	Undivided granite unit; Wright Glacier stock	Granite; Granite, granodiorite	Tertiary (Eocene) Late(?) Tertiary

Table 2. Summary of Isotopic Age Information for Plutons from the Taku Inlet Transect

Body	Sample no.	Dating Method	Mineral	Age (Ma)	Reference
Glass Peninsula stocks	76AF017	K-Ar	Hornblende	90.1	Brew, unpub. data
Everett Peak pluton	87RK143	U-Pb	Zircon	86.5	Brew, unpub. data
Butler Peak pluton	84AF010	U-Pb	Zircon	94.0	Brew, unpub. data
Speel River pluton	74DB426	K-Ar	Biotite	50.8	Drinkwater and others (1989)
			Hornblende		Drinkwater and others (1989)
Tease Lake stock	75SJ425	K-Ar	Biotite	50.7	Brew, unpub. data
			Hornblende	51.7	Brew, unpub. data
Turner Lake batholith	82GS111	U-Pb	Zircon	50.0	Gehrels and others (1984)
Flat Point pluton	82GS112	U-Pb	Zircon	60.0	Gehrels and others (1984)

Table 3A. K-Ar ages and analytical data for plutons associated rocks of the Taku Inlet transect.

Sample	pluton or unit	Mineral	K2O (wt. pct.)	40Ar rad 10-10 mol/gm	40Ar rad (percent)	Age (Ma)
76AF017	Glass Peninsula stocks	Hornblende	1.56	2.1087	88.5	90.1 + 2.6
75SJ425	Tease Lake stock	Hornblende	1.07	0.8072	85.0	51.7 + 3.0
		Biotite	9.41	6.9720	67.0	50.7 + 3.5
76DB015	Western metamorphic belt	Biotite		6.9440	88.6	54.3 + .95
75SJ422	Western metamorphic belt	Hornblende	0.18	0.1524	35.0	57.7 + 3.5
74DB426	Speel River pluton	Hornblende	1.05	0.9294	62.0	60.5 + 1.8
		Biotite	8.04	5.9670	88.0	50.8 + 1.5

Table 3B. U-Pb isotopic ages and analytical data for plutons of the Taku Inlet transect area.

Pluton	Sample no.	Concentrations		Isotopic Pb compositions			Isotopic Ratios (%)			Apparent Ages (Ma)		
		U ppm	Pb ppm	206/204	206/207	206/208	206/238	207/235	207/206	206/238	207/235	207/206
Everett Pk	87RK143	427.1	5.4	5719	19.79	27.4	0.01349	0.08923	0.04795	86.4	86.8	96.7
Butler Pk	84AF010	1477	19.5	9381	20.2	31.2	0.01463	0.09669	0.04747	93.6	93.7	96.6

Table 4. PETROGRAPHIC CHARACTERISTICS OF GRANITOIDS FROM SUBBELTS OF THE TAKU INLET TRANSECT AREA

Feature	Admiralty-Revillagigedo Belt		Great Tonalite Sill Belt		Coast Mountains Belt	
	Grand Island subbelt	Taku Harbor subbelt	Western subbelt*	Eastern subbelt	Turner Lake batholith western subbelt	Turner Lake batholith eastern subbelt
Rock type	quartz diorite, tonalite and granodiorite	quartz monzodiorite	tonalite, quartz diorite	granodiorite, leucotonalite	granodiorite	granite
Texture	foliated, gneissic, and inequigranular	foliated, porphyritic	foliated, equigranular	foliated, inequigranular to heterogeneous	massive, porphyritic to equigranular	massive, porphyritic
Major mafics	hornblend, biotite,	hornblende, epidote	hornblende, biotite	biotite, hornblende	hornblende, biotite	biotite, hornblende
Major acces.	epidote, garnet, sphene, sulfides	sphene, magnetite, apatite	magnetite, sphene, apatite	magnetite, sphene, allanite	sphene, allanite, & magnetite	allanite, apatite, magnetite
Color Index	10 to 35	14 to 23	17 to 35	5 to 25	5 to 18	4 to 13
Plagioclase %	45 to 78	48 to 64	50 to 62	40 to 60	38 to 58	26 to 37
Quartz %	10 to 30	07 to 20	15 to 25	10 to 30	21 to 37	26 to 35
K-Feld. %	0 to 9	11 to 25	0 to 4	02 to 20	5 to 25	22 to 38
K-Feld form	interstitial	granular/phenocrystic	interstitial	interstitial to granular, or phenocrystic	interstitial/poikilitic to granular	phenocrystic
Plagioclase	Subhedral-euhedral, strong multiple zoning strongly altered	Subhedral, multiple normal zoning, partly altered	Subhedral, moderate strong multiple zoning, partly altered	Subhedral, weak to moderate zoning	Subhedral, multiple normal zoned, partly altered	Anhedral-subhedral, moderately zoned, weakly altered
An %	n.d.	33 to 36	34 to 45	28 to 38	27 to 40	26 to 29
Sphene	Euhedral, clustered with mafic minerals	Euhedral, discrete grains	Euhedral, inclusions & flow aligned grains	Intergranular to discrete euhedral grains	Euhedral to subhedral discrete grains	Anhedral/subhedral Interstitial
Notable features	Euhedral zoned epidote with cores of allanite; rounded garnet; lacks magnetite	Primary epidote; brown hornblende; K-feld phenocryst	Much magnetite; coarse-grained flow aligned hornblende	Heterogeneous; phenocrystic K-feldspar	Magnetite-apatite clots; large allanite & sphene grains	Phenocrystic K-feldspar; allanite; fine-grained mafic minerals

Table 5. Modal analyses on samples of plutonic rocks from the Grand Island subbelt

<i>Glass Peninsula stocks</i>								
Sample no	Plag	Qtz	K-feld	Mafics	hornblende	biotite	Accessory	An %
05	67.8	19.1	0.0	13.1	uncommon	minor	sp, ga, ep	n.d.
07	61.3	21.3	5.4	12.0	minor	uncommon	ga, sp, ap, ep	n.d.
08	58.7	29.4	3.4	08.5	uncommon	trace	sp, ap, ep, ilm, su	n.d.
09	49.5	33.3	5.3	11.9	uncommon	minor	sp, ga, ap, ep, su	n.d.
10	77.8	09.2	0.3	12.7	common	trace	sp, ap, ep, ilm	n.d.
16	57.5	22.6	6.7	13.2	trace	uncommon	ga, ap, sp, ilm	n.d.
01	64.2	22.1	0.4	13.3	minor	common	ga, sp, ap, ep, su	n.d.
02	78.0	08.1	0.0	13.9	minor	uncommon	ga, sp, ap, ep, ilm	n.d.
03	72.6	13.2	0.0	14.2	common	minor	sp, ap, al, ep, su	n.d.
04	75.3	11.6	0.0	13.1	uncommon	minor	ga, sp, ap, su	n.d.
15	77.6	11.0	0.0	11.4	uncommon	minor	sp, ap, ep, su	n.d.
14	81.3	07.9	0.0	10.8	uncommon	minor	sp, ap, al, ep, su	n.d.
13	76.6	08.7	0.0	14.7	common	minor	sp, ap, ep, su	n.d.
11	53.1	16.5	8.9	21.5	common	minor	sp, ap, ep, su	n.d.
12	68.3	14.3	4.4	13.0	common	minor	sp, ap, ep, su	n.d.
06	72.0	16.0	0.0	12.1	common	minor	sp, ap, ga, su	n.d.
average	68.2	16.5	2.2	13.1				
<i>Grand Island pluton</i>								
Sample no	Plag	Qtz	K-feld	Mafics	Hbl	Bio	Accessory	An %
21	70.3	14.3	0.0	15.4	common	trace	sp, ap, ep, ilm	n.d.
22	57.8	23.3	3.0	15.9	common	minor	sp, ap, al, ep, su	n.d.
24	54.4	11.0	0.1	34.5	common	minor	sp, ap, ep, su	n.d.
25	48.7	13.3	0.0	38.0	common	minor	sp, ap, al, ep, ilm	n.d.
26	55.8	16.9	2.4	24.9	common	minor	sp, ap, ep, su	n.d.
23	57.1	12.6	0.4	29.9	common	minor	sp, ap, al, ep, su	n.d.
average	57.4	15.2	1.0	26.4				
<i>Irving Peak pluton</i>								
Sample no	Plag	Qtz	K-feld	Mafics	Hbl	Bio	Accessory	An %
31	65.3	11.9	0.0	22.8	common	minor	ap, ilm, ep	n.d.
33	39.6	15.6	0.7	43.9	common	uncommon	ap, al, su, sp	n.d.
32	60.4	00.6	0.0	39.1	common	minor	su, ilm, ap, sp	n.d.
34	57.4	01.3	0.0	41.3	common	minor	su, ap, sp	n.d.
average	55.7	7.4	0.2	36.8				
<i>Butler Peak pluton</i>								
Sample no	Plag	Qtz	K-feld	Mafics	Hbl	Bio	Accessory	An %
27	69.3	25.6	0	06.9	none	uncommon	al, ap, su	n.d.
29	44.9	36.6	8.6	09.8	none	uncommon	ga, ap, ep	n.d.
28	63.8	25.2	0.2	10.8	none	uncommon	ga, ap, ep, ilm	n.d.
average	59.3	29.1	2.9	9.2				

Table 6. Modal Analyses on samples of granitic rocks from the Taku Harbor subbelt

<i>Everett Peak pluton</i>								
Sample no	Plag	Qtz	K-feld	Mafics	hornblende	biotite	Accessory min	An %
45	48.9	19.7	11.3	20.1	common	trace	sp, ep, ap, su, ma	
35	57.7	13.6	13.5	15.2	common	minor	sp, ap, ma	
44	51.4	17.1	16.2	15.3	common	trace	sp, ep, ap,	34
41	53.7	18.4	13.9	14.0	common	minor	sp, ap, al,	
46	55.6	20.0	02.4	22.1	common	none	sp, ap, ma	
43	70.0	10.4	03.3	16.3	common	none	sp, ep, ap	
39	55.8	07.2	19.4	17.6	common	trace	sp, ap, su, ma	
36	55.5	09.5	18.5	16.4	common	minor	sp, ap, su, ma	
37	53.6	08.0	19.5	19.0	common	trace	sp, ap	33
40	55.3	07.0	15.2	22.5	common	trace	sp, ap, su	
38	54.1	04.7	21.7	19.5	common	none	sp, ap, su,	36
49	47.7	06.6	23.4	22.4	common	trace	sp, ep, ap, ma	
48	46.2	09.7	25.1	19.0	common	trace	sp, ep, ap, ma	34
47	51.1	06.9	23.7	18.3	common	trace	sp, ap, ma	
50	49.1	07.6	22.1	21.3	common	trace	sp, ap, zi, ma	
42	63.0	10.6	12.1	14.3	common	trace	sp, ap, ma	
<i>average</i>	<i>54.3</i>	<i>11.1</i>	<i>16.3</i>	<i>18.3</i>				

<i>Arthur Peak pluton</i>								
Sample no.	Plag	Qtz	K-feld	Mafics	hornblende	biotite	Accessory min	An %
53	82.7	11.9	00.0	05.4	common	none	sp, ep, ap, su	
54	61.5	17.1	13.6	07.8	common	trace	ep, sp, ap, su, ma	
55	56.9	12.1	16.8	14.2	common	trace	sp, ep, ap, zi, su	
57	64.0	10.3	17.5	08.2	common	none	sp, ep, ap, zi, ma	
51	54.7	26.3	01.7	17.4	common	none	sp, ep, ap, ma	
56	63.5	17.2	15.2	04.1	common	none	ep, sp, ap, ma	
52	49.5	14.6	24.0	11.9				
<i>average</i>	<i>61.8</i>	<i>15.6</i>	<i>12.7</i>	<i>9.9</i>				

Table 7. Modal analyses on samples of granitic rocks from the Great Tonalite Sill belt

<i>Speel River pluton</i>								
Sample no	Plagioclase	Quartz	K-feldspar	Mafics	hornblende	biotite	accessory	An %
60	53.8	16.5	0.0	29.9	common	uncommon	ap, zi, ma	41
77	55.7	15.9	0.0	28.3	common	common	sp, ap, zi, ma	n.d.
70	51.4	21.4	0.0	27.2	common	common	sp, ap, zi, ma	40
68	58.4	22.8	0.5	18.3	uncommon	common	sp, ap, zi	n.d.
66	53.6	17.8	0.2	28.4	common	uncommon	sp, ap, zi, ma	38
64	53.8	21.4	1.4	23.4	common	uncommon	ap, zi, ma	38
61	55.5	17.9	0.0	26.7	common	common	sp, ap, zi, ma	41
59	56.0	20.7	0.0	23.3	common	uncommon	ap, zi, ma	n.d.
58	57.4	18.9	2.3	21.4	uncommon	common	ap, zi, ma	37
69	54.7	21.9	1.9	21.5	common	uncommon	ap, zi, ma	40
73	49.6	15.1	0.4	34.9	common	common	sp, ap, zi, ma	n.d.
74	59.9	17.4	1.9	20.7	common	uncommon	sp, ap, zi, ma	39
75	55.0	15.6	0.0	29.4	common	common	sp, ap, zi, ma	40
76	51.1	18.4	1.1	29.5	common	common	sp, ap, zi, ilm	n.d.
62	57.7	14.1	0.0	28.1	common	common	sp, ap, zi	n.d.
63	55.6	13.8	3.3	27.3	common	common	ap, zi, ma	40
78	49.9	18.0	0.0	32.3	common	common	ap, sp, zi	n.d.
71	62.6	17.8	0.7	18.9	common	uncommon	ap, zi, ma	n.d.
67	56.1	14.7	0.0	29.2	common	common	ap, zi, ma	n.d.
65	53.8	20.1	2.7	23.4	common	uncommon	sp, ap, zi, ma	38
79	53.0	17.2	2.5	27.3	common	common	sp, ap, zi, ma	40
81	56.6	13.7	0.5	29.2	common	common	sp, ap, zi, ma	n.d.
80	58.1	16.6	2.8	22.5	common	uncommon	ap, zi, ma	n.d.
average	55.2	17.7	1.0	26.1				
<i>Granodiorite layers in Speel River pluton</i>								
82	54.4	24.1	16.4	5.1	trace	uncommon	ap, zi, ma, al	26
72	43.8	28.1	19.6	8.4	minor	uncommon	al, ap, zi, ma	25
83	43.7	27.6	18.6	10.1	trace	uncommon	al, ap, zi, ma	
<i>Taku Cabin pluton</i>								
Sample no	Plagioclase	Quartz	K-feldspar	Mafics	hornblende	biotite	accessory	An %
84	56.5	22.5	4.4	16.6	common	uncommon	sp, ap, zi, ma	38
87	57.8	22.1	3.6	16.5	common	uncommon	sp, ap, zi, ma	39
90	54.5	23.8	2.3	19.4	common	uncommon	sp, ap, zi, ma	40
88	56.1	24.8	3.7	15.4	common	uncommon	sp, ap, zi, ma	39
89	61.5	20.9	0.8	16.8	common	uncommon	sp, ap, zi, ma	34
85	58.4	17.4	2.1	22.1	common	uncommon	sp, ap, zi, ma	39
86	51.2	20.9	4.7	23.2	common	uncommon	sp, ap, zi, ma	41
91	58.1	21.1	0.3	20.5	common	uncommon	sp, ap, zi, ma	40
average	56.8	21.7	2.7	18.8				
<i>Granodiorite layer in pluton</i>								
92	40.6	29	19.4	11	trace	uncommon	al, sp, ap, zi	32

Table 8. Modal analyses on samples from the southern unit of the Turner Lake batholith

Sample no	Plagioclase	Quartz	K-feldspar	Mafics	hornblende	biotite	Accessory	An %
099	53.0	22.0	10.0	15.0	minor	uncommon	sp, ap, ma	43
094	46.4	23.8	13.6	16.0	uncommon	uncommon	ap, zi, ma	
095	49.1	24.0	08.9	17.9	common	uncommon	ap, zi, ma	
105	47.6	25.8	11.4	15.2	uncommon	uncommon	ap, zi, sp, ma	37
103	47.2	31.8	04.4	16.6	common	uncommon	ap, zi, sp, ma	
102	44.1	29.1	11.5	15.3	uncommon	uncommon	al, ap, zi, ma	
098	51.4	23.4	09.4	15.9	uncommon	uncommon	ap, zi, sp, ma	40
097	45.0	31.0	07.0	17.0	minor	uncommon	sp, ap, zi, ma	43
104	49.9	27.4	09.3	13.4	uncommon	minor	sp, ap, zi, ma	
107	45.8	30.0	07.7	16.5	uncommon	uncommon	sp, ap, zi, ma	
108	42.5	31.0	15.6	10.9	minor	uncommon	ap, al, ma	
106	62.0	26.0	01.0	15.0	trace	common	ap, zi, ma	
100	55.0	21.0	03.8	20.0	uncommon	common	ap, ma	
096	52.9	22.3	09.1	15.7	uncommon	common	sp, ap, zi, ma	
093	44.0	29.0	10.0	17.0	uncommon	uncommon	ap, zi, al, ma	42
101	45.7	25.7	16.3	12.3	uncommon	uncommon	ap, sp, zi, ma	
109	53.0	20.3	05.7	20.8	common	uncommon	sp, ap, ma	43
average	49.1	26.1	09.1	15.9				

Table 9. Modal analyses on samples from the central granodiorite unit of the Tumer Lake batholith

Sample no	Plagioclase	Quartz	K-feldspar	Mafics	hornblende	biotite	Accessory	An %
140	43.7	32.8	18.5	05.0	trace	uncommon	sp, ap, zi, ma	31
139	47.5	26.1	17.4	09.0	minor	uncommon	sp, ap, zi, ma	31
138	45.6	34.6	08.2	11.6	uncommon	uncommon	sp, ap, zi, ma	34
137	52.7	26.8	10.4	10.1	uncommon	uncommon	sp, ap, zi, ma	33
136	49.7	28.7	11.0	10.6	uncommon	uncommon	sp, ap, zi, ma	
135	39.4	36.1	13.8	10.7	minor	uncommon	sp, ap, zi, ma	32
134	48.5	29.6	10.8	11.3	uncommon	uncommon	sp, ap, zi, ma	
133	48.9	28.1	12.2	10.8	uncommon	uncommon	sp, ap, zi, ma	
132	50.7	28.1	11.3	09.8	uncommon	uncommon	sp, ap, zi, ma	31
130	37.6	38.6	10.4	13.4	uncommon	uncommon	sp, ap, zi, ma	
131	53.8	25.5	09.9	10.8	uncommon	uncommon	sp, ap, zi, ma	30
125	49.0	26.7	14.1	10.2	uncommon	uncommon	sp, ap, zi, ma	31
126	45.9	33.1	12.3	08.2	minor	uncommon	sp, ap, zi, ma	
127	46.6	30.1	15.2	08.1	minor	uncommon	sp, ap, zi, ma	31
128	43.3	35.6	12.9	08.1	minor	uncommon	sp, ap, zi, ma	30
129	50.7	27.8	10.4	11.1	uncommon	uncommon	sp, ap, zi, ma	
145	50.4	23.4	10.3	15.9	uncommon	uncommon	sp, ap, zi, ma	32
141	57.1	29.4	07.5	06.0	minor	uncommon	sp, ap, zi, ma	34
142	54.2	24.0	06.2	15.6	uncommon	uncommon	sp, ap, zi, ma	36
123	57.7	25.9	05.3	11.1	uncommon	uncommon	sp, ap, zi, ma	31
124	52.9	27.7	11.4	08.0	trace	uncommon	sp, ap, zi, ma	30
120	58.2	24.0	07.2	10.6	uncommon	minor	sp, ap, zi, ma	36
117	52.2	29.1	08.0	10.7	uncommon	uncommon	sp, ap, zi, ma	34
119	54.5	19.8	08.3	17.4	uncommon	uncommon	ap, sp, zi, ma	30
121	60.0	27.2	04.3	08.5	minor	uncommon	sp, ap, zi, ma	
146	49.0	26.5	13.0	11.5	minor	uncommon	ap, zi, ma	
144	49.1	29.6	09.9	11.4	minor	uncommon	sp, ap, zi, ma	32
147	55.0	28.8	06.3	09.9	uncommon	uncommon	sp, ap, zi, ma	37
122	50.5	30.2	13.2	06.1	minor	minor	sp, ap, zi	34
118	55.2	24.4	10.5	09.9	uncommon	uncommon	sp, ap, zi	
115	44.7	29.7	11.9	13.7	uncommon	uncommon	sp, ap, zi, ma	34
148	50.2	26.0	14.6	08.9	minor	minor	sp, ap, zi, ma	32
143	54.6	22.5	09.9	12.3	uncommon	uncommon	sp, ap, zi, ma	34
150	43.0	33.1	12.4	10.5	uncommon	uncommon	sp, ap, zi, ma	32
158	45.7	29.5	12.6	12.0	minor	uncommon	sp, ap, zi	36
149	37.8	28.2	21.7	11.4	uncommon	uncommon	sp, ap, zi, ma	33
151	54.9	27.5	06.2	11.4	uncommon	uncommon	sp, ap, zi, ma	37
154	48.0	26.0	12.0	14.0	uncommon	uncommon	ap, zi, sp, ma	40
156	46.0	31.0	12.0	11.0	uncommon	uncommon	sp, ap, zi, ma	36
157	46.0	26.0	12.0	16.0	uncommon	uncommon	sp, ap, zi, ma	37
152	41.9	27.2	13.5	17.1	uncommon	uncommon	sp, ap, zi, ma	41
116	43.3	30.4	17.7	07.8	uncommon	uncommon	ap, zi, ma	
155	40.5	30.4	18.7	10.1	uncommon	uncommon	sp, ap, zi, ma	32
153	47.1	25.6	10.9	16.4	uncommon	uncommon	al, ap, zi, ma	40
average	48.9	28.4	11.5	11.0				

Southern border zone of central (granodiorite) unit

160	45.2	23.1	12.5	19.3	uncommon	uncommon	sp, al, ap, zi	32
161	56.0	22.1	03.8	18.0	uncommon	uncommon	sp, ap, zi, al	33
162	51.1	24.5	08.5	15.4	uncommon	uncommon	ap, ap, zi	32
164	45.5	27.5	14.7	11.3	uncommon	minor	sp, ap, zi, ma	34
163	47.4	24.5	12.9	15.1	uncommon	uncommon	sp, ap, zi, ma	33
159	50.0	25.0	11.0	14.0	minor	uncommon	sp, ap, zi, ma	32
165	47.5	25.5	11.2	15.8	common	uncommon	ap, zi, sp, ma	34
average	49.0	24.6	10.7	15.6				

Table 10. Modal Analyses on samples of granitic rocks from the northern unit of the Turner Lake batholith

<i>Main phase</i>								
Sample no	Plagioclase	Quartz	K-feldspar	Mafics	hornblende	biotite	accessory	An%
190	38.8	39.0	13.8	08.4	minor	uncommon	zi, ap, al, ma	32
193	50.6	28.7	14.0	06.7	uncommon	minor	sp, ap, zi, ma	29
183	43.4	36.9	15.7	04.0	minor	minor	ap, zi, sp, ma	26
175	49.7	28.0	15.7	06.6	minor	uncommon	sp, ap, zi, ma	31
180	46.5	27.9	18.6	07.0	minor	uncommon	sp, ap, zi, ma	29
182	47.5	32.4	15.6	04.5	minor	minor	sp, ap, zi, al, ma	31
174	47.1	28.4	19.0	05.5	minor	uncommon	sp, al, ap, zi, ma	31
188	45.1	24.7	25.0	05.2	minor	minor	ap, zi, ma	
176	45.2	35.3	14.0	05.5	minor	uncommon	sp, al, ap, zi, ma	29
172	46.1	30.0	20.5	03.4	minor	minor	al, sp, ap, zi, ma	26
187	44.4	32.9	19.4	03.3	minor	minor	ap, sp, al, zi, ma	31
170	47.9	26.0	15.6	10.5	uncommon	uncommon	sp, ap, zi, al, su	
189	49.6	27.6	11.5	11.3	uncommon	uncommon	sp, ap, zi, ma	30
179	47.1	23.3	20.5	09.1	minor	uncommon	sp, al, ap, zi, ma	28
189	45.2	35.3	09.5	10.0	minor	uncommon	al, ap, zi, ma	30
167	46.9	26.3	17.9	08.9	minor	uncommon	sp, ap, zi, ma	29
178	43.1	22.9	25.1	08.9	minor	uncommon	sp, ap, zi, ma	27
194	44.1	28.5	17.0	10.4	minor	uncommon	sp, ap, zi, ma	
181	35.4	24.6	32.5	07.5	minor	uncommon	sp, al, ap, zi, su	27
195	44.6	26.9	20.3	08.2	minor	uncommon	sp, ap, zi, su	30
185	45.0	23.6	20.3	11.1	minor	uncommon	sp, ap, zi, ma	32
168	44.7	20.6	20.9	13.8	uncommon	uncommon	sp, ap, zi, ma	31
192	40.2	29.7	23.5	06.6	minor	minor	sp, ap, al, zi, ma	28
199	46.2	21.5	19.5	12.8	uncommon	uncommon	sp, ap, zi, su, ma	29
173	40.9	30.8	22.6	05.7	minor	minor	sp, ap, zi, ma	28
184	43.8	27.4	22.2	06.6	min	uncommon	sp, ap, zi, al	30
198	38.1	36.1	24.6	01.2	trace	minor	ap, zi, ma	28
191	40.6	26.0	24.4	09.0	minor	uncommon	al, ap, zi, ma	
196	44.0	26.0	18.0	12.0	minor	uncommon	al, ap, zi, ma	30
186	43.4	26.0	20.8	09.8	minor	uncommon	sp, ap, zi, ma	32
197	41.9	26.4	19.1	12.5	minor	uncommon	sp, ap, zi, ma	
177	44.1	24.4	21.6	10.0	minor	uncommon	ap, zi, ma	
166	39.4	28.8	22.9	08.9	minor	uncommon	sp, al, ap, zi, ma	30
251	47.5	26.3	17.1	09.1	minor	uncommon	sp, ap, zi, ma	
171	43.7	30.2	19.9	06.1	minor	minor	ap, ma	
average	44.3	28.3	19.4	08.0				
<i>Southwest Phase</i>								
Sample no	Plagioclase	Quartz	K-feldspar	Mafics	hornblende	biotite	accessory	An %
201	42.2	31.6	24.7	01.5	trace	minor	ap, al, zi, ma	27
204	54.3	32.0	11.3	02.4	minor	minor	sp, ap, zi, ma	34
205	46.6	29.7	19.3	04.4	minor	uncommon	sp, ap, zi, ma	
202	45.6	25.9	20.0	08.5	minor	uncommon	sp, ap, zi, ma	26
207	41.6	18.2	34.1	06.1		uncommon	ap, ma	
203	50.3	20.3	17.5	11.9	minor	uncommon	ap, zi, ma	31
206	54.4	25.0	12.6	08.0	minor	uncommon	sp, al, ap, zi, ma	32
200	40.1	28.4	26.1	05.4	trace	minor	ap, al, zi, ma	
average	46.9	26.4	20.7	06.0				

Table 11 Modal Analyses on samples from granitic rocks of the eastern subbelt of the Turner Lake batholith

<i>Western part of undivided granite</i>								
Sample no	Plagioclase	Quartz	K-feldspar	Mafics	hornblende	biotite	Accessory	An %
213	37.3	32.0	21.6	08.9	minor	uncommon	al, ap, zi, ma	26
211	33.0	31.0	27.0	09.0	minor	uncommon	sp, al, ap, zi	
212	34.2	27.3	30.9	07.5	minor	uncommon	al, ap, zi, ma	29
216	37.3	27.3	28.1	06.9	minor	uncommon	sp, al, ap, zi	27
208	23.3	34.1	40.4	01.0	trace	minor	al, ap, zi, ma	
214	35.1	33.0	23.2	08.4	trace	uncommon	ap, zi, ma	27
209	37.2	26.5	28.2	08.0	minor	uncommon	sp, al, ap, zi	28
215	40.8	27.1	23.0	08.1	minor	uncommon	sp, al, ap, zi	27
210	34.0	27.0	30.0	09.0	trace	uncommon	al, sp, ap, zi	
218	33.9	33.6	21.4	10.5	minor	uncommon	sp, zi, ap, ma	29
217	36.4	26.1	28.5	08.9	minor	uncommon	sp, zi, ap, ma	
219	26.4	34.0	33.6	06.1	none	uncommon	sp, zi, ap, ma	
220	28.0	31.0	28.0	13.0	minor	uncommon	ap, zi, ma	
221	34.7	23.6	27.4	14.3	minor	common	ap, zi, ma	
average	33.7	29.5	28.0	08.5				
<i>Eastern part of undivided granite</i>								
Sample no	Plagioclase	Quartz	K-feldspar	Mafics	hornblende	biotite	Accessory	An %
238	29.5	29.0	37.6	3.8	none	minor	al, ap, zi, ma	
239	30.0	30.0	34.0	6.0	trace	minor	al, ap, ma	
240	27.0	30.0	38.0	5.0	none	minor	al, sp, zi, sp	
224	31.0	27.4	36.2	05.5	none	uncommon	ap, al, zi, ma	
average	29.4	29.1	36.5	05.1				
<i>Wright Glacier stock</i>								
Sample no	Plagioclase	Quartz	K-feldspar	Mafics	hornblende	biotite	Accessory	An %
232	31.8	35.0	27.5	5.5	minor	minor	al, ap, zi	
230	36.0	27.0	28.0	9.0	minor	uncommon	ap, zi	
227	33.0	31.6	32.7	2.7	minor	minor	al, ap, zi	26
225	33.1	27.9	28.6	10.4	minor	uncommon	al, ap, zi	24
231	37.4	27.5	28.5	6.6	minor	uncommon	al, ap, zi, sp	
226	33.6	28.1	30.5	7.8	minor	uncommon	al, ap, zi	27
228	37.3	29.0	23.6	10.1	trace	uncommon	al, ap, zi	
average	34.6	29.4	28.5	7.4				
<i>Wright River stock</i>								
Sample no	Plagioclase	Quartz	K-feldspar	Mafics	hornblende	biotite	Accessory	An %
237	45.0	22.0	19.1	13.9	uncommon	uncommon	ap, zi, cm, ma	
236	52.8	13.5	13.4	20.3	uncommon	common	ap, zi, cm, ma	
235	38.1	18.1	26.3	17.4	uncommon	common	ap, zi, px, cm	
234	37.8	20.8	27.6	13.7	minor	uncommon	ap, zi, cm, ma	
233	50.0	05.3	08.7	36.0	common	uncommon	Px, ap, zi, ma	
average	44.7	15.9	21.6	20.3				

Table 12. Modal analyses for samples of miscellaneous granitic bodies from the Coast Mountains belt

<i>Tease Lake stocks</i>								
Sample no	Plagioclase	Quartz	K-feldspar	Mafics	hornblende	biotite	Accessory	An %
246	56.1	18.1	18.5	07.3	uncommon	minor	sp, ap, ma	
245	65.1	12.1	02.7	20.0	uncommon	common	ap, zi, sp, ma	
244	59.2	20.0	11.7	09.1	uncommon	trace	ap, sp, zi	
242	39.0	22.3	29.4	09.3	none	uncommon	sp, ap, ma	
243	52.0	21.0	18.0	09.0	uncommon	minor	sp, ap, ma	
241	62.1	18.4	12.7	06.8	uncommon	uncommon	al, ap, sp, ma	
<i>average</i>	<i>55.6</i>	<i>18.7</i>	<i>15.5</i>	<i>10.3</i>				

Body at east end of Turner Lake

Sample no	Plagioclase	Quartz	K-feldspar	Mafics	hornblende	biotite	Accessory	An %
169	39.2	29.9	25.1	5.8	minor	uncom	sp, ap, zi, al	29
170	37.2	29.8	25.0	8.0	minor	uncom	sp, ap, zi, al, ma	28
166	40.0	29.0	23.0	8.0	minor	uncom	sp, ap, zi, ma	32
171	35.6	26.3	30.0	8.1	minor	uncom	al, ap, zi, ma	29
167	43.4	23.3	31.5	1.8	none	minor	ga, ap,	
168	36.0	31.4	25.2	7.4	minor	minor	ap, zi, sp, ma	
<i>average</i>	<i>38.6</i>	<i>28.3</i>	<i>26.6</i>	<i>6.5</i>				

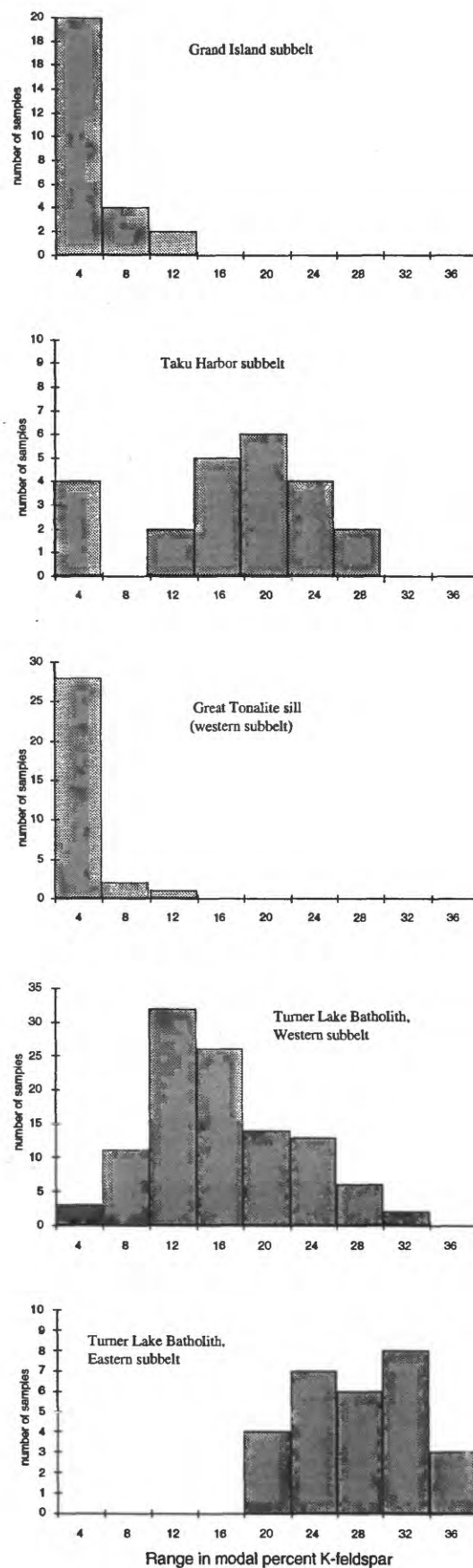


Figure 5. Distribution of K-feldspar (modal percent) for plutons of the Coast Mountains complex along the Taku Inlet transect; grouped according to subbelts.

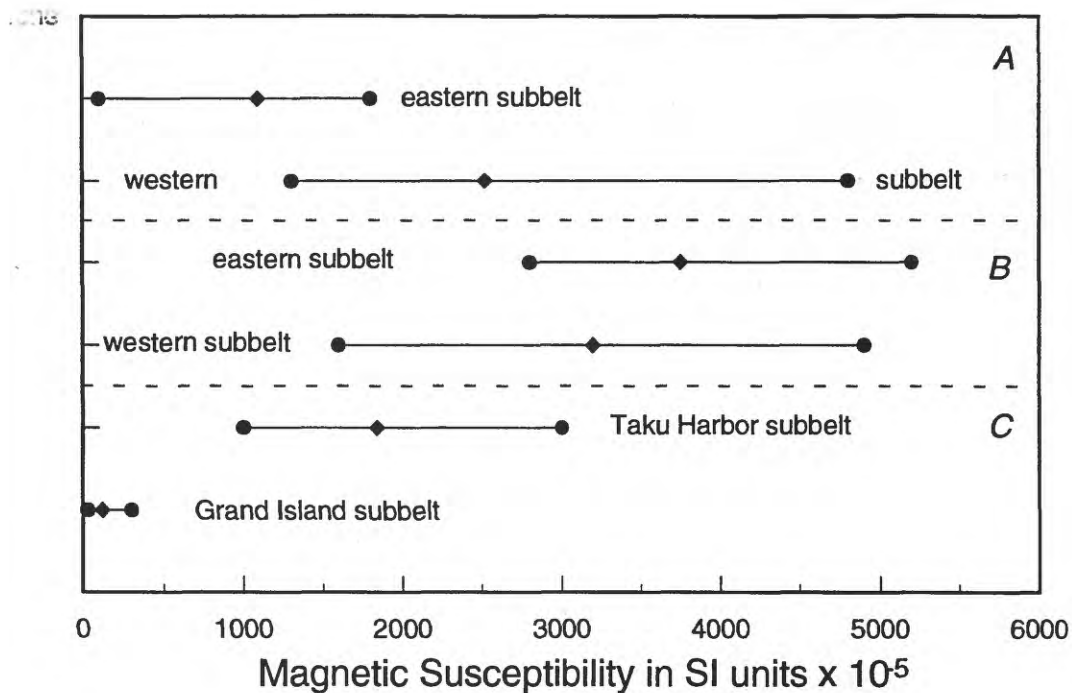
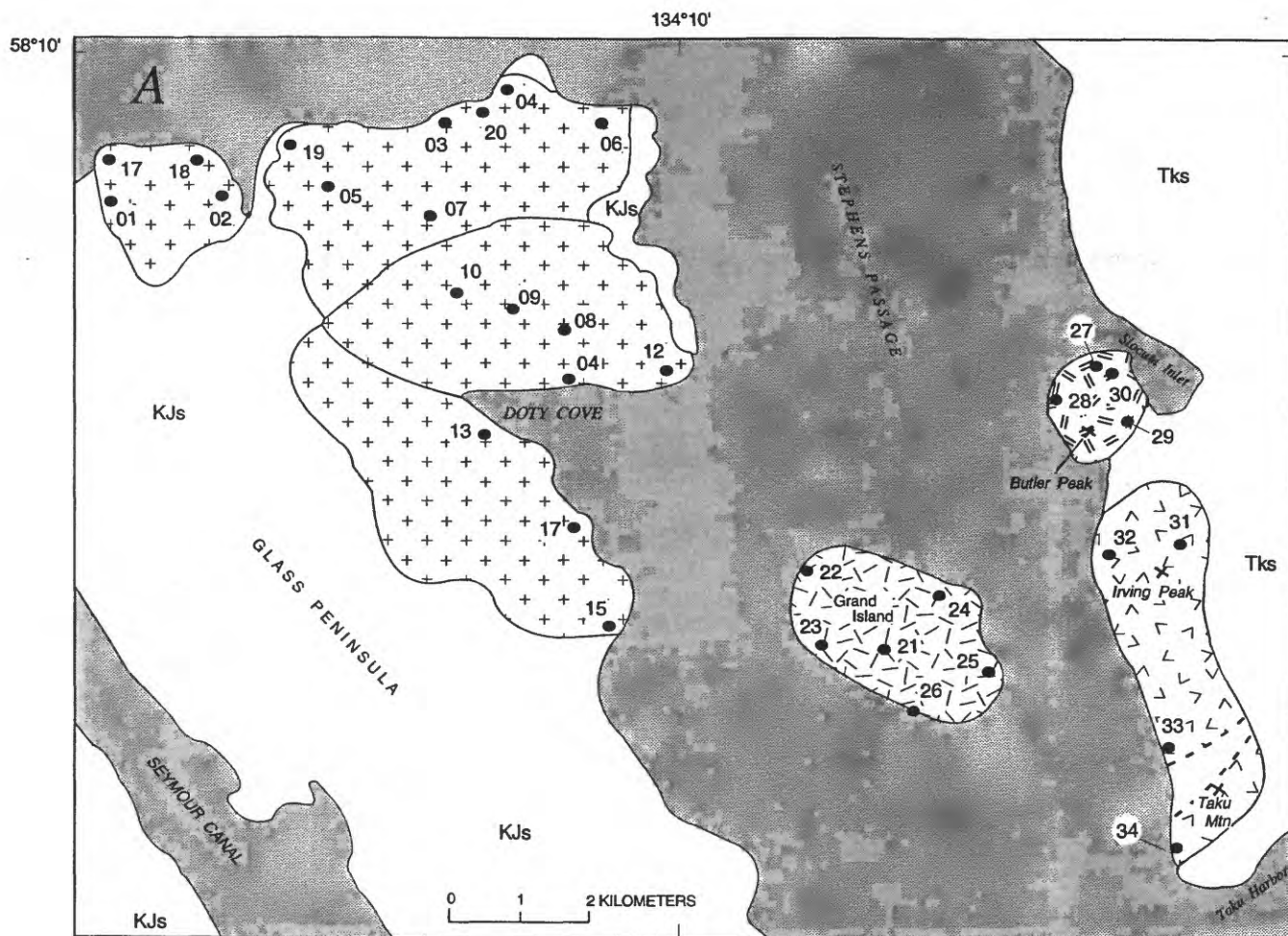


Figure 6. Magnetic susceptibility of granitoids from the Coast Mountains complex along the Taku Inlet transect, grouped according to belts; *A*, Coast Mountains belt; *B*, Great tonalite sill belt; and *C*, Admiralty-Revillagigedo belt



EXPLANATION

- | | |
|--|--|
| | Quartz diorite and tonalite of Glass Peninsula Stocks |
| | Tonalite and quartz diorite of Grand Island pluton |
| | Diorite of Irving Peak pluton |
| | Leucotonalite and granodiorite of Butler Peak pluton |
| | Metasedimentary and metavolcanic rocks of the Stephens Passage Group (Cretaceous and Jurassic) |
| | Mid- to high-grade schist (Late Cretaceous and Tertiary) |
| | Sample |

Figure 7. Generalized geologic maps of the western part of the Taku Inlet transect showing plutons of the Admiralty-Revillagigedo belt. A, plutons of the Grand Island subbelt; and B, plutons of the Taku Harbor subbelt. Sample locations indicated by dot and reference number.

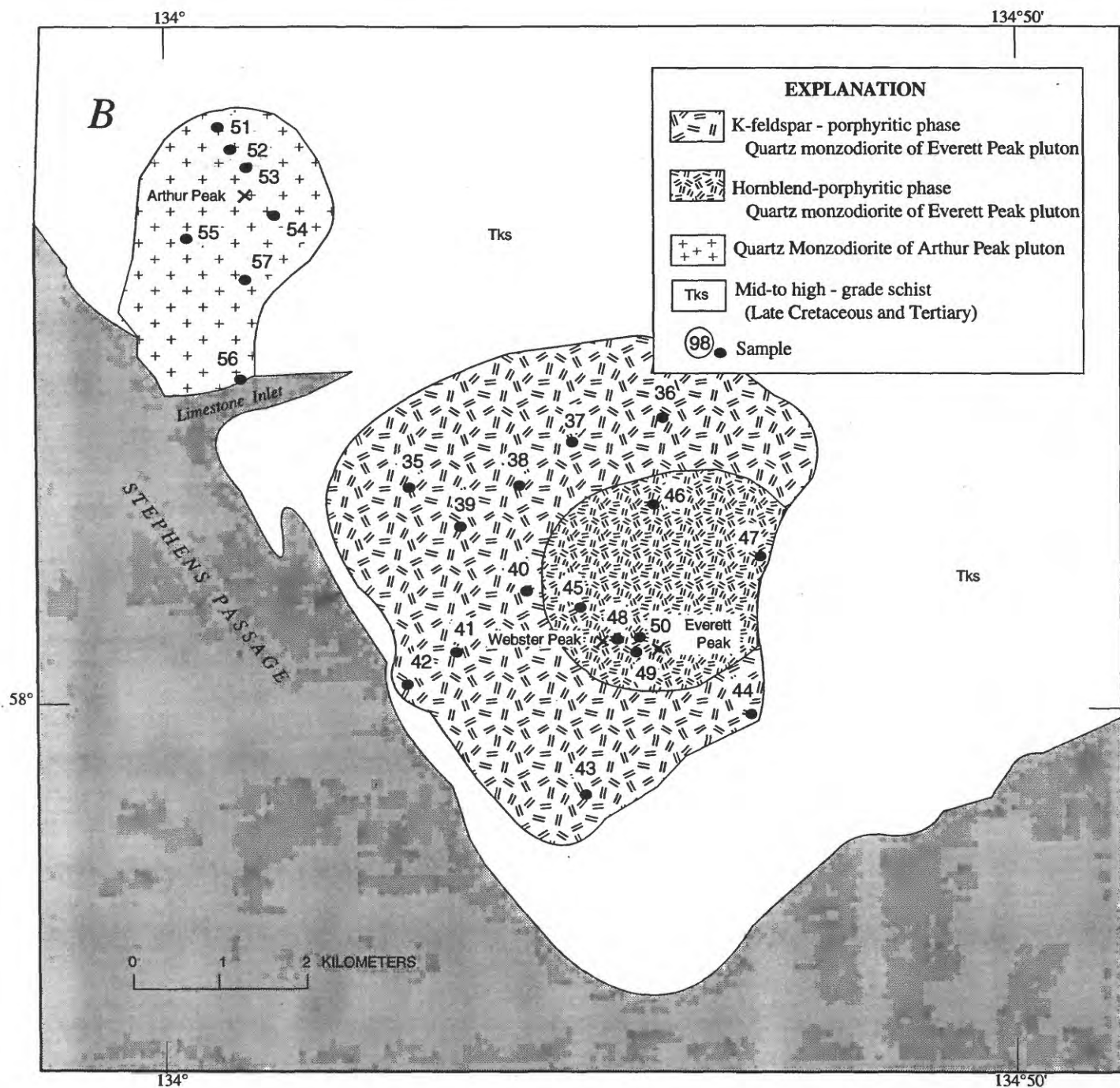
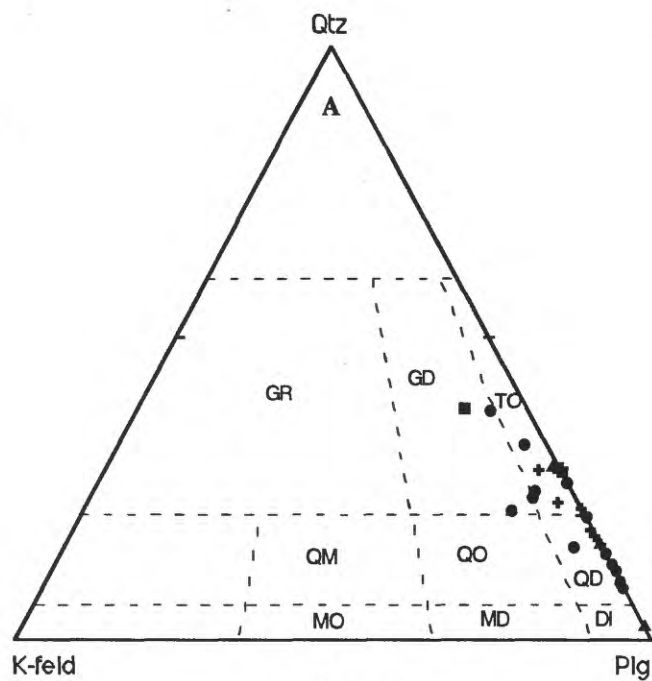
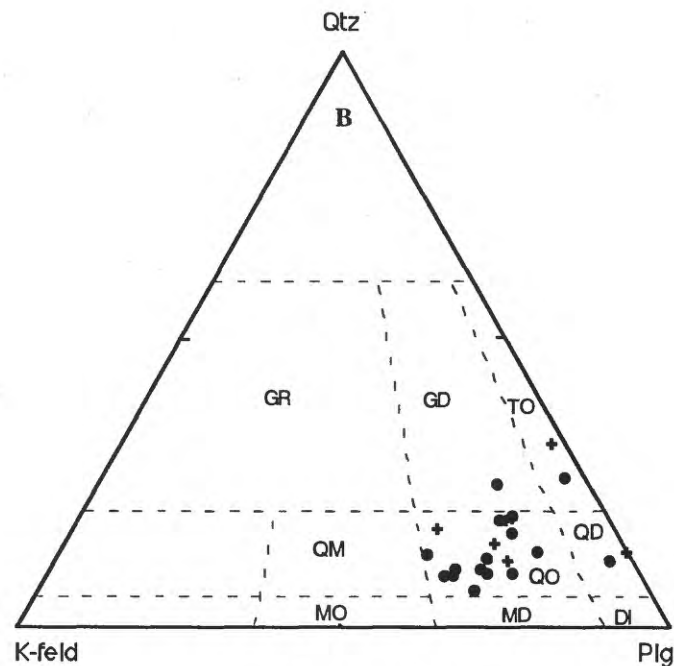


Figure 7. Generalized geologic maps of the western part of the Taku Inlet transect showing plutions of the Admiralty-Revillagiedo belt. A, plutions of the Grand Island subbelt; and B, plutions of the Taku Harbor subbelt. Sample locations indicated by dot and reference number.



Explanation

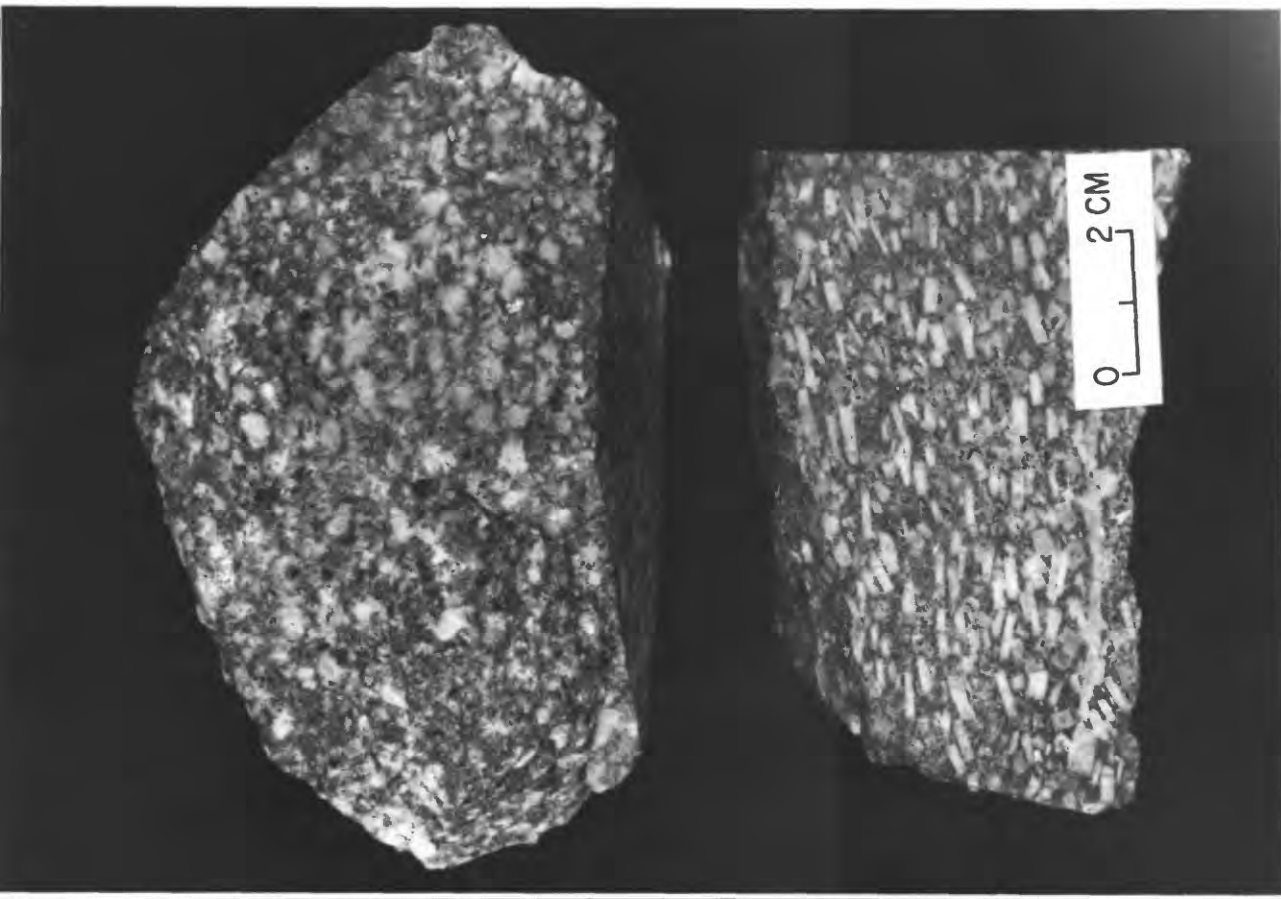
- Glass Peninsula stocks
- ⊕ Grand Island pluton
- Butler Peak pluton
- ▲ Irving Peak pluton



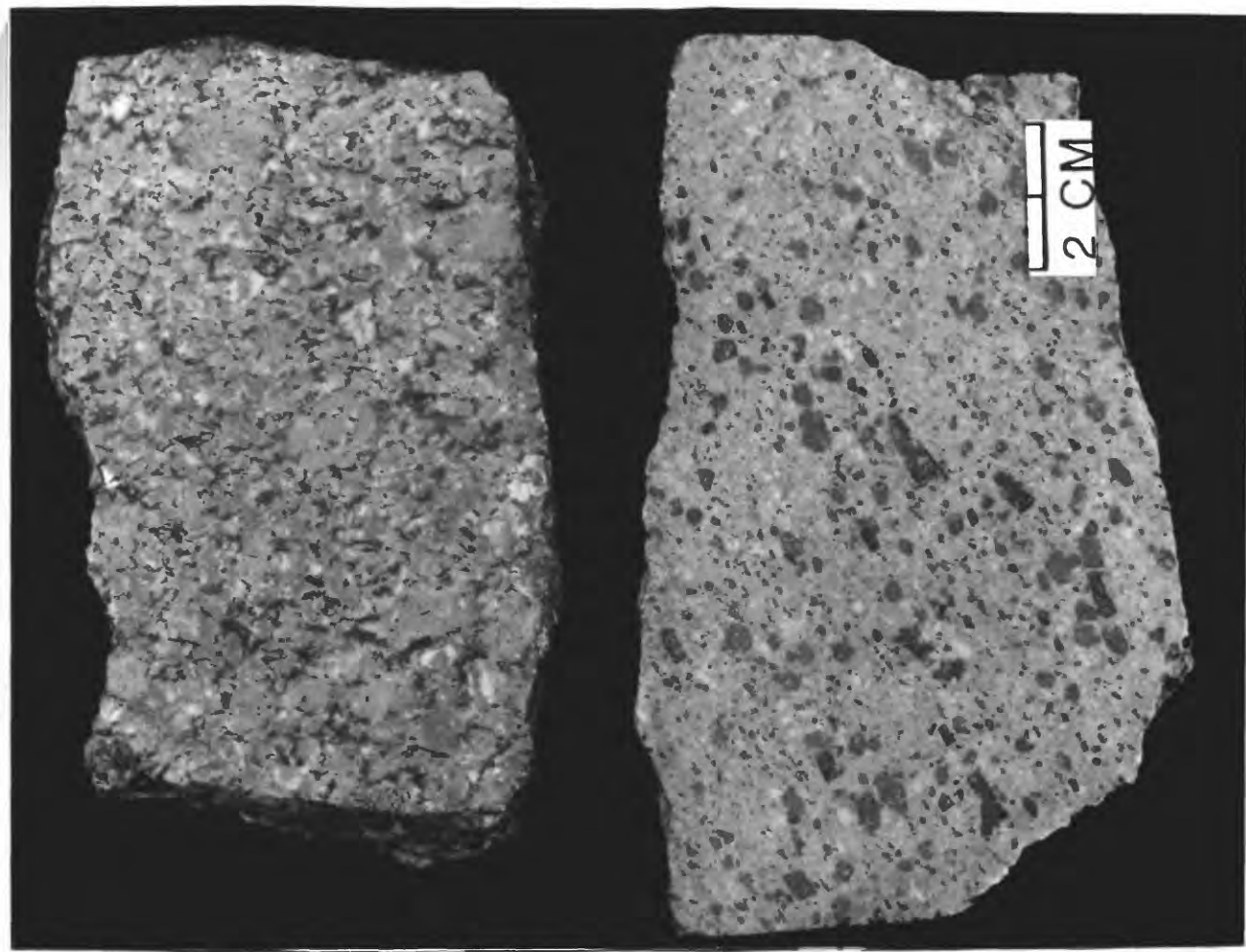
Explanation

- Everett Peak pluton
- ⊕ Arthur Peak pluton

Figure 8. Modal composition of rocks from the Admiralty-Revillagigedo belt within the Taku Inlet transect. A, Grand Island subbelt; B, Taku Harbor subbelt. Rock classification from Streckeisen (1973): GR, granite; GD, granodiorite; TO, tonalite; QM, quartz monzonite; QO, quartz monzodiorite; QD, quartz diorite; MO, monzonite; MD monzodiorite; and DI, diorite.



A



B

Figure 9. Photographs of representative rocks from the Admiralty-Revillagigedo belt. A, typical samples from Glass Peninsula stocks; top sample shows crowded plagioclase-porphyritic texture, and bottom slab shows strongly foliated texture with crowded tabular plagioclase. B, slabbed samples typical of rocks from the Everett Peak pluton; top sample is of K-feldspar-porphyritic main phase, and bottom sample is of hornblende-porphyritic core phase.

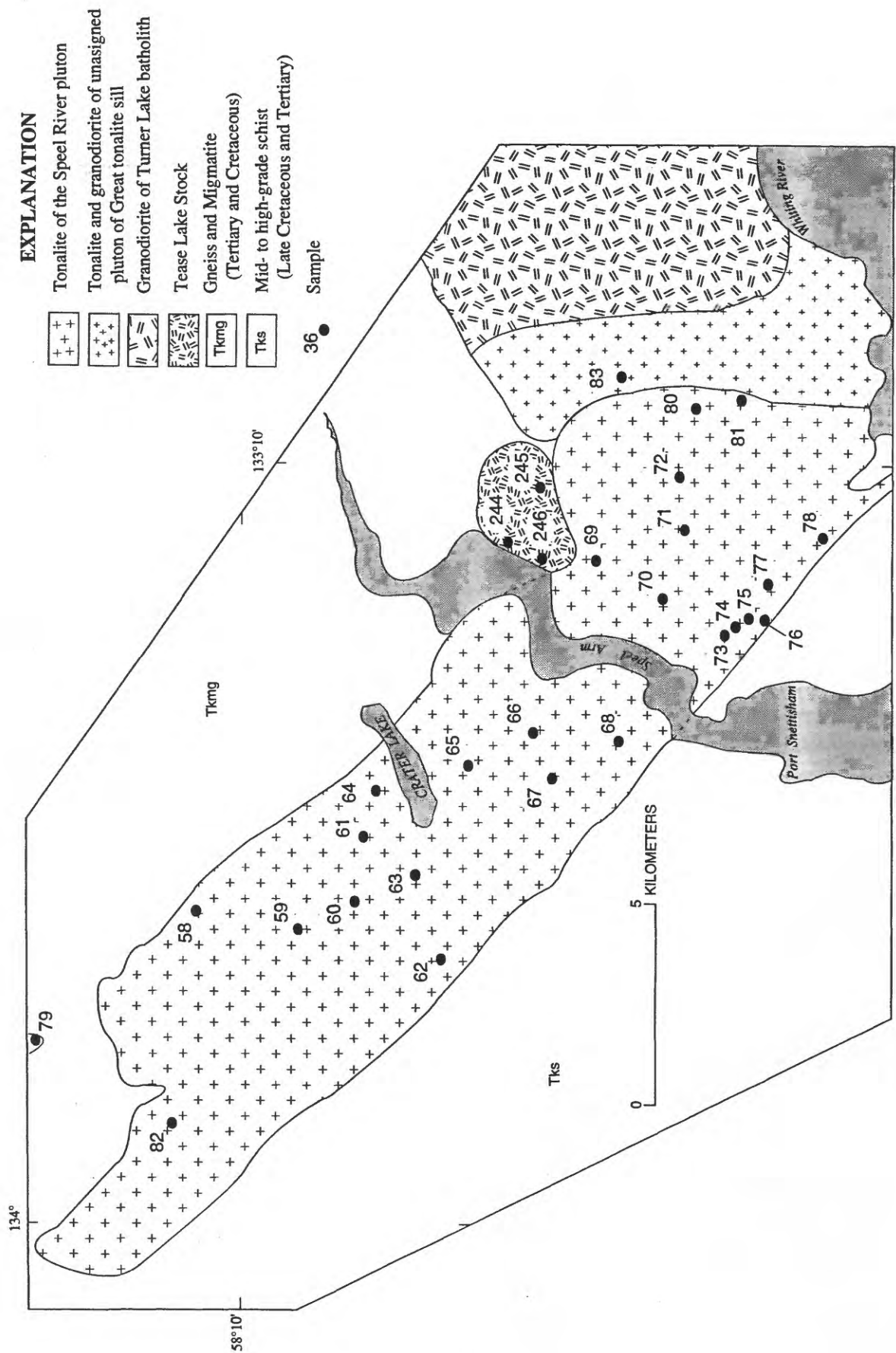


Figure 10. Generalized geologic map of the Speel River pluton and adjacent area. Numbered sample locations (dots) refer to numbers in tables.

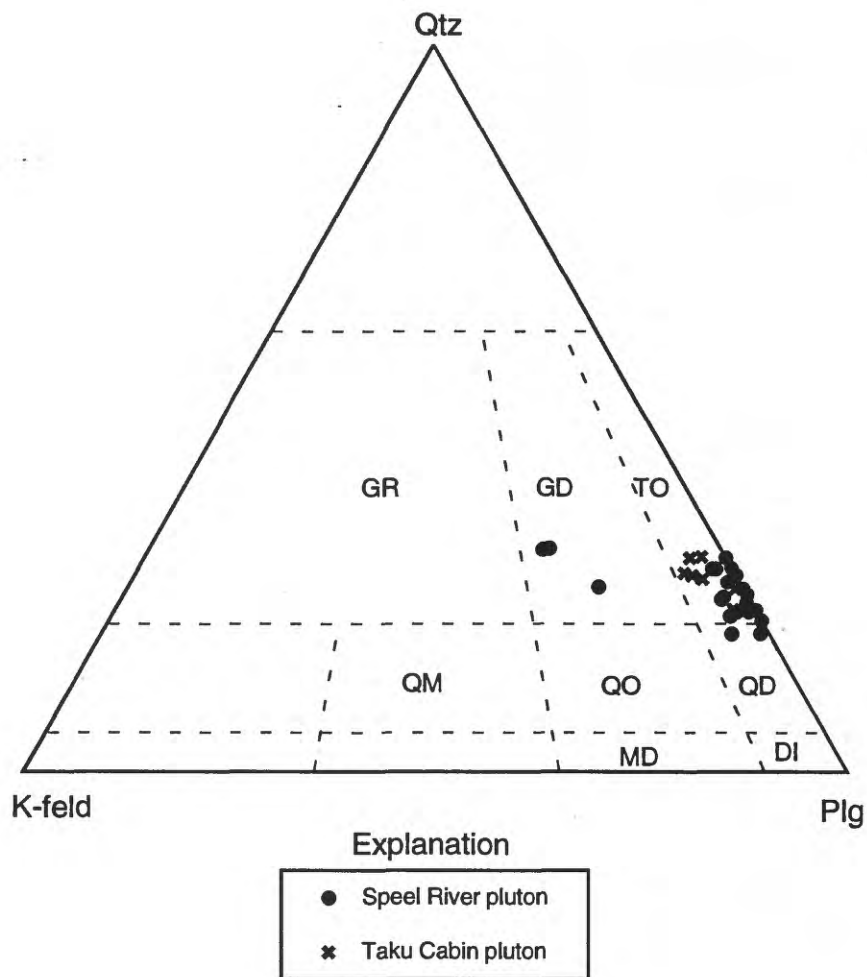
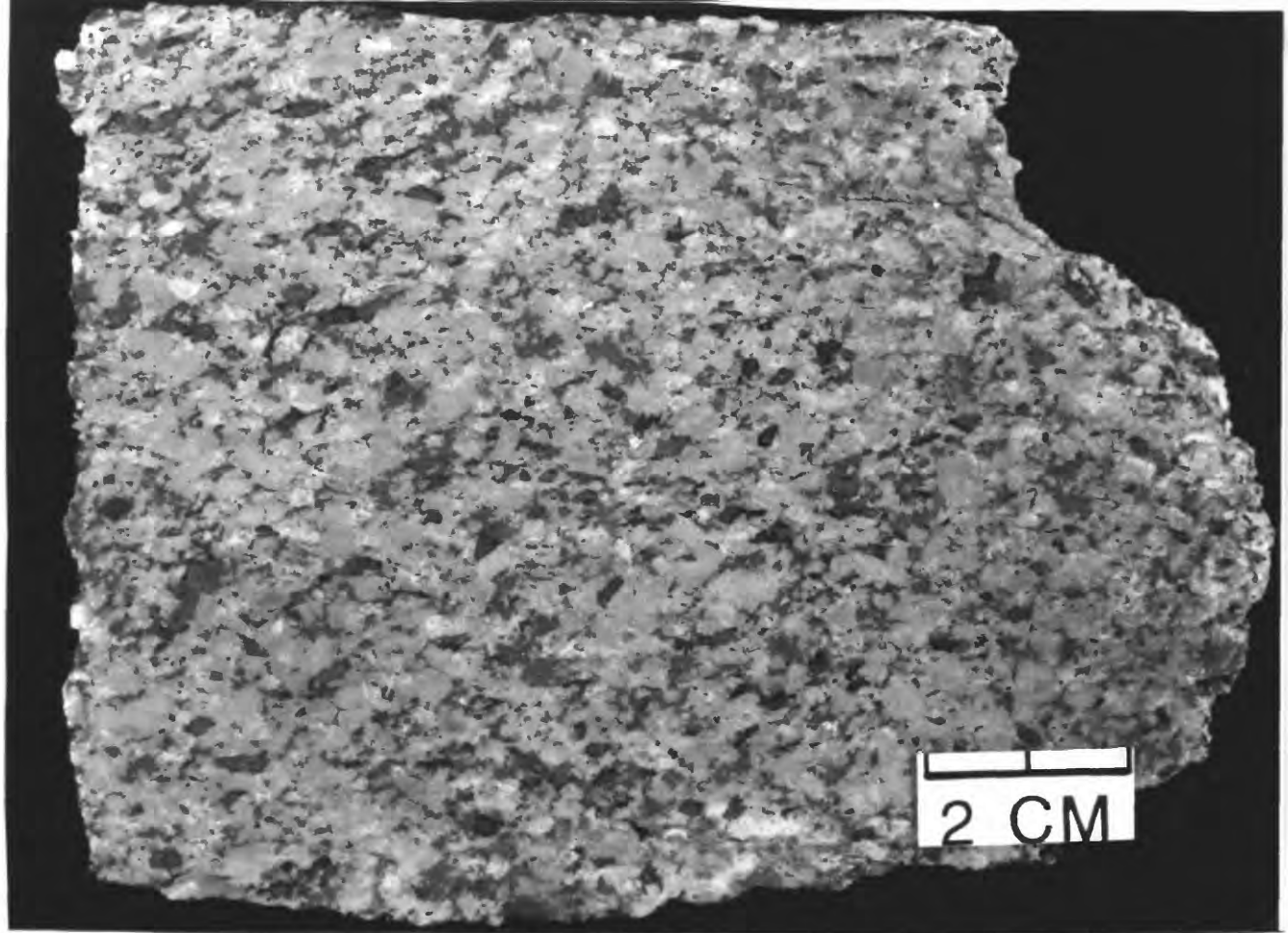
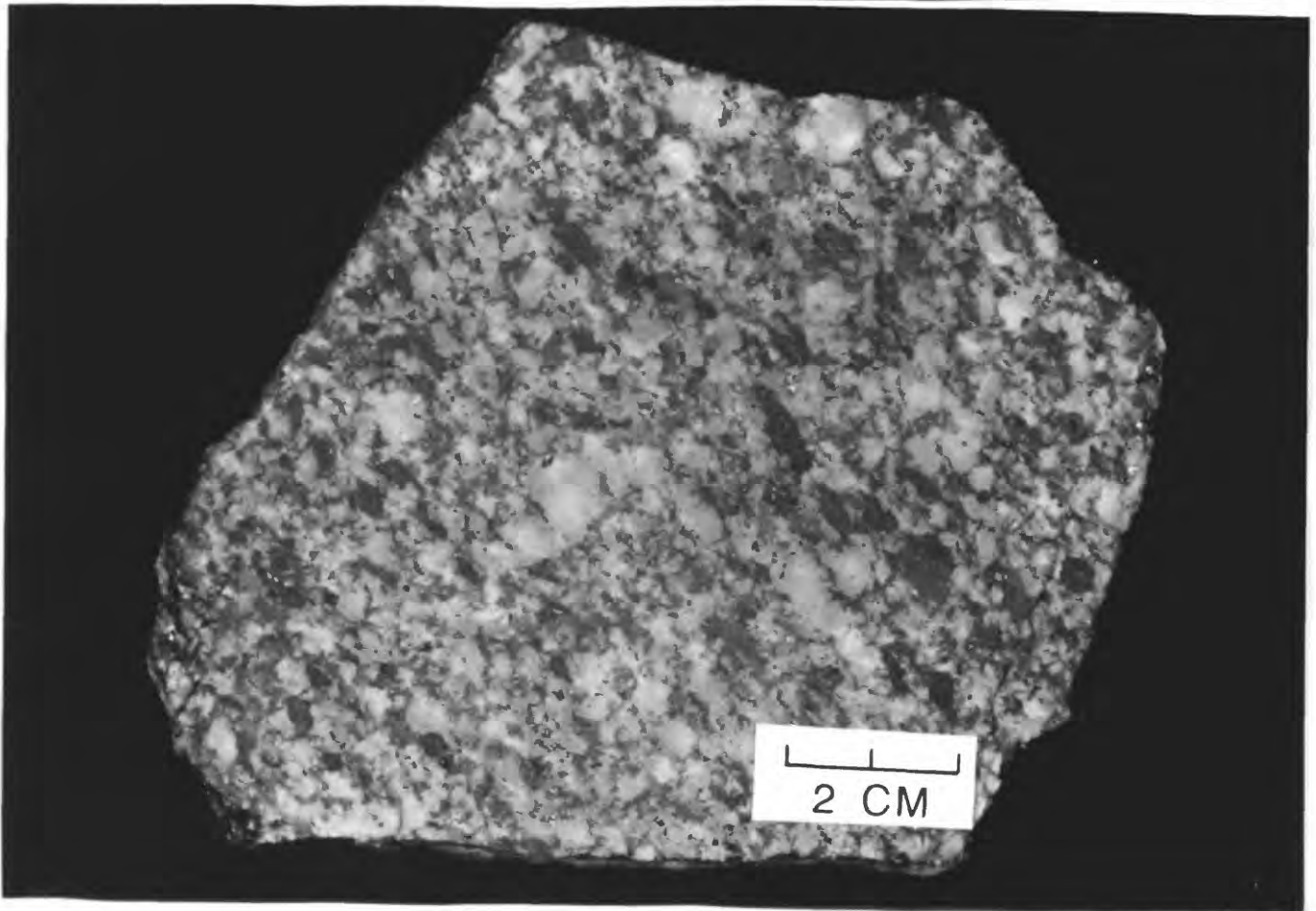


Figure 11. Modal composition of rocks from the Great tonalite sill belt, within the Taku Inlet transect: ●, Speel River pluton; *, Taku Cabin pluton. Rock classification from Streckeisen (1973): GR, granite; GD, granodiorite; TO, tonalite; QM, quartz monzonite; QO, quartz monzodiorite; QD, quartz diorite; MO, monzonite; MD, monzodiorite; and DI, diorite.



A



B

Figure 12. Photographs of typical rocks of the Great tonalite sill belt. *A*, stained slab of foliated, coarse-grained, equigranular tonalite from the Speel River pluton; *B*, stained slab of strongly foliated to nearly gneissic quartz diorite of the southwest margin of the Speel River pluton.

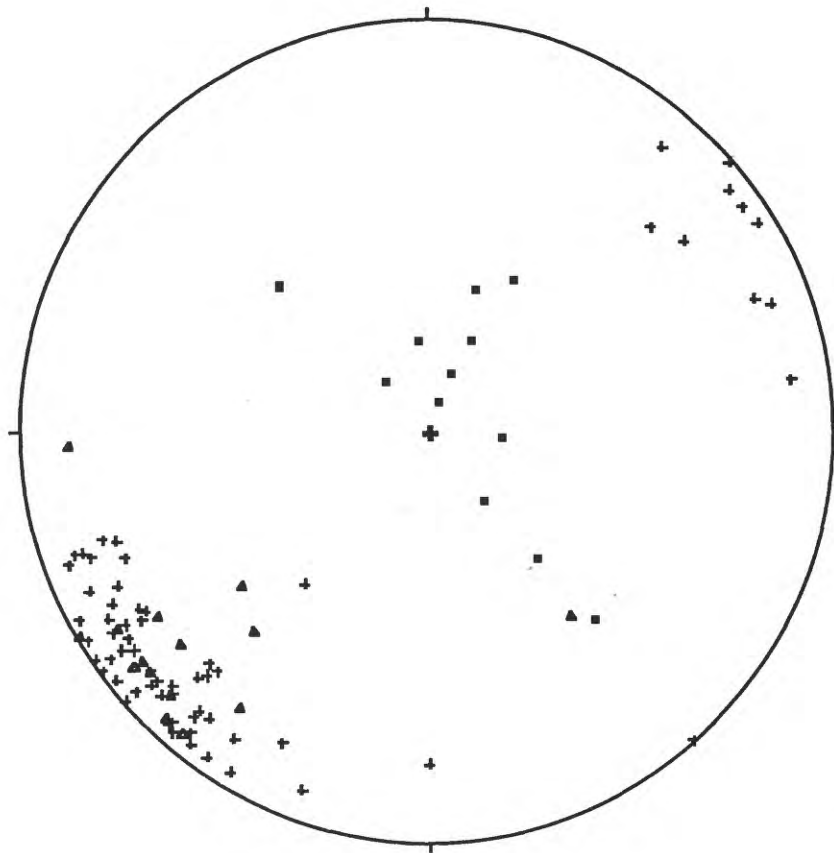


Figure 13. Schmidt equal area projection of foliations and lineations measured from plutons of the Great tonalite sill belt within the Taku Inlet transect. Symbols: +, foliations in Speel River pluton; ▲, foliations in Taku Cabin pluton; and ■, lineations in Speel River pluton.

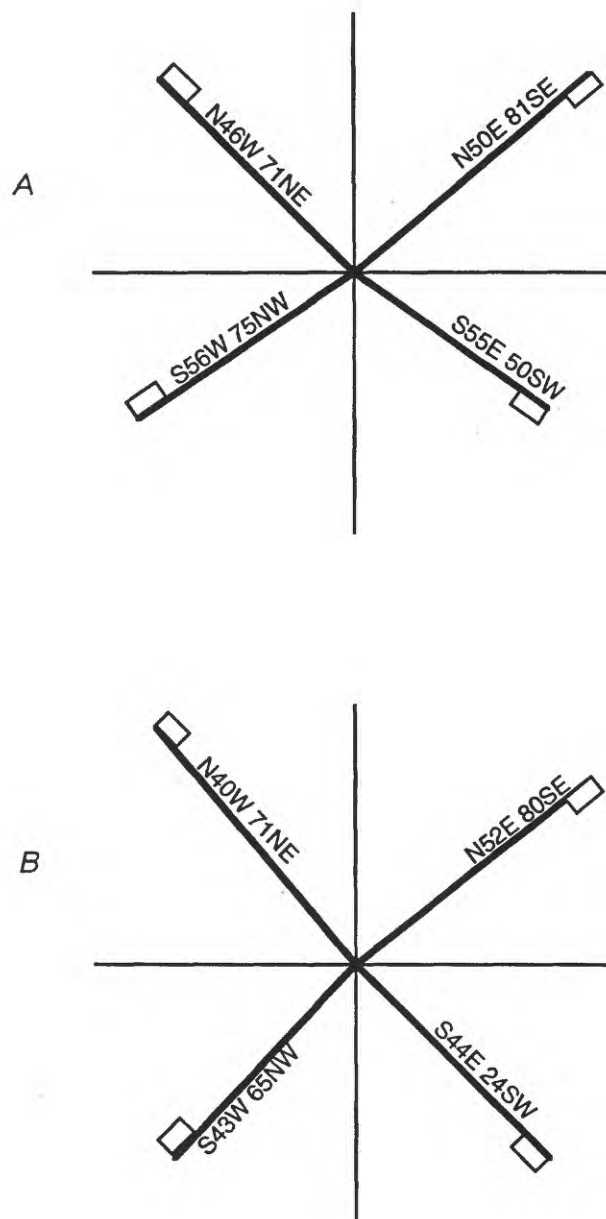


Figure 14. Synthesis of prominent joint sets in plutons of the Great tonalite sill belt. *A*, northern part; *B*, southern part.

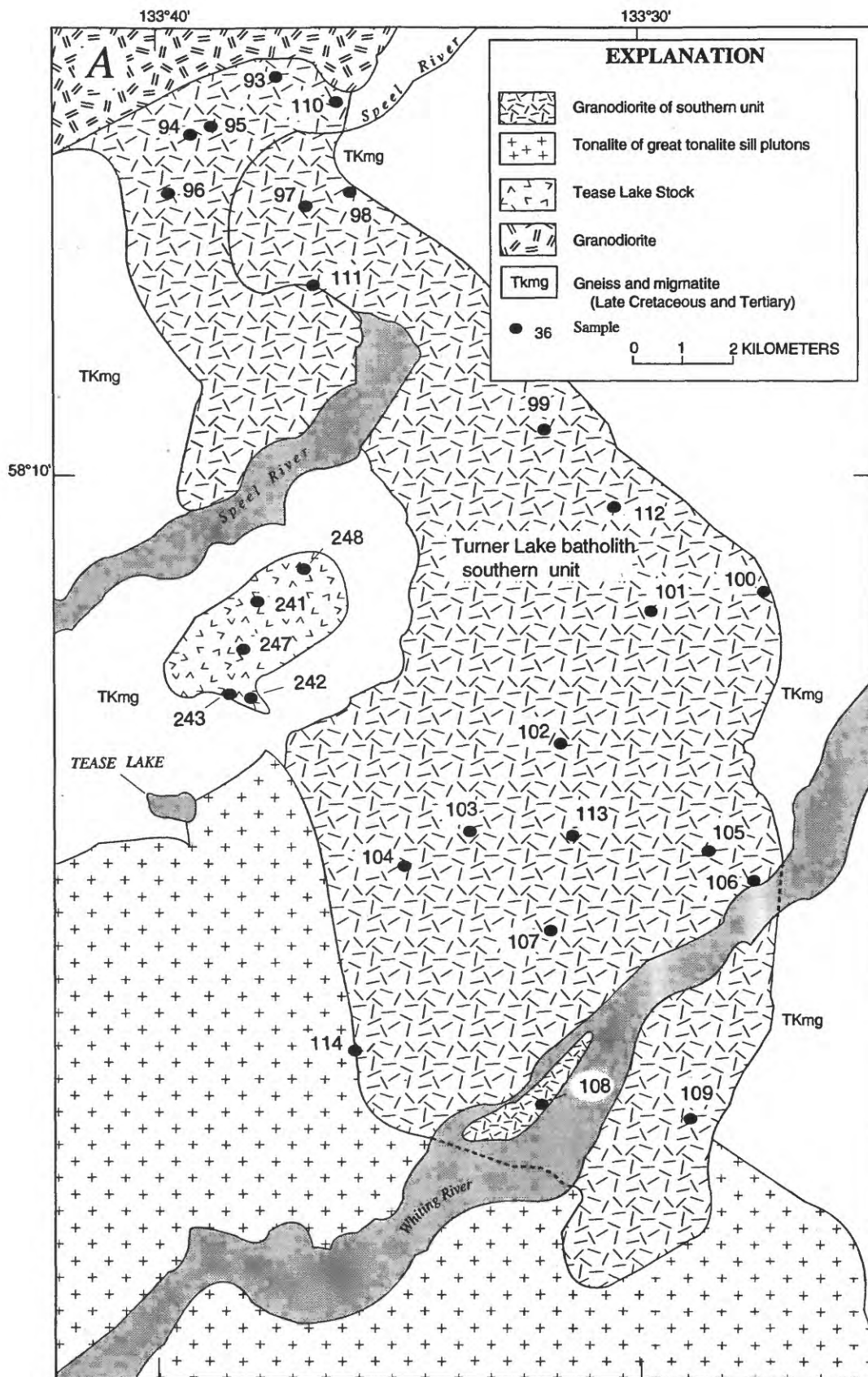


Figure 15. Generalized geologic maps of plutonic units that comprize the western subbelt of the Turner Lake batholith: A , southern unit; B , central unit; C , northern unit. Sample locations shown by numbered dots.

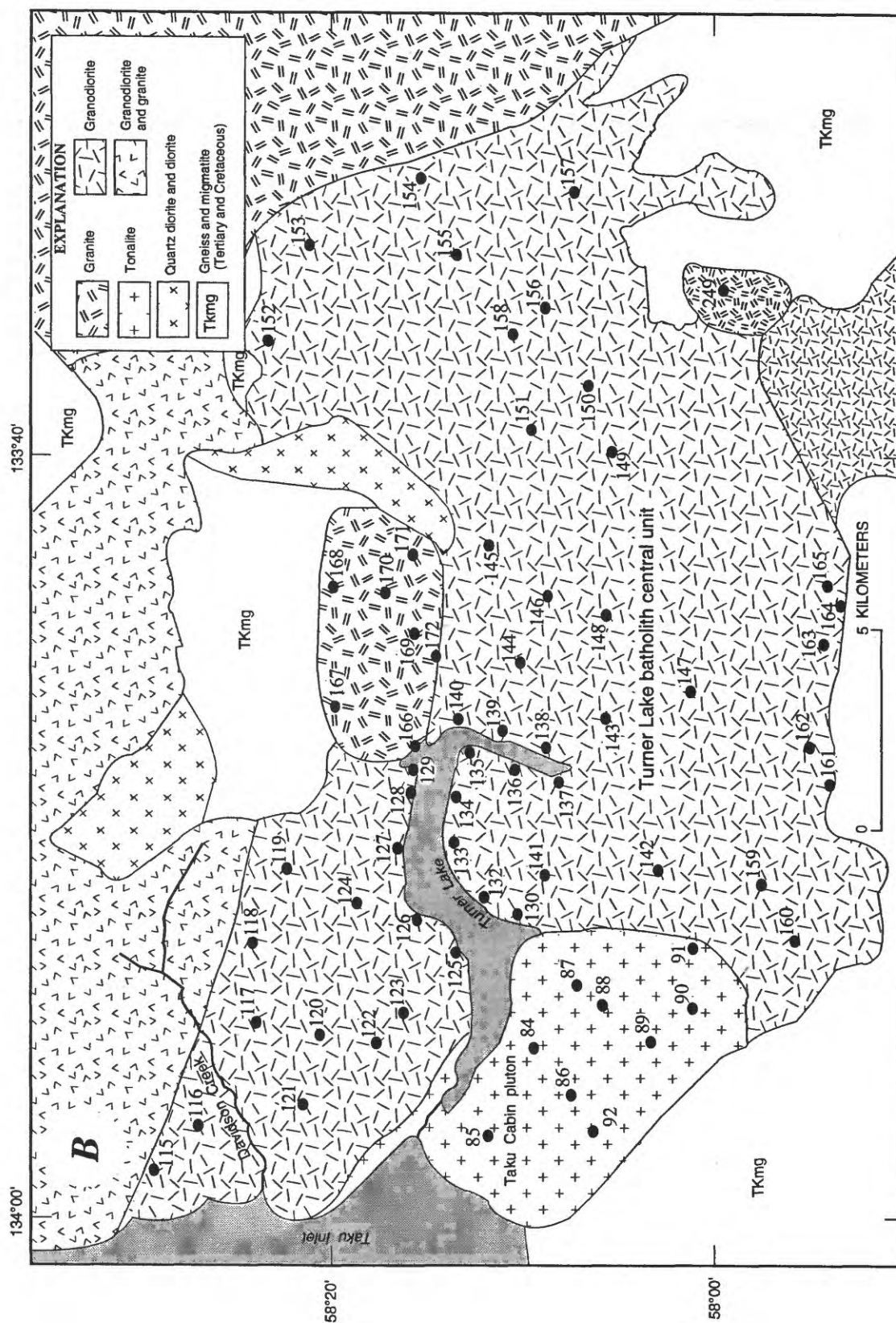


Figure 15 Generalized geologic maps of plutonic units that comprise the western subbelt of the Turner Lake batholith: A, southern unit; B, central unit; and C, northern unit. Sample locations shown by numbered dots. Taku Cabin pluton also shown.

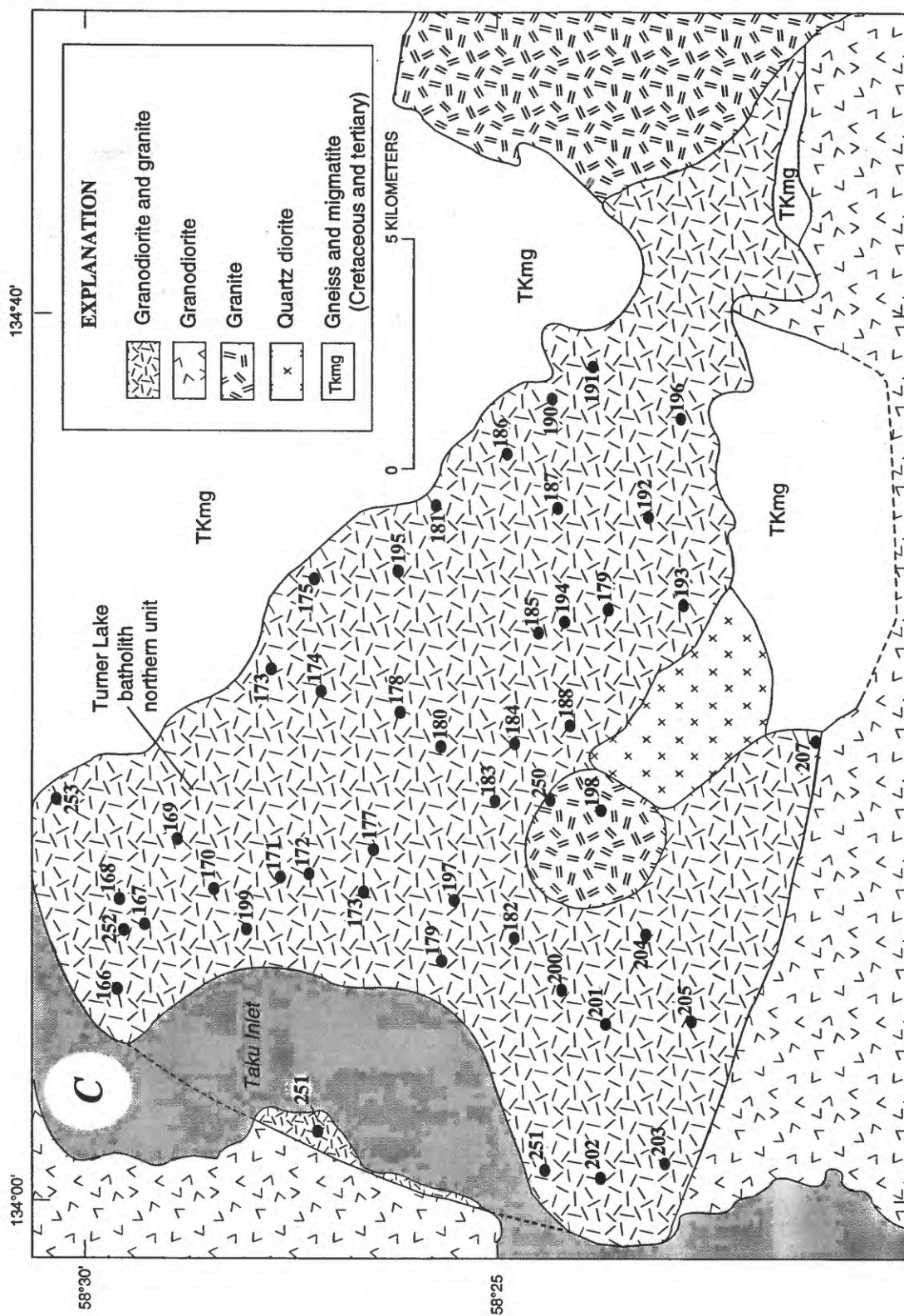


Figure 15. Generalized geologic maps of plutonic units that comprise the western subbelt of the Turner Lake batholith: A, southern unit; B, central unit; and C, northern unit. Sample locations shown by numbered dots.

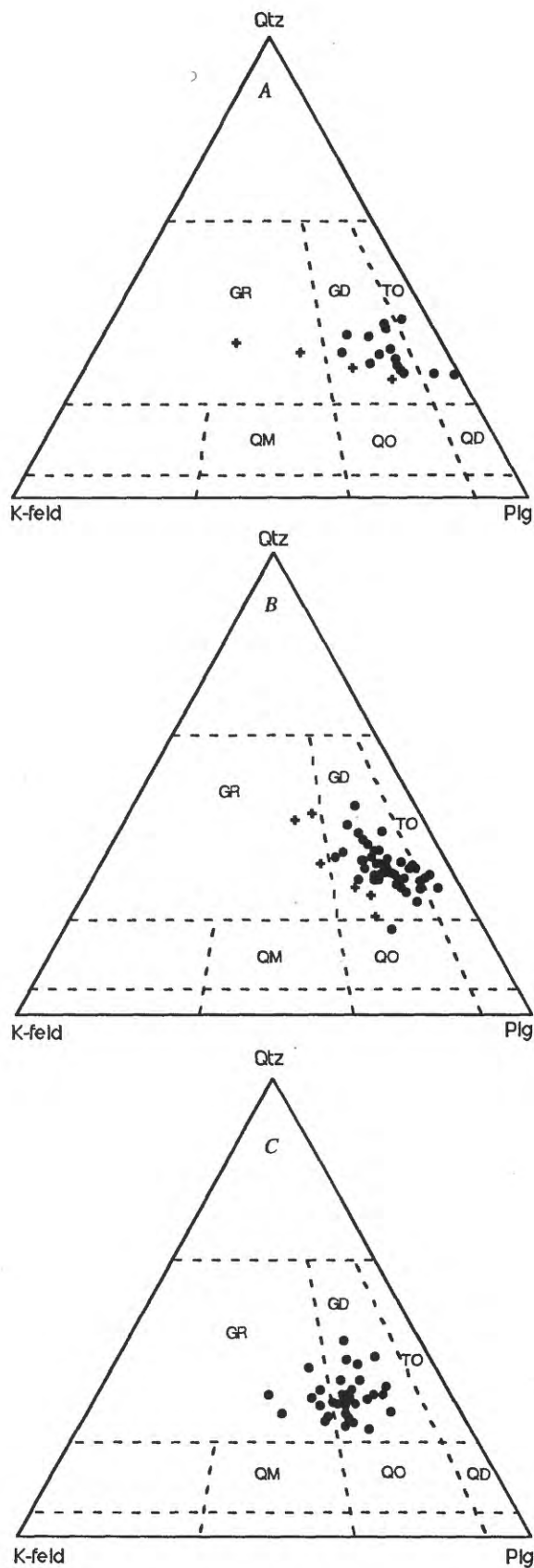
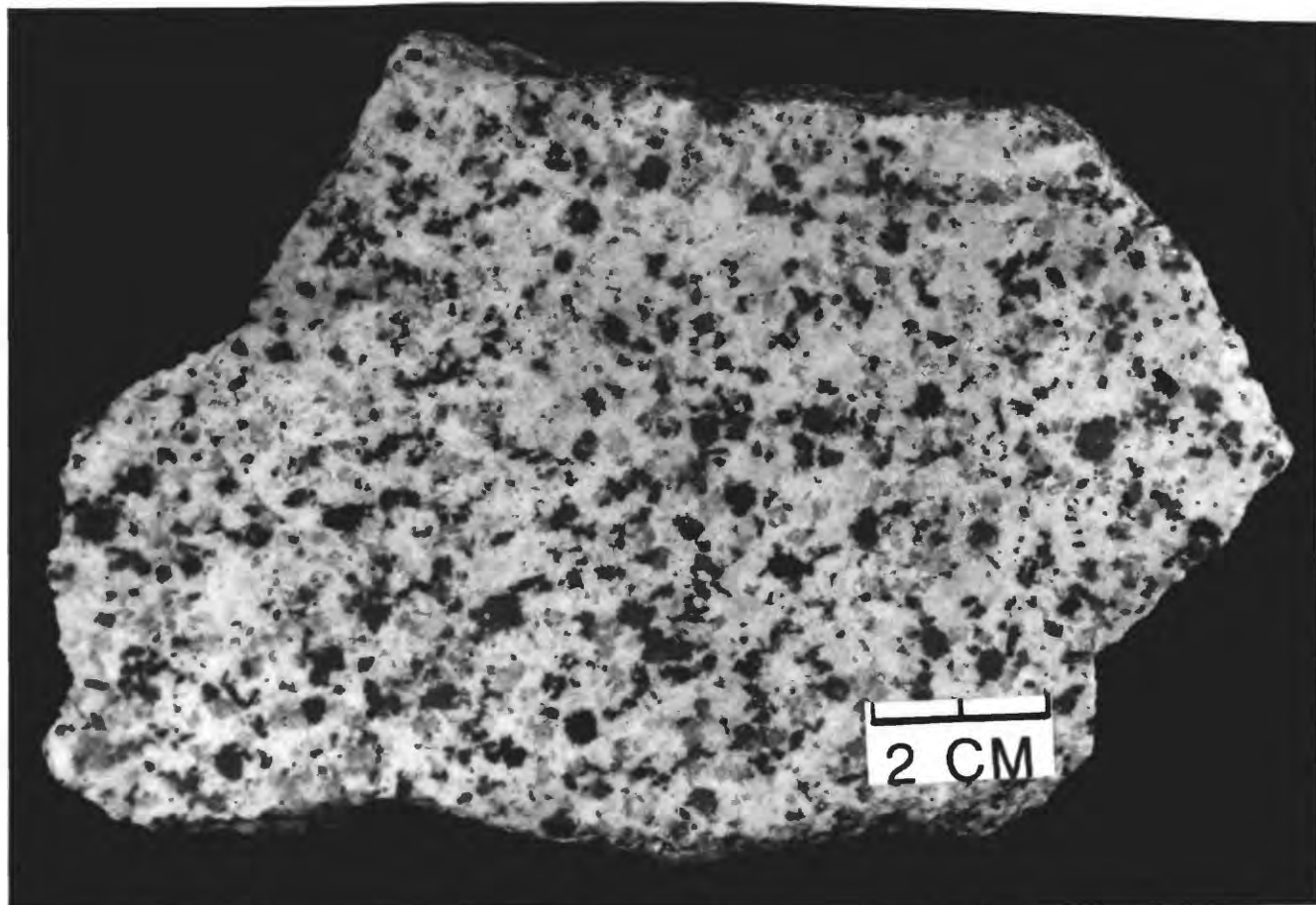
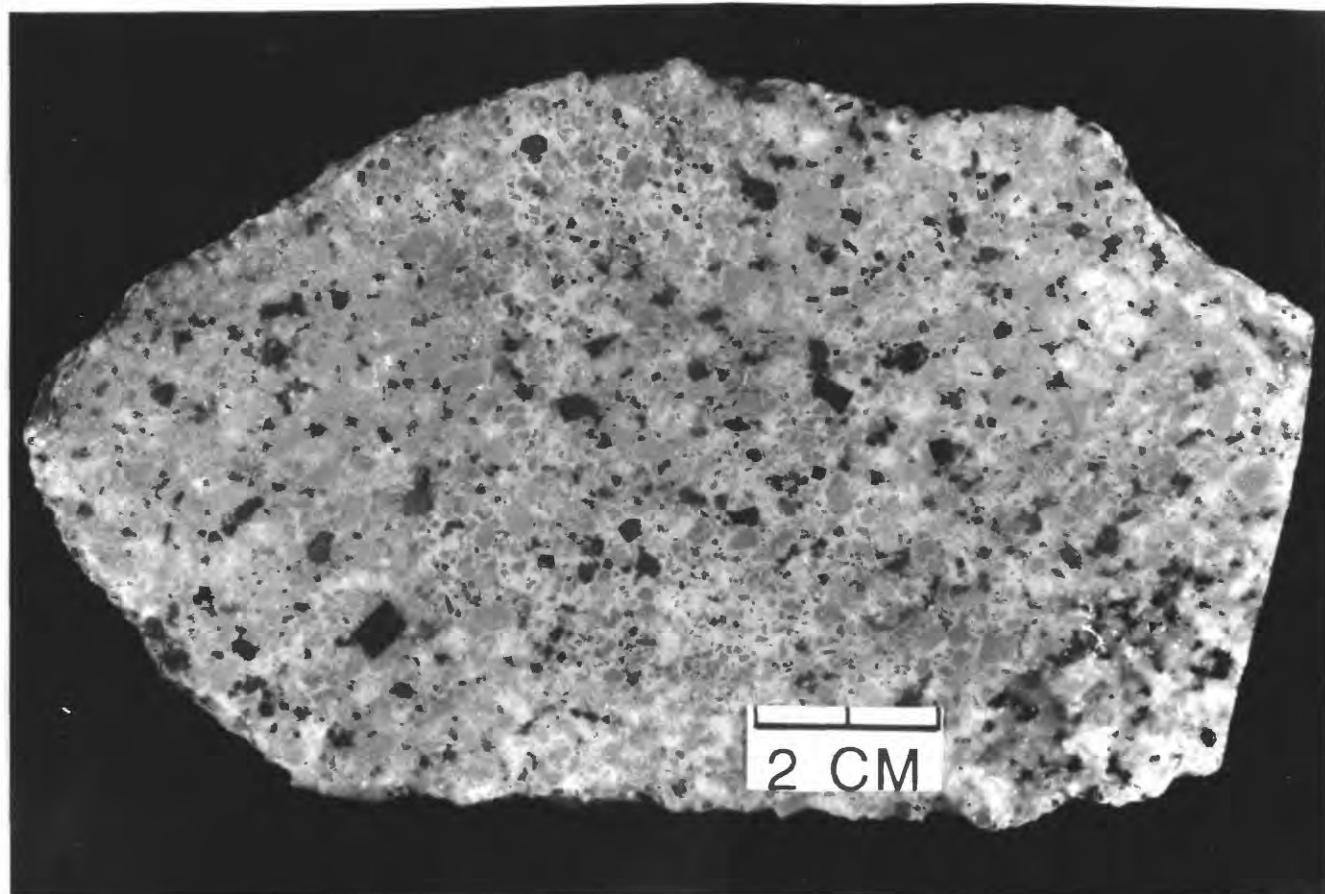


Figure 16. Modal composition of rocks from the western units of the Turner Lake batholith: *A*, southern unit; ●, main phase rocks, +, dikes; *B*, central unit; and *C*, northern unit. Rock classification from Streckeisen (1973): GR, granite; GD, granodiorite; TO, tonalite; QM, quartz monzonite; QO, quartz monzodiorite; QD, quartz diorite; MO, monzonite; and DI, diorite.

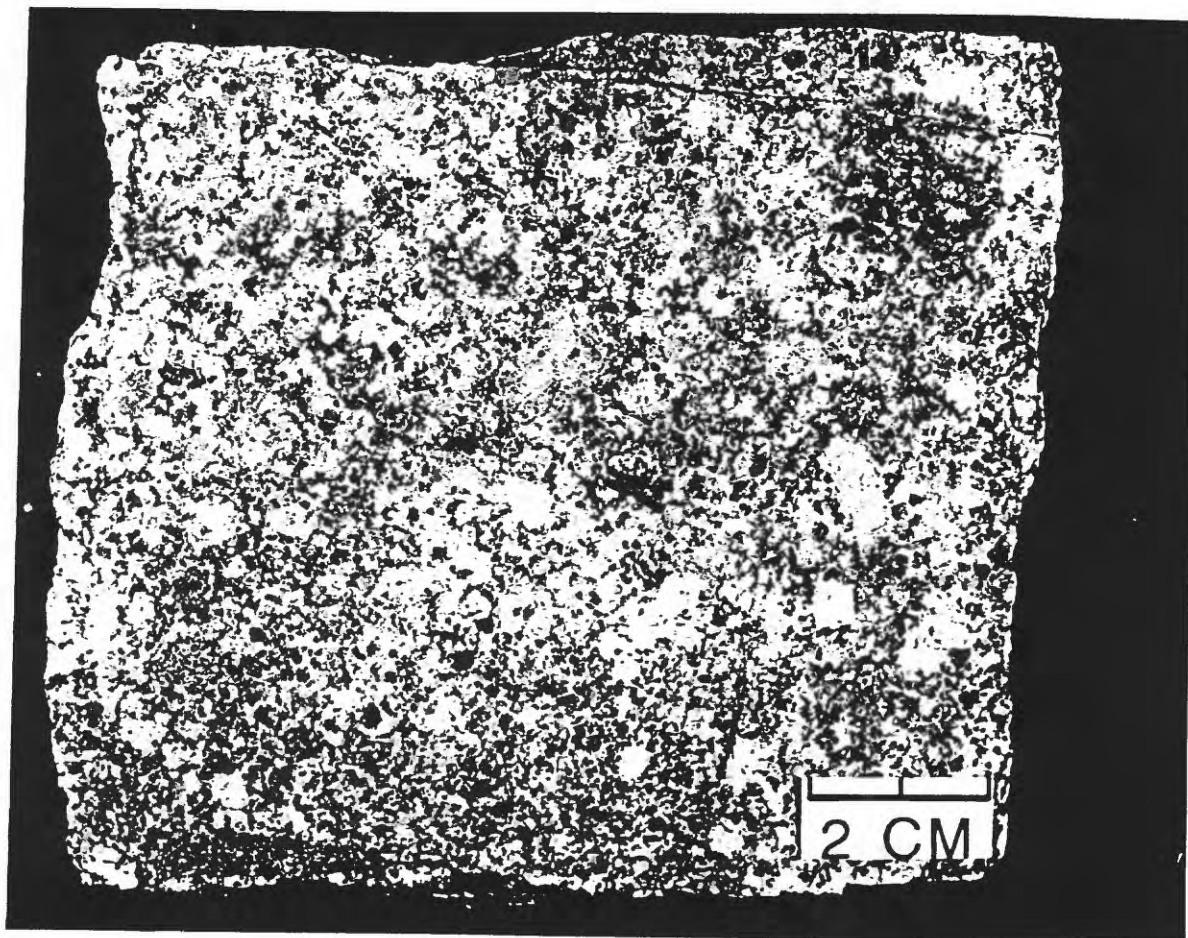


A



B

Figure 17. Photographs of representative rocks from the western units of the Turner Lake batholith: *A*, slab of typical massive, equigranular granodiorite from the southern unit; *B*, stain slab of typical massive, granodiorite from the central unit; and *C*, stain slab of typical massive seriate to slightly porphyritic granodiorite from the northern unit.



C

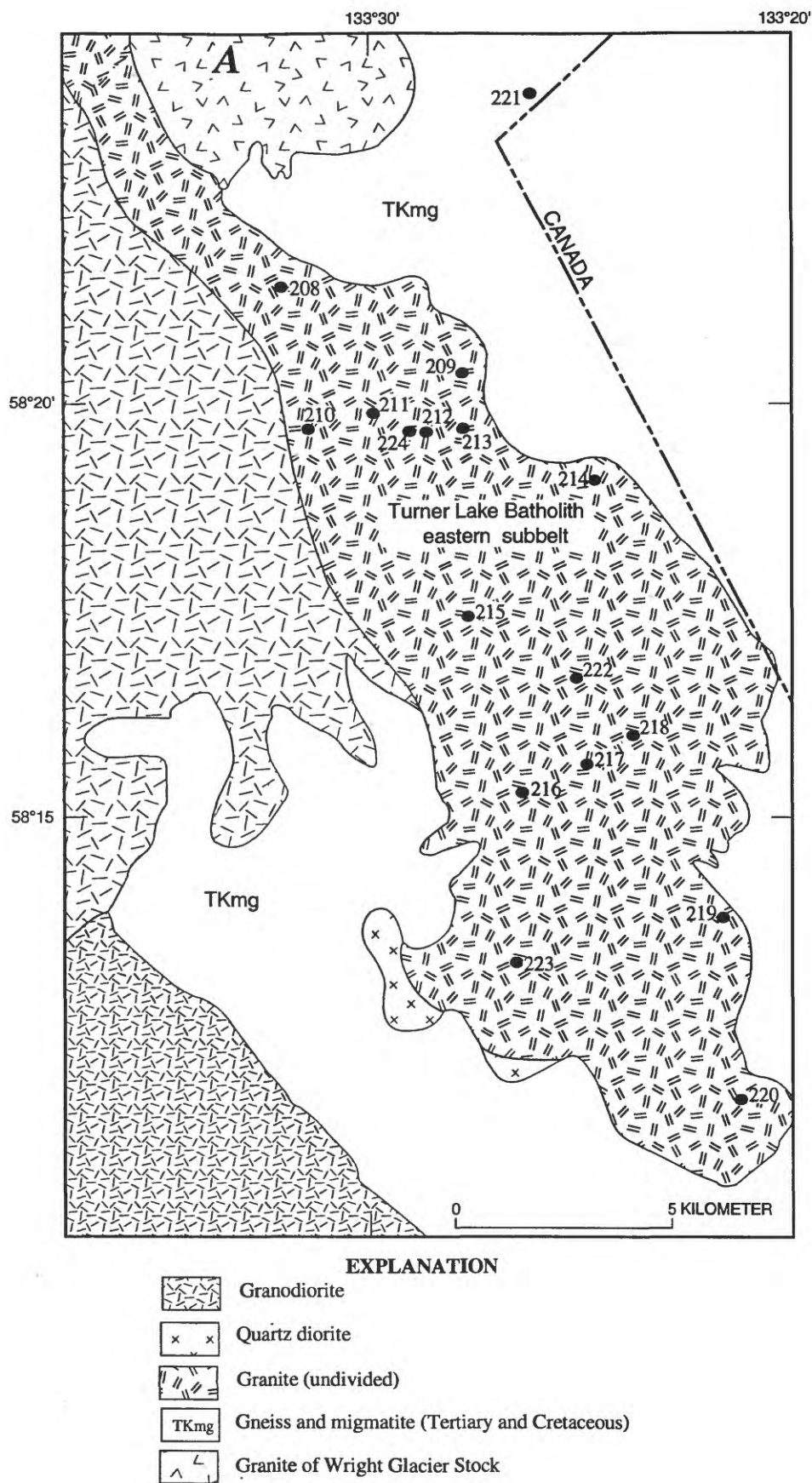
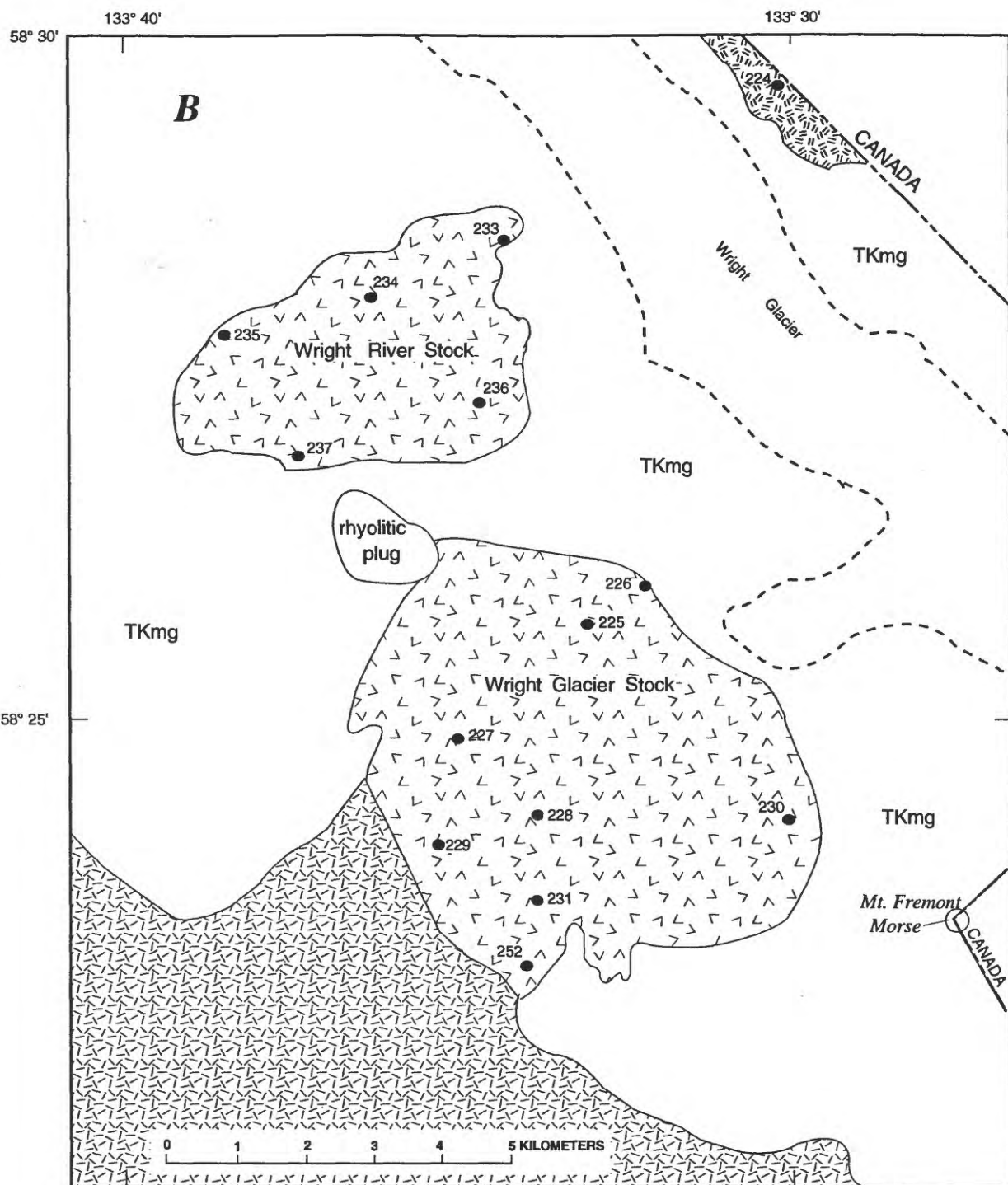


Figure 18. Generalized geologic maps of plutonic units from the eastern part of the Coast Mountains belt (Turner Lake batholith) along the Taku Inlet transect, showing sample locations (numbers and dots). A, undivided granite unit; B, Mid-Tertiary stocks.



EXPLANATION

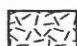
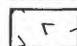

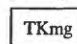
-  Granodiorite and granite, undivided
-  Granitic stocks
-  Granite of eastern unit
-  Gneiss and migmatite (Tertiary and Cretaceous)

Figure 18. Generalized geologic maps of plutonic units from the eastern part of the Coast Mountains belt (Turner Lake batholith) along the Taku Inlet transect, showing sample locations (numbers and dots).
A, undivided granite unit; *B*, Mid-Tertiary stocks.

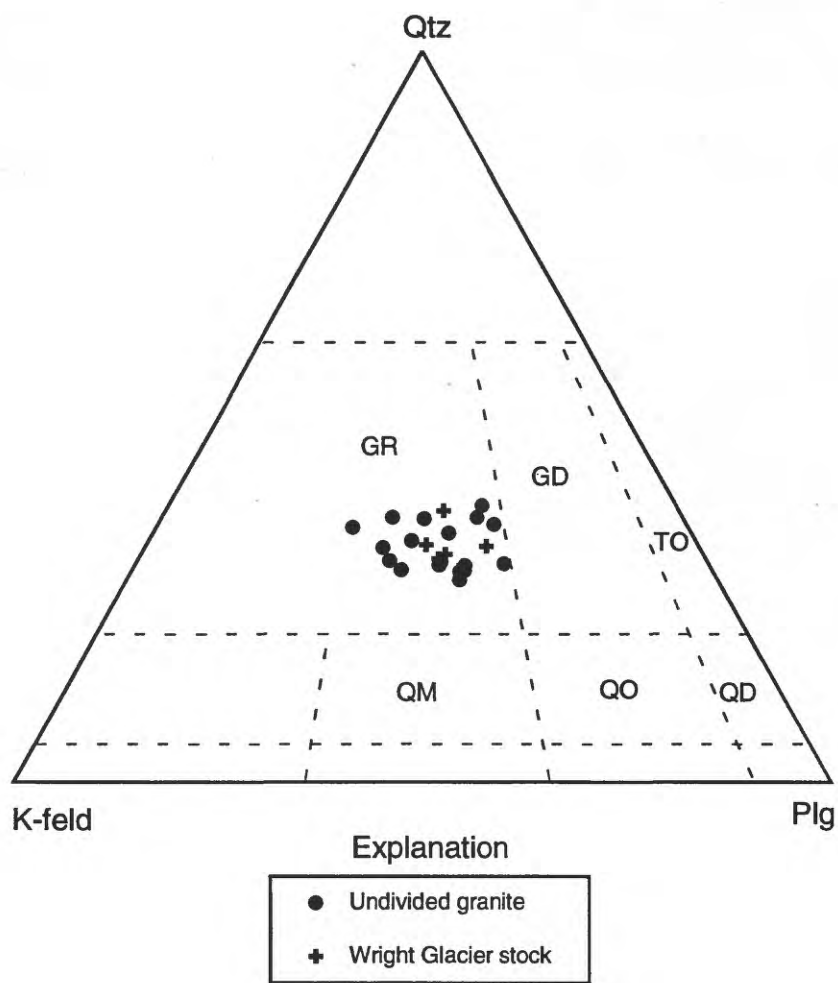
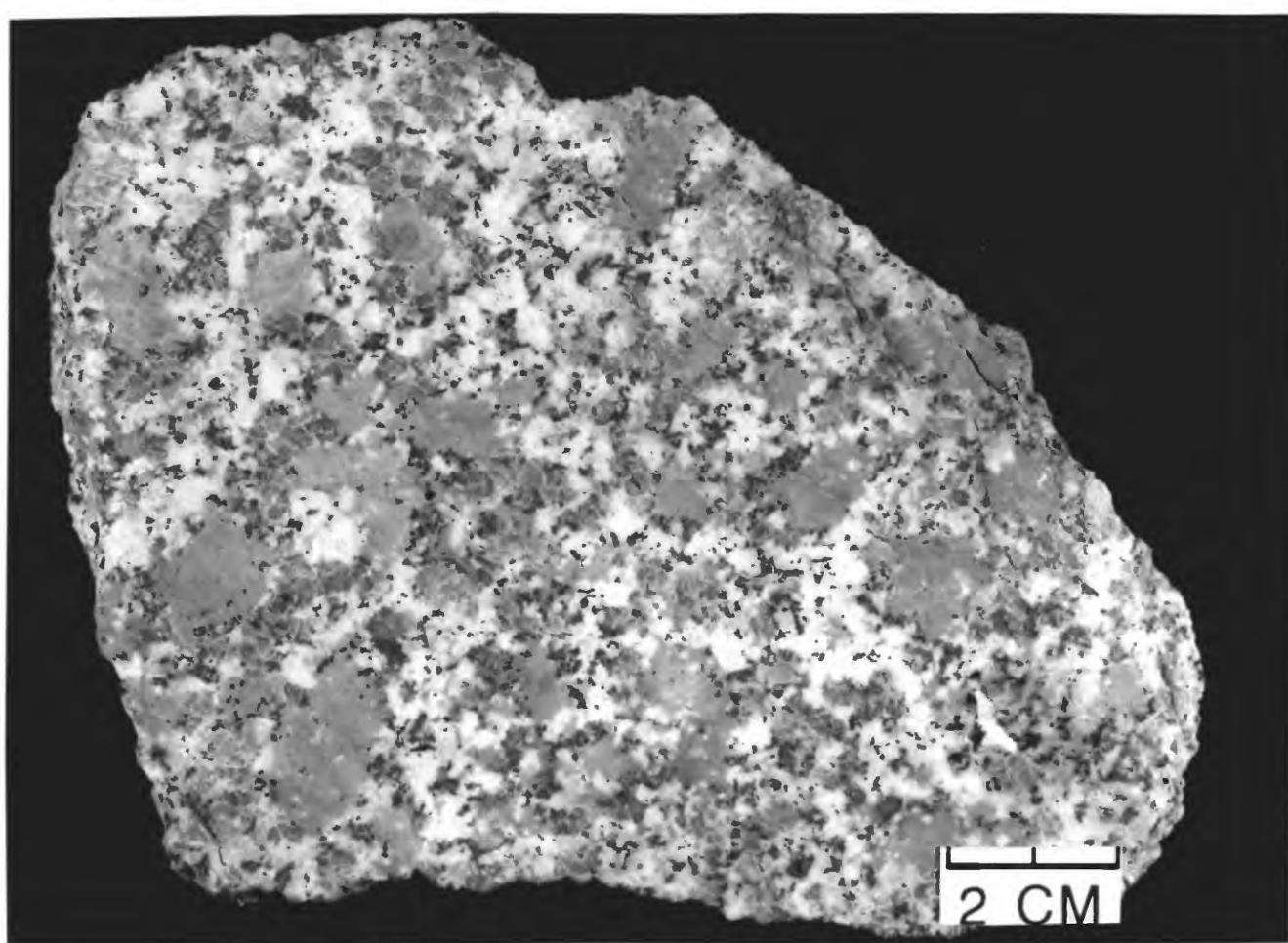


Figure 19. Modal composition of rocks from the eastern subbelt of the Turner Lake batholith. Rock classification from Streckeisen (1973): GR, granite; GD, granodiorite; TO, tonalite; QM, quartz monzonite; QO, quartz monzodiorite; and QD, quartz diorite;



A



B

Figure 20. Photographs of representative rocks from the eastern units of the Turner Lake batholith: *A*, stain slab of typical massive, coars-grained, porphyritic granite of the undivided granite unit; *B*, slab of typical massive, medium-grained, seriate granite of the Wrights Glacier stock.

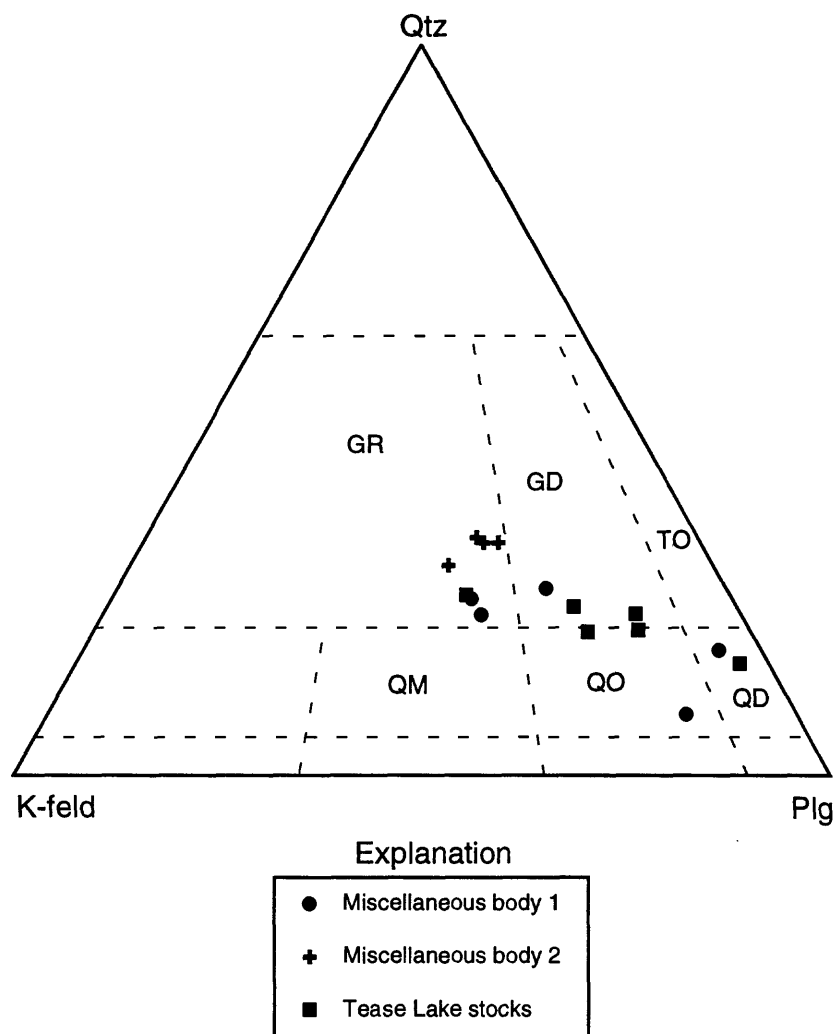


Figure 21. Modal composition of rocks from miscellaneous plutonic bodies associated with the Turner Lake batholith. Rock classification from Streckeisen (1973): GR, granite; GD, granodiorite; TO, tonalite; QM, quartz monzonite; QO, quartz monzodiorite; and QD, quartz diorite.

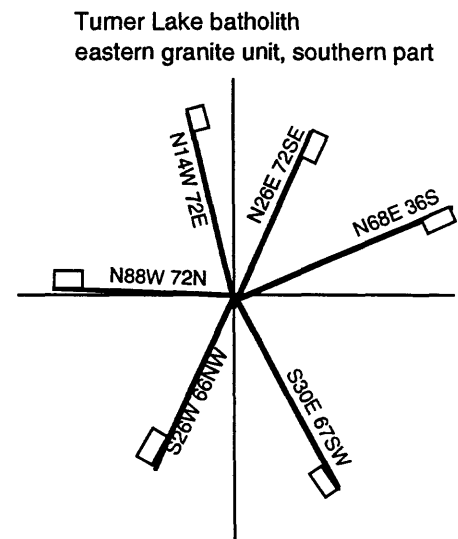
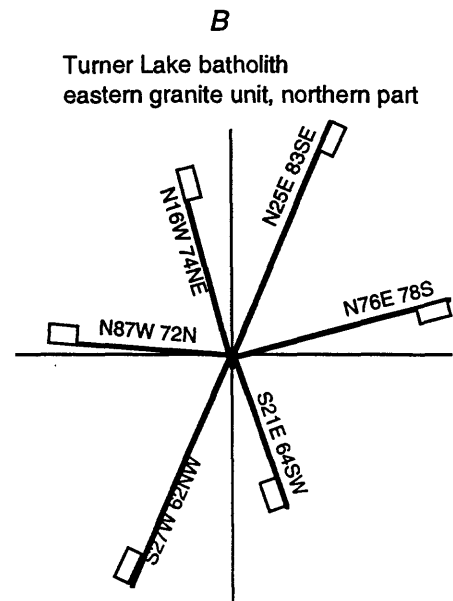
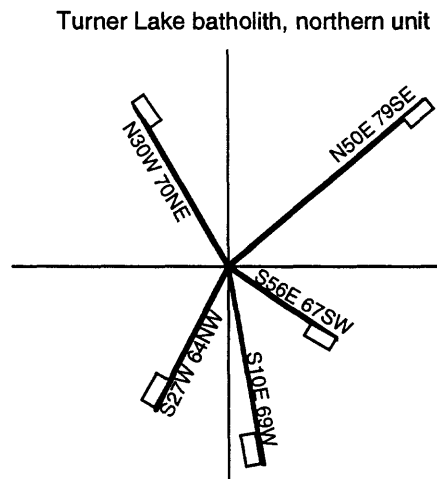
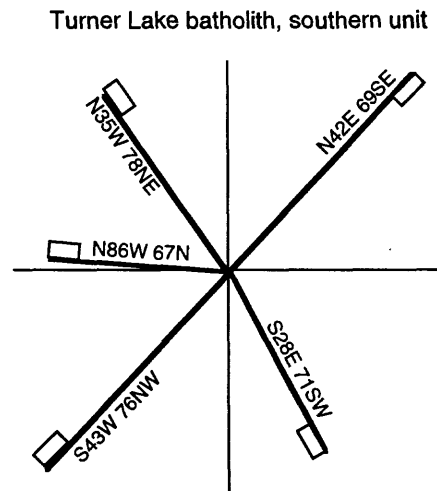
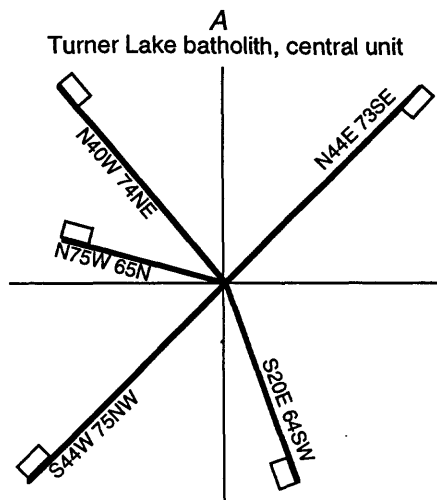


Figure 22. Synthesis of prominent joint sets for plutons of the Turner Lake batholith. A, western subbelt units of the Turner Lake batholith. B, undivided granite of eastern subbelt of the Turner Lake batholith.

where investigated, are foliated, medium-grained, slightly porphyritic biotite-hornblende quartz diorite or granodiorite with a color index of 25 to 35. The rocks consist of medium- to coarse-grained crystals, phenocrysts, and glomerocrystic clots of plagioclase, intergranular quartz, and fine- to medium-grained mafic minerals. Magnetite is relatively common, and sulfides occur in some crystals of magnetite.

Tease Lake stocks: Two small foliated intrusions lie east of the Speel River, near Tease Lake (fig. 4). These stocks are heterogeneous bodies that vary considerably in composition and texture. They are weakly to strongly foliated and locally show gneissic banding. The stocks have discordant intrusive contacts with the country rocks and the southern stock shows discordant intrusive contacts with the Speel River pluton. Foliations within the southern stock trend northeast and normal to the regional fabric and structure, whereas the foliations in the northern stock trend northwest, conformable to the regional structure. The stocks are composed largely of quartz monzodiorite and granodiorite but range from quartz diorite to granite in composition (fig. 21).

The rocks of the Tease Lake stocks are mostly medium- to coarse-grained, porphyritic and allotriomorphic granular in texture. The rocks are generally partly altered and show deformational textures. Plagioclase comprises 39 to 65 percent of the rocks and forms anhedral to subhedral, strained, weakly zoned, and partly altered crystals of calcic oligoclase (An₂₉₋₃₃). K-feldspar varies considerably in abundance (3-29 percent) and forms inclusion-rich, anhedral phenocrysts of perthitic orthoclase in most rocks. Quartz makes up 12 to 22 percent of the rocks and occurs as anhedral, strained, and, in places recrystallized crystals. Hornblende and biotite are the major mafic minerals and comprise 7 to 20 percent of the rocks. They form fine- to medium-grained intergranular crystals. Much of the biotite is altered to chlorite. Titanite is the most common accessory mineral; it forms discrete, well-developed euhedral crystals. Magnetite, apatite, and zircon are other common accessory minerals.

GEOCHEMISTRY

Major-element chemical analysis and minor-element (Nb, Rb, Sr, Zr, Y, Ba, and Zn) concentrations are presented in tables 15 to 20. The chemical characteristics and variations of each subbelt are described under separate sections with Harker diagrams presented for each belt. Additionally, a diagrammatic representation of INAA determined trace elements (U, Th, Hf, Ta, Cs, Sc, Cr, and Co) is also provided. Chondrite-normalized rare-earth element distribution diagrams are also given for plutons from each subbelt, and were constructed using representative samples with the highest and lowest REE abundances and several intermediate REE abundance bearing samples. The light/heavy REE fractionation values used in this report are represented by normalized Ce/Yb ratios.

The chemical distinction between rocks of the three plutonic belts was summarized in Drinkwater and others (1994). Rocks of the three plutonic belts are metaluminous to slightly peraluminous, subalkaline, and calc-alkalic in nature (Brew, 1988; Drinkwater and others, 1994), but chemical plots of rocks from the Admiralty-Revillagigedo belt cluster separately from rocks of the mainland plutonic belts (Great tonalite sill and Coast Mountains belts) on many diagnostic variation diagrams (Drinkwater and others, 1994). Rocks from the Admiralty-Revillagigedo belt are low in silica (fig. 23), and when compared with silica-equivalent rocks of the mainland belts they have lower aluminum saturation indexes (fig. 24), higher alkali contents (fig. 25) and FeO*/MgO ratios (fig. 26). On the non-silica based AFM diagram (fig. 27), rocks of the Admiralty-Revillagigedo belt plot as a separate but parallel

calc-alkalic trend with more iron-rich compositions, and on the normative feldspar composition diagram (fig. 28) they cluster along the K-rich boundary line, whereas the rocks of the mainland belts show a coherent linear distribution within the normal alkali composition field. Rocks of the Admiralty-Revillagigedo belt are generally more enriched in CaO (fig 29) and Sr (fig. 30), but contain relatively low abundances of uranium and thorium (fig. 31), and moderately high abundances of the transition metals (Sc, Cr, and Co). These disharmonic petrogenetic trends support age and isotopic evidence (Barker and Arth, 1990) that separates the Admiralty-Revillagigedo belt plutons as an unrelated magmatic episode from the mainland plutonism east of the megalineament. All the plutons plot as volcanic arc granitoids on the tectonic-affinity diagram of figure 32.

Admiralty-Revillagigedo Belt

Plutons of the Admiralty-Revillagigedo (plutonic belt) within the transect can be separated into two groups or subbelts by distinct chemical traits (figs. 25, 26, 28, 29, and 30). The Grand Island subbelt consists of a highly varied suite of plutons (fig. 33) that range from the more mafic Irving Peak pluton (48-58 percent SiO₂) to the felsic Butler Peak pluton (66-68 percent SiO₂), whereas the plutons of the Taku Harbor subbelt are more uniform rocks of intermediate composition that have a more restricted SiO₂ range (58-64 percent). The higher Fe*/Ti values (>7) from plutons of the Grand Island subbelt clearly separates them from the low Fe*/Ti rocks of the Taku Harbor subbelt (fig 33). The plutons of the Taku Harbor subbelt contain higher abundances of total alkalis, K₂O, Rb, Sr and Ba as well as higher FeO*/MgO ratios and generally higher TiO₂ content (table 13) than silica-equivalent rocks of the Grand Island subbelt (Glass peninsula stocks and Grand Island pluton). When the chemical differences between these two subbelts are viewed with their differences in magnetic susceptibility, mineralogy, and modal compositions, it is evident that the plutons of the two subbelts had evolved under different magmatic conditions.

Grand Island subbelt

The three small plutons and cluster of five stocks that form the Grand Island subbelt are distinguished from each other by chemical traits. For comparison purposes, the stocks of the Glass Peninsula are grouped as a single unit because they are very similar in modal and chemical compositions (tables 5, 15). The stocks are composed of alkali- and iron-rich quartz diorite and tonalite (table 15) that are distinguished from other plutons of the subbelt by their intermediate silica content (58 to 63 percent) and high K₂O/Na₂O ratios (fig 33 B). The Irving Peak pluton, with its low silica and high TiO₂ and ferromagnesian contents (table 15) is the most mafic intrusion of the subbelt, whereas the Butler Peak pluton is the most siliceous and differentiated intrusion. All rocks when plotted on Harker diagrams (fig. 34) show a fairly coherent, linear or semi-linear distribution and inverse correlation with FeO*, MgO, CaO, Al₂O₃, and P₂O₅, although the Glass Peninsula stocks appear to form a separate trend with respect to TiO₂, Sr, and Zn.

The abundance of alkali elements in these rocks shows a scattered distribution (fig. 29) that is due largely to the K₂O content (figs. 33B). Na₂O is relatively high (>3.2 percent) and exceeds K₂O in all rocks; it exhibits a slight positive correlation with SiO₂ with much scatter. K₂O shows a moderate positive correlation with SiO₂, but rocks of the Glass Peninsula stocks show a rough negative correlation with much scatter. Many of the rocks exhibit a borderline K-rich trend on the ternary feldspar-composition diagram (fig. 28) although one sample of the Butler Peak pluton is borderline sodic-rich. The elevated abundance and scattered distribution of K₂O in these rocks is probably due to alteration and, in particular, to metasomatic addition of

K₂O. This enrichment in K₂O is more prevalent in the stocks of the Glass Peninsula than in the other plutons, and is manifested in the form of secondary muscovite.

The trace element abundances vary little between plutons of the Grand Island subbelt. The Sr content (600-970 ppm) is relatively high (fig. 31) in these rocks, but shows a scattered distribution with SiO₂ (fig. 34). The average Rb and Ba contents are relatively low (30-55 ppm and 450-700 ppm). The zinc content varies between 60 and 150 ppm and shows a moderate negative correlation with SiO₂ with much scatter (fig. 34).

The chondrite-normalized rare-earth element (REE) abundances for plutons of the Grand Island subbelt are similar (fig. 35); the rocks are highly enriched in light REEs (LREE) compared to the heavy REEs (La, 55-90 times chondrite, and Yb, 7-10 times chondrite), although there is a slight decrease in total REE abundances with an increase in SiO₂ content (fig. 35). The REE fractionation patterns are also generally similar, with all rocks forming a relatively steep semi-linear to slightly concave distribution. Rocks of the Glass Peninsula stocks and Grand Island pluton show a characteristic slight positive Tm spike. The lowest light/heavy REE fractionation values (normalized Ce/Yb=4.8 to 5.2) occur in rocks of the Grand Island and Irving Peak plutons, and the highest value is found in the more silicious Butler Peak pluton (Ce/Yb= 9.9). The Ce/Yb values of the Glass Peninsula stocks range from 6.8 to 7.8. The similar REE abundances and fractionation trends indicate a common source and magmatic evolutionary history for these plutons.

Taku Harbor subbelt

The two plutons that form the Taku Harbor subbelt are composed of relatively low silica and high K₂O rocks. Rocks from the Everett Peak pluton, with one exception, show very uniform compositions within the narrow silica range of 57.9 to 58.8 percent (table 16, fig. 34), whereas the Arthur Peak pluton is composed of more felsic rocks within the SiO₂ range of 60.8 to 64.1 percent (table 16, fig. 34). Both plutons are alkali-rich, but the Arthur Peak pluton contains lower concentrations of mafic elements (FeO*, MgO, CaO, and TiO₂), but when plotted on Harker diagrams the two plutons show a relatively coherent, linear distribution and negative correlation with FeO*, MgO, CaO, TiO₂, and P₂O₅ (fig. 34). The Everett Peak pluton also contains higher concentrations of Sr, Ba, Nb, and Y than the Arthur Peak pluton. The wider range in MgO, K₂O, and P₂O₅ content in comparison to the narrow range in other components shown for the Everett Peak pluton may be due to hydrothermal alteration.

REE abundances are higher in the Everett Peak pluton (La, 85-100 times chondrite) than in the Arthur Peak pluton (La, 48-65 times chondrite) but both plutons show similar REE distribution patterns (fig. 35) and light/heavy REE fractionation (Ce/Yb=5.1-6.3). The differences in REE abundances between the Everett Peak and Arthur Peak plutons correlates with major-element composition differences between the plutons (fig. 39). REE abundances decrease fairly systematically as the SiO₂ contents increase (fig. 34), similar to the REE trends in rocks of the Grand Island subbelt. REE depletion with differentiation of calc-alkalic rocks is attributed to fractionation of REE-rich accessory phases such as titanite and apatite (Miller and Mittlefehldt, 1982; Sawka and others, 1984). Rocks of the Taku Harbor subbelt show slightly less REE fractionation than rocks of the Glass Peninsula stocks (Ce/Yb=6.8-7.8) but are slightly more fractionated than rocks of the Grand Island and Irving Peak plutons (Ce/Yb=4.8-5.2), however, they exhibit similar semi-linear or slightly warped distribution patterns. The highest concentrations of heavy REE occur in the Everett Peak pluton and reflects the abundance of primary titanite in rocks of this pluton.

Mainland Plutonic Belts

The two major plutonic belts of the mainland Coast Range mountains represent a cogenetic, calc-alkalic magmatic suite (Brew, 1988; Drinkwater and others, 1994). The more mafic-rich foliated tonalites and quartz diorites of the Great tonalite sill belt (western subbelt) contrast sharply with the more felsic-rich and massive granodiorites and granites of the Coast Mountains belt. Chemically, rocks of the Great tonalite sill generally contain lower SiO_2 (59 to 65 percent) and alkalis (figs. 25B, 39A), and higher ferromagnesian contents (fig. 36) than the more silica-rich (65 to 72 percent) and K_2O -abundant rocks of the Coast Mountains belt. Both belts form coherent, continuous, linear distribution patterns on the Harker diagrams (fig. 41) that are typical of calc-alkalic continental-margin plutonic suites. Both belts do contain tonalites with overlapping SiO_2 contents (62-65 percent), but the tonalites of the Coast Mountains belt contain higher abundances of TiO_2 , and Sr, slightly higher contents of K_2O , FeO^* , and Y, and lower CaO content than silica-equivalent rocks of the Great tonalite sill (Table 21, fig. 39). These differences between silica-equivalent rocks from the two belts imply differences in magmatic evolution and fractionation history. The two belts produce a curvi-linear distribution when plotted on the alkali/CaO versus SiO_2 diagram (fig. 37) with a deflection point at 65 percent SiO_2 . On the AFM diagram (fig. 27B) the two belts exhibit a fairly tight, continuous and nearly linear distribution and calc-alkalic trend. The three subbelts are clearly distinguished by their relative Fe^*/Ti (molecular proportions) values (fig. 38); low-silica rocks of the Great tonalite sill show higher Fe^*/Ti values (>7) than the felsic rocks of the western subbelt of the Turner Lake batholith (<7). Together, the Fe^*/Ti values of these two suites show a negative correlation with SiO_2 content whereas rocks of the eastern subbelt (Turner Lake batholith) produce a steep positive trend (fig. 38). Rocks of the Great tonalite sill belt contain much lower abundances of uranium, thorium, cesium, and tantalum, but higher abundances of transition metals (Sc, Cr, and Co) than rocks of the Coast Mountains belt (fig. 30).

Great Tonalite Sill Belt

Rocks of the Speel River and Taku Cabin plutons are typical granitoids of the western subbelt of the Great tonalite sill belt (Brew, 1988; Drinkwater and others, 1994). The plutons consist largely of metaluminous, calc-alkalic rocks of intermediate composition (59-66 percent SiO_2) although some rocks of more siliceous composition (>71 percent SiO_2) occur as thin layers or lenses of granodiorite. Rocks with 66 to 71 percent silica content are absent in these plutons. In comparison to other belt rocks, the main-phase rocks of the Speel River and Taku Cabin plutons are relatively low in alkali content and have higher CaO and ferromagnesium contents. The relatively high Ca and Sr contents are attributed to higher amounts of plagioclase, and the low K and Rb contents reflect the very low abundance of K-feldspar. Main-phase rocks exhibit a narrow range in their differentiation Index (fig. 39B) and in TiO_2 content (fig. 39C).

The major oxides in relation to the SiO_2 content show systematic variations (fig. 40); FeO , MgO , and P_2O_5 show a strong negative correlation, whereas Al_2O_3 and CaO show weaker negative correlations, and TiO_2 shows a more irregular and scattered decreasing distribution. The branching at the low SiO_2 end of the FeO^* and MgO plots implies two fractionation trends that may be explained by the presence of more than one cooling unit or sheet. Na_2O varies little and exceeds K_2O in all rocks. The flat Na_2O trend and the scattered, but otherwise flat, distribution of K_2O in the main-phase rocks is typical of Great tonalite sill rocks (Brew, 1988).

Minor element concentrations are presented in table 15 and summarized in figures 30 and 31. For main phase rocks, the Sr content varies between 500 and 800 ppm and shows a flat trend with much scatter (fig. 45), whereas Zn ranges from 40 to 90 ppm and exhibits a fairly tight distribution and negative correlation with SiO₂. Rb also shows a flat trend with concentrations between 59 and 66 ppm. Barium concentrations vary between 750 and 1200 ppm. The rocks contain the highest concentrations of transition metals (fig. 30) within the transect, and average 15 ppm scandium and chromium, 13 ppm cobalt, and 73 ppm zinc.

The tonalitic rocks of the Speel River pluton are enriched in light REE (La 55-105 times chondrite) and moderately enriched in heavy REE (Yb 4-9 times chondrite) which represents an approximate 2-fold difference in REE abundances through the series (fig. 41). Total REE abundances tend to decrease with increase in SiO₂ content. The rocks show pronounced light/heavy REE fractionation that varies little through the series (Ce/Yb=9-11) and is reflected in their relatively steep linear distribution patterns, which also show a characteristic slight positive Tm spike. As a group, they show steeper patterns and stronger light/heavy REE fractionation than most rocks of the Admiralty-Revillagigedo belt.

The felsic rock members of the Speel River pluton are high-silica, peraluminous granodiorites in composition (figs. 7, 40). Although fairly similar in major-element composition to granodiorites of the Coast Mountains belt, they are more evolved in their REE compositions (fig. 41), showing much higher light/heavy REE fractionation (Ce/Yb=14-46). The REE patterns for the felsic rocks are steeper than the tonalitic rocks but they do show the similar nearly linear distribution pattern with a slight Tm spike. In contrast to the tonalitic rocks, the LREE content of the felsic rocks increases with an increase in SiO₂ content. One felsic sample is highly fractionated and nearly depleted in heavy REE (fig. 41). The depletion in HREE in the residual felsic magma may be explained as a result of fractionation of hornblende (Frey and others, 1978) and possibly titanite (Sawka, 1988), two minerals that are abundant and common, respectively, in the main phase tonalites but are scarce to absent in the granodiorites.

Coast Mountains Belt

Major and minor element chemistry further substantiates the division of the rocks of the Turner Lake batholith into many units (fig. 4) that can be grouped into two subbelts. Where rocks from the two subbelts overlap in SiO₂ content (70-73 percent), granitic rocks from the eastern units contain higher alkalis (fig. 28), higher K₂O/Na₂O and FeO*/MgO ratios (fig. 39; table 13) and generally higher Rb concentrations (fig. 31). The higher alkali/CaO ratios of the eastern granites further distinguish them from silica-equivalent rocks of the western units (fig. 37). When these rocks are plotted by differentiation index versus TiO₂ content (fig. 39B), the eastern granitic units form a separate trend that diverges from the subparallel trends shown by the major units of the western subbelt. The range in uranium, thorium, and tantalum content (fig. 33) overlaps between the two subbelts, but the average abundances of these high-valence trace elements are much lower in rocks of the western subbelt.

Western subbelt: The three large granodiorite units that form the western subbelt contain rocks of similar major-element chemical composition (Tables 16-18) but significant differences do occur in their chemical diversity and minor element abundances. Rocks of the southern unit exhibit the widest range in SiO₂ (62-71 percent) and corresponding major element oxides (fig. 42), whereas rocks of the northern unit have very restricted compositions (69-72 percent SiO₂). Rocks of the central unit are intermediate in compositional range (65-70 percent SiO₂). Together,

oxides of the three units form a coherent, continuous, single-trend distribution on Harker diagrams (fig. 42) that reflects their common magmatic evolution. The oxides of Fe, Mg, Ca, Ti, and Al show strong negative correlations with SiO₂, whereas K₂O shows a positive correlation with much scatter, and Na₂O varies little with SiO₂. Na₂O exceeds K₂O in all but one sample. These trends are typical of plutonic rocks of the Coast Mountains Complex (Brew, 1988) and of continental-margin calc-alkalic magmatism.

The abundances of the LIL elements Sr, Rb, and Zr vary between units, whereas the concentrations of Ba, Nb, and Y vary little between units (tables 16-18). The restricted range in Sr abundance for the central unit (550-630 ppm) distinguish it from the collectively low Sr abundance of the northern unit (390-530 ppm) and the higher wide range in Sr for the southern unit (500-850 ppm). Collectively, Sr decreases with increasing SiO₂ content with much scatter (fig. 42). Rb concentrations vary from 22 to 97 ppm in all rocks and in general it increases with increasing SiO₂ content but also varies between units (fig. 42). Zr abundances in rocks of the central and northern units are nearly the same and average about 205 to 212 ppm, whereas in rocks of the southern unit Zr occurs in less abundance, averaging about 160 ppm. Ba occurs in amounts generally greater than 700 ppm in all units and averages from 1220 to 1235 ppm in the three units.

The REE abundances and fractionation patterns are very similar for the three units (fig. 43). The rocks are highly enriched in light REE (La, 45-95 times chondrite) and moderately enriched in heavy REE (Yb, 4.5-7 times chondrite). All the units produce a similar steep, nearly-linear distribution pattern that levels off in the heavy REE, and they show similar light/heavy REE fractionation (Ce/Yb=8-11), with the exception of one sample from the central unit which is less fractionated (Ce/Yb=6.3). Some samples show slight negative Eu anomalies. All the units show a relatively narrow range in total REE abundances, and REE abundances in the central unit decrease with an increase in SiO₂ content (fig. 43).

Eastern Subbelt: The undivided granitic masses and stocks that comprise the eastern subbelt of the Turner Lake batholith form an abrupt change in composition from rocks of the western subbelt. These rocks are more siliceous (71-75 percent SiO₂) and K₂O-rich (fig. 39A) in composition. They form the similar distribution patterns on Harker diagrams (fig. 42) as rocks from the western subbelt, with the exception of K₂O which forms a flat trend but exceeds Na₂O in all rocks. The granites contain higher concentrations of high-valence LILE (uranium, thorium, hafnium, and tantalum), except Zr, than other subbelt rocks (fig. 31). Sr contents vary between 100 and 400 ppm, and Rb content ranges mostly between 98 and 190 ppm. Two samples from separate masses along the Canadian border have higher K₂O and Rb contents and lower Zr content than main phase granites to the west, which suggest the presence of more than one pluton. Rocks of the Wrights Glacier stock produced a separate and flatter distribution trend with respect to MgO and CaO on the Harker diagrams (fig. 49), and have higher concentrations of Zr (270-380 ppm), Y (30-50 ppm), and Ba (1500-2000 ppm) than rocks of the undivided main phase (Table 19). The granites of the Wright Glacier stock and eastern unit contain elevated Fe*/Ti values (>7) that distinguish them from granites of the main undivided phase and western subbelt (fig. 38).

REE abundances and fractionation patterns vary between the three granite phases, although all the rocks show a negative Eu anomaly, indicating plagioclase fractionation (fig. 44). The undivided granites are highly enriched (La, 80-180 times chondrite; and Yb, 6-8 times chondrite) and are highly fractionated (Ce/Yb=8-17) showing a curvi-linear distribution pattern. The LREE (La, Ce, and Nd) contents increase with an increase in SiO₂, but the HREE (Yb and Lu) decrease with increasing

SiO₂. The rocks along the eastern border are much less fractionated (Ce/Yb=4.1-4.7) and are more enriched in the heavy REE (Yb, 14-16 times chondrite), and have a more pronounced Eu anomaly. These rocks produce a cupped or broad U-shaped distribution pattern, which results from the relative depletion in the middle REE and may reflect the removal or fractionation of hornblende and titanite, which concentrate middle REE (Hanson, 1978; Lipman, 1987). Rocks of the Wrights Glacier stock are also enriched (La, 100-150 times chondrite) and show an intermediate light/heavy REE fractionation (Ce/Yb=7.8-7.9) and a slight Eu anomaly (fig. 44).

In comparison to granitic rocks of the western subbelt, the granites of the eastern subbelt contain generally higher REE abundances, particularly more HREE, and they produce a more curved pattern with the characteristic negative Eu anomaly. Fractionation of plagioclase may slightly increase the LREE content as well as produce a negative Eu anomaly (Hanson, 1980), but hornblende separation may also deplete the HREE (Frey and others, 1978). Allanite is a common phase in rocks of the eastern subbelt, which explains the increase in LREE (Sawka and others, 1984) but the increase in HREE is more difficult to explain by fractionation alone, because the rocks lack hornblende and titanite (euhedral), two minerals that concentrate HREE. This relationship suggests that the eastern granites were derived from a different or varied but HREE-rich source. The decrease of HREE with differentiation, though, is compatible with the removal of these mineral phases.

Miscellaneous Plutonic Rocks

Major and minor element chemistry for the Wrights River stock and Tease Lake stocks are given in Table 20. Additionally, several chemical analyses of granitic rocks from small granite masses that lie within the western subbelt of the Turner Lake batholith are also provided. The two samples from the Wrights River body are a quartz monzodiorite and granodiorite with corresponding SiO₂ content of 60 and 69 percent. The Rb and Sr contents of these rocks are highly varied (74-160 ppm Rb and 310-510 ppm Sr), but their relatively high Y (35-36 ppm) and Zr (180-340 ppm) contents are similar to those concentrations found in the Wright Glacier stock. The Sr and Ba concentrations, though, are closer to values of the undivided granite and northern units of the Turner Lake batholith, indicating that this stock may be a hybrid body with components from several different plutons. The REE abundances and fractionation patterns for both bodies are very similar (figs. 50, 51), although rocks from the Wrights River stock show a less pronounced negative Eu anomaly.

The Tease Lake stocks are chemically heterogeneous (table 20) and have a SiO₂ range of 61 to 72 percent, although the rocks show uniform high K₂O abundance (3.1-4.1 percent) and Zr content (154-315 ppm). One sample produced anomalously high Sr (1700 ppm) and Ba (2600 ppm) concentrations. Because of the diverse chemical nature of these two stocks, it is difficult to correlate them with either the Great Tonalite sill belt or the western subbelt of the Turner Lake batholith.

The nature of the small granitic masses that lie within the granodiorite units of the western subbelt is uncertain. Chemically, they are granites in composition (table 20), and most of them contain the low Sr (< 300 ppm) and high Rb (> 100 ppm) abundances that is more typical of the younger granites of the eastern subbelt. Other components, such as Ba and Zr abundances, vary widely in these rocks making it difficult to correlate them with other plutons or subbelts. The sample from the granite body at the head of Turner Lake is less enriched in REE than most other rocks, but it displays a fractionation pattern with a pronounced negative Eu anomaly (fig. 45) that is similar to the granites of the eastern subbelt (fig. 44). A granite sample from the north end of the northern unit of the western subbelt of the Turner Lake batholith yielded a highly evolved REE fractionation pattern (Ce/Yb=22) that is more similar to those produced by the granodiorites of the Great Tonalite sill belt than by the granodiorites or granites of the Turner Lake batholith.

Summary of Chemical Features and Variations

The three major belts and their constituent subbelts of the Taku Inlet transect (table 1) can be characterized by distinctive chemical traits (Table 13, and figs. 24–29). The division of plutons of the Admiralty-Revillagigedo belt into the Taku Harbor and Grand Island subbelts is based on differences in their alkali content (fig. 25), FeO^*/MgO ratios (fig. 26), and Ba, Sr, and Rb abundances (fig. 31). Although the total iron content of both groups is comparable, the relative percentage of trivalent iron (Fe_2O_3) and corresponding magnetic susceptibility is higher in plutons of the Taku Harbor subbelt (Drinkwater and others, 1992). Rocks from the mainland plutonic belts, within the transect, can be grouped into 3 subbelts according to abrupt changes in chemical composition along the transect (west to east). On the basis of normative feldspar compositions (fig. 28B) the rocks range from tonalites of the Great tonalite sill belt (western subbelt) to granodiorites of the western subbelt of the Turner Lake batholith to granites of the eastern subbelt of the Turner Lake batholith. This normative chemical classification correlates well with modal compositions (figs. 8, 16, 19). All the plutons plot predominantly as volcanic arc granitoids (fig. 32) on the tectonic diagram of Pearce and others (1984).

Admiralty-Revillagigedo Belt

The plutons of the Admiralty-Revillagigedo belt are largely metaluminous calc-alkalic rocks with elevated FeO^*/MgO ratios and high Sr content, they show an iron-rich calc-alkalic trend on the AFM diagram. The Grand Island subbelt consists of a varied suite of magnetite-free plutons of quartz diorite to granodiorite composition, whereas the Taku Harbor subbelt consist of two oxidized plutons of quartz monzodiorite composition. The high K_2O content of rocks from the Grand Island subbelt is partly due to metasomatic alteration, whereas in rocks of the Taku Harbor subbelt it reflects the high K-feldspar content. The two plutons of the Taku Harbor subbelt contain higher amounts of Rb, Sr, and Ba than plutons of the Grand Island subbelt, and the higher abundances of Y, Nb, and heavy REE in rocks of the Everett Peak pluton are attributed to the abundance of titanite in them. Both groups of plutons show the rough systematic decrease of REE with increasing SiO_2 content, which indicates fractionation of accessory phases as differentiation proceeds.

The plutons of the Admiralty-Revillagigedo belt are linked by similar REE abundances and fractionation patterns, but the differences in major and minor element compositions, and oxidation state between the two subbelts indicates differences either in the source rock composition or in the melting and crystallization history. Plutons of the two subbelts are believed to have been emplaced in different terranes (fig. 46) that are separated by a major structural brake, the Fanshaw fault (Gehrels and others, 1991), although Brew and Ford (1984) believe that the rocks of the Taku terrane of Berg and others (1978) may be the high-grade metamorphic equivalents of the Alexander-Wrangellia terrane. The emplacement of plutons of the two subbelts occurred after major collision and accretion events took place so differences in composition and structural regime between the two host terranes may or may not have caused significant differences between the rocks of the two subbelts.

Mainland Plutonic Rocks

The plutons that form the mainland Coast batholith along the Taku Inlet transect are calc-alkalic and range from metaluminous tonalitic rocks of the Great tonalite sill belt to peraluminous granitic rocks of the Turner Lake batholith. All the rocks show balanced feldspar compositions that become more sodic west to east. These rocks form coherent continuous trends on SiO_2 variation diagrams indicating that they belong to a cogenetic, calc-alkalic magmatic suite, but other chemical

Table 13. Characteristic chemical features of the major plutonic divisions of the Taku Inlet transect

<i>Unit</i>	SiO ₂	K ₂ O	FeO*	TiO ₂	Sr (ppm)	Rb	Nb+Y	Ba	FeO*/MgO	Alk/lime
Grand Island subbelt	49-68	1.0-3.0	3.5-10.5	.48-1.3	670-970	30-58	32-40	420-800	2.4-3.7	.43-1.2
Taku Harbor subbelt	58-64	2.7-3.4	3.8-6.1	.46-.85	830-1150	52-92	34-62	850-2000	3.1-3.9	1.0-1.3
Great Tonalite sill belt	59-66	1.0-1.9	3.3-6.1	.40-.72	560-780	20-46	20-34	750-1200	2.0-2.4	.67-.98
Turner Lake batholith (western subbelt)	62-72	1.7-3.6	2.0-5.0	.32-.63	390-780	26-97	20-44	800-1700	2.4-3.9	.95-3.1
Turner Lake batholith (eastern subbelt)	71-75	3.6-4.7	1.0-3.1	.19-.39	156-365	98-140	20-32	1000-2000	2.5-7.1	3.0-5.6

Table 14 A Major and Minor Element Chemical Data for rocks of the Grand Island Subbelt

Glass Peninsula stocks									
Whole rock analyses in weight percent (oxides normalized volatile free)									
sample no.-	17	18	20	19	12	9	8	4	2
SiO ₂	62.54	62.78	61.6	58.5	60.91	58.85	60.38	60.68	58.51
Al ₂ O ₃	18.78	18.44	17.56	17.52	17.46	17.98	17.85	17.85	18.68
Fe ₂ O ₃	1.62	1.81	1.95	2.78	3.16	3.51	3.04	1.57	1.80
FeO	2.74	3.02	3.39	3.63	2.64	3.00	3.04	4.51	4.75
MgO	1.22	1.41	2.16	2.28	1.96	2.30	1.96	2.33	2.09
CaO	5.79	5.64	6.26	5.79	5.84	6.88	6.19	6.34	7.43
Na ₂ O	4.26	3.93	4.11	5.43	4.05	3.90	3.94	3.74	3.64
K ₂ O	2.23	2.12	2.05	2.74	2.92	2.33	2.45	1.88	1.87
TiO ₂	0.49	0.49	0.60	0.76	0.60	0.72	0.64	0.64	0.67
P ₂ O ₅	0.19	0.20	0.23	0.37	0.28	0.34	0.33	0.32	0.36
MnO	0.13	0.14	0.11	0.21	0.18	0.19	0.18	0.15	0.19
LOI	1.17	1.38	1.31	0.82	0.92	1.29	1.21	1.39	0.86
FeO*	4.2	4.66	5.14	6.13	5.48	6.16	5.78	5.92	6.37
CIPW normative minerals									
Quartz	14.5	16.7	13.5	2.5	12.2	10.8	12.8	13.4	10.4
Orthoclase	13.2	12.5	12.1	16.2	17.3	13.8	14.5	11.1	11.1
Albite	36.1	33.3	34.7	45.9	34.3	33.0	33.3	31.7	30.8
Anorthite	25.5	26.4	23.4	15.4	20.8	24.7	23.8	26.4	29.2
Diopside	1.6	0.21	5.1	8.9	5.0	5.8	3.9	2.5	4.5
Hypersthene	5.4	6.9	6.7	4.8	4.1	4.8	5.4	10.7	9.5
Magnetite	2.36	2.63	2.83	4.0	4.6	5.1	4.4	2.3	2.6
Ilmenite	0.93	0.94	1.13	1.43	1.14	1.36	1.22	1.22	1.28
Apatite	0.45	0.48	0.52	0.86	0.66	0.78	0.76	0.73	0.83
Norm Cl	10.3	10.7	15.7	19.2	14.8	17.0	15.0	16.8	17.8
Norm An	41.4	44.3	40.3	25.1	37.8	42.8	41.7	45.4	48.7
Diff. index	63.8	62.4	60.3	64.6	63.7	57.6	60.6	56.2	52.2
Minor elements in ppm									
Nb	7.1	11	7	n.d.	n.d.	12	14	18	16
Rb	n.d.	n.d.	n.d.	n.d.	n.d.	56	58	34	54
Sr	890	880	590	n.d.	n.d.	970	910	750	820
Zr	68	87	40	n.d.	n.d.	160	172	166	164
Y	12	16	9	n.d.	n.d.	22	20	14	22
Ba	570	500	420	n.d.	n.d.	680	790	710	620
Zn	64	60	46	n.d.	n.d.	86	96	60	92

Table 14 B Major and Minor Element Chemical Data for rocks of the Grand Island Subbelt

Whole rock analyses in weight percent (oxides normalized volatile free)									
sample no.-	Grand Island pluton			Irving Peak pluton			Butler Peak pluton		
	25	83-6-30	22	33	32	34	30	27	28
SiO ₂	49.21	57.49	57.57	57.77	48.78	48.24	68.62	68.40	65.77
Al ₂ O ₃	19.36	19.23	19.02	17.80	20.66	19.56	16.39	17.02	17.77
Fe ₂ O ₃	4.43	2.55	2.85	2.65	2.05	3.73	0.86	1.10	1.52
FeO	6.45	4.13	3.94	4.86	8.10	7.50	2.71	2.09	2.02
MgO	3.50	2.11	2.08	2.58	2.71	4.05	1.22	0.92	0.89
CaO	10.60	7.94	8.18	7.58	10.33	10.64	4.23	4.57	5.41
Na ₂ O	3.47	3.81	3.68	3.73	4.15	3.23	3.16	4.42	3.94
K ₂ O	1.12	1.69	1.59	1.82	1.08	1.17	2.28	0.98	2.03
TiO ₂	1.10	0.61	0.59	0.71	1.35	1.15	0.32	0.31	0.32
P ₂ O ₅	0.51	0.28	0.31	0.32	0.54	0.48	0.14	0.15	0.18
MnO	0.26	0.18	0.19	0.18	0.26	0.26	0.08	0.03	0.14
LOI	0.67	0.62	0.48	0.84	1.15	0.59	1.18	1.28	1.25
FeO*	10.44	6.42	6.50	7.25	9.94	10.86	3.48	3.08	3.39
CIPW normative minerals									
Quartz		08.9	10.1	09.2			29.3	27.1	21.9
Corundum							01.4	00.7	
Orthoclase	06.6	10.0	09.4	10.8	06.4	06.9	13.5	05.8	12.0
Albite	29.4	32.2	31.2	31.6	27.9	27.2	26.7	37.4	33.4
Anorthite	33.9	30.4	30.7	26.4	34.5	35.4	20.0	21.7	24.8
Diopside	12.5	05.9	06.4	07.5	11.1	00.1			00.7
Hypersthene	03.7	07.2	06.3	08.6			06.9	04.8	04.1
Olivine	04.2				09.4	09.9			
Magnetite	06.4	03.7	04.1	03.9	03.0	05.4	01.2	01.6	02.2
Ilmenite	02.1	01.2	01.1	01.4	02.6	02.2	00.6	00.6	00.6
Apatite	01.2	00.7	00.7	00.7	01.3	01.1	00.3	00.4	00.4
Norm Cl	28.9	17.9	18.0	21.3	26.0	29.3	08.8	07.0	07.6
Norm An	53.6	48.6	49.6	45.6	50.1	56.4	42.9	36.7	42.6
Diff. index	36.0	51.1	50.6	51.5	38.2	34.2	69.5	70.3	67.2
Minor elements in ppm									
Nb	n.d	n.d	16	14	24	n.d	n.d	18	20
Rb	n.d	n.d	30	44	16	n.d	n.d	34	46
Sr	n.d	n.d	780	670	920	n.d	n.d	750	690
Zr	n.d	n.d	152	138	178	n.d	n.d	166	174
Y	n.d	n.d	24	20	38	n.d	n.d	14	20
Ba	n.d	n.d	510	450	435	n.d	n.d	710	710
Zn	n.d	n.d	98	98	152	n.d	n.d	60	80

Table 15. Major and Minor Element Chemical Data for rocks of the Taku Harbor Subbelt

Whole rock analyses in weight percent (oxides normalized volatile free)											
sample no.-	Everett Peak pluton								Arthur Peak pluton		
	45	44	35	48	40	49	50	47	55	51	52
SiO ₂	58.74	58.33	62.94	58.70	58.18	58.49	58.30	57.95	63.82	60.83	64.08
Al ₂ O ₃	17.77	18.80	17.77	17.58	19.46	18.08	18.00	18.06	17.30	18.31	17.72
Fe ₂ O ₃	3.19	2.85	2.54	2.86	2.74	3.01	2.92	2.90	2.73	4.24	2.08
FeO	3.11	3.21	2.03	3.51	3.02	3.01	3.22	3.29	1.81	1.14	1.94
MgO	1.81	1.50	1.11	1.98	1.41	1.74	1.82	1.85	1.12	1.36	1.11
CaO	6.87	7.17	5.52	6.80	7.06	7.03	7.07	7.13	5.32	6.33	5.53
Na ₂ O	3.94	4.08	4.11	3.81	4.30	3.97	3.87	3.94	3.89	3.92	3.99
K ₂ O	3.24	2.78	3.10	3.36	2.65	3.29	3.37	3.44	3.12	2.87	2.72
TiO ₂	0.79	0.79	0.53	0.88	0.74	0.82	0.86	0.85	0.54	0.56	0.47
P ₂ O ₅	0.33	0.27	0.20	0.32	0.25	0.35	0.38	0.39	0.20	0.25	0.21
MnO	0.20	0.22	0.16	0.20	0.20	0.20	0.20	0.20	0.15	0.18	0.15
LOI	0.28	0.61	0.61	0.39	0.49	0.28	0.34	0.26	0.66	1.01	0.41
FeO*	6.00	5.77	4.31	6.08	5.48	5.72	5.85	5.90	4.26	5.00	3.81
CIPW normative minerals											
Quartz	8.3	7.9	14.9	8.0	7.0	7.5	7.3	6.2	17.6	13.5	17.7
Orthoclase	19.2	16.5	18.3	19.9	15.6	19.5	19.9	20.3	18.4	16.9	16.1
Albite	33.3	34.5	34.8	32.2	36.4	33.6	32.7	33.3	32.9	33.1	33.8
Anorthite	21.3	24.8	20.9	20.9	26.0	21.8	21.8	21.5	20.6	23.9	22.4
Diopside	8.6	7.4	4.2	8.7	6.0	8.7	8.8	9.3	3.6	4.5	2.9
Hypersthene	2.5	2.8	1.8	3.7	3.0	2.2	2.7	2.7	1.6	1.3	2.7
Magnetite	4.6	4.1	3.7	4.2	4.0	4.4	4.3	4.2	4.0	2.7	3.0
Ilmenite	1.5	1.5	1.0	1.7	1.4	1.6	1.6	1.6	1.0	1.1	0.9
Apatite	0.8	0.6	0.5	0.8	0.6	0.8	0.9	0.9	0.5	0.6	0.5
Norm Cl	17.2	15.8	10.7	18.2	14.4	16.8	17.4	17.8	10.1	12.0	9.6
Norm An	39.0	41.8	37.5	39.4	41.7	39.3	40.0	39.2	38.5	41.9	40.0
Diff. index	60.8	58.8	68.0	60.1	59.0	60.6	60.0	59.9	68.8	63.6	67.6
Minor elements in ppm											
Nb	n.d	n.d.	n.d	16	26	22	20	20	n.d	18	16
Rb	n.d	52	68	76	46	70	70	68	50	92	60
Sr	n.d	1050	940	890	1150	950	930	940	870	860	830
Zr	n.d	114	62	186	235	152	156	148	57	162	152
Y	n.d	n.d	n.d	20	32	26	24	24	n.d	18	18
Ba	n.d	1650	1260	1350	1950	1350	1400	1250	2150	850	1100
Zn	n.d	n.d	n.d.	88	106	96	92	86	n.d	132	80

Table 16. Major and Minor Element Chemical Data for rocks of the Great Tonalite Sill Belt

Whole rock analyses in weight percent (oxides normalized volatile free)																
sample no.-	Speel River pluton										felsic sill layers			Taku Cabin pluton		
	67	68	66	64	62	63	61	59	76	81	65	72	82	83	84	90
SiO ₂	60.33	65.75	63.21	64.64	62.57	59.60	61.68	62.17	62.42	61.35	63.77	72.23	71.72	72.94	61.56	61.68
Al ₂ O ₃	18.52	17.63	17.80	17.25	17.41	18.08	18.41	17.59	17.75	18.40	17.73	15.31	16.20	15.36	16.97	16.92
Fe ₂ O ₃	2.29	1.29	2.19	1.64	2.00	2.98	2.16	2.28	1.74	1.94	2.05	0.85	0.10	0.59	2.66	2.48
FeO	3.33	2.15	2.75	2.68	3.31	3.34	2.98	3.37	3.28	3.35	2.56	1.04	1.00	0.86	3.64	3.89
MgO	2.53	1.48	2.00	1.93	2.41	3.00	2.15	2.42	2.38	2.33	1.80	0.52	0.63	0.34	2.78	2.68
CaO	7.19	6.06	6.20	5.70	5.81	6.92	6.92	6.33	6.61	7.11	6.38	3.05	2.65	2.92	6.22	6.30
Na ₂ O	3.87	3.92	3.71	3.67	3.78	3.69	3.82	3.58	3.69	3.80	3.88	3.77	4.46	3.99	3.38	3.34
K ₂ O	0.97	1.02	1.35	1.66	1.75	1.31	1.01	1.34	1.26	0.93	1.10	2.91	2.90	2.70	1.76	1.67
TiO ₂	0.59	0.42	0.47	0.51	0.63	0.69	0.52	0.58	0.56	0.45	0.40	0.19	0.25	0.16	0.68	0.68
P ₂ O ₅	0.28	0.23	0.25	0.23	0.22	0.28	0.26	0.25	0.23	0.25	0.25	0.11	0.08	0.11	0.22	0.23
MnO	0.10	0.06	0.09	0.07	0.11	0.11	0.08	0.10	0.09	0.11	0.08	0.03	0.02	0.03	0.13	0.12
LOI	0.36	0.30	0.40	0.45	0.50	0.41	0.30	0.36	0.45	0.40	0.27	0.25	1.84	0.25	0.52	0.51
FeO*	5.32	3.31	4.72	4.16	5.11	6.03	4.93	5.42	4.84	5.09	4.40	1.80	1.08	1.39	6.03	6.12

CIPW normative minerals																
Quartz	14.9	23.7	20.0	21.4	17.3	14.2	17.5	18.5	18.0	16.6	20.7	31.8	27.6	32.6	17.4	17.9
Corundum												0.7	1.1	0.83		
Orthoclase	5.7	6.1	7.8	9.8	10.4	7.8	5.9	7.9	7.5	5.5	6.5	17.1	17.2	15.9	10.4	9.9
Albite	32.7	33.2	31.4	31.1	31.9	31.2	32.4	30.3	31.2	32.2	32.8	31.9	37.8	33.8	28.6	28.3
Anorthite	30.3	27.5	28.0	25.7	25.4	28.9	30.1	28.0	28.1	30.4	27.7	14.4	12.6	13.8	25.9	26.2
Diopside	2.8	0.9	0.9	0.9	1.6	2.9	2.1	1.5	2.5	2.6	1.8				2.8	2.9
Hypersthene	8.4	5.6	7.2	7.2	8.8	8.8	7.3	8.8	8.5	8.5	6.1	2.3	2.9	1.7	9.2	9.5
Magnetite	3.3	1.9	3.2	2.4	2.9	4.3	3.1	3.3	2.5	2.8	3.0	1.2	0.1	0.85	3.9	3.6
Ilmenite	1.1	0.8	0.9	1.0	1.2	1.3	1.0	1.1	1.1	0.9	0.8	0.4	0.5	0.31	1.3	1.3
Apatite	0.7	0.5	0.6	0.5	0.5	0.7	0.6	0.6	0.5	0.6	0.6	0.3	0.2	0.26	0.5	0.5
Norm Cl	15.6	9.1	12.2	11.5	14.5	17.3	13.5	14.7	14.6	14.8	11.7	3.8	3.6	2.9	17.1	17.2
Norm An	48.1	45.3	47.1	45.2	44.3	48.1	48.2	48.0	47.4	48.6	45.8	31.1	25.0	29	47.5	48.1
Diff. index	53.4	62.9	59.3	62.3	59.6	53.1	55.8	56.8	56.7	54.2	60.0	80.8	82.5	82.3	56.4	56.0

Minor elements in ppm																
Nb	n.d	<10	10	12	16	12	12	10	14	<10	10	<10	<10	10	<10	<10
Rb	n.d	20	26	30	46	32	24	28	30	22	24	46	53	48	30	33
Sr	n.d	760	710	680	560	730	780	730	680	790	730	480	840	520	660	640
Zr	n.d	150	130	146	120	116	160	130	156	130	172	144	260	162	130	130
Y	n.d	<10	14	14	16	18	16	14	16	18	16	10	14	12	22	24
Ba	n.d	900	1100	1540	730	960	760	1000	910	870	1050	1800	n.d	1750	1130	1140
Zn	n.d.	52	74	66	80	92	72	80	72	80	64	38	n.d.	40	n.d.	n.d.

Table 17. Major and minor element chemical data for rocks from the western subbelt of the Turner Lake Batholith

Southern Granodiorite unit							
Whole rock analyses in weight percent (oxides normalized volatile free)							
sample no.-	97	110	96	111	112	113	114
SiO ₂	67.09	64.63	67.21	62.30	71.71	66.23	63.16
Al ₂ O ₃	16.09	16.02	16.83	17.83	15.00	16.61	17.44
Fe ₂ O ₃	1.51	2.50	1.47	2.28	1.67	2.93	3.26
FeO	2.62	2.31	1.81	3.09	0.92	1.57	1.95
MgO	1.41	2.05	1.21	2.22	0.77	1.62	1.92
CaO	4.43	5.19	5.11	5.87	2.90	4.64	5.83
Na ₂ O	3.82	3.69	3.77	3.84	3.64	3.78	3.76
K ₂ O	2.31	1.90	1.95	1.57	2.97	1.85	1.73
TiO ₂	0.47	0.60	0.38	0.66	0.28	0.50	0.61
P ₂ O ₅	0.17	0.21	0.20	0.24	0.10	0.19	0.25
MnO	0.08	0.10	0.07	0.10	0.06	0.09	0.09
LOI	0.80	0.54	0.31	0.45	0.91	0.56	0.34
FeO*	3.97	4.56	3.14	5.14	2.42	4.20	4.88
CIPW normative minerals							
Quartz	23.8	21.9	25.1	17.6	32.1	25.4	20.4
Corundum					0.77	0.42	
Orthoclase	13.7	11.3	11.5	9.3	17.5	10.9	10.2
Albite	32.3	31.2	31.9	32.5	30.7	32	31.8
Anorthite	19.9	23.7	23.2	26.8	13.7	21.8	25.6
Diopside	0.75	0.51	0.63	0.59			1.3
Hypersthene	6.1	6.2	4.3	8.1	1.9	4.1	4.2
Magnetite	2.2	3.6	2.1	3.3	2.4	3.9	4.7
Ilmenite	0.9	1.2	0.71	1.3	0.52	0.94	1.2
Apatite	0.4	0.49	0.47	0.56	0.24	0.45	0.59
Norm Cl	9.9	11.5	7.8	13.3	4.8	9.1	11.4
Norm An	38.1	43.2	42.1	45.2	30.8	40.5	44.6
Diff. index	69.8	64.3	68.5	59.4	80.5	68.3	62.4
Minor elements in ppm							
Nb	nd	<10	20	9	9	8	12
Rb	nd	34	34	22	54	26	22
Sr	nd	700	740	850	460	710	780
Zr	nd	114	188	194	124	106	182
Y	nd	16	22	18	12	12	24
Ba	nd	1200	1700	810	1300	750	1100
Zn	nd	60	58	74	54	50	62

Table 18. Major and minor element chemical data for rocks from the western subbelt of the Turner Lake Batholith

Central Granodiorite unit												
Whole rock analyses in weight percent (oxides normalized volatile free)												
sample no.-	124	115	120	122	119	116	144	146	141	159	145	129
SiO ₂	70.26	69.12	68.46	68.31	65.27	70.41	69.06	68.75	68.26	67.43	62.18	68.26
Al ₂ O ₃	16.18	15.97	16.08	16.47	16.24	16.05	16.00	15.75	16.20	16.35	16.91	16.21
Fe ₂ O ₃	1.24	1.36	1.62	1.70	2.27	0.94	1.32	1.62	1.90	1.92	2.14	1.24
FeO	0.91	1.66	1.66	1.24	2.74	0.96	1.70	1.87	1.67	2.43	3.22	1.90
MgO	0.63	1.06	1.17	1.02	1.98	0.56	1.10	1.27	1.30	1.26	2.61	1.20
CaO	3.36	3.65	4.00	3.81	5.03	3.52	3.78	3.78	4.07	3.91	6.04	3.93
Na ₂ O	4.37	4.10	4.09	4.02	3.66	4.17	3.79	3.92	4.34	4.15	3.80	4.18
K ₂ O	2.55	2.41	2.25	2.79	1.94	2.78	2.63	2.39	1.51	1.68	2.09	2.41
TiO ₂	0.32	0.48	0.46	0.39	0.58	0.33	0.43	0.44	0.53	0.64	0.68	0.46
P ₂ O ₅	0.16	0.14	0.16	0.18	0.19	0.24	0.13	0.14	0.15	0.17	0.24	0.16
MnO	0.03	0.06	0.06	0.06	0.10	0.05	0.06	0.07	0.07	0.06	0.10	0.06
LOI	0.42	0.40	0.39	0.51	0.40	0.31	0.25	0.51	0.46	0.36	0.51	0.60
FeO*	2.03	2.89	3.11	2.77	4.79	1.80	2.89	3.32	3.38	4.16	5.14	3.02
CIPW normative minerals												
Quartz	27.4	26.5	25.8	24.9	22.6	27.6	26.9	26.6	26.7	26.2	15.7	24.2
Corundum	0.52	0.32	0.03	0.35		0.38	0.38	0.19	0.4	1.02		
Orthoclase	15.1	14.2	13.3	16.5	11.5	16.5	15.6	14.1	8.9	9.9	12.3	14.2
Albite	36.9	34.7	34.6	34.0	31.0	35.3	32.1	33.1	36.7	35.1	32.1	35.4
Anorthite	15.6	17.2	18.8	17.7	22.2	15.9	17.9	17.8	19.2	18.3	22.9	18.4
Diopside					1.3						4.4	0.05
Hypersthene	1.7	3.9	4.0	2.9	6.7	1.9	4.2	4.7	4	5.1	7.6	4.8
Magnetite	1.8	2.0	2.4	2.5	3.3	1.4	1.9	2.3	2.8	2.8	3.1	1.8
Ilmenite	0.61	0.90	0.86	0.75	1.1	0.62	0.81	0.84	1	1.2	1.3	0.88
Apatite	0.38	0.33	0.38	0.42	0.44	0.57	0.31	0.33	0.35	0.40	0.56	0.37
Norm Cl	4.1	6.8	7.2	6.1	12.4	3.9	6.9	7.8	7.7	9.1	16.4	7.5
Norm An	29.7	33.1	35.2	34.2	41.7	31.0	35.8	35.0	34.4	34.2	41.7	34.2
Diff. index	79.4	75.4	73.6	75.4	65.0	79.3	74.5	73.8	72.3	71.2	60.1	73.8
Minor elements in ppm												
Nb	<10	10	10	<10	10	<10	13	10	12	10	10	nd
Rb	60	52	50	58	40	62	50	50	42	42	44	nd
Sr	570	580	630	590	620	580	590	580	580	600	550	nd
Zr	190	240	210	200	210	205	190	250	220	390	130	nd
Y	13	19	18	18	20	14	21	22	20	17	30	nd
Ba	995	1400	1410	1770	1010	1700	1600	1140	768	586	1060	nd
Zn	nd	nd	nd	nd	nd	60	nd	nd	nd	nd	nd	nd

Table 19. Major and minor element chemical data for rocks from the western subbelt of the Turner Lake Batholith

sample no.-	Northern Granodiorite Unit														Whole rock analyses in weight percent (oxides normalized volatile free)													
	178	189	183	185	190	171	201	205	251	167	168	252	253		178	189	183	185	190	171	201	205	251	167	168	252	253	
SiO ₂	71.14	71.12	69.12	69.54	70.56	70.23	72.06	71.13	70.00	69.19	69.15	70.23	69.03		71.14	71.12	69.12	69.54	70.56	70.23	72.06	71.13	70.00	69.19	69.15	70.23	69.03	
Al ₂ O ₃	14.59	14.75	15.48	15.75	15.06	15.35	15.44	15.54	15.66	15.66	15.77	15.48	15.41		14.59	14.75	15.48	15.75	15.06	15.35	15.44	15.54	15.66	15.66	15.77	15.48	15.41	
Fe ₂ O ₃	1.08	1.04	1.42	1.08	1.09	0.92	0.93	1.27	1.37	1.27	1.19	0.91	1.78		1.08	1.04	1.42	1.08	1.09	0.92	0.93	1.27	1.37	1.27	1.19	0.91	1.78	
FeO	1.49	1.54	1.81	1.54	1.48	1.46	0.77	0.91	1.36	1.58	1.56	1.54	1.44		1.49	1.54	1.81	1.54	1.48	1.46	0.77	0.91	1.36	1.58	1.56	1.54	1.44	
MgO	1.05	1.01	1.26	1.04	0.96	0.92	0.41	0.64	0.88	1.13	1.08	1.02	1.37		1.05	1.01	1.26	1.04	0.96	0.92	0.41	0.64	0.88	1.13	1.08	1.02	1.37	
CaO	2.88	2.76	3.23	3.48	3.07	2.93	2.44	3.15	3.23	3.53	3.39	3.27	3.20		2.88	2.76	3.23	3.48	3.07	2.93	2.44	3.15	3.23	3.53	3.39	3.27	3.20	
Na ₂ O	3.43	3.70	3.68	3.97	3.77	3.86	3.91	4.15	4.08	3.98	3.89	3.66	3.62		3.43	3.70	3.68	3.97	3.77	3.86	3.91	4.15	4.08	3.98	3.89	3.66	3.62	
K ₂ O	3.74	3.55	3.32	3.01	3.39	3.66	3.68	2.71	2.83	2.99	3.33	3.33	3.42		3.74	3.55	3.32	3.01	3.39	3.66	3.68	2.71	2.83	2.99	3.33	3.33	3.42	
TiO ₂	0.40	0.40	0.50	0.39	0.41	0.43	0.22	0.32	0.40	0.44	0.43	0.36	0.52		0.40	0.40	0.50	0.39	0.41	0.43	0.22	0.32	0.40	0.44	0.43	0.36	0.52	
P ₂ O ₅	0.16	0.10	0.13	0.16	0.16	0.20	0.10	0.14	0.12	0.18	0.17	0.15	0.16		0.16	0.10	0.13	0.16	0.16	0.20	0.10	0.14	0.12	0.18	0.17	0.15	0.16	
MnO	0.04	0.04	0.05	0.04	0.04	0.05	0.03	0.04	0.07	0.05	0.04	0.04	0.05		0.04	0.04	0.05	0.04	0.04	0.05	0.03	0.04	0.07	0.05	0.04	0.04	0.05	
LOI	0.64	0.42	0.45	0.24	0.44	0.50	0.26	0.47	0.44	0.50	0.36	0.42	0.55		0.64	0.42	0.45	0.24	0.44	0.50	0.26	0.47	0.44	0.50	0.36	0.42	0.55	
FeO*	2.47	2.47	3.09	2.52	2.46	2.29	1.60	2.05	2.60	2.72	2.63	2.36	3.05		2.47	2.47	3.09	2.52	2.46	2.29	1.60	2.05	2.60	2.72	2.63	2.36	3.05	

CIPW normative minerals													
Quartz	29.1	28.3	25.9	25.8	27.6	26.1	29.5	29.3	27.2	25.4	24.8	27.4	26.3
Corundum	0.1	0.1	0.3	0.0	0.0	0.2	0.8	0.4	0.3	0.0	0.0	0.3	0.3
Orthoclase	22.1	20.9	19.6	17.8	20.0	21.6	21.8	16.0	16.7	17.7	19.7	19.7	20.2
Albite	29.0	31.3	31.2	33.6	31.9	32.7	33.1	35.1	34.5	33.7	32.9	31.0	30.6
Anorthite	13.2	13.0	15.2	16.2	14.2	13.2	11.5	14.7	15.2	16.0	15.7	15.2	14.8
Diopside										0.2			
Hypersthene	3.9	3.9	4.6	4.0	3.6	3.6	1.4	1.7	3.0	3.9	3.9	4.1	3.8
Magnetite	1.6	1.5	2.1	1.6	1.6	1.3	1.4	1.8	2.0	1.9	1.7	1.3	2.6
Ilmenite	0.8	0.8	0.9	0.8	0.8	0.8	0.4	0.6	0.8	0.8	0.8	0.7	1.0
Apatite	0.4	0.2	0.3	0.4	0.4	0.5	0.2	0.3	0.3	0.4	0.4	0.4	0.4
Norm Cl	6.2	6.2	7.6	6.3	6.0	5.7	3.1	4.2	5.8	6.8	6.5	6.1	7.4
Norm An	31.3	29.4	32.7	32.6	30.8	28.8	25.7	29.5	30.6	32.2	32.2	32.9	32.6
Diff. index	80.1	80.5	76.7	77.1	79.5	80.4	84.4	80.4	78.4	76.7	77.4	78.1	77.1

Minor elements in ppm													
Nb	<10	<10	<10	<10	10	<10	<10	10	12	<10	10	10	<10
Rb	97	96	92	74	94	112	78	60	66	83	92	78	78
Sr	390	400	460	470	420	400	460	500	530	460	470	450	425
Zr	200	200	210	200	220	194	190	210	220	220	210	180	114
Y	22	20	19	18	22	16	16	18	23	19	19	14	14
Ba	1270	1050	1270	1230	1160	1300	1340	1140	1340	1070	1220	1300	1200
Zn	nd	nd	nd	nd	nd	62	nd	nd	nd	nd	nd	44	52

Table 20. Major and minor element chemical data for rocks from the eastern subbelt of the Turner Lake Batholith

Whole rock analyses in weight percent (oxides normalized volatile free)												
sample no.-	Undivided unit							Wright Glacier stock				
	214	216	221	224	223	212	222	229	225	231	227	226
SiO ₂	72.43	71.14	71.08	75.67	75.27	71.68	71.37	71.31	72.92	72.86	74.68	71.83
Al ₂ O ₃	14.47	14.45	14.36	13.60	13.25	14.50	14.68	14.81	14.16	14.77	13.66	15.07
Fe ₂ O ₃	0.93	1.61	0.90	0.62	1.28	1.34	1.52	1.21	0.65	0.75	0.76	0.69
FeO	1.21	1.41	2.24	0.43	0.77	1.17	1.05	1.91	1.89	1.06	1.09	1.46
MgO	0.69	0.78	0.90	0.12	0.35	0.99	1.01	0.42	0.44	0.36	0.37	0.32
CaO	2.02	2.40	2.42	0.67	1.33	2.51	2.48	1.71	1.64	1.67	1.61	1.63
Na ₂ O	3.74	3.81	3.38	3.98	3.46	3.68	3.64	4.23	3.97	4.00	3.64	4.28
K ₂ O	4.05	3.91	4.12	4.74	4.00	3.59	3.69	3.93	3.95	4.24	3.88	4.37
TiO ₂	0.31	0.34	0.47	0.08	0.19	0.39	0.40	0.33	0.29	0.20	0.21	0.23
P ₂ O ₅	0.09	0.09	0.10	0.05	0.06	0.11	0.11	0.08	0.06	0.06	0.05	0.07
MnO	0.05	0.05	0.06	0.05	0.03	0.05	0.05	0.06	0.05	0.03	0.04	0.05
LOI	0.67	0.64	0.51	0.24	0.30	0.49	0.43	0.71	0.21	0.44	0.40	0.39
FeO*	2.05	2.85	3.05	1.00	1.93	2.37	2.42	3.00	2.46	1.74	1.78	2.08
CIPW normative minerals												
Quartz	29.6	27.7	28.3	32.8	36.6	29.8	29.5	26.7	29.6	29.02	34.3	25.6
Corundum	0.47		0.21	0.84	0.97	0.26	0.45	0.68	0.53	0.74	0.67	0.51
Orthoclase	23.9	23.1	24.3	28.0	23.6	21.2	21.8	23.2	23.3	25.1	22.9	25.8
Albite	31.7	32.3	28.5	33.7	29.3	31.14	30.8	35.8	33.6	33.7	30.8	36.2
Anorthite	9.4	10.8	11.3	3.0	6.2	11.7	11.6	8.0	7.7	7.9	7.7	7.6
Diopside		0.49										
Hypersthene	2.8	2.5	4.9	0.55	0.97	3.0	2.6	3.1	3.6	2.0	2.1	2.6
Magnetite	1.4	2.3	1.3	0.89	1.9	1.9	2.2	1.8	0.94	1.1	1.1	1.0
Ilmenite	0.60	0.65	0.88	0.15	0.37	0.73	0.75	0.63	0.56	0.38	0.4	0.44
Apatite	0.21	0.21	0.23	0.12	0.14	0.26	0.20	0.19	0.14	0.14	0.12	0.16
Norm Cl	4.7	6.0	7.2	1.6	3.2	5.6	5.6	5.5	5.1	3.4	3.5	4.1
Norm An	23.0	25.0	28.5	8.1	17.4	27.4	27.3	18.2	18.7	18.9	19.9	17.4
Diff. index	85.2	83.1	81.1	94.5	89.5	82.1	82.1	85.6	86.5	87.8	88	87.7
Minor elements in ppm												
Nb	n.d	n.d	n.d	n.d	<10	10	<10	n.d	12	12	10	12
Rb	n.d	n.d	140	190	70	100	98	n.d	110	112	120	120
Sr	n.d	n.d	230	50	156	365	340	n.d	205	240	220	200
Zr	n.d	n.d	98	59	124	118	130	n.d	330	270	280	380
Y	n.d	n.d	n.d	nd	12	16	20	n.d	40	30	34	50
Ba	n.d	n.d	1530	365	1300	1000	1000	n.d	2030	1750	1470	1990
Zn	n.d	n.d	n.d	n.d	36	48	54	n.d	n.d	n.d	n.d	n.d

Table 21. Chemical data for miscellaneous plutons in the Coast Mountains Belt

Whole rock analyses in weight percent (oxides normalized volatile free)									
sample no.-	Wright River stock		Tease Lakes stocks			Miscellaneous Granitic bodies			
	234	236	246	247	248	172	167	250	249
SiO ₂	69.14	60.41	65.51	60.70	71.89	70.52	73.88	74.99	73.03
Al ₂ O ₃	15.51	17.61	16.63	17.66	15.09	15.98	15.20	13.89	14.61
Fe ₂ O ₃	1.18	1.44	1.85	2.59	1.36	1.46	0.15	0.62	0.79
FeO	1.91	4.27	2.08	2.42	0.68	1.06	0.50	0.36	1.18
MgO	1.12	2.66	1.20	2.17	0.53	0.80	0.15	0.20	0.50
CaO	2.72	5.79	3.92	5.40	1.93	3.57	0.88	1.37	2.02
Na ₂ O	3.49	3.86	4.55	4.51	3.91	3.87	4.41	3.46	3.30
K ₂ O	4.33	2.69	3.06	3.36	4.15	2.27	4.62	4.86	4.20
TiO ₂	0.45	0.86	0.69	0.69	0.28	0.32	0.08	0.14	0.23
P ₂ O ₅	0.12	0.31	0.37	0.39	0.14	0.11	0.04	0.05	0.06
MnO	0.05	0.11	0.06	0.12	0.04	0.04	0.09	0.04	0.04
LOI	0.61	0.79	0.37	0.30	0.41	0.32	0.17	0.05	0.27
FeO*	2.96	5.56	3.75	4.75	1.90	2.37	0.64	0.92	1.89
CIPW normative minerals									
Quartz	24.3	10.6	17.9	8.6	28.74	30.7	28.2	33.2	32.4
Corundum	0.44				1.0	0.95	1.5	0.56	1.1
Orthoclase	25.6	15.9	18.1	19.9	24.5	13.4	27.3	28.7	24.8
Albite	29.5	32.6	38.5	38.1	33.1	32.7	37.3	29.3	27.9
Anorthite	12.7	22.8	15.9	18.1	8.7	17	4.1	6.5	9.6
Diopside		3.2	0.9	5.0					
Hypersthene	4.7	10.5	3.8	4.4	1.3	2.3	1.2	0.5	2.4
Magnetite	1.7	2.1	2.7	3.8	1.5	2.1	0.22	0.89	1.2
Ilmenite	0.85	1.6	1.3	1.3	0.54	0.62	0.15	0.27	0.44
Apatite	0.28	0.73	0.86	0.89	0.33	0.26	0.09	0.12	0.14
Norm Cl	7.2	17.4	8.7	14.5	3.7	5	1.6	1.67	4.1
Norm An	30.1	41.1	29.2	32.1	20.8	34.2	9.9	18.1	25.6
Diff. index	79.4	59.1	74.5	66.6	86.4	76.8	92.8	91.2	85.1
Minor elements in ppm									
Nb	18	14	n.d	16	10	<10	n.d	10	<10
Rb	160	74	n.d	60	96	46	280	118	96
Sr	310	510	n.d	1700	460	600	140	176	275
Zr	340	180	n.d	315	154	164	30	102	144
Y	36	35	n.d	18	10	<10	n.d	13	18
Ba	1300	1230	n.d	2600	1500	1600	622	930	2000
Zn	n.d.	n.d	n.d	76	40	58	n.d	46	48

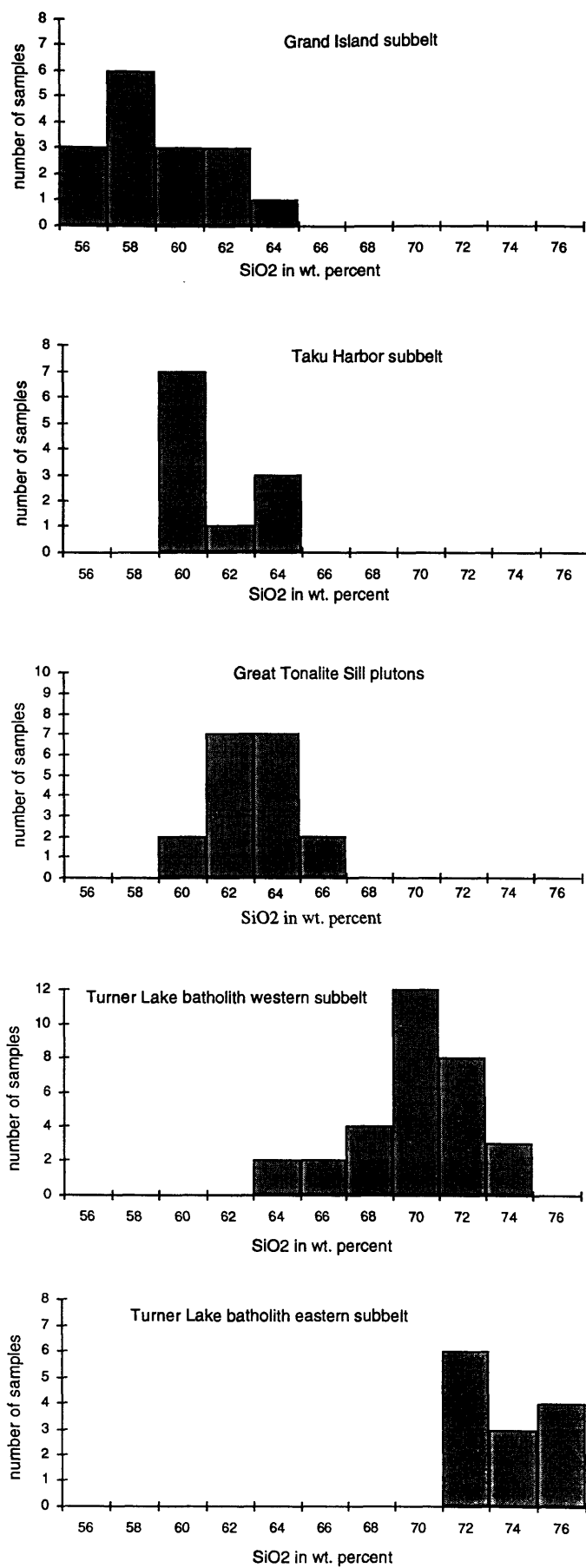


Figure 23. SiO₂ distribution of plutonic rocks, grouped according to subbelt, along the Taku Inlet transect.

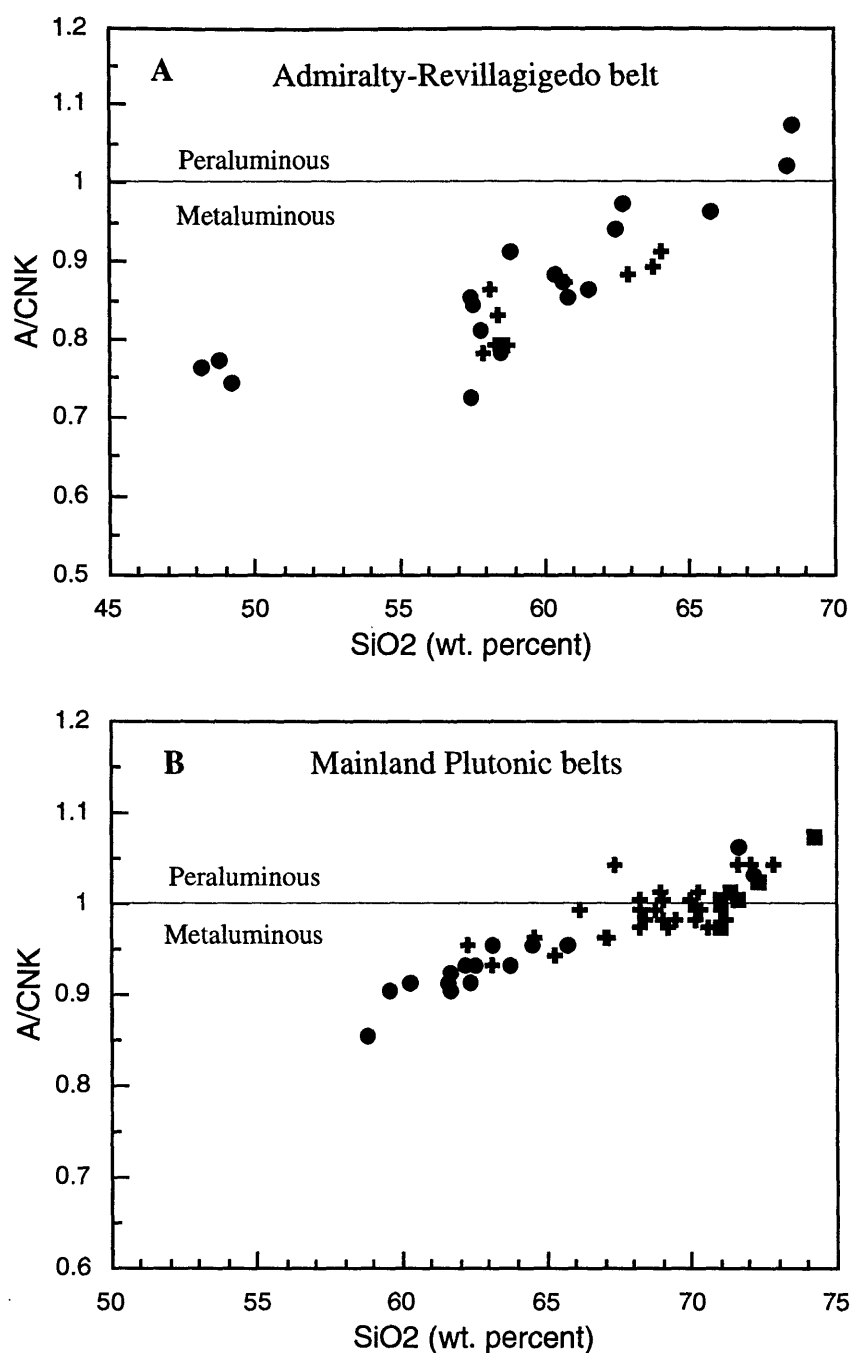


Figure 24. Binary plot of the Alumina saturation index (A/CNK) versus SiO₂ for plutonic rocks along the Taku Inlet transect. *A*, Admiralty-Revillagigedo belt; ●, Grand Island subbelt; ✕, Taku Harbor subbelt. *B*, Mainland batholith; ●, Great tonalite sill belt; ✕, western units of Turner Lake batholith; and ■, eastern units of Turner Lake batholith.

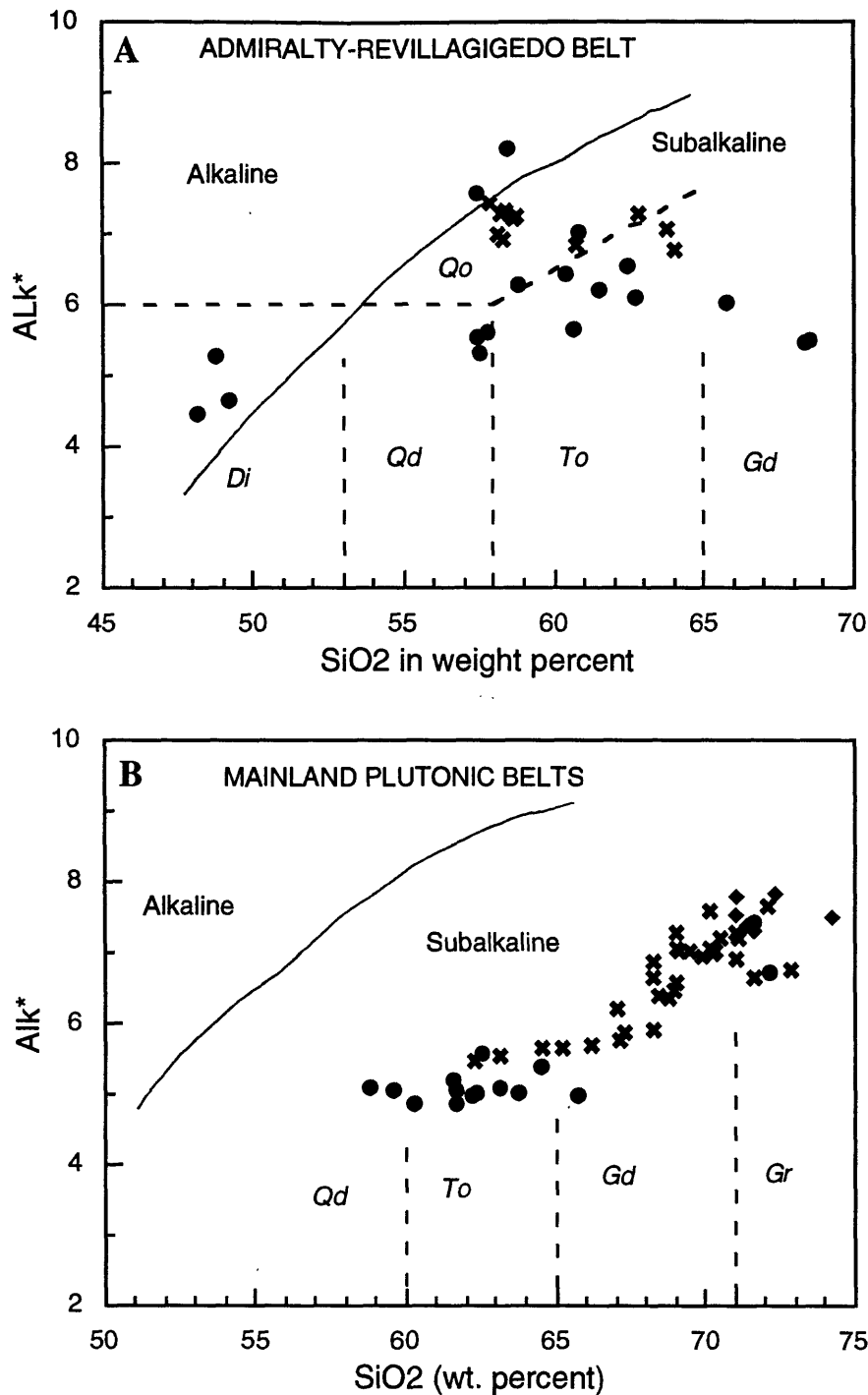


Figure 25. Binary plots of total alkalis (Na_2O+K_2O) versus SiO_2 for plutonic units along the Taku Inlet transect. Field boundaries from Irvine and Baragar (1971). A, Admiralty-Revillagigedo Belt; ●, Grand Island subbelt; *, Taku Harbor subbelt. B, Mainland batholith; ●, Great tonalite sill belt; *, western units of Turner Lake batholith; ◆, eastern units of Turner Lake batholith. Rock types indicated by: Gr, granite; Gd, granodiorite; To, tonalite; Qd, quartz diorite; Di, diorite; and Qo, quartz monzodiorite. Rock types determined by modal analyses.

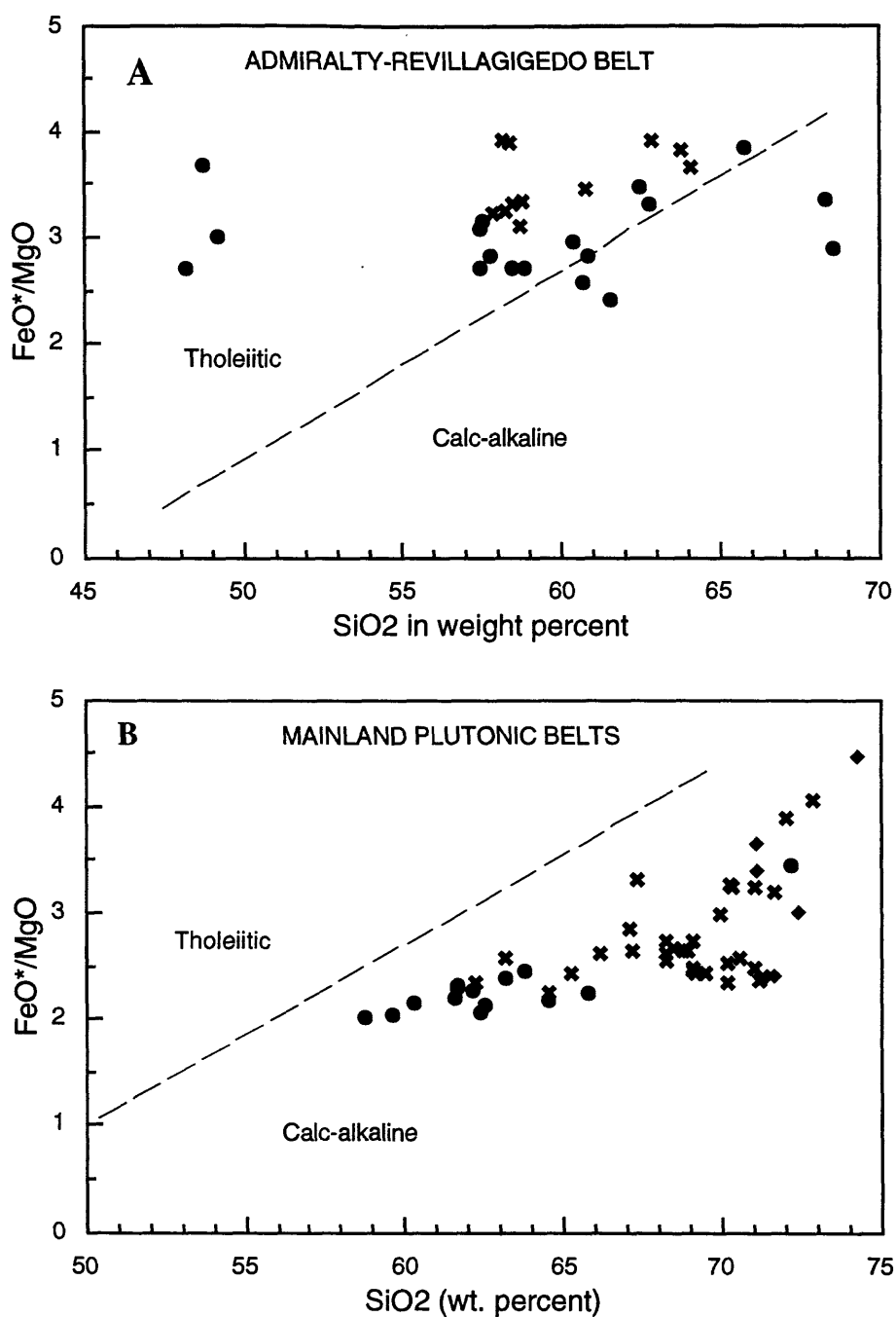


Figure 26. Binary plots of Fe* (total iron)/MgO versus SiO₂ for plutonic rocks along the Taku Inlet transect. Boundary fields from Miyashiro (1974). *A*, Admiralty-Revillagigedo belt: ●, Grand Island subbelt; *, Taku Harbor subbelt. *B*, Mainland batholith: ●, Great tonalite sill belt; *, western units of Turner Lake batholith; and ♦, eastern units of Turner Lake batholith.

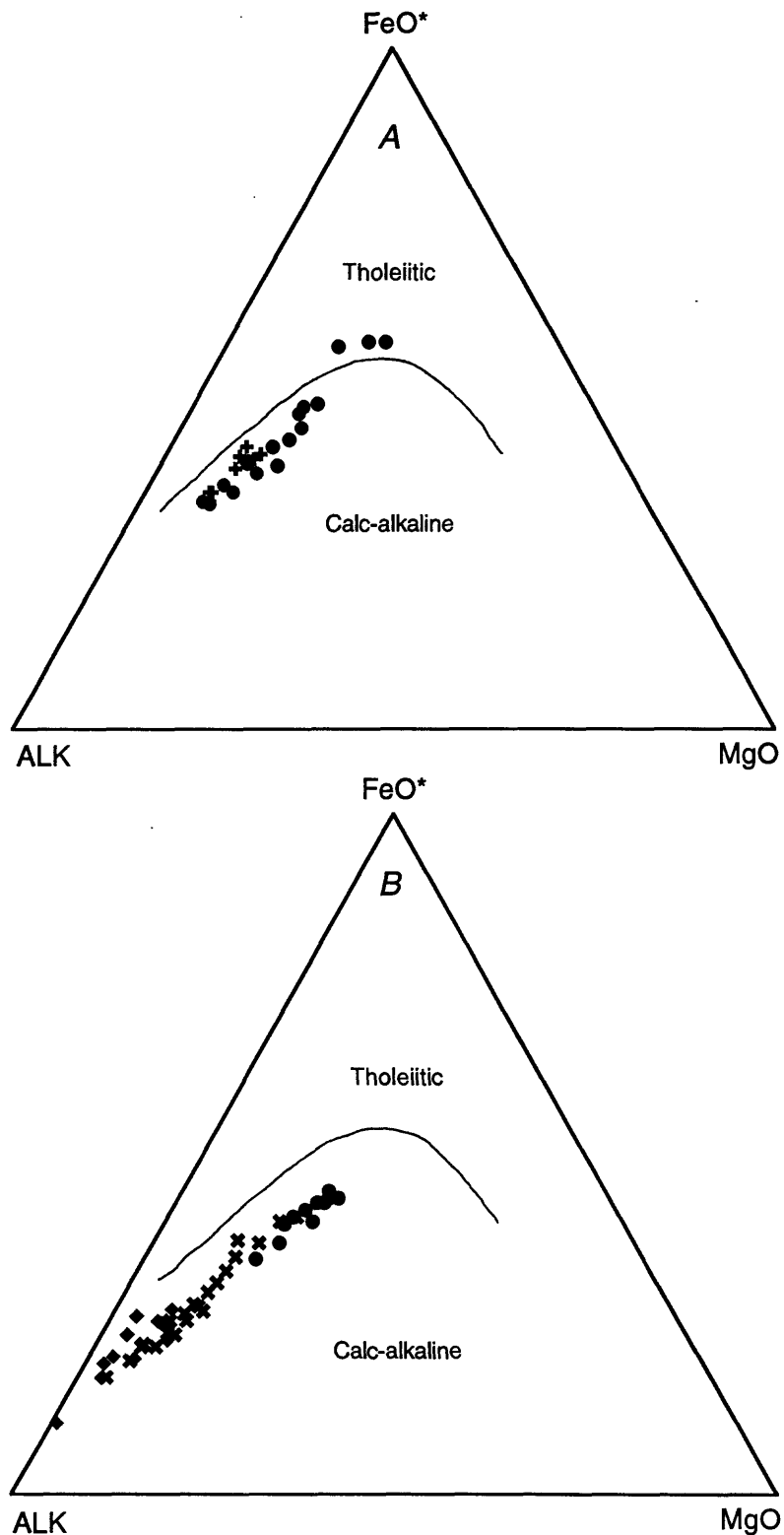


Figure 27. Ternary AFM plots for plutonic rocks along the Taku Inlet transect. Boundary fields from Irvine and Baragar (1971). *A*, Admiralty-Revillagigedo belt; ●, Grand Island subbelt; ✕, Taku Harabor subbelt. *B*, Mainland batholith: ●, Great tonalite sill belt; ✕, western units of Turner Lake batholith; ◆, eastern units of Turner Lake batholith.

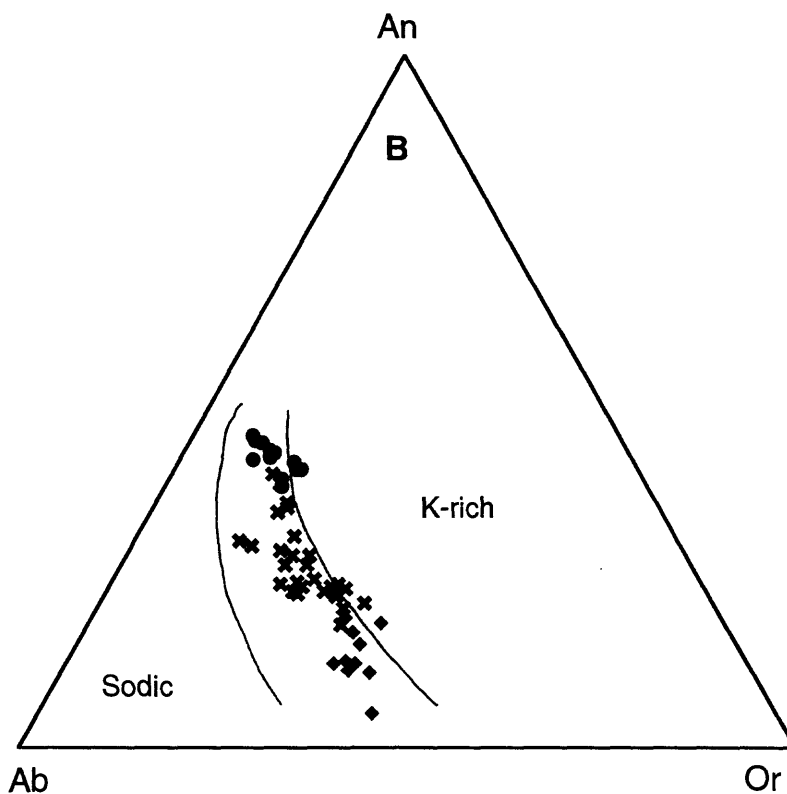
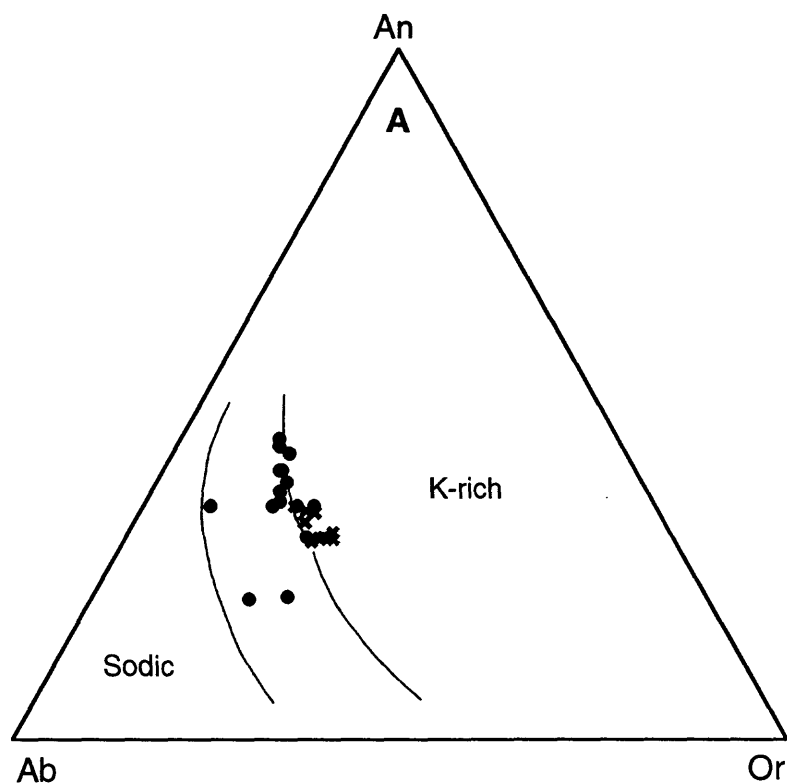


Figure 28. Ternary plots of normative feldspar composition (Ab, albite; An, anorthite; Or, K-feldspar) for plutonic rocks along the Taku Inlet transect. Boundary fields from Irvine and Baragar (1971). *A*, Admiralty-Revillagigedo belt: ●, Grand Island subbelt; ✱, Taku Harbor subbelt. *B*, Mainland batholith; ●, Great tonalite sill belt; ✱, western units of Turner Lake batholith; ◆, eastern units of Turner Lake batholith.

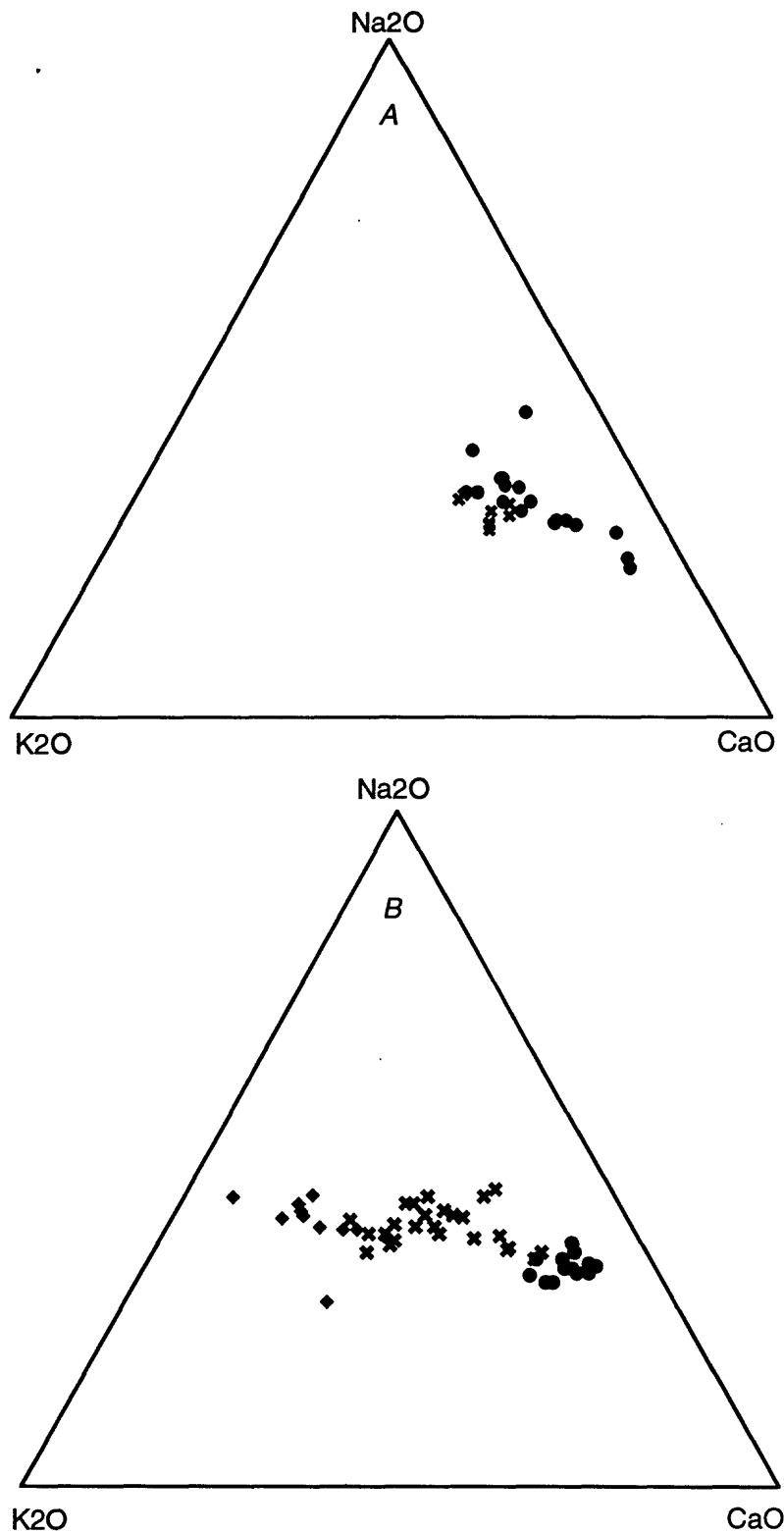


Figure 29. Ternary plots of K₂O-Na₂O-CaO for plutonic rocks along the Taku Inlet transect. *A.*, Admiralty-Revillagigedo belt; ●, Grand Island subbelt; ✕, Taku Harbor subbelt. *B.* Mainland batholith; ●, Great tonalite sill belt; ✕, western units of the Turner Lake batholith; ◆, eastern units of the Turner Lake batholith.

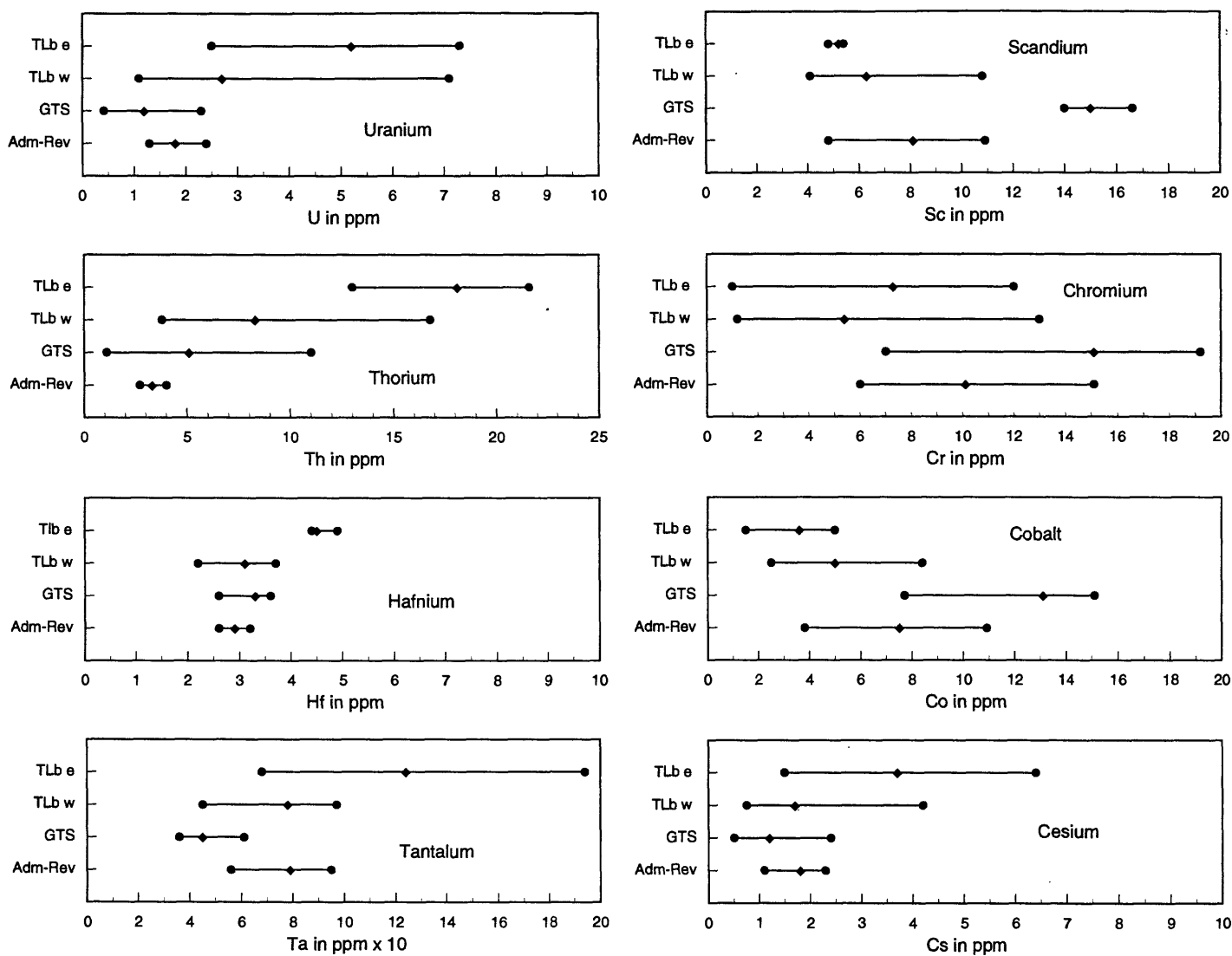


Figure 30. Range in selected trace elements for plutonic rocks of the major belts along the Taku Inlet transect. *Adm-Rev*, Admiralty-Revillagigedo belt; *GTS*, Great tonalite sill belt; *TLb e*, eastern subbelt of the Turner Lake batholith; and *TLb w*, western subbelt of the Turner Lake batholith.

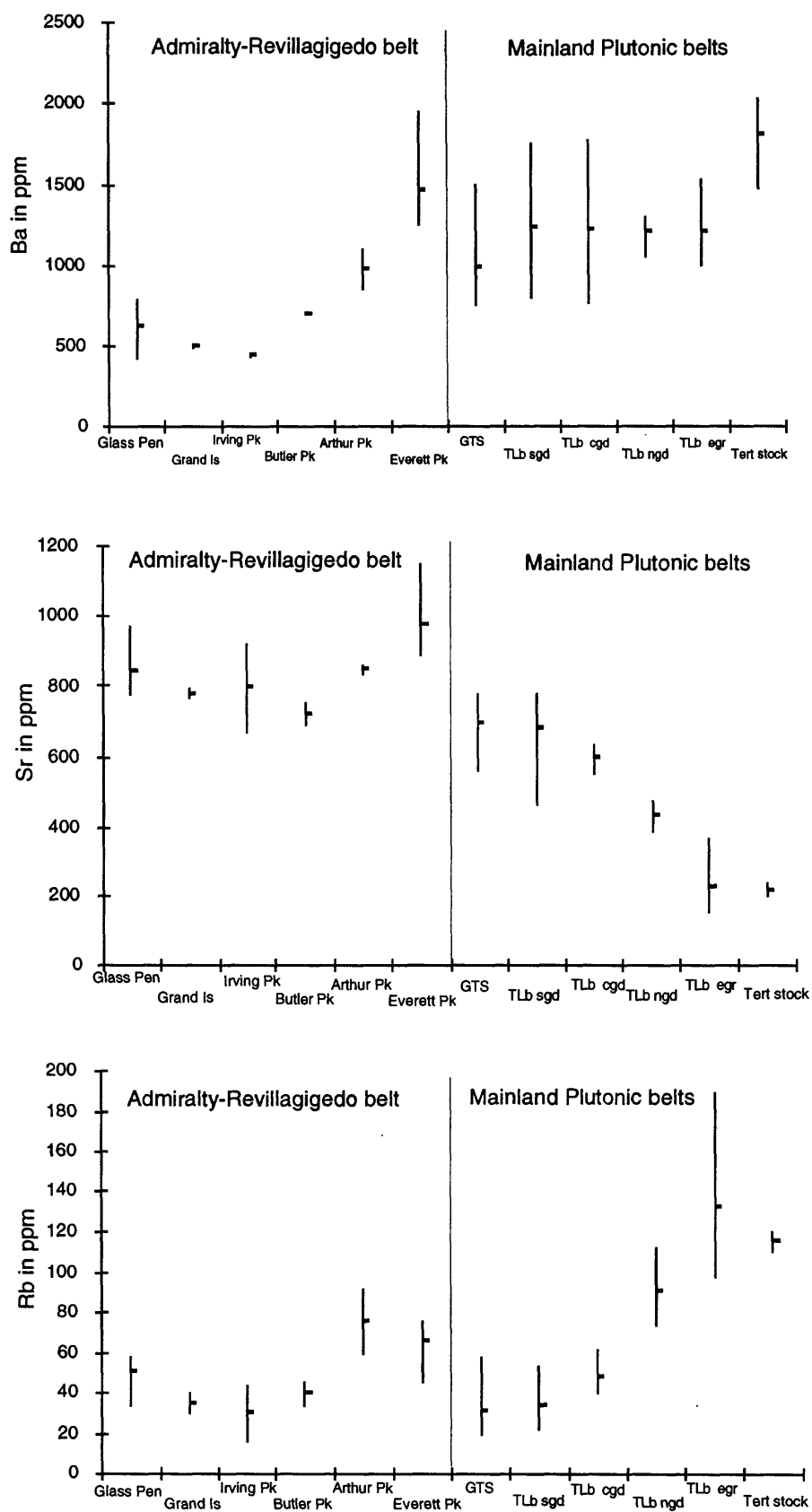


Figure 31. Range charts for barium, strontium, and rubidium abundances for plutons along the Taku Inlet transect.

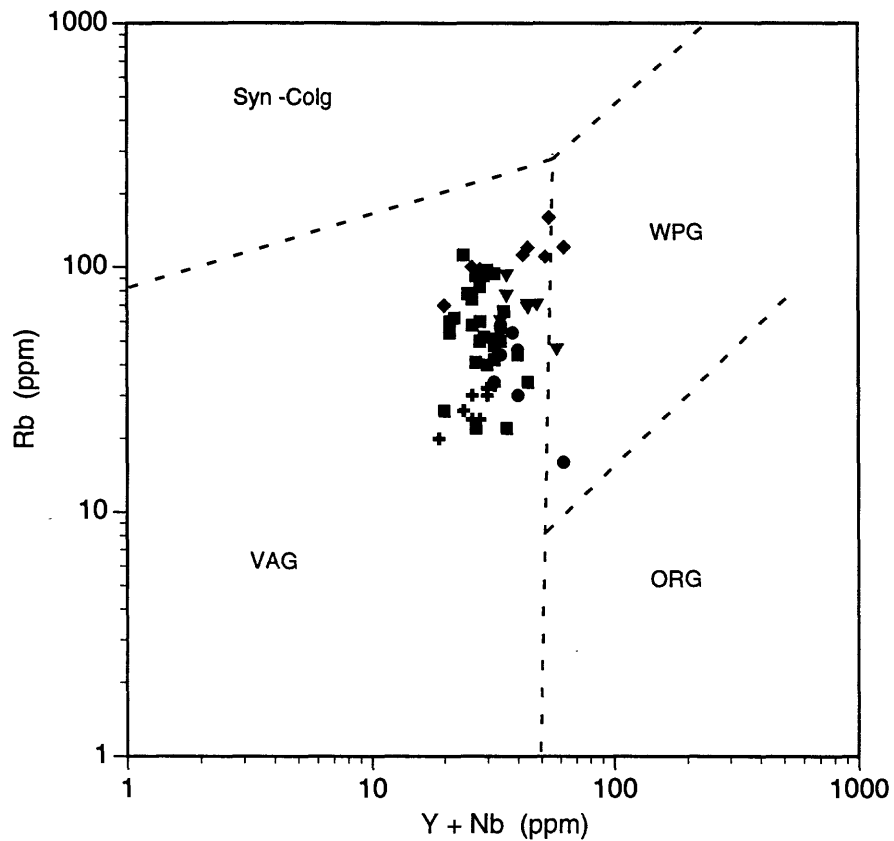


Figure 32. Variation diagram of Y+Nb versus Rb for plutonic rocks along the Taku Inlet transect. Tectonic affinity boundaries from Pearce and others (1984). Symbols: ●, Grand Island subbelt; ▼, Taku Harbor subbelt; ✱, Great tonalite sill belt; ■, western units of Turner Lake batholith; ◆, eastern units of Turner Lake batholith. VAG, volcanic arc granitoids; ORG, ocean ridge granitoids; WPG, within plate granitoids; Syn-Colg, late or post tectonic granitoids.

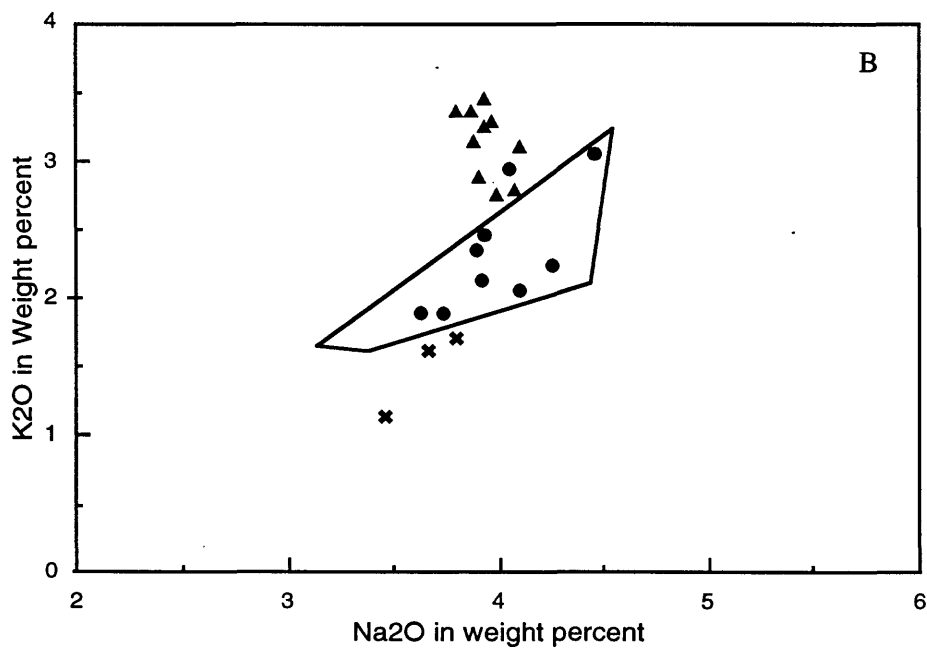
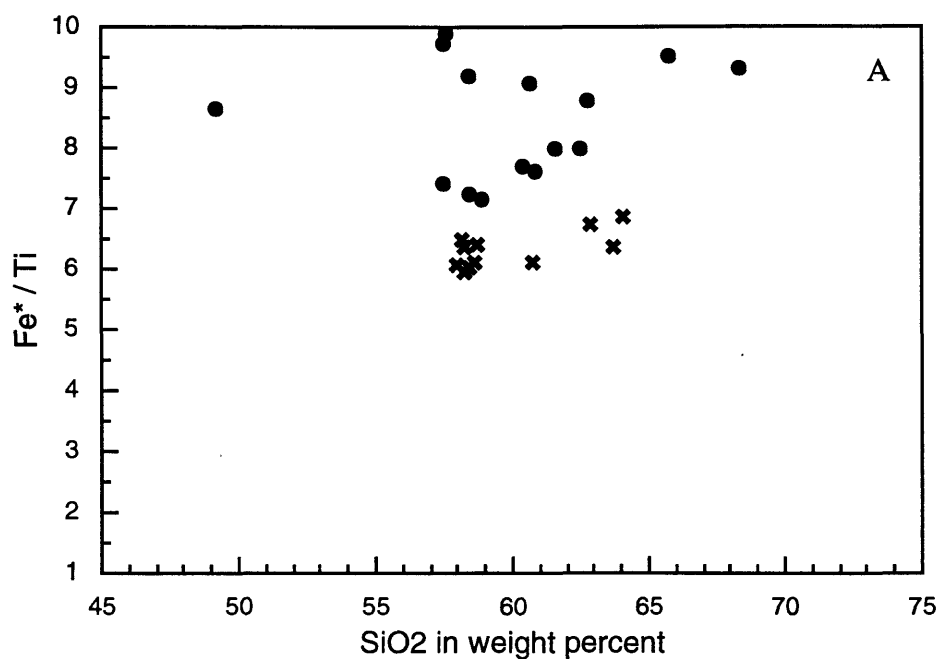


Figure 33. Binary variation diagrams for plutonic rocks of the Admiralty- Revillagigedo belt. A, Total Fe/Ti ratio versus SiO₂ plot: ●, Grand Island subbelt; ✕, Taku Harbor subbelt. B, K₂O versus Na₂O plot: ●, Glass Peninsula stocks; ✕, Grand Island pluton; ▲, Taku Harbor plutons.

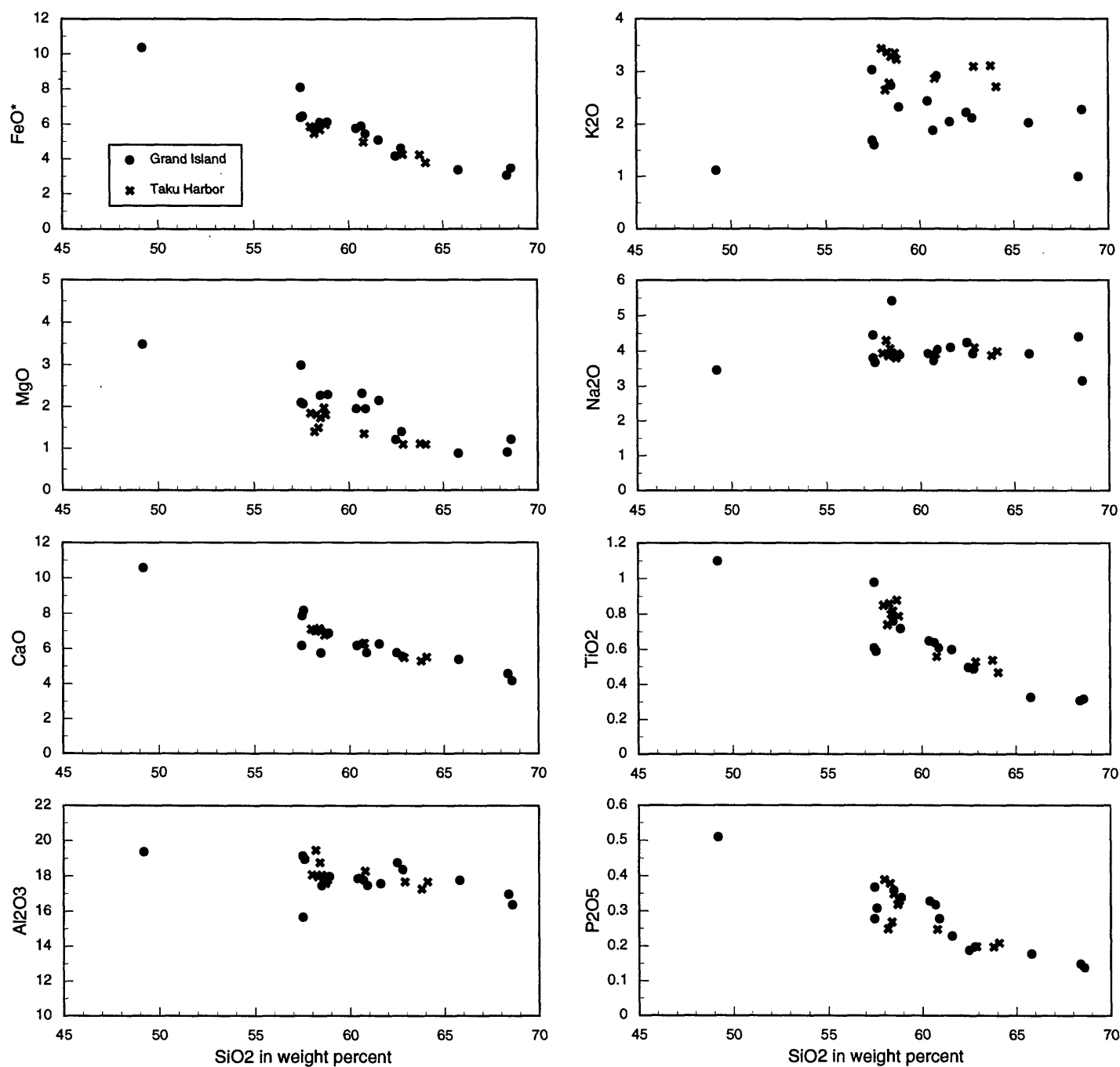


Figure 34. Harker type variation diagrams for plutonic rocks of the Admiralty-Revillagigedo belt.
 Symbols: ●, Grand Island subbelt; ✱, Taku Harbor subbelt.

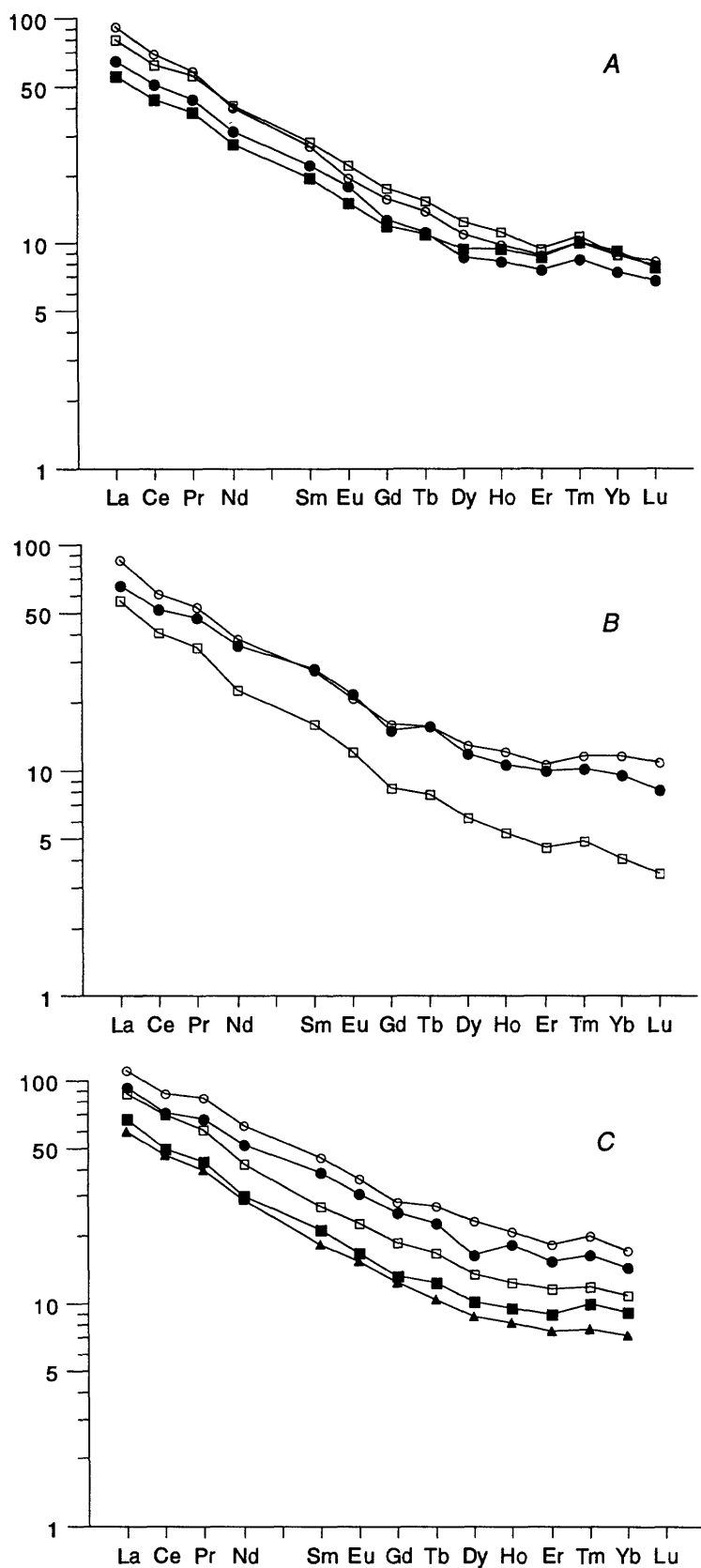


Figure 35. Chondrite-normalized rare-earth-element (REE) plots of representative plutonic rocks from the Admiralty-Revillagigedo belt. A, REE plot of plutonic rocks from the Glass Peninsula stocks and Grand Island pluton; B, REE plot of plutonic rocks from the Irving Peak and Butler Peak plutons; and C, REE plot of plutonic rocks from the Everett and Arthur Peaks plutons.

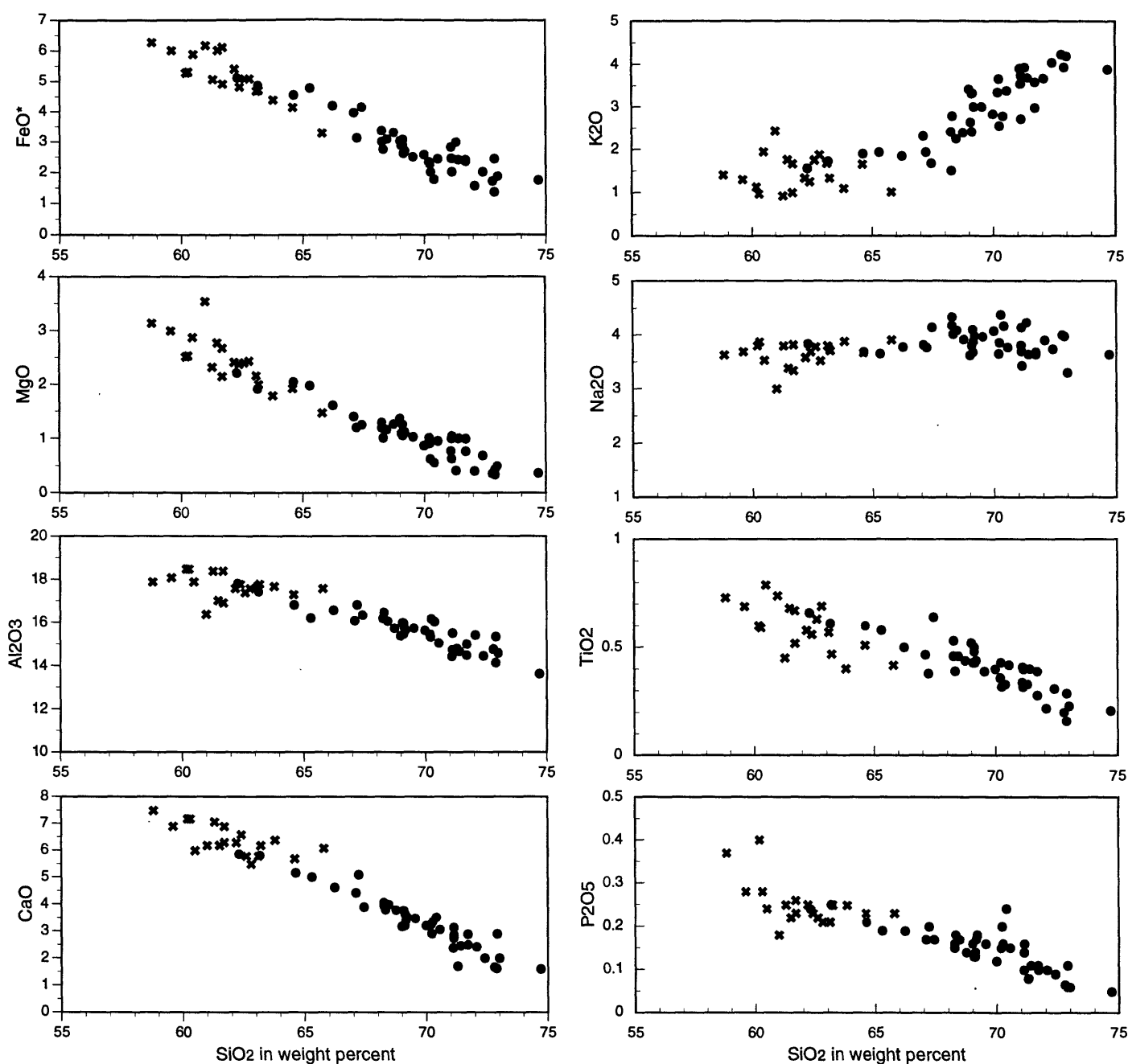


Figure 36. Harker type variation diagrams for plutonic rocks from the mainland plutonic belts.
 Symbols: x, Great tonalite sill belt; ●, Coast Mountains belt (Turner Lake batholith).

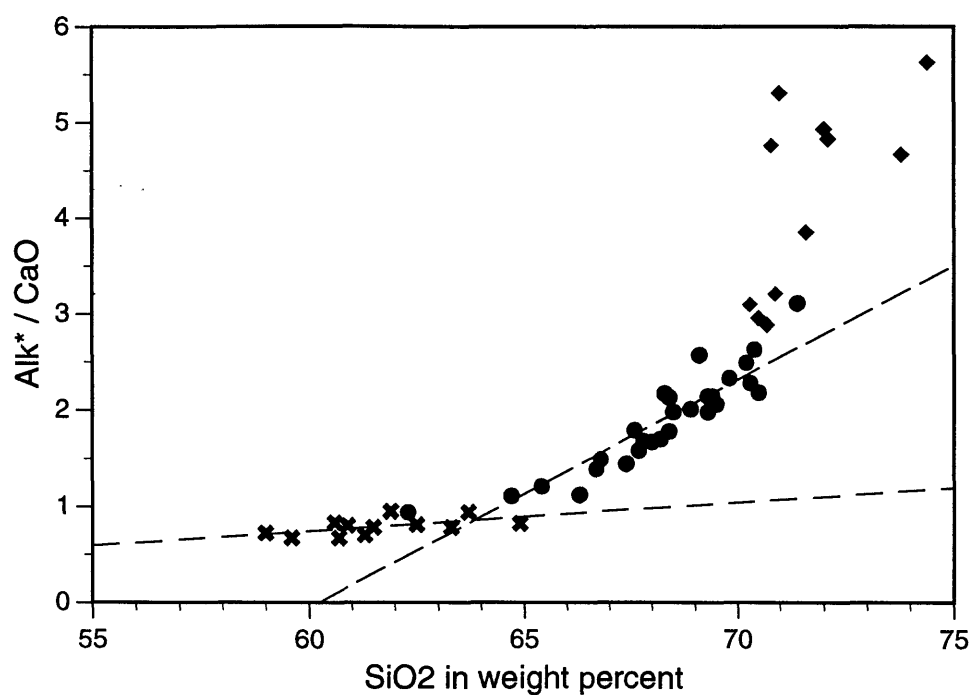


Figure 37. Binary plot of SiO₂ versus ratio of K₂O+Na₂O/CaO for rocks of the mainland batholith. Symbols: ✕, Great tonalite sill belt; ●, western units of the Turner Lake batholith; ◆, eastern units of the Turner Lake batholith

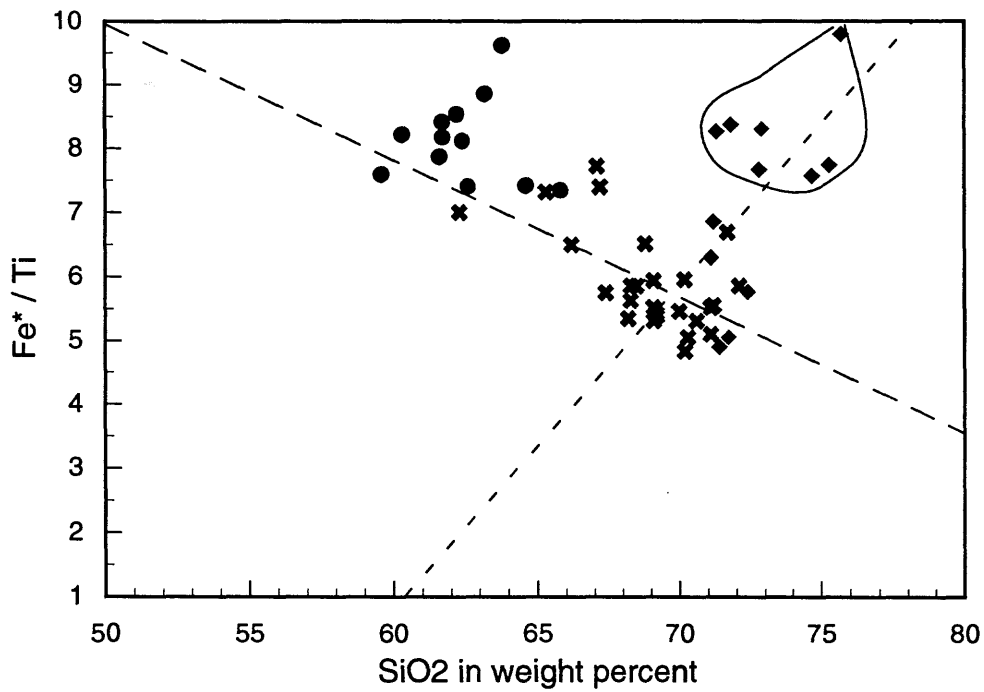


Figure 38. Binary plot of molecular ratio of Fe^*/Ti versus SiO_2 for rocks of the mainland batholith. Symbols: ●, Great tonalite sill belt; ✱, western units of the Turner Lake batholith ; and ◆, eastern units of the Turner Lake batholith.

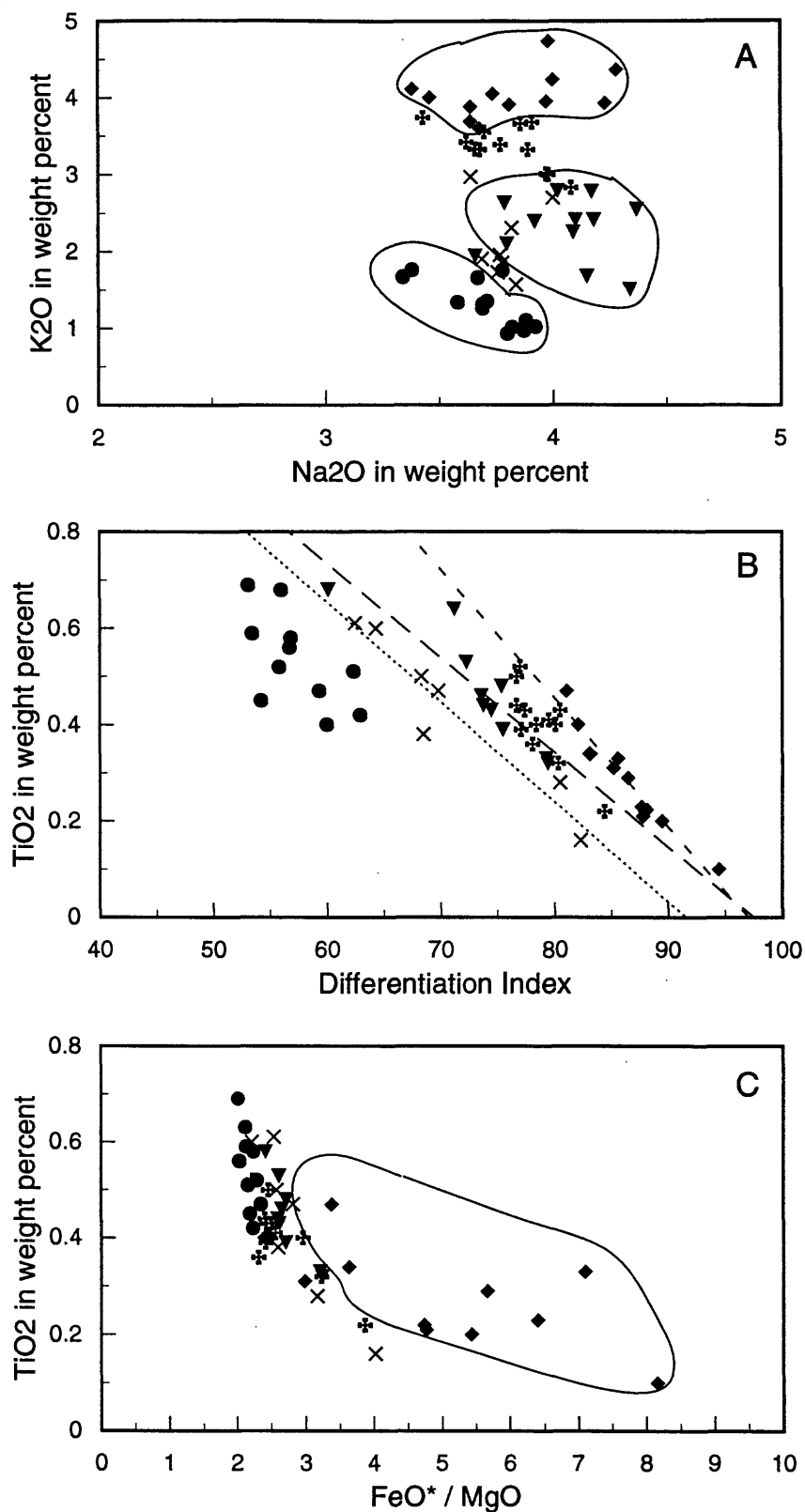


Figure 39. Binary variation diagrams for rock units of the mainland plutonic belts. Symbols: ●, Great tonalite sill belt; ×, southern unit of Turner Lake batholith; ▼, central unit of Turner Lake batholith; +, northern unit of Turner Lake batholith; and ◆, eastern units of Turner Lake batholith.

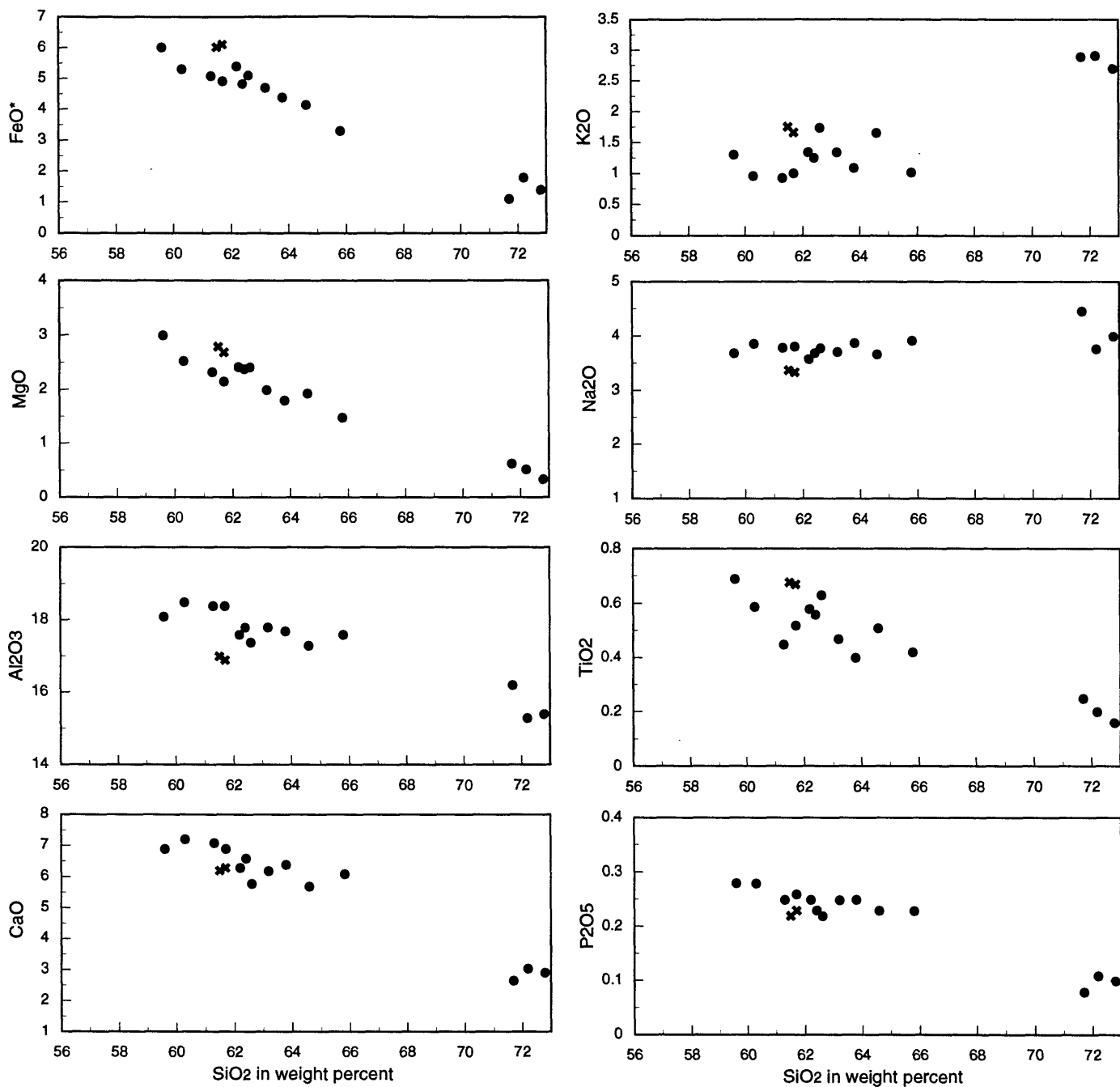


Figure 40. Harker-type variation diagrams for plutonic rocks from the Great tonalite sill belt along the Taku Inlet transect. Symbols: ●, Speel River pluton; *, Taku Cabin pluton.

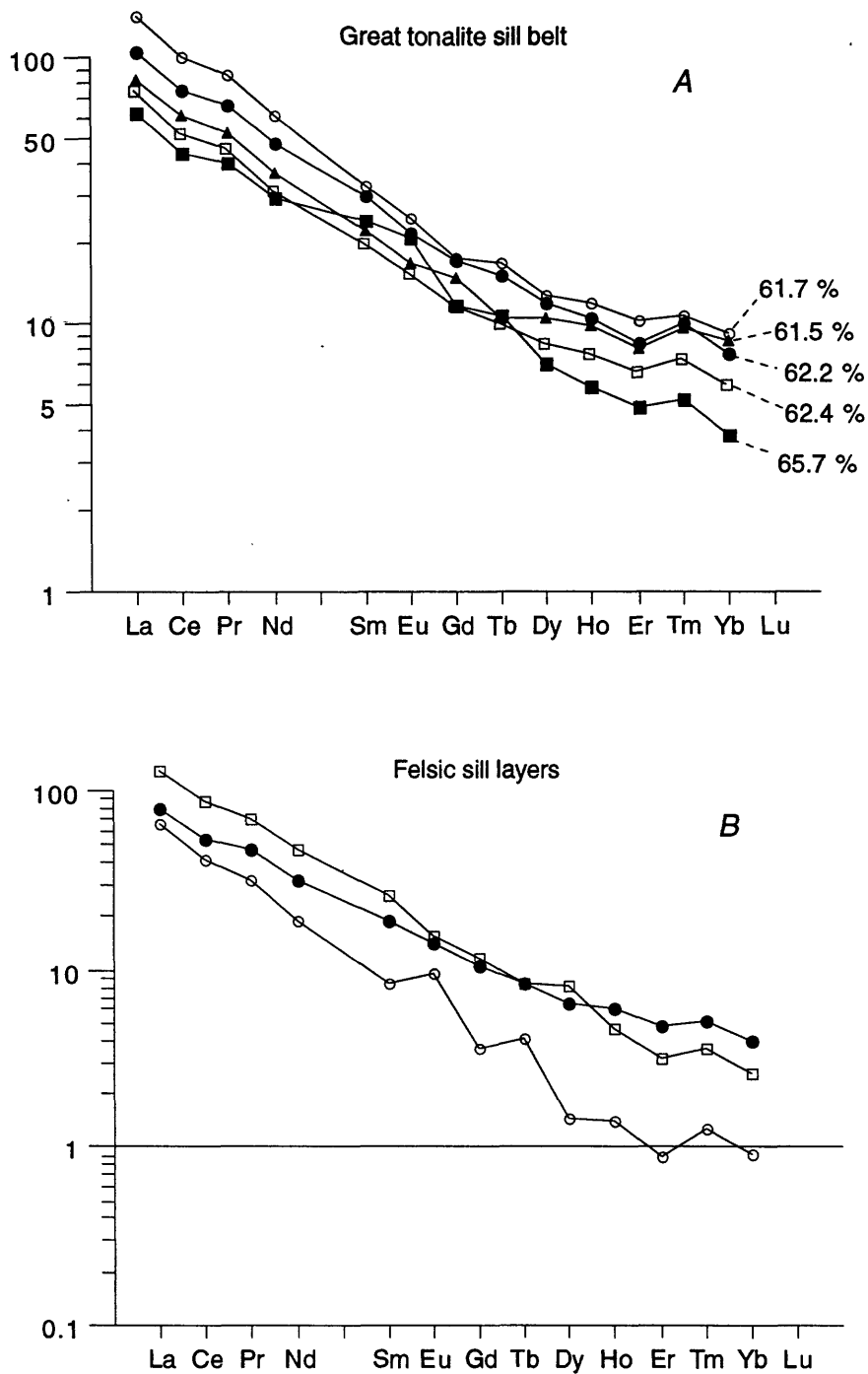


Figure 41. Chondrite-normalized rare-earth-element (REE) plots of representative plutonic rocks from the Speel River and Taku Cabin plutons. *A*, main phase tonalites with 61 to 66 percent SiO₂ content. *B*, felsic rocks associated with the Speel River pluton. Percentage numbers indicate whole-rock SiO₂ content (weight percent)

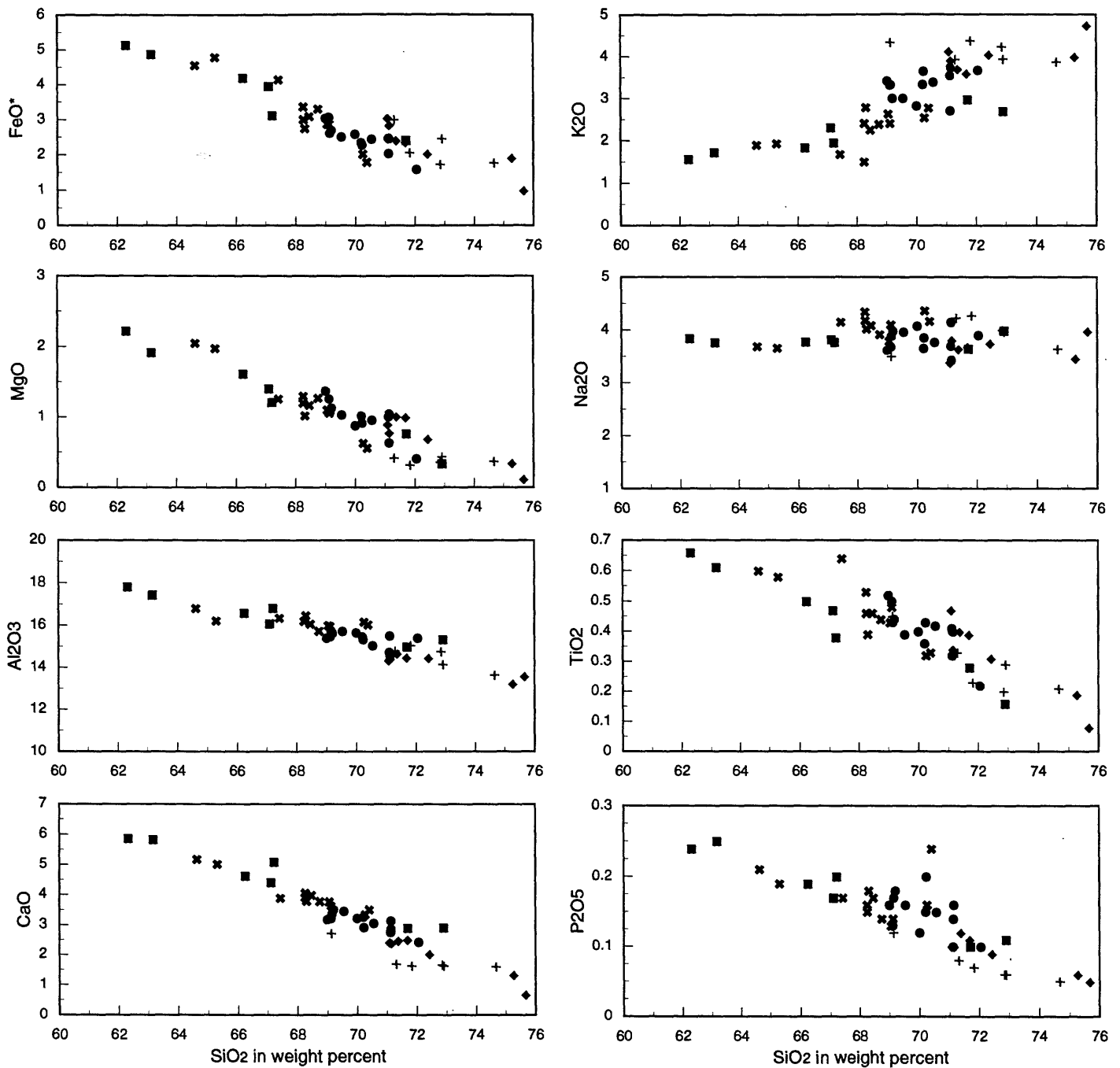


Figure 42. Harker type variation diagrams for plutonic rocks from the Coast Mountains belt (Turner Lake batholith) along the Taku Inlet transect: Symbols: ●, southern unit; ✕, central unit; ■, northern unit; ◆, undivided granite unit; and +, Wright Glacier stock.

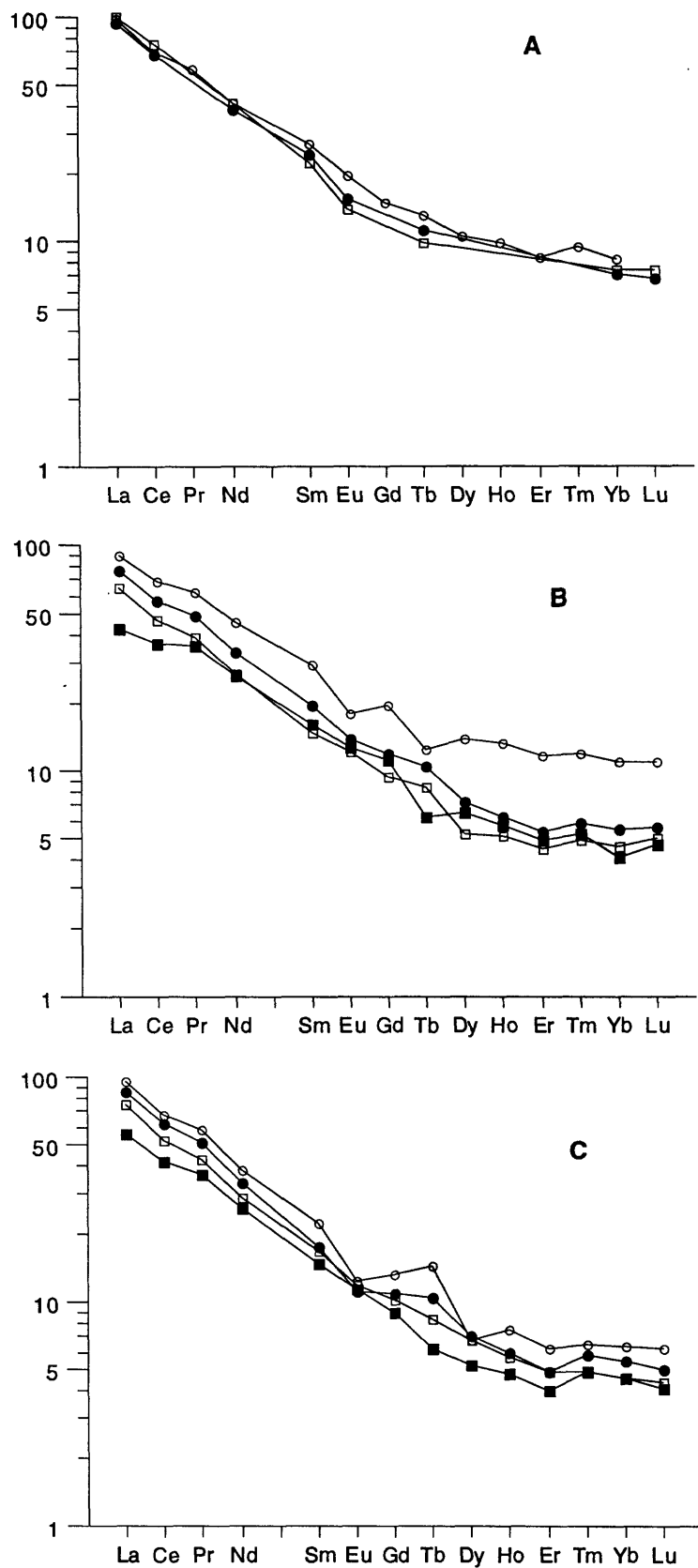


Figure 43. Chondrite-normalized rare-earth-element (REE) plots of representative plutonic rocks from the western units of the Turner Lake batholith. A, southern unit; B, central unit; C, northern unit.

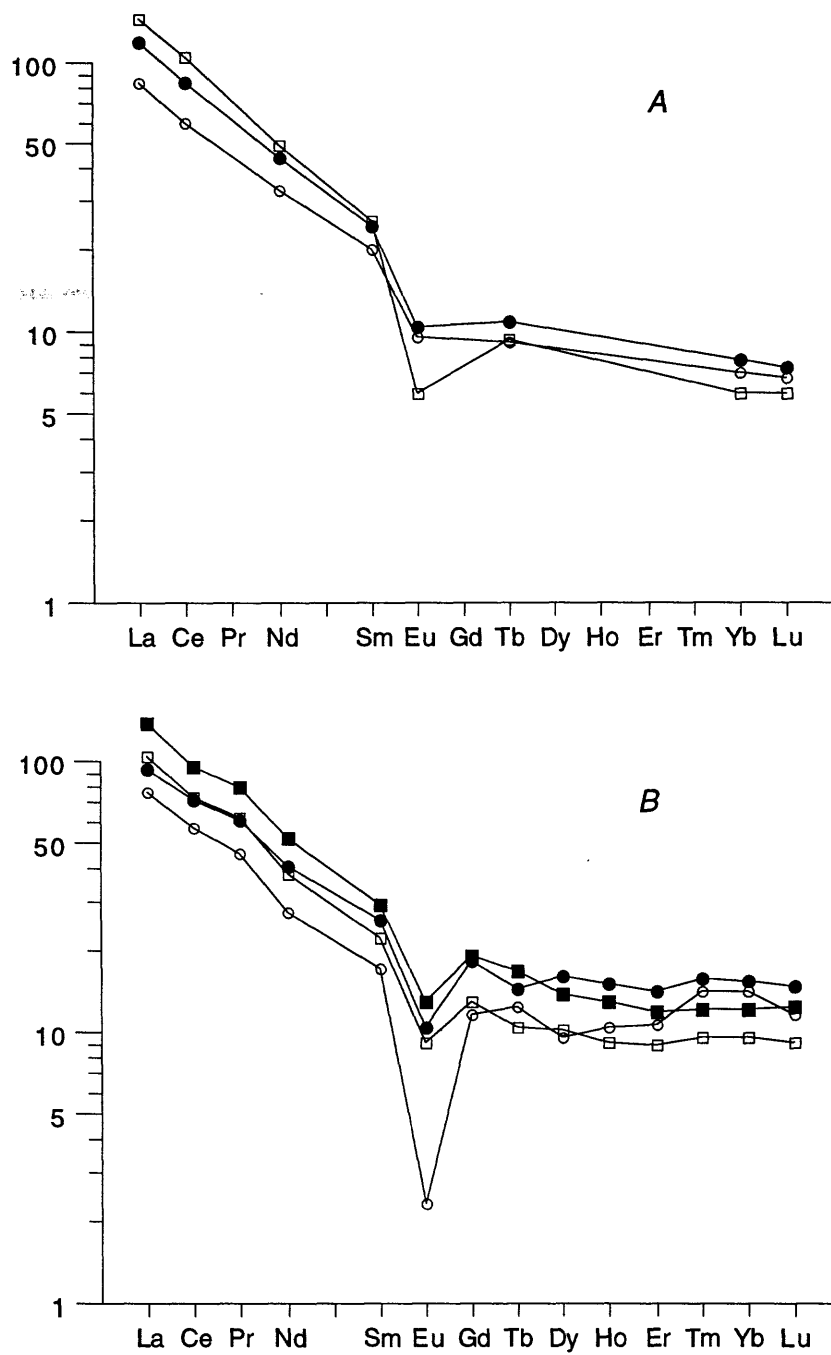


Figure 44. Chondrite-normalized rare-earth-element (REE) plots of representative plutonic rocks from the eastern units of the Turner Lake batholith. *A*, undivided granite unit; *B*, eastern unit and Wright Glacier stock.

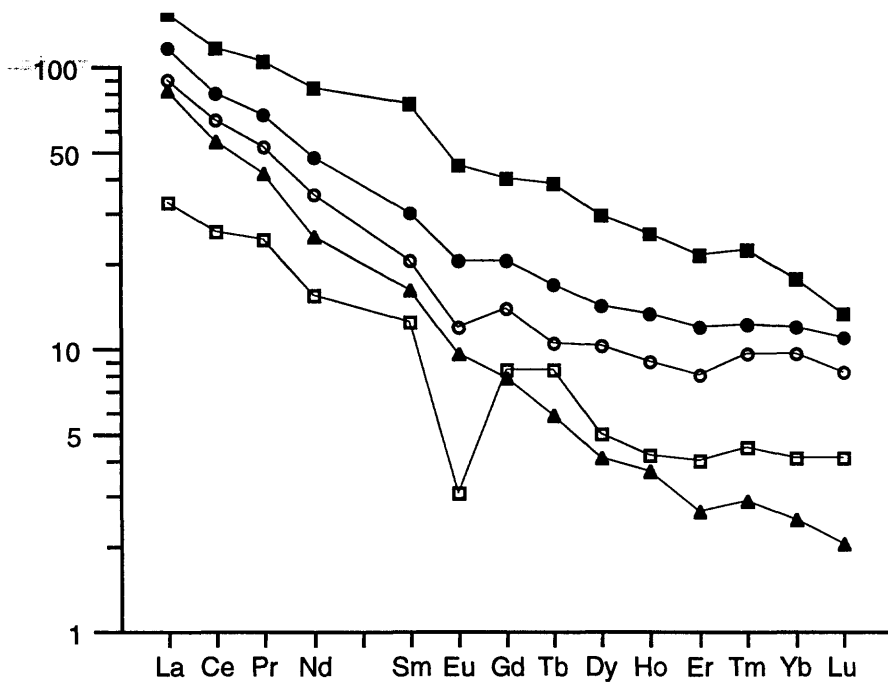


Figure 45. Chondrite-normalized rare-earth-element (REE) plots of representative plutonic rocks from miscellaneous (unsigned) plutonic bodies associated with the Turner Lake batholith. Samples: ■, granodiorite dike; ●, Wright River stock; ○, Wright River stock; ▲, granitic dike; and □, small granite body.

features suggest that the eastern granites evolved separately from the rest of the Coast Mountains belt. The major chemical features and variations are summarized below.

Felsic components, SiO_2 and K_2O , abruptly increase from west to east along the transect, but K_2O increases with increasing SiO_2 content only in the plutons from the western subbelt of the Turner Lake batholith, and shows no systematic variations with SiO_2 in rocks of the Great tonalite sill belt or eastern subbelt of the Turner Lake batholith. Na_2O varies little across the three subbelts showing a flat trend with SiO_2 .

Mafic components, (FeO^* , MgO , CaO , and TiO_2) show abrupt decreases eastward along the transect, and also exhibit systematic variations (negative correlation) with SiO_2 in all rocks.

Sr abundance decreases abruptly eastward and also decreases systematically with SiO_2 in rocks of the Turner Lake batholith. Rb shows an opposite trend to this and like Sr varies little with SiO_2 in rocks of the Great tonalite sill.

Uranium and thorium abundances are lowest in rocks of the Great tonalite sill but they increase rapidly in the rocks of the Turner Lake batholith.

Nb and Y show very little variation in abundance along the transect except for the Y enrichment (30-50 ppm) in the Wrights Glacier and Wrights River stocks.

The transition metals (Sc, Cr, Co, and Zn) are most abundant in rocks of the Great tonalite sill and with the exception of Cr decline rapidly across the Turner Lake batholith.

REE distributions vary little between rocks of the Great tonalite sill and western subbelt of the Turner Lake batholith whereas the granites of the eastern subbelt show significant differences in REE distribution patterns from other plutons of the CMC. The grossly similar REE abundances and fractionation patterns of the plutons of the Great tonalite sill and western subbelt of the Turner Lake batholith indicate they shared the same source rock and underwent similar crystal fractionation histories. Differences in some chemical attributes between silica- and K_2O -equivalent rocks of the two groups, however, indicates they evolved from separate but related magmas.

Granites (>70 % SiO_2) from the western and eastern subbelts of the Turner Lake batholith show significant differences in chemical attributes that indicate they are not genetically linked but probably evolved from separate unrelated magmas. The dissimilar REE patterns between these two granites may also indicate different or varied source material and or different mechanisms of melting and fractionation. In experimental studies (Hanson, 1980), various partial melting processes of mantle- or crustal-derived material could produce the observed REE patterns of the eastern granites.

SUMMARY AND DISCUSSION

Cretaceous and early Tertiary plutonic rocks of the northern part of the Coast Mountains Complex are products of three major periods of magmatism, and were emplaced in six separate pulses of plutonism. The presence of these pulses or subbelts is evident by abrupt rather than gradual changes in lithology, chemistry, and ages across the complex. The plutons of the Admiralty-Revillagigedo belt show characteristic features of an oceanic island arc environment (Brew, 1992; Pitcher, 1982), whereas the plutonic rocks of the two mainland belts are typical of calc-alkaline, subduction- or collision-related, continental-margin magmatic arcs elsewhere (Brew, 1992; Pitcher, 1982; Barker and Arth, 1990). The small Cretaceous plutons of the Admiralty-Revillagigedo belt represent a separate two-phase magmatic episode that ended approximately 20 m.y. prior to inception of plutonism in the mainland Coast Mountains. In the mainland Coast Mountains, U-Pb ages record a

history of shifting of loci of magmatism eastward with the emplacement of four distinct northwest-trending suites (subbelts) of plutonic rocks that have time spans of 2 to 8 m.y. between suites. Two of the subbelts comprise the Great tonalite sill belt of sheet-like tonalitic to granodioritic plutons, that were emplaced mostly near the end of early Paleocene time. The other two subbelts form the Coast Mountains belt, and within the Taku Inlet transect area, were emplaced in Eocene time as large massive granodioritic and granitic plutons of the Turner Lake batholith.

The Cretaceous tonalites and quartz diorites of the Admiralty-Revillagigedo belt differ from similar-appearing rocks of the mainland belts by the occurrence of primary epidote and garnet. The very low magnetic susceptibilities of most of these rocks reflects the presence of ilmenite and sulfides rather than magnetite. These rocks are also distinguished by their crowded plagioclase-porphyritic textures, and higher FeO^*/MgO ratios and Sr content than other belt rocks.

The mostly Paleocene tonalites of the Great tonalite sill belt are characterized by their coarse-grained, foliated, equigranular textures and relatively high color index, and by their very high magnetic susceptibility, low K_2O and Rb content, and low FeO^*/MgO ratios. These rocks typically contain higher abundances of ferromagnesian trace elements (Ti, Cr, Sc, and Co) than other belt rocks. A silica-gap of 66-71 percent occurs between these rocks and the high-silica, peraluminous, granodioritic phase of these plutons.

The Eocene massive granodiorites, tonalites, and minor granites that form the western subbelt of the Coast Mountains belt are titanite-bearing equigranular to slightly porphyritic rocks with moderate to high magnetic susceptibilities. Chemically, they show a strong genetic relationship to the tonalites of the Great tonalite sill belt.

The massive granites that form the eastern subbelt of the Coast Mountains belt are middle and late Eocene in age and are allanite-bearing porphyritic to seriate rocks which have a moderately low magnetic susceptibility signature. These are K_2O -rich rocks that contain higher Rb and lower Sr abundances than silica-equivalent rocks of the western subbelt. The coherent distribution of major element-oxides on Harker diagrams suggest a natural petrogenetic continuum or evolution from the granitic rocks of the western subbelt, but conversely, the abrupt increases in the alkali/lime index, $\text{K}_2\text{O}/\text{Na}_2\text{O}$ and Rb/Sr ratios, and the dissimilar REE fractionation patterns indicate significant differences in the magmatic evolution of the eastern granities.

The differences between the three major plutonic belts are related to the ages of the plutons and the host terranes in which the plutons were emplaced (Drinkwater and others, 1994). The cause of the compositional and textural differences between progressively younger plutons from adjacent subbelts is less clear but may also be related to slight differences in age, composition of host terranes, depths of generation, and the tectonic-structural regime of emplacement (fig. 52). If the eastern granites are indeed unrelated to the rest of the CMC, then they may warrant designation as a plutonic belt rather than the subbelt usage we are using.

Petrogenetic Implications

The three plutonic belts of the northern part of the CMC differ in age, magnetic susceptibility, and chemical characteristics, and were emplaced in different terranes (fig. 52) and structural-tectonic regimes (Drinkwater and others, 1994). The older age, low magnetic susceptibility, accessory mineralogy, chemical characteristics, and position west of the megalineament separate rocks of the Admiralty-Revillagigedo belt as representing a distinct episode of plutonism from the mainland batholith east of the megalineament. Because these plutons are unrelated

to the Great tonalite sill and Coast Mountains belts, they need to be discussed separately.

Any interpretation of the origin of the Admiralty-Revillagigedo belt of plutons in the northern part of the CMC must take into account the many unique features of these granitoids including 1) the small size of the plutons; 2) the absence of magnetite and the reduced nature of the rocks of most of the plutons; 3) presence of primary (magmatic) epidote; 4) the differences between the two subbelts; and, 5) the low pressure outer contact aureoles and regional rock assemblage (Brew and others, 1990). Many features of these plutons, including their small size, discordant contacts, narrow bands of contact metamorphism, porphyritic textures and oscillatory zoned plagioclase, and K-metasomatism with disseminated sulfides are generally considered characteristics of relatively shallow emplacement (McBirney, 1984). However, the presence of primary epidote, which indicates relatively high pressures (>8 Kbars) and deep emplacement (>25 km) (Zen and Hammarstrom, 1984), and the geobarometry work of Hammarstrom and Brew (1993) and Stowell and others (1993) which indicates pressures of emplacement of 7 - 9 Kbars, suggest moderately deep crustal levels of emplacement. The fact that most of these plutons are magnetite-free puts further constraints on their origin and emplacement history.

These plutons represent an unusual occurrence of epidote- and titanite-bearing magnetite-free granitoids that reflect unique magmatic conditions of formation or emplacement. Barker and Arth (1990) concluded from their measured low initial Sr ratios that plutons of the Admiralty-Revillagigedo belt originated either as fractionation products from mantle-derived melts, or from melts of deep-seated, juvenile, immature crust of the accreted terranes. The heat source, in both cases, was believed to be subduction-generated. The borderline tholeiitic affinity, relatively high TiO_2 and ferromagnesium element content, and moderately evolved REE patterns exhibited by these plutons from the Taku Inlet transect would indicate a relatively immature island arc or back arc derivation, but these plutons also intrude the Douglas Island volcanics which show geochemical affinity to Wrangellia continental terrane rocks (Ford and Brew, 1988). The origin of these epidote-bearing magnetite-free I-type plutons must be related to particular thermal and pressure conditions of generation and emplacement that occur within a high tectonic stress regime that formed the narrow fault-bounded wedge of imbricated polygenetic terrane rocks into which the plutons were emplaced.

The magnetite-free plutons of the Admiralty-Revillagigedo belt along the transect are iron-rich rocks that have relatively low iron oxidation states (Drinkwater and others, 1993) and therefore were either generated as reduced magmas or as oxidized magmas that became reduced during the subsequent magmatic history and emplacement. Most reduced plutons or "ilmenite series granitoids" (Ishihara, 1977) are considered to be either S-type granitoids (Chappell and White, 1974; Tulloch, 1989; Todd and Shaw, 1988) or strongly contaminated I-type rocks of granite or quartz monzonite composition (Ague and Brimhall, 1987, 1988; Ishihara and Sasaki, 1989). The plutons of the Grand Island subbelt are unique in that they are neither S-type granitoids nor granite in composition, but rather are reduced I-types of intermediate to mafic composition (Drinkwater and others, 1992). Additionally, primary (magmatic) epidote is conceived to have formed under oxidizing conditions (Zen and Hammarstrom, 1984), and primary titanite, which was thought to occur only in magnetite series (oxidized) granitoids (Ishihara, 1977; and Ague and Brimhall, 1987), commonly occurs in the magnetite-free plutons of the Grand Island subbelt. All plutons from the Admiralty-Revillagigedo belt along the transect contain primary epidote and titanite, but garnet occurs only in plutons of the Grand Island subbelt indicating that garnet is a more-reduced component of this magmatic system, which is compatible with the observations of Ishihara (1981) and Gastil (1990) that primary garnet occurs only in the magnetite-free granitoids. Whether the plutons

were intrinsically reduced or oxidized is uncertain, however, the lack of euhedral magnetite inclusions (or relicts of) and presence of euhedral garnet inclusions in plagioclase suggest that the magma was originally more-reduced. The common occurrence of hornfelsed sedimentary and volcanic rock inclusions, secondary muscovite, and disseminated sulfides in these plutons indicates that contamination and hydrothermal interaction were also important factors in the formation of these rocks.

The origin of two spatially and temporally related suites of plutons, one more-reduced (ilmenite and garnet+titanite+epidote), and the other more-oxidized (magnetite+titanite+epidote) would be difficult to explain by mantle-derived magmatic processes alone. However, they may have been generated at different depths in a vertically heterogeneous source, or derived in different terranes separated by the Fanshaw fault. A simple explanation for the magnetite-free plutons is that they were generated in the upper mantle or lower crust below the zone of oxidation, but emplacement and rapid solidification above the zone of oxidation would be necessary to explain the occurrence of titanite and epidote. Also, the more-reduced plutons with oxidized components could be explained either as mixtures (assimilation) or due to late magmatic-hydrothermal interaction. If assimilation was an important factor, the source of contamination could be pelitic metasedimentary rocks of the Alexander-Wrangellia terrane, which contain graphitic and carbonaceous material (Brew and others, 1984; Brew and Ford, 1986), but other plutonic belts to the west (Brew and Morrell, 1983) that were also emplaced into the Alexander-Wrangellia terrane are magnetite-bearing (Brew and Ford, 1986; Fukuhara, 1986), thus making this terrane an unlikely source. A better alternative are the rocks of the Gravina overlap assemblage which are largely restricted to the same region as the plutons of the Grand Island subbelt.

Plutons of the mainland batholith, within the Taku Inlet transect, are spatially and temporally related, and form three distinct northwest-trending, progressively younger groups of plutons. Although plutons of the Great tonalite sill and western subbelt of the Coast Mountains belt had different mechanisms of emplacement within different tectonic-stress environments (Barker and Arth, 1990; Brew and others, 1991; Drinkwater and others, 1994), they are genetically linked by coherent chemical characteristics and variations and thus form a comagmatic suite of plutons. The granitic rocks of the eastern subbelt however, show distinct chemical characteristics from granites of the western subbelt of the Turner Lake batholith. The differences in the joint pattern distribution between the two subbelts also implies differences in the tectonic-thermal stress environment of emplacement. This implies that the eastern granities evolved separately from the tonalitic and granodioritic magmatism to the west and are not linked to them as simple fractionation products. Barker and Arth (1990); and Samson and others (1991) determined, through Sr and Nd isotope studies, that plutons of the Great tonalite sill and Coast Mountains belt are genetically related to the same source and magmatic evolution, but Arth and others (1988) also found that the younger granitic rocks in the eastern part of their transect in the Ketchikan area were isotopically distinct from the plutons of the mainland batholith and may be similar to the granites of the eastern part of the Taku Inlet transect.

It is beyond the scope of this report to extrapolate on the nature of the protolith and magmatic evolution of the plutons of this part of the mainland CMC. Previous interpretations on the source and petrogenesis of the CMC were based on Sr and Nd isotopic systematics studies of Barker and Arth (1990); Arth and others (1988); and Samson and others (1991); and the U-Pb geochronology studies of Gehrels and others (1991). In the Ketchikan area, the plutons of the CMC were interpreted by Arth and others (1988) as fractionated products of a two-component system, partial melts of the mantle and assimilated juvenile, immature and largely oceanic crust of the accreted terranes. In the northern part of the CMC, Samson and others (1991)

determined that the plutons were derived largely from crustal rocks, possibly with some influx of mantle-derived melts, and that isotopic evidence indicates a substantial amount of old evolved continental crust was incorporated into the melts. Gehrels and others (1991) found inherited zircons in plutons of the northern part of the CMC and suggest that they were derived from assimilated crustal rocks of Early Proterozoic to mid-Paleozoic age, that they correlated with the Yukon-Tanana terrane. Himmelberg and others (1990) reasoned that the Great tonalite sill plutons were, in part, mantle derived, and Ingram and Hutton (1994) also argued for a largely mantle-source based on physical and petrographic evidence.

Our results support a common source and magmatic evolution for plutons of the Great tonalite sill and western subbelt of the Coast Mountains belt regardless of the essential source component; the main subbelts probably evolved separately from similar parent magmas. The sodic composition ($\text{Na}_2\text{O} > \text{K}_2\text{O}$), high Sr content, and steep REE distributions with fractionated HREE and absence of Eu anomalies supports derivation of Great tonalite sill rocks from deep-seated crustal or upper mantle sources. The very homogeneous composition and textures of the Great tonalite sill plutons also indicates a relatively deep and equilibrated source. The plutons that form the western subbelt of the Turner Lake batholith are also sodic, contain relatively high but variable Sr content, and have negligible Eu anomalies, that implies that they are more like the Great tonalite sill rocks than the eastern granites.

The plutons of the western subbelt of the Turner Lake batholith are also the most diverse group in composition within the transect; from south to north the plutonic units become less mafic and more silicious and potassic in composition, which suggest a temporal and spatial evolution of magmatic compositions that are linked to changes in source region composition or conditions of magma generation. However, linear trends on Harker variation diagrams are generally attributed to mixing (or unmixing) of two components rather than to fractional crystallization of partial melts, which produce more curved patterns on Harker diagrams (Wall and others, 1987; Chappell and others, 1987). This indicates that the variations in compositions may be due to variations in the host rock (crustal assimilation) rather than the source rock. If the three plutonic units were derived from the same source regime, then their north-south compositional trends must reflect either a slightly changing source composition or variations in crustal thickness. The regular variation in SiO_2 , Sr, Rb, and alumina saturation index from north to south along the CMC of southeastern Alaska (Brew, 1988; Drinkwater and others, 1994) may also reflect differences in source composition or crustal thickness along the orogen. Whatever the scenario, the high LILE abundances and highly fractionated REE distribution patterns for these rocks support isotopic evidence (Barker and Arth, 1990; Samson and others, 1991) that significant amounts of crustal material were involved in the petrogenesis of these plutons.

The eastern granites show petrographic and chemical evidence for a separate magmatic evolution from plutonism to the west. The potassic composition ($\text{K}_2\text{O} > \text{Na}_2\text{O}$), low Sr content, high iron oxidation states, and pronounced negative Eu anomalies and unfractionated HREE patterns shown for the eastern granites is compatible with derivation from a relatively shallow crustal source of more felsic and garnet-free composition. These rocks also contain relict pyroxene rimmed by amphibole, a feature considered by some workers (Chappell and others, 1987) to be re-equilibrated restite (source material) but which also is attributed to crystallization under low water fugacities and subsequent partial reaction at relatively low crystallization pressures (Wall and others, 1987). The differences in the REE distribution and fractionation patterns between the two suites of plutons may reflect the nature of the country terrane rocks. The less fractionated REE assemblage of the more felsic granites of the eastern subbelt may reflect greater amounts of juvenile or mantle-derived material in the source region, and the more fractionated REE assemblage of the western

tonalites and granodiorites may indicate larger amounts of crustal derived material. This scenario is compatible with the interpretations of Samson and others (1991) who concluded through their isotopic studies that a substantial amount of evolved PreCambrian crustal component, that they linked with the Yukon-Tanana terrane, as well as some mantle-derived material or juvenile terrane crust was involved in the petrogenesis of plutons in the west side of the northern Coast Mountains batholith. If this is so, then the boundary between the western and eastern subbelts of the Turner Lake batholith may mark or be near a major structural break that represents the eastern limit of the piece of Yukon-Tanana (Nisling) terrane or of the Tracy Arm terrane of Berg and others (1978) and Monger and Berg (1987). This structural break may represent the southern extension of the Meade Glacier fault that Brew and Ford (1987) mapped as a possible tectonic boundary between the Stikine terrane to the east and the outboard terranes of the compressional orogen to the west, but was later interpreted by Brew and others (1991) as a transtensional fault contact between upper and lower parts of the Stikine terrane.

The granites of the Wrights Glacier stock and eastern unit along the Canadian boundary are also chemically different from the main-phase granites of the eastern subbelt. These more felsic granities of the eastern subbelt may represent a separate magmatic event derived from a different source terrane. The Wright Glacier stock and felsic granites of the eastern part of the transect also resemble the younger and less evolved granitic rocks of the Ketchikan and Skagway areas (Barker and Arth, 1990), which are believed to have been emplaced at shallow levels (Gehrels and others, 1991) as largely crustal melts of immature oceanic type crust (Barker and Arth, 1990) in a tensional- or slightly transtensive to extensional stress regime (Barker and Arth, 1990; Brew and others, 1991; and Brew, 1992). The transitional chemical nature of the main (western part) phase granites suggest that they may be mixtures of components from two different terranes whereas the more felsic granites to the east may have been derived solely from the Stikine terrane.

Emplacement of the Mainland Batholith

The regular spatial and temporal distribution, continuity, and homogeneous compositions of the major plutonic belts indicates that their emplacement was structurally controlled by tectonic processes. All the intrusions of the mainland batholith within the Taku Inlet transect reflect some degree of structural control indicating that both faults and structural trends of the metamorphic country rocks influenced the form of the various plutons. Structural control is more pronounced in the older plutons (Great tonalite sill belt), which are elongated and concordant with the regional northwest-trending structures. The Speel River pluton, which is intruded by by a younger pluton of the Turner Lake batholith, contains large screens of schist that parallel the foliation in the pluton indicating that it had strong structural control. The younger plutons of the mainland batholith (Turner Lake batholith) are areally more semi-equidimensional or irregular in outline and tend to show both concordant and discordant relations to the host rocks, indicating less influence by structures of the country rocks. The episodic nature of the different suites of plutons and the compositional differences between them may reflect differences in the composition and structural-stress regime of the host terranes (fig. 46), and to different depths of magma generation and emplacement.

Great Tonalite Sill (Belt) Plutons

The concordant thick sheet-like plutons of the Great tonalite sill belt were emplaced along a crustal-scale linear structural orogen (Crawford and others, 1987; Brew, 1988; Brew and others, 1989) believed to have been the loci of major collision and thrust-fault tectonics (Rubin and others, 1990; Gehrels and others, 1992). The

structurally controlled emplacement occurred synchronously with uplift, high-grade metamorphism and east-side-up displacement of the central metamorphic belt (Stowell and Hooper, 1990; Wood and others, 1991; Gehrels and others, 1992). The Speel River and Taku Cabin plutons show the pervasive northwest-trending and northeast-inclined fabrics typical of Great tonalite sill rocks. This fabric formed from magmatic-state deformation modified by solid-state deformation during the synkinematic emplacement of the plutons in a compressional orogen (Hutton and Ingram, 1992; Ingram and Hutton, 1994). Ingram and Hutton (1994) used structural fabric analysis to interpret the emplacement zone as a steeply-dipping, contractional ductile shear zone, which they concluded was an unusual environment for major pluton emplacement.

The emplacement of plutons of the Great tonalite sill in the northern part of the CMC is believed to have been at mid-crustal depths corresponding to pressures of 5-6 Kbar (Hollister and others, 1988; Stowell and others, 1989), although Himmelberg and others (1991) suggested that initial emplacement of these sills was actually at greater pressures corresponding to depths of 30-35 kilometers, and that the 5-6 Kbar figure represents final emplacement after uplift. Ingram and Hutton (1994) postulated that magma generation occurred at the base of a crustal-thickened shear zone near the Moho boundary that they believe is a crustal-scale longitudinal discontinuity that represents the boundary of the Insular and Intermontane superterrane. The problems of sill emplacement at substantial depths has been discussed by many workers (for example, Mudge, 1968), particularly in compressional tectonic environments where very large magmatic pressures would be required to overcome the lithostatic pressures of overburden and compressional stress. This problem was recognized by Ingram and Hutton (1994) who postulated that emplacement by repeated internal dike propagation and sheet wedging could overcome wall-rock stresses and overburden pressures. The presence of granodiorite segregations and screens of metasedimentary wall rocks in the Speel River pluton indicates that this pluton is composed of multiple coalesced sheet-like intrusions as envisaged by Ingram and Hutton (1994). Some plutons of the Great tonalite sill show decrease in K-Ar ages from west to east across the bodies (Stowell and others, 1989) that were interpreted by Wood and others (1991) not as sequential magma injections but rather as sequential cooling from west to east in response to uplift. It is probable that both mechanisms occurred in the formation of individual plutons of the Great tonalite sill belt.

Coast Mountains Belt

Plutons of the Coast Mountains belt are post-tectonic (post-thrusting) intrusions that formed a continental-margin uplift batholith (Brew, 1989). They show evidence of late-synkinematic to post-kinematic emplacement in either a slightly extensional or transtensional (Crawford and other, 1987; Barker and Arth, 1990) or transpressional to extensional (Brew and others, 1991; Brew, 1992) stress environment that followed the crustal-thickening compressional event associated with the emplacement of plutons of the Great tonalite sill belt. Although these two major plutonic belts were emplaced in different tectonic-structural stress regimes, most of the plutons are genetically linked by chemical and isotopic signatures. Samson and others (1991) proposed a thrusting-related crustal-thickening and anatexis model for the origin of these rocks based on the results of their Sr and Nd isotopic studies. The rocks were interpreted by Barker and Arth (1990) as being largely mantle-derived and representing subduction-related continental-margin magmatism that developed possibly as an Andean-type magmatic arc. Our results support derivation of most of the Turner Lake batholith as strongly-contaminated mantle-derived magmas emplaced along a convergent continental margin during a transtensional or extensional tectonic episode, but are results are also compatible

with an anatexis model for the granites of the Wrights Glacier stock and eastern unit, which show evidence of shallower emplacement.

The western and eastern subbelts of the Turner Lake batholith show abrupt changes in chemistry and joint patterns between them which indicate that they are not directly related by magmatic processes or to the same source region. Differences in age, source rock composition, and regional stress field are indicated and suggest that the plutons of the two subbelts are separated at depth by a discontinuity that may be the boundary between unlike terranes. If this is true, then the eastern granites should be considered as a distinct plutonic belt. The generation and emplacement of the eastern granites at relatively shallower crustal levels is indicated by their proximity to cogenetic volcanic rocks (Ford and Brew, 1987), isotopic signatures of similar granites elsewhere in the CMC (Barker and Arth, 1990), relatively high iron oxidation states (Drinkwater and others, 1993), presence of pyroxene as an indicator of low crystallization pressures, and weakly evolved REE fractionation patterns.

Resource Potential

There is very little evidence for substantial mineralization directly associated with the plutons of the Taku Inlet transect. The only major ore deposits and occurrences in the region are found in the mother-lode-type rocks (schist, slates, and greenstones) of the Juneau gold belt which lies between the Great tonalite sill and 90-Ma plutons of the Admiralty-Revillagigedo belt. Although iron-stained rocks commonly occur in or near the plutons of the Taku Inlet transect, there are very few known mineral prospects or occurrences in them within this region of the CMC (Kimball and others, 1984; Wells and others, 1986; Cobb, 1978). The only former productive mine was the lode gold deposit at Limestone Inlet near the southern margin of the Arthur Peak pluton. This deposit consisted of auriferous quartz veins in altered slate and greenstone, as well as granitic rocks of the Arthur Peak pluton, that were briefly worked between 1908 and 1916 (Wells and others, 1986; Cobb, 1978). The mineralized veins, which contained free gold, galena, sphalerite, and chalcopyrite, are considered part of the Juneau gold belt that extends northward through the Juneau area (Twenhofel, 1952; Redman and others, 1985). A major silver-gold lode prospect, located just south of the Whiting River, was extensively worked in the early 1900s (Wells and others, 1986; Kimball and others, 1984; Cobb, 1978). The deposit consisted of sulfide-bearing quartz veins in dolomitic rocks near the southern margin of the southern (granodiorite) unit of the Turner Lake batholith. The mineralized veins, which contained arsenopyrite, pyrite, galena, sphalerite and chalcopyrite yielded fairly high silver values when it was worked between 1908 and 1916. South of the transect in the Sumdum region, are many iron-stained zones and minor mineralized occurrences found near gneiss-granite contacts in the central granitic belt (Kimball and others, 1984), but no major mineralized occurrences have been found.

Molybdenite occurs in granitic rocks along the Canadian boundary, and it may offer a greater resource potential than the mineralization described previously. A molybdenite prospect occurs in an altered granitic porphyry stock at Mount Ogden (Souther, 1971; Wells and others, 1986). Most of the mineralization is within Canada, but it may be similar to the molybdenite occurrences in porphyritic granite north of the transect known as the Boundary Creek occurrence (Brew and Ford, 1969; Koch and others, 1987). These molybdenite occurrences are found in the more felsic and oxidized granites of the eastern subbelt and indicate that the eastern subbelt granites may be favorable environments for porphyry molybdenum type deposits. Molybdenite-bearing granites also occur in the southern CMC (Hudson and others, 1979; 1981) east of Ketchikan, as small stocks of Miocene age. Porphyry

copper/molybdenum deposits are also related to oxidized granites of Cretaceous to early Tertiary age throughout the Circum-Pacific region (Ishihara, 1981).

There are no known prospects or mineralized occurrences in or near the non-magnetic 90-Ma plutons of the Admiralty-Revillagigedo belt. However, in the Circum-Pacific region, tin and tungsten deposits occur in non-magnetic granitic terranes and are associated with I-type reduced plutons (Ishihara, 1981). These mineralized plutons occur along the Asian-Pacific margin and are more granitic in composition than the quartz diorites and tonalites of the Admiralty-Revillagigedo belt. Lithophile element mineralization (W, Sn, Be, Li, Rb, F) is also associated with reduced granitoids in the Great Basin of western USA (Barton, 1990). According to Candela (1992), in granite-related ore systems tungsten and tin form ore solutions from reduced-type granitic magmas. However, making any analogy between this type of mineralization and the magnetite-free plutons of the Admiralty-Revillagigedo belt is difficult or inappropriate because most mineralized reduced granitic plutons are alkalic or S-type granites in composition, whereas the 90-Ma plutons of the Admiralty-Revillagigedo belt are calc-alkalic, metaluminous rocks of intermediate composition. The occurrence of ubiquitous disseminated sulfides in the plutons of the Grand Island subbelt may indicate that ore solutions did not form there. Although pyrrhotite is the common sulfide of deep level reduced plutons (Ishihara, 1981; 1977), we have analyzed only one sample, which proved to be pyrite.

REFERENCES CITED

- Ague, J.J., and Brimhall, G.H., 1987, Granites of the batholiths of California: Products of local assimilation and regional-scale crustal contamination; *Geology*, v. 15, p. 63-66.
- Arculus, R.J., 1987, The significance of source versus process in the tectonic controls of magma genesis: *Journal of Volcanology and Geothermal Research*, v. 32, p. 1-12.
- Arth, J.G., Barker, F., and Stern, T.W., 1988, Coast batholith and Taku plutons near Ketchikan, Alaska: petrography, geochronology, geochemistry, and isotopic character: *American Journal of Science*, v. 288, p. 461-489.
- Baedecker, P.A., 1987, Methods for geochemical analysis: U.S. Geological Survey Bulletin 1770
- Barker, Fred, Arth, J.G., and Stern T.W., 1986, Evolution of the Coast batholith along the Skagway Traverse, Alaska and British Columbia: *American Mineralogist*, v. 71, p. 632-643.
- Barker, Fred, and Arth, J.G., 1990, Two traverses across the Coast batholith, southeastern Alaska: in Anderson, J.L., ed., *The nature and origin of Cordilleran magmatism: Geological Society of America Memoir 174*, p. 395-404.
- Bateman, P.C., Dodge, F.C., and Kistler, R.W., 1991, Magnetic susceptibility and relation to initial $^{87}\text{Sr}/^{86}\text{Sr}$ for granitoids of the central Sierra Nevada, California: *Journal of Geophysical Research*, v. 96, no. B12, p. 19,555-19,568.
- Berg, H.C., Jones, D.L., and Coney, P.J., 1978, Map showing pre-Cenozoic tectonostratigraphic terranes of southeastern Alaska and adjacent areas: U.S. Geological Survey Open-File Report 78-105, scale 1:1,000,000.
- Bingler, E.C., Trexler, D.T., Kemp, W.R., and Bonham, H.P., Jr., 1976, PETCAL--A Basic language computer program for petrologic calculations: Nevada Bureau of Mines and Geology Report 28, 27 p.

- Brew, D.A., 1988, Latest Mesozoic and Cenozoic igneous rocks of southeastern Alaska--A synopsis: U.S Geological Survey Open-file Report 88-405, 29p.
- Brew, D.A., 1992a, Origin and distribution of granitic rocks in the Coast plutonic-metamorphic complex, N American Cordillera, southeastern Alaska, U.S.A. (abs): Transactions of the Royal Society of Edinburgh, Earth Sciences, v. 83, p. 486.
- Brew, D.A., 1992b, Mesozoic and Cenozoic intrusions and batholiths of the circum-Pacific region as analogues of pre-Phanerozoic batholiths: A summary: Basement Tectonics 8, Proceedings of the 8th International Conference on Basement Tectonics (Butte, Montana, 1988), p. 169-177.
- Brew, D.A., and Ford, A.B., 1977, Preliminary geologic and metamorphic-isograd map of the Juneau B-1 quadrangle, Alaska: U.S. Geological Survey Miscellaneous Field Studies Map MF-846, scale 1:31,680.
- 1978, Megalineament in southeastern Alaska marks southwest edge of Coast Range batholithic complex: Canadian Journal of Earth Science, v. 15, no. 11, p. 1763-1772.
- 1981, The Coast plutonic complex sill, southeastern Alaska, in Albert, N.R.D., and Hudson, T., eds., The United States Geological Survey in Alaska: Accomplishments during 1979: U.S. Geological Survey Circular 823-B, p. B96-B99.
- 1984, The northern Coast plutonic complex, southeastern Alaska and northwestern British Columbia, in Coonrad, W.L., and Elliott, R.L., eds., The U.S. Geological Survey in Alaska--Accomplishments during 1981: U.S. Geological Survey Circular 868, p. 120-124.
- 1986, Preliminary reconnaissance geologic map of the Juneau, Taku River, Atlin, and part of the Skagway 1:250,000 quadrangles, southeastern Alaska: U.S. Geological Survey Open-File Report 85-395, 23 p.
- Brew, D.A., and Grybeck, D., 1984, Geology of the Tracy Arm-Fords Terror wilderness study area and vicinity, Alaska: U.S. Geological Survey Bulletin 1525, 308 p.
- Brew, D.A., Himmelberg, G.R., Douglass, S.L., Zen, E., and Sutter, J.F., 1990, Contrasting metamorphic and emplacement environment of a distinctive 95 Ma plutonic suite, southeastern Alaska [abs.]: Geological Society of America, Abstracts with Programs, v. 22, no. 3, p. 10.
- Brew, D.A., Himmelberg, G.R., Loney, R.A., and Ford, A.B., 1992, Distribution and characteristics of metamorphic belts in the south-eastern Alaska part of the North American Cordillera: Journal of Metamorphic Geology, v. 10, p. 465-482.
- Brew, D.A., and Karl, S.M., 1988, A reexamination of the contacts and other features of the Gravina belt, southeastern Alaska, Supplemental data: U.S. Geological Survey Open-File Report 88-652, 8 p.
- Brew, D.A., and Morrell, R.P., 1983, Intrusive rocks and plutonic belts in southeastern Alaska, in Roddick, J.A., ed., Circum-Pacific plutonic terranes: Geological Society of America Memoir 159, p. 171-193.
- Brew, D.A., Ford, A.B., and Himmelberg, G.R., 1989, Evolution of the western part of the Coast plutonic-metamorphic complex, southeastern Alaska, USA--A summary; in Daly, J.S., and

others, eds., Evolution of metamorphic belts, Geological Society of America Special Publication no. 42, p. 447-452

- Brew, D.A., Karl, S.M., Barnes, D.F., Jachens, R.C., Ford, A.B., and Horner, R., 1991, A northern Cordilleran ocean-continent transect: Sitka Sound, Alaska, to Atlin Lake, British Columbia: Canadian Journal of Earth Sciences, v. 28, no. 6, p. 840-853.
- Brew, D.A., Ford, A.B., and Himmelberg, G.R., and Drinkwater, 1994, The Coast Mountains complex of southeastern Alaska, and adjacent regions, in Koozmin, E.A., ed., Stratigraphic notes--1994: U.S. Geological Survey Bulletin_____(in press)
- Buddington, A.F., 1927, Coast Range intrusives of southeastern Alaska: Journal of Geology, v. 35, no. 3, p. 224-246.
- Buddington, A.F., and Chapin, T., 1929, Geology and mineral deposits of southeastern Alaska: U.S. Geological Survey Bulletin 800, 398 p.
- Chappell, B.W., and White, A.J.R., 1974, Two contrasting granite types: Pacific Geology, v. 8, p. 173-174.
- Chappell, B.W., White, A.J.R., and Wyborn, D., 1987, The importance of residual source material (Restite) in granite petrogenesis: Journal of Petrology, v. 28, p. 1111-1138.
- Cobb, E.H., 1978, Summary of references to mineral occurrences in the Sumdum and Taku River quadrangles, Alaska: U.S. Geological Survey Open-File Report 78-698, 64 p.
- Cohen, H.A., and Lundberg, N., 1993, Detrital record of the Gravina arc, southeastern Alaska: Petrology and provenance of Seymour Canal Formation sandstones: Geological Society of America Bulletin, v. 105, p. 1400-1414.
- Coney, P.J., Jones, D.L. and Monger, J.W.H., 1980, Cordilleran suspect terranes: Nature, v. 288, p. 329-333.
- Crawford, M.L., Hollister, L.S., and Woodsworth, 1987, Crustal deformation and regional metamorphism across a terrane boundary, Coast plutonic complex, British Columbia: Tectonics, v. 6, no. 3, p. 342-361.
- Currie, L., and Parrish, R.R., 1993, Jurassic accretion of Nisling terrane along the western margin of Stikinia, Coast Mountains, northwestern British Columbia: Geology, v. 21, p. 235-238.
- Douglas, R.J.W., Gabrielse, H., Wheeler, J.O., Stott, D.F., and Belyea, H.R., 1970, Geology of western Canada; in Geology and economic minerals of Canada: Canada Geologic Survey Economic Geology Report 1, p. 366-488.
- Drinkwater, J.L., Brew, D.A., and Ford, D.A., 1989. Petrographic and chemical description of the variably deformed Speel River pluton, south of Juneau, southeastern Alaska: in Dover, J.H., and Galloway, J.P., Geological studies in Alaska by the U.S. Geological Survey, 1988: U.S. Geological Survey Bulletin 1903, p. 104-112.
- _____, 1990, Petrographic and chemical data for the large Mesozoic and Cenozoic plutonic sills east of Juneau, southeastern Alaska: U.S. Geological Survey Bulletin 1918, 47p.
- Drinkwater, J.L., Ford, D.A., and Brew, D.A., 1992, Magnetic susceptibilities and iron content of plutonic rocks across the Coast plutonic-metamorphic complex near Juneau, Alaska: in

- Bradley, D. and Dusel-Bacon, C., eds., *Geologic Studies in Alaska by the U.S. Geological Survey*, 1991, U.S. Geological Survey Bulletin 2041, p. 125-139.
- Drinkwater, J.L., Brew, D.A., and Ford, D.A., 1994, Chemical characteristics of major plutonic belts of the Coast Plutonic-metamorphic complex near Juneau, southeastern Alaska, *in* Till, A., and Moore, T., eds., *Geologic Studies in Alaska by the U.S. Geological Survey*, 1993, U.S. Geological Survey Bulletin 2107, p. 118-
- Ford, A.B., and Brew, D.A., 1977, Preliminary geologic and metamorphic-isograd map of northern parts of the Juneau A-1 and A-2 quadrangles, Alaska: U.S. Geological Survey Miscellaneous Field Studies Map MF-847, 1 sheet, scale 1:31,680.
- _____, 1987, The Wright Glacier volcanic plug and dike swarm, southeastern Alaska, *in* Hamilton, T.D., and Galloway, J.P., eds., *Geologic studies in Alaska by the U.S. Geological Survey during 1986: U.S. Geological Survey Circular 998*, p. 116-118.
- _____, 1988, Major-element geochemistry of metabasalts of the Juneau-Haines region, southeastern Alaska: *in* Galloway, J.P., and Hamilton, T.D., eds., *Geologic studies in Alaska by the U.S. Geological Survey during 1987: U.S. Geological Survey Circular 1016*, p. 150-155.
- Frey, F.A., Chappell, B.W., and Roy, S.D., 1978, Fractionation of rare-earth elements in the Tuolumne Intrusive Series, Sierra Nevada batholith, California: *Geology*, v. 6, p. 239-242.
- Fukuhara, C.R., 1986, Descriptions of plutons in the western part of the Juneau and parts of the Adjacent Skagway 1:250,000 quadrangles, southeastern Alaska: U.S. Geological Survey Open-File Report 86-393, 56 p.
- Gastil, G., Diamond, J., Knaack, C., Walawender, M., Marshall, M., Boyles, C., Chadwick, B., and Erskine, B., 1990, The problem of the magnetite/ilmenite boundary in southern and Baja California, California, *in* Anderson, J.L., ed., *The nature and origin of Cordilleran magmatism: Geological Society of America Memoir 174*, p. 19-31.
- Gehrels, G.E., Brew, D.A., and Saleeby, J.B., 1984, Progress report on U-Pb (zircon) geochronologic studies in the Coast plutonic-metamorphic complex east of Juneau, southeastern Alaska; *in* Reed, K.M., and Bartsch-Winkler, S., eds., *The United States Geological Survey in Alaska: Accomplishments during 1982: U.S. Geological Survey Circular 939*, p. 100-102.
- Gehrels, G.E., McClelland, W.C., Samson, S.D., Patchett, P.J., and Brew, D.A., 1991, U-Pb geochronology of Late Cretaceous and early Tertiary plutons in the northern Coast Mountains batholith: *Canadian Journal of Earth Science*, v. 28, p. 899-911.
- Gehrels, G.E., McClelland, W.C., Samson, S.D., Patchett, P.J., and Jackson, J.L., 1990, Ancient continental margin assemblage in the northern Coast Mountains, southeast Alaska and northwest Canada: *Geology*, v. 18, no. 3, p. 208-211.
- Gehrels, G.E., McClelland, W.C., Samson, S.D., Patchett, P.J., and Orchard, M.J., 1992, Geology of the western flank of the Coast Mountains between Cape Fanshaw and Taku Inlet, southeastern Alaska: *Tectonics*, v. 11, no. 3, p. 567-585.
- Hammarstrom, J.M., and Brew, D.A., 1993, Petrology and geobarometry of Admiralty-Revillagigedo belt granitoids near Petersburg, southeastern Alaska (abs.): *Geological Society of America Abstracts with Programs, Cordilleran and Rocky Mountain Sections*, v. 25, no. 5, p. 47.

- Hanson, G.N., 1978, The application of trace elements to the petrogenesis of igneous rocks of granitic composition: *Earth and Planetary Science Letters*, v. 38, p. 26-43
- Hanson, G.N., 1980, Rare Earth elements in petrogenetic studies of igneous systems: *Annual Reviews in Earth and Planetary Science*, v. 8, p. 371-406.
- Himmelberg, G.R., Brew, D.A., and Ford, A.B., 1991, Development of inverted metamorphic isograds in the western metamorphic belt, Juneau, Alaska: *Journal of Metamorphic Geology*, v. 9, p. 165-180.
- Himmelberg, G.R., Ford, A.B., and Brew, D.A., 1984a, Progressive metamorphism of pelitic rocks in the Juneau area, southeastern Alaska, in Coonrad, W.L., and Elliott, R.L., eds., *The United States Geological Survey in Alaska: Accomplishments during 1981: U.S. Geological Survey Circular 868*, p. 131-134.
- Himmelberg, G.R., Ford, A.B., and Brew, D.A., 1984b, Reaction isograds in pelitic rocks of the Coast plutonic-metamorphic complex near Juneau, Alaska, in Reed, K.M., and Bartsch-Winkler, S., eds., *The United States Geological Survey in Alaska: Accomplishments during 1982: U.S. Geological Survey Circular 939*, p. 105-108.
- Himmelberg, G.R., Ford, A.B., and Brew, D.A., 1986, The occurrence and chemical composition of chloritoid in the metamorphic rocks of the Coast plutonic-metamorphic complex near Juneau, in Bartsch-Winkler, Susan, and Reed, K.M., eds., *Geologic studies in Alaska by the United States Geological Survey during 1985: U.S. Geological Survey Circular 978*, p. 99-102.
- Himmelberg, G.R., Brew, D.A., and Ford, A.B., 1995a, Low-grade, M1 metamorphism of the Douglas Island Volcanics, western metamorphic belt near Juneau, Alaska: in Schiffman, P., and Day, H.W., eds., *Low-Grade Metamorphism of Mafic Rocks: Geological Society of America Special Paper 296*, p. 51-66.
- Himmelberg, G.R., Brew, D.A., and Ford, A.B., 1995b, Evaluation and application of garnet-hornblende thermobarometry, western metamorphic belt near Juneau, Alaska, in Till, A.B., and Moore, T.E., eds., *The U.S. Geological Survey in Alaska: Geologic Studies in Alaska by the U.S. Geological Survey in 1993: U.S. Geological Survey Bulletin 2107*, p. 185-198.
- Hollister, L.S., Grissom, G.C., Peters, E.K., Stowell, H.H., and Sisson, V.B., 1987, Confirmation of the empirical correlation of Al in hornblende with pressure of solidification of calc-alkaline plutons: *American Mineralogist*, v. 72, p. 231-239.
- Hutton, D.H.W., and Ingram, G.M., 1992, The Great tonalite sill of southeastern Alaska: emplacement into an active contractional high angle reverse shear zone: *Transactions of the Royal Society of Edinburgh, Earth Sciences*, v. 83, parts 1 and 2, p. 383-386 and *The Second Hutton Symposium on the Origin of Granites and Related Rocks: Boulder, Colorado, Geological Society of America, Special Paper 272*, p. 383-386.
- Ingram, G.M., and Hutton, D.H.W., 1994, The Great Tonalite Sill: Emplacement into a contractional shear zone and implications for Late Cretaceous to early Eocene tectonics in southeastern Alaska and British Columbia; *Geological Society of America Bulletin*, v. 106, p. 715-728.
- Irvine, T.N., and Baragar, W.R., 1971, A guide to the chemical classification of the common volcanic rocks: *Canadian Journal of Earth Sciences*, v. 8, p. 523-548.

- Ishihara, S., 1977, The magnetite-series and Ilmenite-series granitic rocks: *Mining Geology*, v. 27, p. 293-305.
- Ishihara, S., and Sasaki, A., 1989, Sulfur isotopic ratios of the magnetite-series and ilmenite-series granitoids of the Sierra Nevada batholith--A reconnaissance study: *Geology*, v. 17 p. 788-791.
- Karl, S.M., and Brew, D.A., 1984, Migmatites of the Coast plutonic-metamorphic complex, southeastern Alaska, in Bartsch-Winkler, S., and Reed, K.M., eds., *The United States Geological Survey in Alaska: Accomplishments during 1982: U.S. Geological Survey Circular 939*, p. 108-111.
- Kimball, R.A., Still, J.C., and Rataj, J.L., 1984, Mineral deposits and occurrences in the Tracy Arm-Fords Terror Wilderness Study Area and vicinity, Alaska, in *Mineral resources of the Tracy Arm-Fords Terror Wilderness Study Area and vicinity, Alaska: U.S. Geological Survey Bulletin 1525*, p. 105-210.
- Lathram, E.H., Pomeroy, J.S., Berg, H.C., and Loney, R.A., 1965, Reconnaissance geology of Admiralty Island, Alaska: *U.S. Geological Survey Bulletin 1181-R*, p. R1-R48.
- Lipman, P.W., 1987, Rare-Earth-Element compositions of Cenozoic volcanic rocks in the southern Rocky Mountains and adjacent areas: *U.S. Geological Survey Bulletin 1668*, 23 p.
- McBirney, A.R., 1984, *Igneous Petrology*: Freeman, Cooper, and Company, San Francisco, 504 p.
- Miller, J.C., 1962, Geology of waterpower sites on Crater Lake, Long lake, and Speel River near Juneau, Alaska: *U.S. Geological Survey Bulletin 1031-D*, p. D71-D101.
- Monger, J.W.H., and Berg, H.C., 1987, Lithotectonic terrane map of western Canada and southeastern Alaska: *U.S. Geological Survey Miscellaneous Field Studies Map MF-1874B*, scale 1: 2,500,000.
- Miyashiro, Akiho, 1974, Volcanic rock series in island arcs and active continental margins: *American Journal of Science*, v. 274, no. 4, p. 321-355.
- Mudge, M.R., 1968, Depth control of some concordant intrusions: *Geological Society of America Bulletin*, v. 79, p. 315-332.
- Norman, M.B., 1974, Improved techniques for selective staining of feldspar and other minerals using amaranth: *U.S. Geological Survey Journal of Research*, v. 2, no. 1, p. 73-79.
- Pearce, J.A., Nigell, Harris, N.B.W., and Tindle, A.G., 1984, Trace element discrimination diagrams for the tectonic interpretation of granitic rocks: *Journal of Petrology*, v. 25, no. 4, p. 956-983.
- Pitcher, W.S., 1982, Granite type and tectonic environment: in Hsu, K.J., ed., *Mountain Building Processes*; Academic Press, London, 263 p.
- Plafker, George, 1962, Geologic investigations of proposed power sites at Sheep Creek, Carlson Creek, and Turner Lake, Alaska: *U.S. Geological Survey Bulletin 1031-F*, p. F127-F148.
- Rubin, C.M., Saleeby, J.B., Cowan, D.S., Brandon, M.T., and McGroder, M.F., 1990, Regionally extensive mid-Cretaceous west-vergent thrust system in the northwestern Cordillera: Implications for continent-margin tectonism: *Geology*, v. 18, p. 276-280.

- Samson, S.D., Patchett, P.J., McClelland, W.C., and Gehrels, G.E., 1991, Nd and Sr isotopic constraints on the petrogenesis of the west side of the northern Coast Mountains batholith, Alaskan and Canadian Cordillera: *Canadian Journal of Earth Science*, v. 28, p. 939-946.
- Sawka, W.N., Chappell, B.W., and Norrish, K., 1984, Light-rare-earth-element zoning in sphene and allanite during granitoid fractionation: *Geology*, v. 12, p. 131-134.
- Shapiro, L., 1975, Rapid analysis of silicate, carbonate, and phosphate rocks: *U.S. Geological Survey Bulletin* 1401, 76 p.
- Stowell, H.H., Onstott, T.C., and Wood, D.J., 1989, Tectonic history of the Coast plutonic complex sill and adjacent metamorphic rocks, northern Coast Ranges, SE Alaska [abs.]: *Geological Society of America, Abstracts with Programs*, v. 21, no. 6, p. A181.
- Stowell, H.H., Menard, T., and Inman, K., 1993, Episodic Ca-metasomatism in overlapping thermal aureoles, Juneau goldbelt, SE Alaska: *Geological Society of America Abstracts with Programs*, v. 25, no. 5.
- Streckeisen, A.L., 1973, Plutonic rocks--Classification and nomenclature recommended by IUGS Subcommittee on Systematics of Igneous Rocks: *Geotimes*, v. 18, p. 26-30.
- Tulloch, A.J., 1989, Magnetic susceptibilities of Westland-Nelson plutonic rocks: Discrimination of Paleozoic and Mesozoic granitoid suites: *New Zealand Journal of Geology and Geophysics*, v. 32, p. 197-203.
- Wall, V.J., Clemens, J.D., and Clarke, D.B., 1987, Models for granitoid evolution and source compositions: *Journal of Geology*, v. 95, p. 731-749.
- Wells, D.E., Pittman, T.L., Brew, D.A., and Douglas, S.L., 1986, Map and description of the mineral deposits in the Juneau, Taku River, Atlin, and part of the Skagway quadrangles, Alaska: *U.S. Geological Survey Open-File Report* 85-717, 332 p.
- Wheeler, J.O., McFeely, P., 1991, Tectonic Assemblage Map of the Canadian Cordillera: *Geological Survey of Canada, Map* 1712A, scale 1:2,000,000.
- Wheatley, M.R., and Rock, N.M.S., 1988, A Macintosh program to generate normalized multi-element spidergrams: *American Mineralogist*, v. 73, p. 919-921.
- Wood, D.J., Stowell, H.H., Onstott, T.C., and Hollister, L.S., 1991, $^{40}\text{Ar}/^{39}\text{Ar}$ constraints on the emplacement, uplift, and cooling of the Coast plutonic complex sill, southeastern Alaska: *Geological Society of America Bulletin*, v. 103, no. 7, p. 849-860.
- Zen, E-an, and Hammarstrom, J.M., 1984, Magmatic epidote and its petrologic significance: *Geology*, v. 12, p. 515-518.